LEABHARLANN CHOLÁISTE NA TRÍONÓIDE, BAILE ÁTHA CLIATH | TRINITY COLLEGE LIBRARY DUBLIN
Ollscoil Átha Cliath | The University of Dublin

Terms and Conditions of Use of Digitised Theses from Trinity College Library Dublin

Copyright statement

All material supplied by Trinity College Library is protected by copyright (under the Copyright and Related Rights Act, 2000 as amended) and other relevant Intellectual Property Rights. By accessing and using a Digitised Thesis from Trinity College Library you acknowledge that all Intellectual Property Rights in any Works supplied are the sole and exclusive property of the copyright and/or other IPR holder. Specific copyright holders may not be explicitly identified. Use of materials from other sources within a thesis should not be construed as a claim over them.

A non-exclusive, non-transferable licence is hereby granted to those using or reproducing, in whole or in part, the material for valid purposes, providing the copyright owners are acknowledged using the normal conventions. Where specific permission to use material is required, this is identified and such permission must be sought from the copyright holder or agency cited.

Liability statement

By using a Digitised Thesis, I accept that Trinity College Dublin bears no legal responsibility for the accuracy, legality or comprehensiveness of materials contained within the thesis, and that Trinity College Dublin accepts no liability for indirect, consequential, or incidental, damages or losses arising from use of the thesis for whatever reason. Information located in a thesis may be subject to specific use constraints, details of which may not be explicitly described. It is the responsibility of potential and actual users to be aware of such constraints and to abide by them. By making use of material from a digitised thesis, you accept these copyright and disclaimer provisions. Where it is brought to the attention of Trinity College Library that there may be a breach of copyright or other restraint, it is the policy to withdraw or take down access to a thesis while the issue is being resolved.

Access Agreement

By using a Digitised Thesis from Trinity College Library you are bound by the following Terms & Conditions. Please read them carefully.

I have read and I understand the following statement: All material supplied via a Digitised Thesis from Trinity College Library is protected by copyright and other intellectual property rights, and duplication or sale of all or part of any of a thesis is not permitted, except that material may be duplicated by you for your research use or for educational purposes in electronic or print form providing the copyright owners are acknowledged using the normal conventions. You must obtain permission for any other use. Electronic or print copies may not be offered, whether for sale or otherwise to anyone. This copy has been supplied on the understanding that it is copyright material and that no quotation from the thesis may be published without proper acknowledgement.

Investigations into the Physiological Expression of UCP1 and UCP3

A dissertation submitted to Trinity College Dublin
for the degree of Doctor of Philosophy
by

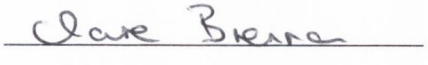
Clare M. Brennan

Department of Biochemistry
Trinity College Dublin
March 2005

TRINITY COLLEGE
13 NOV 2006
LIBRARY DUBLIN
THESIS
8007

Declaration

I, the undersigned, declare that this thesis is entirely my own work, except where otherwise accredited, and that it has not been submitted for a degree in any other university or institution. This thesis may be borrowed or copied upon request with the permission of the Librarian, University of Dublin, Trinity College.



Clare Brennan

Abstract

Previous studies have indicated that acute exercise induces large increases in uncoupling protein 3 in skeletal muscle, whereas endurance training results in marked decreases in skeletal muscle uncoupling protein 3 at both mRNA and protein levels. Using an uncoupling protein 3 specific antibody we confirm that uncoupling protein 3 protein is expressed in rat skeletal muscle mitochondria. In addition, we show that absolute uncoupling protein 3 expression is elevated in *gastrocneumis* and *plantaris* muscle homogenates following acute exercise (2 weeks). Furthermore, we show the novel finding that uncoupling protein 3 protein expression per unit mass of mitochondria is increased by acute exercise (2 weeks) in *gastrocnemius* muscle of mice. We also show that the increase in uncoupling protein 3 protein expression is transient with levels returning to pre-exercise levels 22 hours after the final exercise bout. Acute exercise is shown to have no effect on uncoupling protein 3 protein expression in *plantaris*, *soleus* or *extensor digitorum longus* muscle homogenates. Furthermore, we present novel results illustrating that endurance exercise (17 weeks) results in no significant changes in uncoupling protein 3 protein expression in whole muscle homogenates of *gastrocnemius*, *soleus*, *plantaris* or *extensor digitorum longus*.

Using uncoupling protein 1 knockout technology, our study provides novel evidence demonstrating the occurrence of uncoupling protein 1 in thymus isolated from wild type but not uncoupling protein 1 knock-out mice. Preliminary evidence also suggests that the immunological condition of the animal may have some bearing on the role of uncoupling protein 1 in thymus mitochondria since non-specific pathogen free mice express more uncoupling protein 1 in their thymus than specific pathogen free mice. Anti-peptide uncoupling protein 1 antibodies, that have been previously shown to be specific for uncoupling protein 1, detected a significant increase in uncoupling protein 1 protein expression in thymus mitochondria isolated from cold acclimated (5-weeks) rats, akin to the increase in uncoupling protein 1 observed in brown adipose tissue mitochondria following cold exposure. In addition, we have presented novel results showing that thymus mitochondrial state 4 oxygen consumption rates are more sensitive to inhibition by

guanosine 5'-diphosphate and more sensitive to subsequent reactivation by palmitate, in cold acclimated rats when compared to room temperature rats. Abundance of uncoupling protein 1 was also determined using a radiolabelled binding assay. It was determined that [^{3}H] guanosine 5'-diphosphate binding to Dowex-treated thymus mitochondria isolated from cold acclimated rats (5-weeks) was significantly increased when compared to Dowex-treated thymus mitochondria isolated from rats housed at room temperature, without altering the K_D for guanosine 5'-diphosphate binding. Our findings also confirm that the purine nucleotide binding site in thymus mitochondria isolated from rats housed at room temperature is masked and that Dowex-treating thymus mitochondria for 1 hour at room temperature results in the binding site being unmasked. Therefore, we conclude the novel finding that rat thymus mitochondria contain uncoupling protein 1 protein whose expression and activity appear to be temperature sensitive. However, our results suggest that thymic uncoupling protein 1 is not a general source of heat in the body of these animals.

Our study has shown that purine nucleotides inhibit and nanomolar amounts of fatty acids activate uncoupling protein 1 in both brown adipose tissue mitochondria and thymus mitochondria. Guanosine 5'-diphosphate and palmitate, known to inhibit and activate the uncoupling activity of uncoupling protein 1, had no effect on oxygen consumption rates in uncoupling protein 2 (kidney) and uncoupling protein 3 (spleen) containing mitochondria. Brown adipose tissue and thymus mitochondria bind guanosine 5'-diphosphate with high affinity due to the presence of the guanosine 5'-diphosphate binding protein uncoupling protein 1. Since, many of the amino acid residues reported to be essential for the binding of guanosine 5'-diphosphate by uncoupling protein 1 are conserved in uncoupling protein 2 and uncoupling protein 3, it was suggested that uncoupling protein 2 and uncoupling protein 3 can bind guanosine 5'-diphosphate. However, our results illustrate that guanosine 5'-diphosphate binding to uncoupling protein 2 (kidney) and uncoupling protein 3 (spleen) containing mitochondria is of low affinity, with no saturable binding up to 6 μM [^{3}H] guanosine 5'-diphosphate. Taken together, our functional and binding results suggest that in contrast to uncoupling protein 1, uncoupling protein 2 and uncoupling protein 3 do not exhibit uncoupling activity in isolated mitochondria, thereby suggesting a different role for uncoupling protein 2 and uncoupling protein 3

Acknowledgements

I'd like to start with Richie my 'super' supervisor! Thanks a million for all the (**fact a**) encouragement, (**fact b**) inspiration and (**fact c**) many, many laughs along the way. It's been a pleasure to work with you over the last few years. Now that I have finished, I feel as though I have not lost a supervisor but have gained a friend!

Many thanks to everyone, past and present, in Richie's lab especially (in no particular order guys):

Oliver, thank you for your enormous patience with me. Lordy, the questions I had for you! Your kindness, help and friendship will never be forgotten. Dublin's loss was most definitely Sligo's gain. Thanks also to Lorna for her friendship and always knowing when not to ask the terrible thesis question!

Eamo, thanks for your kindness and for always being there to give me a hand in the lab when I needed it. Thanks also for keeping me up to date on 'what's hot and what's not' in fashion, people and just stuff in general! Sorry the whole 'I'd marry you if we aren't married by the time we're 30' thing fell through. Still, we may never have Barbuda (or the Vera Wang creation!) but we'll always have the lab!

Audrey, thank you for your patience, help and friendship over the last few years. It has been wonderful to know I could rely on you in the midst of another experimental crisis! I've enjoyed all our 'girly' chats too and look forward to many, many more. We're on our way now missus!

I feel exceptionally lucky to have joined such a wonderful lab and met all of you. Each of you made it a delight to come into college every day. What wonderfully educated conversations we had about all the important things in life – remembering (and singing) children's TV theme tunes of our youth (Ollie wins that one), launching our ACE clothing line (Whatever happened there lads? It was such a winner) and discussing hot topics of the day such as 'Do Leprechauns really exist?' (Audrey, I'm afraid you're going to have to discuss that one with your da again). Thanks guys... It's been wonderful and I'll miss our little party of 5.

Thanks to everyone in the Bioresources Unit, in particular to Anne and Brian for their kind assistance always. Thanks also to the guys in the prep room and to Kyran in stores for always being ready to assist at the last minute.

Thanks also to Dr. Stuart Warmington and Professor Christopher Bell in the Department of Physiology, Trinity College for all the help at the start of my PhD and for the use of the facilities in their department.

Special thanks to my wonderful friends who have provided laughter, friendship, spooky castle adventures, lots and lots of pizza, sambuca (never again Katherine!), shoulders to cry on when times were tough, rude jokes (you know who I'm talking about Trish!), oodles of bath-bombs, lively debate (I'm striving Lesley!), fantastic nights on the town in Aberdeen (Aoife - Miss Irish Rover 2000) and ridiculous conversations about scientific inventions that never were - sodium umbrella anyone? (How did we ever get our degrees Frances?). You lot are the best.

Special thanks to my fantastic brothers- Ciaran, Niall, Mick and Conor and also to their wives Tina, Florence, Pat and Cliodhna and to their wonderful kids Emma, Gillian, Aoife, Mia, Iseult and Fiachra. I love each and every one of you. Thanks for your support and encouragement throughout everything.

Very special thanks to mam and dad for believing that I could do this, for their encouragement and support and for making this PhD a possibility for me. I love you both very much.

Finally, thanks to Cathal for his unending support, love and encouragement and for always keeping my thermally challenged feet warm. I love you. Let's go get married!

Financial support from the Trinity Postgraduate award is acknowledged

Abbreviations

ADP	Adenosine 5'– diphosphate
AMP	Adenosine 5'– monophosphate
ANOVA	Analysis of variance
APS	Ammonium persulfate
ATP	Adenosine 5' -triphosphate
AtUCP/AtPUMP	*Arabidopsis thaliana* uncoupling protein
avUCP	Avian uncoupling proteins
BAT	Brown adipose tissue
B_{MAX}	Maximal binding capacity
BMCP-1	Brain-specific mitochondrial uncoupling protein
BRU	Bioresources Unit
BSA	Bovine serum albumin
cAMP	cyclic adenosine monophosphate
CCCP	carbonyl cyanide m-chlorophenylhydrazone
CpUCP	*Candida parapsilosis* uncoupling protein
CREB	camp-response-element-binding protein
DNA	Deoxyribonucleic acid
2,4-DNP	2,4- dinitrophenol
dpm	Disintegrations per minute
DTNB	5,5-dithio-bis-nitrobenzoic acid
ECL	Enhanced chemiluminescence
EDL	*Extensor digitorum longus*
EDTA	Ethylenediamine tetraacetic acid
EGTA	Ethyleneglycol-bis(aminoethylether)-N,N-tetraacetate
ETC	Electron transport chain
FAD^+	Flavin adenine dinucleotide oxidised form
$FADH_2$	Flavin adenine dinucleotide reduced form

FCCP	Carbonyl cyanide *p*-trifluoromethoxyphenylhydrazone
FDA	U.S. food and drug administration
FFA	Free fatty acid
FCCP	carbonyl cyanide *p*-trifluoromethoxyphenylhydrazone
FCS	Fetal calf serum
Folins	Folin's Ciocalteau's phenol reagent
g	Relative gravitational force
GDP	Guanosine 5'-diphosphate
GMP	Guanosine 5'- monophosphate
GTP	Guanosine 5'- triphosphate
HEPES	N-(2-hydroxymethyl) piperazine-N'-(2-ethanesulfonic acid)
hUCP	human uncoupling protein
HRP	Horse radish peroxidase
K_D	Michaelis dissociation constant
MIM	Mitochondrial inner membrane
MOM	Mitochondrial outer membrane
$_m$RNA	Messenger RNA
NAD^+	Nicotinamide adenine dinucleotide oxidised form
NADH	Nicotinamide adenine dinucleotide reduced form
OD	Optical density
Δp	Proton electrochemical gradient
ΔpH	pH gradient across the mitochondrial inner membrane
PA	Palmitic acid
PAGE	Polyacrylamide gel electrophoresis
PBS	Phosphate buffered saline
PBS-Tween	PBS containing 0.1% (w/v) Tween
PKA	Protein kinase A
PUMP	Plant uncoupling protein
PVDF	polyvinylidene difluoride
RCR	Respiratory control ratio
RNA	Ribonucleic acid
ROS	Reactive oxygen species

SDS	Sodium dodecyl sulfate
S.E.M	Standard error of the mean
SPF	Specific pathogen free
STE	Sucrose-trizma-EGTA medium
StUCP	*Solanum tuberosum* uncoupling protein
TAG	triacylglycerol
TES	N-Tris[hydroxymethyl]methyl-2-aminoethane-sulfonic acid
Tris	2-amino-2-[hydroxymethyl]-1,3-propanediol
Tween	Tween 20 (polyoxyethylenesorbitan monolaurate)
UCP	Uncoupling protein
$UCP3_L$	Uncoupling protein 3 long-form
$UCP3_S$	Uncoupling protein 3 short-form
VDAC	Voltage-dependent anion channel
v/v	volume per unit volume
$\Delta\Psi$	Membrane potential
WAT	White adipose tissue
w/v	weight per unit volume

Table of Contents

Declaration I

Abstract II

Acknowledgements IV

Abbreviations VI

1. Introduction

1.1 The Mitochondrion 1

1.2 Oxidative Phosphorylation 1

1.3 Mitochondrial Proton Leak 3

1.3.1 Natural Proton Leak 3

1.3.2 Artificially induced proton leak 6

1.3.3 Protein Mediated Proton Leak 6

1.4 Brown Adipose Tissue 8

1.4.1 Structure of UCP1 8

1.4.2 Activation of UCP1 10

1.4.3 Expression of UCP1 14

1.5 Uncoupling Protein Homologues 15

1.5.1 Uncoupling Protein 2 16

1.5.2 Uncoupling Protein 3 16

1.5.3 Uncoupling Protein 4 19

1.5.4 Uncoupling Protein 5 19

1.5.5 Plant Uncoupling Proteins 19

1.6 Metabolic Adaptations to Training 20

1.6.1 Muscle mitochondrial Density 20

1.7 UCPs and Reactive Oxygen Species 21

1.8 Effects of fatty acids and purine nucleotides on UCP function 22

1.8.1 Heterologous Yeast expression systems 23

1.8.2 UCPs reconstituted in liposomes 24

1.8.3 Transgenic over-expression and gene knock-out studies .. 25
1.8.4 Evidence from physiologically perturbed natural models.. 27
1.8.5 Evidence from site-directed mutagenesis studies 27
1.9 Purine nucleotide binding to UCPs 28

2. Materials and Methods

2.1 Materials 34
2.2 Ethics Approval 34
2.3 Animal Treatments 35
2.3.1 Acute Exercise 35
2.3.2 Endurance Training 35
2.3.3 Temperature Acclimation 35
2.3.4 Wild Type (WT) and UCP1 Knock-Out (KO) mice 35
2.3.5 Specific Pathogen Free Mice 36
2.4 Training Protocols 36
2.4.1 Endurance Swimming Training 36
2.4.2 Acute Swimming Exercise 36
2.5 Whole Body Oxygen Consumption 37
2.6 Skeletal Muscle Dissection 37
2.7 Preparation of Skeletal Muscle Homogenates 37
2.8 Mitochondrial Isolations 38
2.8.1 Isolation of Brown Adipose Tissue 38
2.8.2 Isolation of Skeletal Muscle Mitochondria 39
2.8.3 Isolation of Liver and Spleen Mitochondria 39
2.8.4 Isolation of Kidney Mitochondria 40
2.8.5 Isolation of Thymus Mitochondria 40
2.9 Mitochondrial Protein Determination – Markwell Assay 41
2.10 Citrate Synthase Assay 41
2.11 Sodium Dodecyl Sulfate Polyacrylamide Gel Electrophoresis 42
2.11.1 Preparation of samples for Gel Electrophoresis 42
2.11.2 Gel Electrophoresis 42
2.12 Western Immunoblotting 42
2.13 Coomassie BlueR Staining of SDS-PAGE Gels 43

2.14 Densitometry 44
2.15 Antibodies 44
2.16 Purification of Polyclonal Antibodies Using Protein A-Sepharose 44
2.17 Dowex Treatment of Isolated Mitochondria 45
2.18 GDP Binding Assay 45
2.19 Liquid Scintillation Counting 46
2.20 Analysis of Saturable Binding Data 46
2.21 Measurement of Oxygen Consumption Rates in Mitochondria Isolated from BAT, thymus, liver, kidney, muscle and spleen 47
2.22 Fatty Acid Activation Assay 47
2.23 Statistical Analysis 48

3. The effects of acute and endurance exercise on UCP3 protein expression in mouse *gastrocnemius*, *plantaris*, *soleus* and *EDL* muscles

3.1 Introduction 49
3.2 Results 54
3.3 Discussion 74
3.4 Conclusions 80

4. Detection of UCP 1 protein expression using Western Blot analysis

4.1 Introduction 81
4.2 Results 83
4.3 Discussion 90
4.4 Conclusions 93

5. The effect of fatty acids and purine nucleotides on UCP function in cold-acclimated rats

5.1 Introduction 94
5.2 Results 97
5.3 Discussion 112
5.4 Conclusions 115

6. Application of a radiolabeled purine nucleotide binding assay to UCP-containing mitochondria

6.1 Introduction 116

6.2 Results 118

6.3 Discussion 128

6.4 Conclusions 132

7. General Discussion 133

References 141

Appendix 168

List of Figures

1.1 Anatomy of the mitochondrion 2

1.2 An overview of the redox carriers in the mitochondrial respiratory chain 4

1.3 The chemiosmotic proton circuit across the mitochondrial inner membrane of isolated mitochondrial 7

1.4 Tripartite structural model of hamster uncoupling protein 1 9

1.5 The mechanism of hormonally-induced uncoupling of oxidative phosphorylation in brown fat mitochondria 11

1.6 Proposed mechanism by which free fatty acids activate H^+ transport by UCP1 13

1.7 Proposed mechanism for the masking/unmasking phenomenon 30

1.8 C- terminal amino acid sequence of rat uncoupling proteins 1, 2 and 3 32

3.2.1 Effect of acute exercise on body mass 55

3.2.2 Citrate synthase activity in gastrocnemius, plantaris, soleus and EDL muscle homogenates 56

3.2.3 $F_1\beta$ expression in gastrocnemius, plantaris, soleus and EDL muscle homogenates 57

3.2.4 Effect of acute swimming on expression of UCP3 protein in gastrocnemius homogenates 59

3.2.5 Effect of acute swimming on expression of UCP3 protein in plantaris homogenate 60

3.2.6 Effect of acute swimming on expression of UCP3 protein in soleus homogenate 62

3.2.7 Effect of acute swimming on expression of UCP3 protein in EDL homogenate 63

3.2.8 Effect of endurance training on body mass 65

3.2.9 Whole body resting oxygen consumption pre, mid and post training 66
3.2.10 Citrate synthase activity in gastrocnemius, plantaris, soleus and EDL muscle homogenates of endurance trained mice 67
3.2.11 Effect of 17 weeks endurance swimming training on expression of UCP3 protein in gastrocnemius homogenate 69
3.2.12 Effect of 17 weeks endurance swimming training on expression of UCP3 protein in plantaris homogenate 70
3.2.13 Effect of 17 weeks endurance swimming training on expression of UCP3 protein in soleus homogenate 71
3.2.14 Effect of 17 weeks endurance swimming training on expression of UCP3 protein in EDL homogenate 72

4.2.1 UCP1 is expressed in thymus mitochondria isolated from WT C57BL/6J mice but is not detected in thymus mitochondria from UCP1 KO C57BL/6J mice 84
4.2.2 UCP1 is expressed in thymus mitochondria isolated from specific pathogen free (SPF) and non-SPF mice 85
4.2.3 UCP1 is expressed in BAT mitochondria isolated from room temperature and cold acclimated rats but is not detected in liver mitochondria isolated from these groups 86
4.2.4 UCP1 is not detected in spleen, muscle or kidney mitochondria isolated from room temperature and cold acclimated rats 88
4.2.5 UCP1 protein expression is increased in thymus mitochondria isolated from rats acclimated to the cold for 5 weeks 89

5.2.1 State 4 oxygen consumption rates in BAT mitochondria, isolated from rats kept at room temperature, are sensitive to purine nucleotides and fatty acids 98
5.2.2 State 4 oxygen consumption rates in BAT mitochondria, isolated from rats kept at 4°C for 5 weeks, are sensitive

to purine nucleotides and fatty acids 99
5.2.3 State 4 oxygen consumption rates in thymus mitochondria, isolated from rats kept at room temperature, are sensitive to purine nucleotides and fatty acids 100
5.2.4 State 4 oxygen consumption rates in thymus mitochondria, isolated from rats kept at 4°C for 5 weeks, are sensitive to purine nucleotides and fatty acids 102
5.2.5 Comparison of state 4, GDP and palmitate rates in thymus mitochondria isolated from rats housed at room temperature and 4°C 103
5.2.6 State 4 oxygen consumption rates in liver mitochondria, isolated from rats kept at room temperature, are insensitive to purine nucleotides and fatty acids 104
5.2.7 State 4 oxygen consumption rates in liver mitochondria, isolated from rats kept at 4°C for 5 weeks, are insensitive to purine nucleotides and fatty acids 105
5.2.8 State 4 oxygen consumption rates in kidney mitochondria, isolated from rats kept at room temperature, are insensitive to purine nucleotides and fatty acids 106
5.2.9 State 4 oxygen consumption rates in kidney mitochondria, isolated from rats kept at 4°C for 5 weeks, are insensitive to purine nucleotides and fatty acids 107
5.2.10 State 4 oxygen consumption rates in spleen mitochondria, isolated from rats kept at room temperature, are insensitive to purine nucleotides and fatty acids 109
5.2.11 State 4 oxygen consumption rates in spleen mitochondria, isolated from rats kept at 4°C for 5 weeks, are insensitive to purine nucleotides and fatty acids 110

6.2.1 Comparison of [^{3}H] GDP binding parameters in Dowex-treated BAT mitochondria isolated from room temperature and cold acclimated rats 120

6.2.2 Comparison of [^{3}H] GDP binding parameters in Dowex-treated liver mitochondria isolated from room temperature and cold acclimated rats 121
6.2.3 Comparison of [^{3}H] GDP binding parameters in Dowex-treated thymus mitochondria isolated from room temperature and cold acclimated rats 122
6.2.4 Comparison of [^{3}H] GDP binding parameters in Dowex-treated BAT and thymus mitochondria isolated from room temperature and cold acclimated rats 124
6.2.5 [^{3}H] GDP binding parameters in Dowex treated and non-Dowex treated thymus mitochondria isolated from room temperature rats 125
6.2.6 Comparison of [^{3}H] GDP binding parameters in Dowex-treated kidney mitochondria isolated from room temperature and cold acclimated rats 126
6.2.7 Comparison of [^{3}H] GDP binding parameters in Dowex-treated spleen mitochondria isolated from room temperature and cold acclimated rats 127

List of Tables

1.1 Summary of structure, function and location of the three principal uncoupling proteins 15

1.2 Summary of adaptations of skeletal muscle to endurance training 21

3.1 Muscle fibre composition 53

5.2.1 Respiratory control ratios for mitochondria isolated from rats acclimated to the cold for 5-weeks and from rats kept at room temperature 111

7.1 Summary of the effects of 5-weeks cold acclimation on tissue mass, mitochondrial protein yield/g tissue, B_{MAX} and UCP1/F1β protein expression in BAT mitochondria 137

7.2 Summary of the effects of 5-weeks cold acclimation on tissue mass, mitochondrial protein yield/g tissue, B_{MAX} and UCP1/F1β protein expression in thymus mitochondria 138

Lovingly dedicated to mam and dad

'The most exciting phrase to hear in science, the one that heralds new discoveries, is not 'Eureka!' (I found it) but 'that's funny…'

Isaac Asimov

1920 – 1992

U.S Science Fiction Novelist and Scholar

Chapter 1
Introduction

1.1 The Mitochondrion

It is generally believed that mitochondria are the descendants of bacteria that invaded or were engulfed by primitive cells early in evolutionary history. A symbiotic relationship subsequently evolved, with the bacteria eventually becoming permanent organelles. Present in virtually all eukaryotic cells, both plant and animal, mitochondria are about the size of an *Escherichia coli* bacterium, having a typically ellipsoid shape, being approximately 0.5 μm in diameter and 1 μm in length. Their structure consists of a smooth mitochondrial outer membrane (MOM) and a mitochondrial inner membrane (MIM) which together form two compartments, the intermembrane space and the matrix (Figure 1.1). The matrix holds high concentrations of the soluble enzymes of oxidative metabolism, as well as substrates, nucleotide cofactors and inorganic ions. The matrix also contains mitochondrial genetic machinery, namely DNA, RNA, and ribosomes. The MOM is freely permeable to most small molecules including protons. The MIM is not. The MIM is extensively folded to form cristae, a structural feature that substantially increases the surface area available for mitochondrial functions, in particular adenosine triphosphate (ATP) production. As such, the MIM also contains the ATP synthase molecule, responsible for ATP production, and the various protein components of the electron transport chain (ETC). The main function of the mitochondrion is the production of ATP via oxidative phosphorylation.

1.2 Oxidative Phosphorylation

The endergonic synthesis of ATP from adenosine diphosphate (ADP) and P_i in mitochondria is known as oxidative phosphorylation (reviewed in Nicholls & Ferguson, 1992). This process is catalysed by a MIM proton translocating ATP synthase molecule and driven by the ETC (Figure 1.2). The chemiosmotic theory proposed by Mitchell in 1961 gives the best description of what occurs during oxidative phosphorylation.

Briefly, metabolism of fuel (either dietary or stored) leads to the production of the reducing equivalents nicotinamide adenine dinucleotide ($NADH_2$) and flavin adenine dinucleotide ($FADH_2$). Large membrane-bound enzymes, such as glycerol phosphate dehydrogenase, the dehydrogenases of β-oxidation, NADH-Q oxidoreductase (Complex I) or succinate-Q oxidoreductase (Complex II) pass electrons down the gradient of redox potential to the mobile lipid-soluble carrier, ubiquinone (Q). From Q, the electrons pass

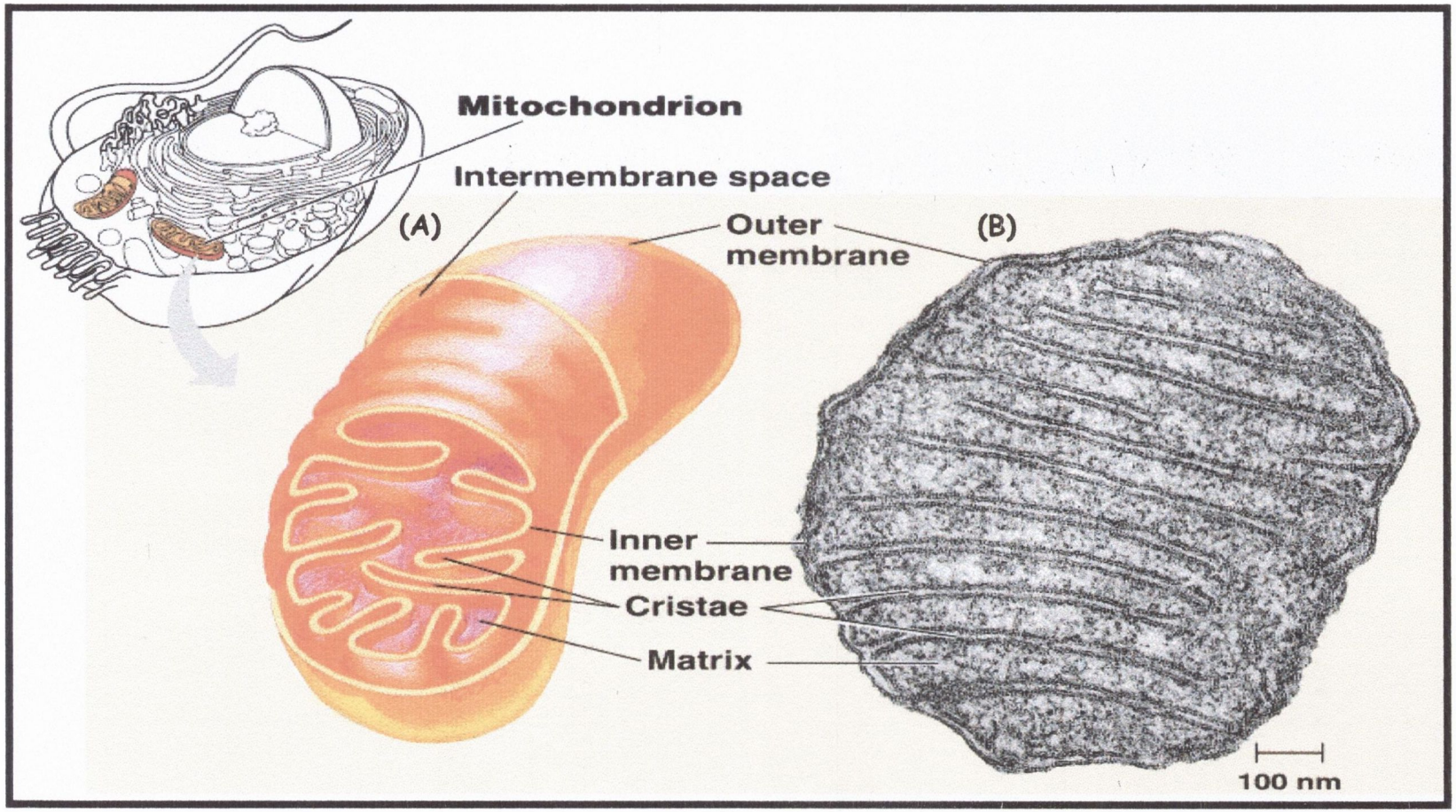


Figure 1.1 Anatomy of the Mitochondrion. (A) Schematic representation of a mitochondrion. Each mitochondrion will hold thousands of copies of the electron transport chain and ATP synthase complexes which are found on the mitochondrial inner membrane. **(B)** An electron micrograph of a mitochondrion illustrating the extensive folding of the cristae some of which span the width of a single mitochondrion.

(www.uwinnipeg.Ca/~simmons/cm1503/mitochondria.htm)

down through the bc_1 complex (Complex III), cytochrome c (a water-soluble, mobile carrier) and cytochrome oxidase (Complex IV) to the final acceptor, oxygen. As electrons are moved down through the protein complexes of the ETC, complex I, III and IV translocate protons across the mitochondrial inner membrane from the matrix in to the intermembrane space hence setting up an electrochemical gradient (Δp). Protons are then able to re-enter the mitochondrial matrix via the ATP synthase molecule (which is distinct from the ETC) in a reaction that is tightly linked to ATP synthesis, and driven by the Δp. The MIM contains an ATP/ADP translocator which exchanges ADP (a by-product of cytosolic ATP hydrolysis) for ATP (synthesised within the mitochondrial matrix). ATP generated in the matrix via oxidative phosphorylation can be used to drive such energy requiring processes as muscle contraction, active transport, nucleic-acid synthesis and protein synthesis, virtually all cellular processes requiring energy.

Electron transport chain reactions lead to proton pumping and the generation of the Δp. Assuming all proton backflow is through the ATP synthase molecule, then substrate oxidation and ATP phosphorylation are said to be 'coupled'. However, it has long been recognised that the ATP synthase molecule is not the only means by which the Δp may be dissipated (Nicholls, 1974). Oxidative phosphorylation is never fully coupled in either isolated mitochondria or in mitochondria *in situ* (Brand *et al.*, 1994). An inefficiency of the system exists whereby protons translocated from the matrix into the intermembrane space may re-enter the matrix via flux through a non-productive (no ATP synthesis) proton conductance channel in a phenomenon known as proton leak.

1.3 Mitochondrial Proton Leak

1.3.1 Natural Proton leak

Isolated mitochondria consume oxygen at low rates even when they are prevented from producing ATP by either the addition of oligomycin (an ATP synthase inhibitor), or by removal of all ADP (Brand *et al.*, 1977). This observation illustrates 'imperfect coupling' of mitochondria and hence the occurrence of natural proton leak, a non-enzymatic (*i.e.* ATP synthase is not involved) diffusion of protons across the MIM of mitochondria both isolated and *in situ* (Figure 1.3). The relationship between proton leak and its driving force, Δp, is non-linear. That is, proton leak proceeds maximally when mitochondria are not making ATP (State 4 respiration) and minimally when they are

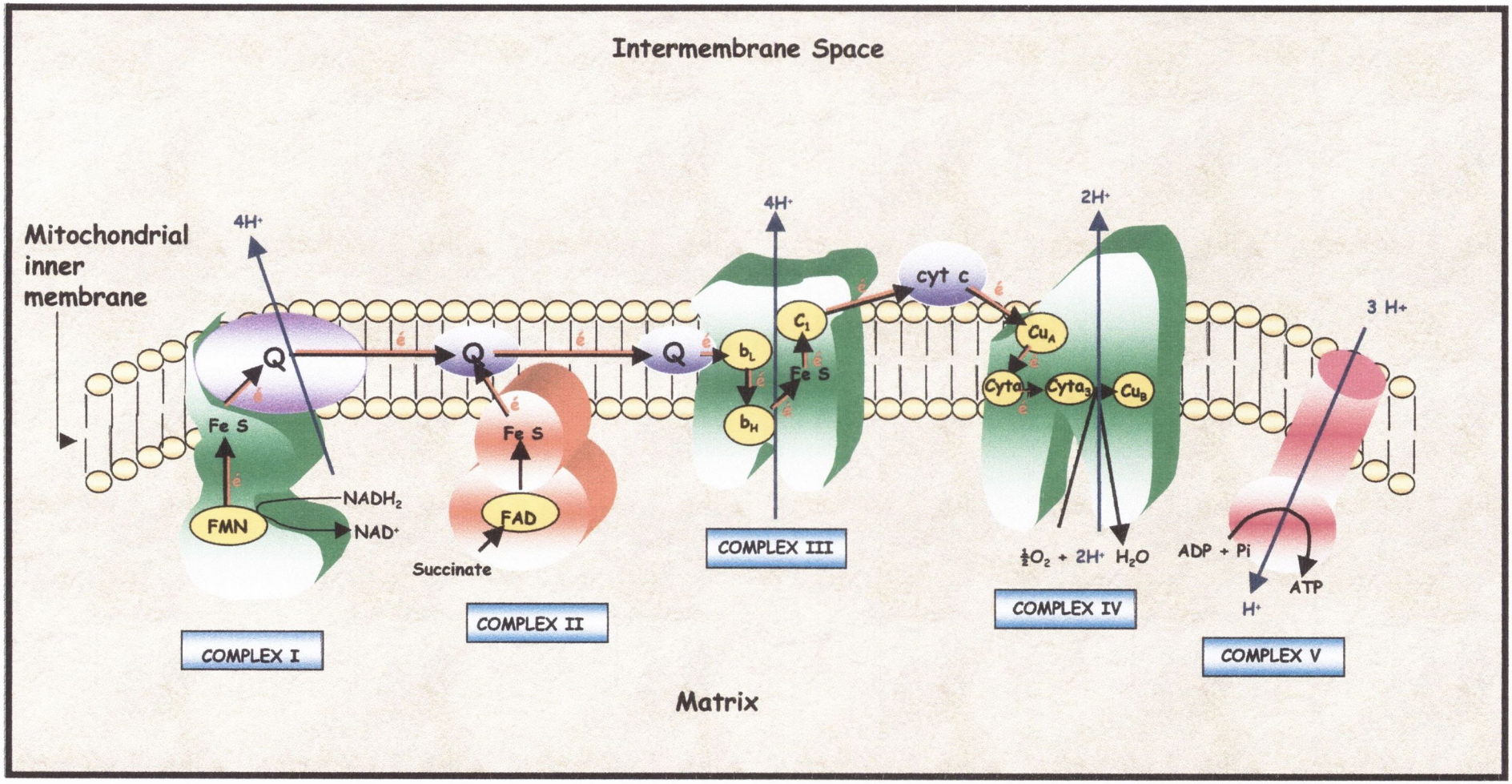


Figure 1.2: An overview of the redox carriers in the mitochondrial respiratory chain.

A diagram of the mitochondrial electron transport chain indicating the pathway of electron transfer (black) and proton pumping (red). Electrons are transferred between Complexes I and III by the membrane-soluble CoQ and between Complexes III and IV by the peripheral membrane protein, cytochrome C. Complex II transfers electrons from succinate to CoQ.Diagram reproduced with kind permission of Dr. Audrey Carroll.

synthesising ATP (State 3 respiration) (Nicholls & Rial, 1974; Brown and Brand, 1986; Porter & Andrews, 1998). A basal proton conductance is therefore a feature of undamaged mitochondria. However, the mechanism by which proton leak occurs remains to be elucidated. The weight of evidence in the literature suggests that oxygen consumed under these non-phosphorylating conditions is controlled by the inner membrane permeability to protons (Brand, 1990; Brand *et al.*, 1994; Porter & Brand, 1995; Porter, 2001).

Initially proton leak was believed to be an artefact of damage to mitochondria, sustained upon isolation from cells and tissues and not a physiological phenomenon (Stuart *et al.*, 1999). However, it was shown that the proton leak across the MIM was present when mitochondria were functioning in intact rat hepatocytes (Nobes *et al.*, 1990). Since then other research groups have shown that the properties of proton leak (*i.e.* the ability to circumvent the ATP synthase, the non-ohmic relationship proton leak displays with its driving force, Δp and its apparent lack of dependence on fatty acids and purine nucleotides) are the same in all tissues (*e.g.* skeletal muscle or liver) and cells (*e.g.* hepatocytes or thymocytes), isolated or *in situ* (Brand *et al.*, 1993; Harper and Brand, 1993).

In rat liver cells 25% of energy consumption is used to drive proton leak alone (Nobes *et al.*, 1990). However, it is more pertinent to examine whole body energetics to estimate the significance of proton leak on metabolism. By far the greatest oxygen consuming tissue of the body is skeletal muscle (Rolfe and Brand, 1996). Results have suggested that approximately 50% of metabolic rate may be dedicated to countering the leak of protons across the MIM of resting muscle (Rolfe and Brand, 1996). Experiments on contracting skeletal muscle indicate that, even as metabolism increases to accommodate increasing workloads, proton leak still accounts for a large quantity, approximately 35%, of the overall energy expenditure (Rolfe *et al.*, 1999). Therefore proton leak is a large consumer of whole body energy supplies.

In addition to diffusion mediated proton leak there is a MIM protein in brown adipose tissue (BAT) which displays uncoupling activity (Cannon *et al.*, 1982). This protein, originally called thermogenin, allows the dissipation of the Δp generated by the ETC as heat (Nicholls and Locke, 1984). Unlike diffusion mediated proton leak, thermogenin is highly regulated. Free fatty acids (nanomolar amounts) activate

thermogenin (Skulachev, 1991), while purine nucleotides (mainly GDP) inhibit its activity (Rafael *et al.*, 1969).

1.3.2 Artificially induced proton leak

One of the most notable early successes of the chemiosmotic theory was its explanation of the action of uncoupling agents. Uncoupling agents abolish the link between oxidation and phosphorylation, allowing electron transport to proceed without coupled ATP synthesis (Brand, 2000). Over the years, many compounds, including 2,4-dinitrophenol (DNP) and carbonylcyanide-*p*-trifluoromethoxy-phenylhydrazone (FCCP) have been found to "uncouple" oxidative phosphorylation. DNP and FCCP are lipophilic weak acids that can cross the mitochondrial inner membrane in either a protonated or unprotonated state. This sets up a catalytic cycle that dissipates Δp and so allows substrate oxidation to proceed without providing the driving force for coupled ATP synthesis (Brand, 2000) (Figure 1.3). In fact, uncoupling of mitochondria has been used to reduce body fat in humans. The artificial uncoupler DNP has been used for this purpose for many years (Parascandola, 1974). DNP was introduced as an anti-obesity drug in the 1930s and used with considerable success, though reports of side effects and some deaths from overdose led to it being removed from the market by the U.S. Food and Drug Administration (FDA) in 1938.

1.3.3 Protein Mediated Proton Leak

Thermogenin was discovered in the 1970s (Heaton *et al.*, 1978). In 1997, upon discovery of several homologues it was renamed Uncoupling Protein 1 (UCP1) (Fleury *et al.*, 1997). As already mentioned, UCP1 is expressed in BAT where it exerts its thermogenic effect by allowing the re-entry of protons into the matrix without ATP synthesis (Klaus *et al.*, 1991). The net result of this (and function of UCP1) is the oxidation of substrate, and the dissipation, as heat, of the liberated energy (Figure 1.3). UCP1 is activated in response to cold exposure or chronic overeating (Swick & Swick, 1986; Sundin *et al.*, 1987; Klaus *et al*, 1991) and as such is an important contributor to whole body energy expenditure in rodents, which conserve their BAT supplies throughout their lifetime (Trayhurn and Nicholls, 1986). In cold adapted rodents, UCP1 may form as much as 10 - 15% of the mitochondrial membrane proteins (Lin and Klingenberg, 1980; Ricquier *et al.*, 1982). In addition to its proton translocating properties, UCP1 is also permeable to Cl^- ions (Huang & Klingenberg, 1996).

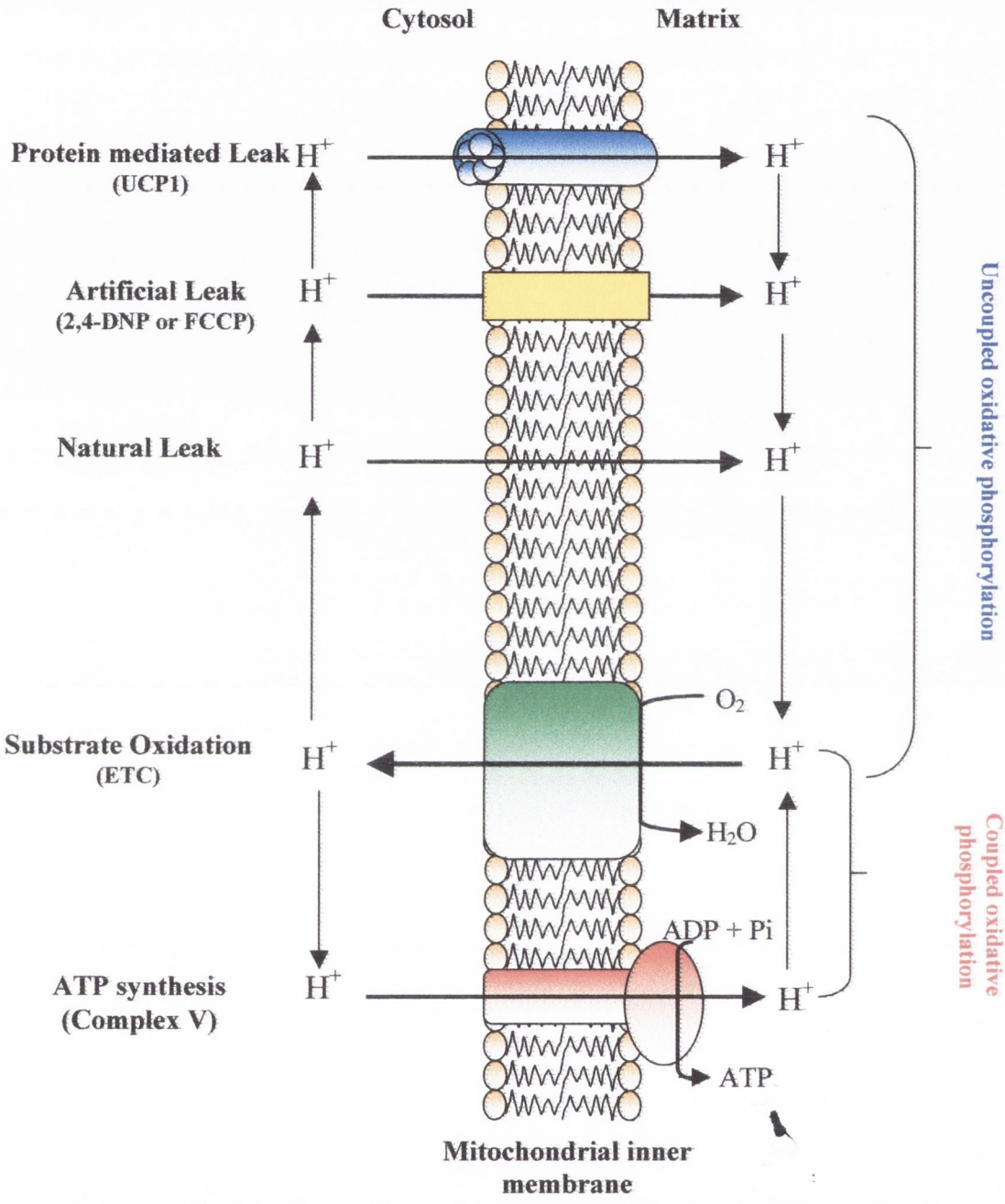


Figure 1.3 The chemiosmotic proton circuit across the mitochondrial inner membrane of isolated mitochondria.

The lower circuit, consisting of substrate oxidation (electron transport chain) and the enzymes of ATP production, results in coupled oxidative phosphorylation. Uncoupling of oxidative phosphorylation occurs via substrate oxidation, a natural leak, artificially-induced leak (2,4-DNP & FCCP) and a protein-mediated proton leak pathway (UCP) (Brand, 2000). ETC = electron transport chain; UCP1 = uncoupling protein 1; 2,4-DNP = 2,4 – dinitrophenol; FCCP = Carbonyl cyanide *p*-trifluoromethoxyphenylhydrazone. Diagram reprinted with kind permission of Dr. Audrey Carroll.

1.4 Brown Adipose Tissue and Uncoupling protein 1

BAT is found in newborn mammals incapable of shivering, hibernators, and throughout the life of rodents (Himms-Hagen, 1990). It is a highly specialised, metabolically active tissue, involved in thermoregulation via non-shivering thermogenesis (Himms-Hagen, 1990). BAT contributes to both the maintenance of body temperature in a cold environment through non-shivering thermogenesis and the control of body weight through the regulatory part of diet-induced thermogenesis (Rothwell & Stock, 1979). It has been shown that during cold acclimation, the capacity of BAT to produce heat is determined by the UCP1 content of their mitochondria (Hansen & Knudsen, 1986). Active BAT accounts for approximately 50% of heat production in non-shivering thermogenesis in the cold acclimated rat and accounts up to 1% of the body mass of a rat (Foster & Frydman, 1979; Foster 1986). Accordingly, BAT shows considerable adaptive change related to cold acclimation including dense adrenergic innervation, vast mitochondrial content (which gives BAT its brown colouring) and it is highly vascular for rapid deployment of generated heat (Néchad, 1986).

UCP1, cloned in 1985 (Bouillaud *et al.*, 1985), is thought to be exclusively expressed in the brown adipocyte (Cannon *et al.*, 1982). UCP1 is the key molecule in the thermogenic function of brown adipose tissue (BAT).

1.4.1 Structure of UCP1

UCP1 has been successfully purified from BAT mitochondria (Lin & Klingenberg, 1980). The primary structure of UCP1 has also been elucidated by N-terminal sequencing (Aquila *et al.*, 1985).

UCP1 is a 32kDa monomer of 306 amino acids (Heaton *et al.*, 1978). Its amino acid sequence is highly homologous to several ubiquitous MIM carriers including oxoglutarate, a glutamate/malate exchanger (Runswick *et al.*, 1987) and the ADP/ATP carrier (Aquila *et al.*, 1985). Among species there is high sequence homology of amino acids. Human and rat UCP1 for example are 79% identical (Klaus *et al.*, 1991). It is proposed that UCP1 contains 6 amphiphilic transmembrane α-helices with the C- and N- termini protruding into the cytosolic side of the MIM (Figure 1.4) (Klingenberg, 1990; Casteilla *et al.*, 1990). The

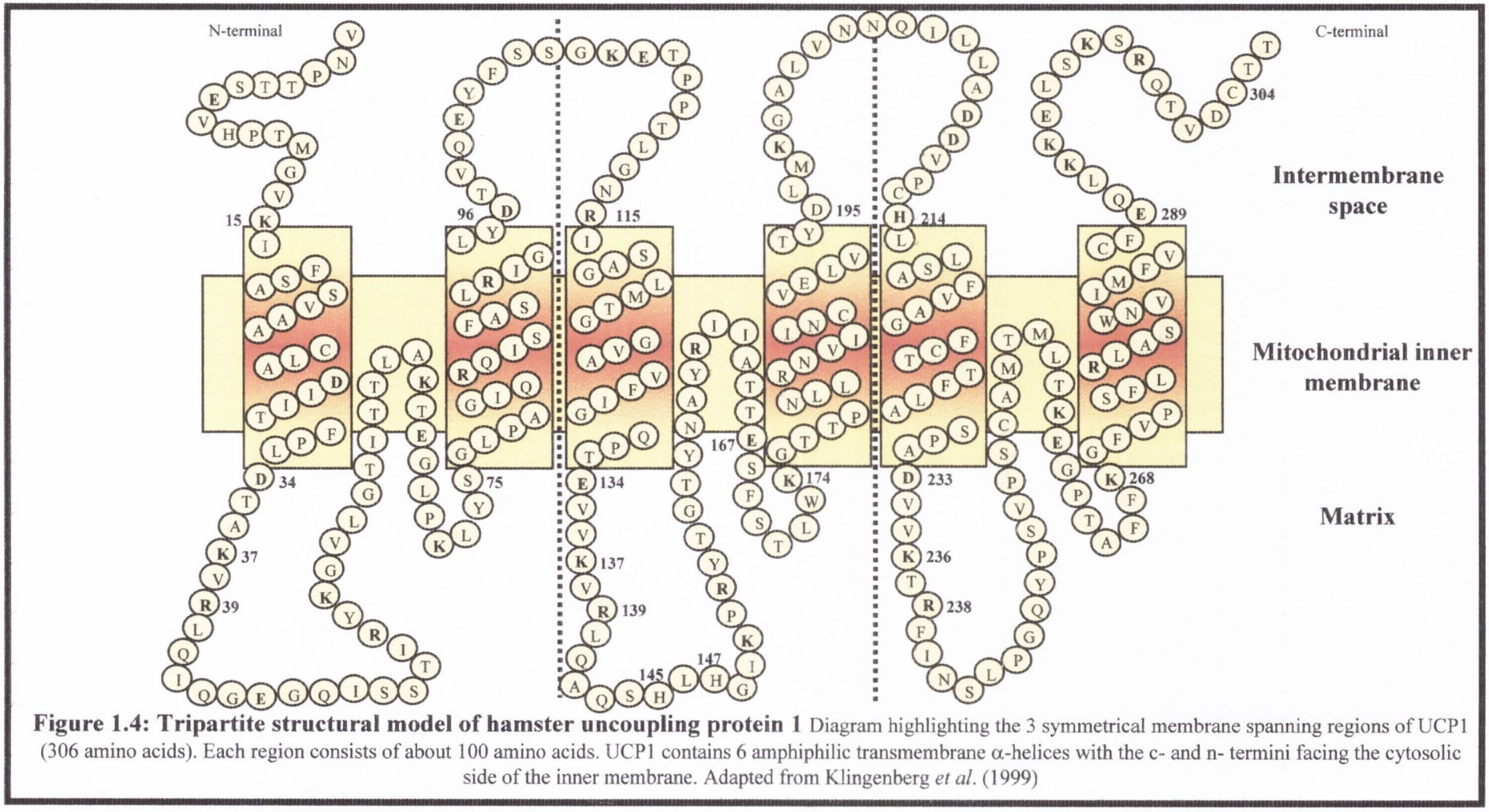


Figure 1.4: Tripartite structural model of hamster uncoupling protein 1 Diagram highlighting the 3 symmetrical membrane spanning regions of UCP1 (306 amino acids). Each region consists of about 100 amino acids. UCP1 contains 6 amphiphilic transmembrane α-helices with the c- and n- termini facing the cytosolic side of the inner membrane. Adapted from Klingenberg *et al.* (1999)

overall protein structure comprises 50 % α-helix, 30 % β- structure, 15 % β-turns and 7 % random (Nedergaard and Cannon, 1992).

1.4.2 Activation of UCP1

Noradrenaline, released from sympathetic terminals, activates BAT UCP1 in response to chronic overeating, cold exposure and β–adrenergic agonists (Ricquier *et al.*, 1986). The major adrenoreceptor mediating the effects of noradrenaline in mature BAT cells is β_3-adrenoreceptor, which is mainly expressed in white and brown adipocytes. The main role of BAT is to promote thermogenesis (*i.e.* UCP1 activation), cell division and UCP1 synthesis (Cannon *et al.*, 1996). It does this by creating a cascade of events culminating in UCP1 activation (Figure 1.5). Activation of surface β-adrenoceptors coupled via G-proteins to adenylyl cyclase leads to an increase in cyclic adenosine monophosphate (cAMP). cAMP typically activates protein kinase A (PKA) which acts to phosphorylate hormone sensitive lipase, the enzyme which hydrolyses triacylglycerol (TAG) stores releasing free fatty acids (FFA) which activate UCP1 resulting in subsequent thermogenesis. FFA also activate cAMP-response-element-binding-protein (CREB) which stimulates transcription from the UCP1 gene (Palou *et al.*, 1998). UCP1 proton transport activity is inhibited by binding of purine nucleotides (GDP, GTP, ADP, ATP) to a specific site located on the outer leaflet of UCP1 itself.

Fatty acids activate UCP1 via a mechanism which is poorly understood. There are currently two proposed models for activation of UCP1 by fatty acids.

(A) Fatty Acid Buffering Model

Firstly, the fatty acid buffering model (Figure 1.6 **(A)**) suggests protons are directly transported by UCP1 (Winkler and Klingenberg, 1994). This group propose that fatty acids act as cofactors, lining the aqueous channel of UCP1. Protons are then shuttled from one fatty acid to another until they reach the matrix. In this model fatty acids act in conjunction with proton conducting amino acids such as histidines. Indeed, in support of this theory, it has been shown that mutation of two histidine residues (His 145 and His 147) in UCP1 cause a loss of proton transport (Bienengraeber *et al.*, 1998). In this case the α-carboxyl end of the fatty acid inserts into the protein.

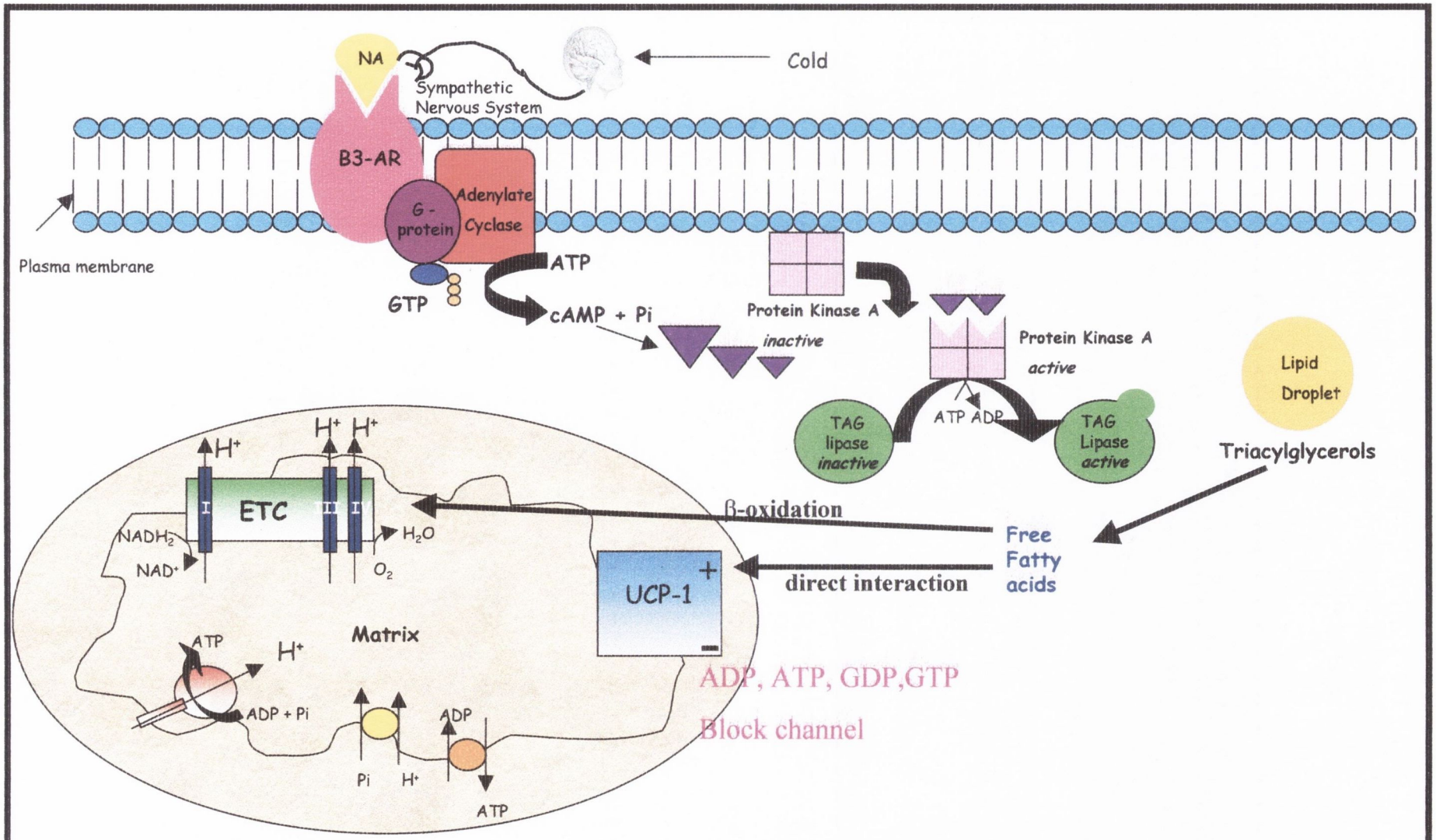


Figure 1.5: The mechanism of hormonally-induced uncoupling of oxidative phosphorylation in brown fat mitochondria. Diagram reprinted with kind permission of Dr. Audrey Carroll.

(B) Fatty Acid Protonophore Model

Secondly, fatty acids may act as cycling protonophores (Garlid *et al.*, 1996). This group has suggested that UCP1 catalyses the movement of the fatty acid anionic head group from inner to outer leaflet of the MIM (Figure 1.6 **(B)**). Transport of the anion is driven by the high, inside negative membrane potential ($\Delta\Psi$). Once the head group reaches the intermembrane space it becomes protonated and spontaneously 'flops' back to the matrix side where deprotonation occurs. The net result of the cycle is the delivery of protons with charge to the matrix. In this model UCP1 does not conduct protons at all. Rather, like all other members of the mitochondrial super-family, they transport anions. This mechanism of activation has been nicknamed the 'flip flop' theory of UCP1-mediated proton flux. In this case the ω-end of the fatty acid inserts into the protein.

Much evidence exists both supporting and contradicting the two mechanisms of activation of UCP1. The discovery that alkylsulfonates, ranging in alkyl chain length between C_{11} and C_{16}, are transported by UCP1 (Ježek and Garlid 1990; Ježek *et al.*, 1994; Garlid *et al.*, 2001) favours the fatty acid protonphore model proposed by Garlid (1996). Aikylsulfonates can be regarded as "permanent" fatty acid anion analogs, since at physiological pH they cannot pick up a proton. In addition, they are competitive inhibitors of UCP-mediated Cl^- transport (Garlid *et al.*, 2001). Ježek *et al.* (1994) attempted to derive the alkylsulfonate transport activity by measuring the competition with Cl^- uptake. Competitive suppression of the lauric acid catalyzed proton transport was demonstrated with the longer chain C_{11}-sulfonate only. A major problem with these experiments is the sensitivity towards GDP. With increasing chain length the uptake of alkylsulfonate (C_6 and C_{11}) becomes more insensitive to GDP (Ježek *et al.*, 1994). Since this model requires that the protonated acid permeate across the lipid bilayer, Ježek *et al.* (1994) tested the model by comparing the activation of UCP1 by a number of organic acids with the ability to permeate across the bilayer. These authors found that the bulky-planar structure of the benzene ring prevented the flip-flop of compounds like the phenylhexanoic acid. However, the demonstration that all *trans* retinoic acids are powerful activators of UCP1 seems to violate this hypothesis (Rial *et al.*, 1999). In addition, Rial *et al.* (2004) have now shown that alkylsulfonates, fatty acids anion analogs which cannot cross the lipid bilayer, activate UCP1 in respiring BAT mitochondria. Furthermore, Klingenberg & Huang (1999) have

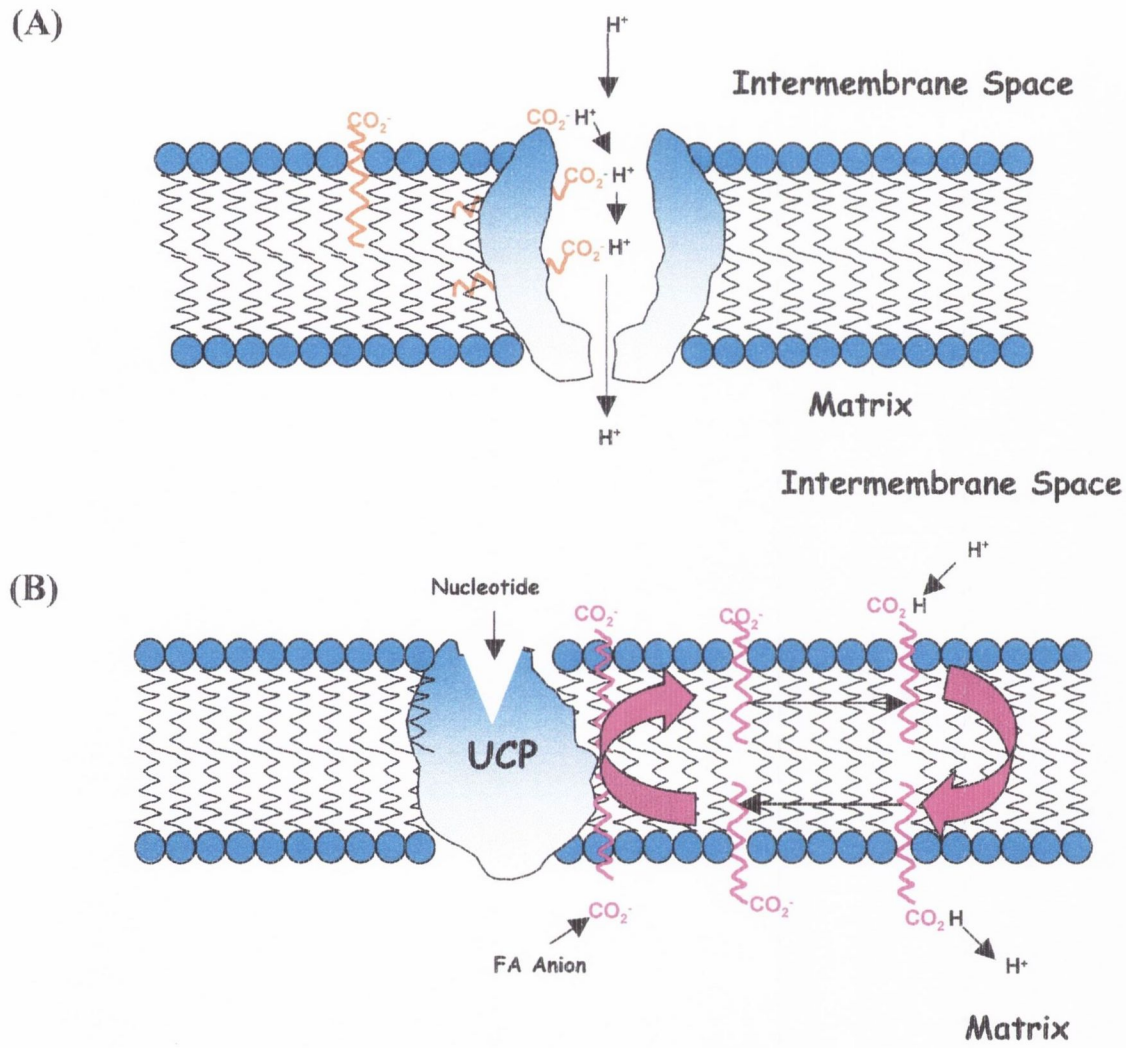


Figure 1.6: Proposed mechanisms by which free fatty-acids activate H^+ transport by UCP 1.

(A) Proton buffering model, proposed by Klingenberg, where fatty-acid carboxyl groups acting as H^+ buffers in conjunction with resident H^+ buffering amino acids in the translocation channel. **(B)** Fatty-acid protonophore model, proposed by Garlid, where fatty-acids act as cycling protonophores. Fatty-acid anions are transported out from the matrix and protonated fatty-acids return into the mitochondrial matrix by flip flop. The H^+ is then released in the mitochondrial matrix. Diagram reproduced with kind permission of Dr. Audrey Carroll.

allegedly found a fatty acid derivative, ω-glucopyranoside-o-palmitic acid that should not permeate the bilayer but does activate UCP1.

There is a lot of evidence to support the fatty acid protonophore model. As with purine nucleotide binding to UCP1 (section 1.9), one of the first striking features of the fatty acid activation of UCP1 is its pH dependency. There is a sharp increase in proton conductance over the pH range 7.0 - 8.0 (Nicholls, 1974). The pH dependency may be an indication of the involvement of an amino acid side chain in UCP1. Klingenberg & Huang, (1999) have shown that His 145 and His 147 were required for fatty acid dependent proton transport while anion transport was unaffected when these residues were mutated. Klingenberg & Huang, (1999) proposed that these residues, which are located on the matrix side of the protein, could be the final acceptors in the proton translocation chain. Biengraeber *et al.* (1998) has also reported the involvement of Asp 27 in proton but not chloride transport.

1.4.3 Expression of UCP1

UCP1 antibodies have been shown to recognise UCP1 protein in rats, hamsters, guinea pigs, rabbits and mice (Ricquier & Bouillaud, 1986). Commercial and in-house anti-UCP1 peptide antibodies have been successful in determining factors affecting the expression of UCP1 protein. Until recently, UCP1 has been exclusively associated with BAT mitochondria since immunological studies of liver, heart, epididymal white fat, parametrial white fat or thigh muscle, even from cold acclimated animals, revealed no significant quantities of UCP1 (Ricquier & Bouillaud, 1986). However, several recent studies have provided attention-grabbing results contradicting the popularly held belief that UCP1 is exclusively expressed in BAT. UCP1 mRNA was detected in the liver of newborn rats and in the liver of cold exposed adult rats (Shinohara *et al.*, 1991). A second study suggests that the β_3-adrenergic agonist, CL316243, induces a functionally active uncoupling protein in white fat and slow twitch muscle fibres (Yoshida *et al.* 1998). A study by Nibbelink *et al.* (2001) showed that UCP1 is expressed in uterine longitudinal smooth muscle cells, but this finding has since been discredited (Rousset *et al.*, 2003). More recently, in our laboratory we have generated novel, well-substantiated results illustrating the presence of UCP1 mRNA and protein in thymus mitochondria and UCP1 protein in thymus cell (thymocyte) mitochondria (Carroll *et al.*, 2005). UCP1 expression

was established using a commercially available (Calbiochem), polyclonal anti-UCP1 antibody. Specificity of the UCP1 antibody, over UCP2 and UCP3, was established prior to use and sequence analysis studies on a purified sample of thymus mitochondria unequivocally revealed the occurrence of UCP1 (Carroll *et al.*, 2005).

It has been shown that cold acclimation induces an increase in UCP1 protein expression in BAT mitochondria isolated from rats (Desautels *et al.*, 1978; Heaton *et al.*, 1978; Swick & Swick, 1986; Sundin *et al.*, 1987; Klaus *et al*, 1991; Nicholls & Rial, 1999; Nedergaard *et al.*, 2001a). In contrast, starvation has been shown to decrease UCP1 protein expression in BAT mitochondria (Rothwell *et al.*, 1984; Trayhurn and Jennings, 1988; Boss *et al.*, 1998b; Nedergaard *et al.*, 2001a). In addition, certain dietary regimes such as cafeteria diets, high-fat diets and high-sucrose diets have been shown to increase UCP1 protein content in BAT (Himms-Hagen, 1986; Nedergaard *et al.*, 2001a).

1.5 Uncoupling protein homologues

Since the discovery of UCP1 in the mid 1970s, other mitochondrial uncoupling proteins have been discovered which occur in many different tissues in both humans and rodents (Fleury *et al.*, 1997; Boss *et al.*, 1997; Vidal-Puig *et al.*, 1997; Gong *et al.*, 1997). These newly discovered UCPs share high sequence homology with UCP1 and with the MIM carrier proteins (Table 1.1)

Table 1.1: Summary of structure, function and location of the three principal uncoupling proteins

	Structure	Location	Function
UCP1	32kDa protein 306 amino acids	Brown adipose tissue Thymus	Heat production Unknown
UCP2	30kDa protein 309 amino acids	Macrophages, Spleen, Gut, Lung, WAT, Pancreatic islets, Thymus, Thymocytes, Kidney	Unclear
UCP3	34kDa protein 312 amino acids	Skeletal muscle BAT of rodents Spleen Thymus	Unclear

1.5.1 Uncoupling Protein 2

Screening of a skeletal muscle library using UCP1 cDNA as a probe led to the discovery of Uncoupling Protein 2 (UCP2) (Fleury *et al.*, 1997). Further analysis indicated that this novel UCP2 shared 59 % sequence homology with UCP1 (in rats) and had an approximate molecular mass of 30 kDa (Fleury *et al.*, 1997). Northern blot analysis from mouse, rat and human tissues showed widespread expression of UCP2 mRNA in a number of tissues including, white adipose tissue, BAT, skeletal muscle, heart, placenta, brain, stomach, kidney, lung, female reproductive tract, myocytes, lymphocytes, macrophages and the Kupffer cells of liver (Fleury *et al.*, 1997; Gimeno *et al.*, 1997; Larrouy *et al.*, 1997; Nègre-Salvayre *et al.*, 1997; Gong *et al.*, 1997; Boss *et al.*, 1998a; Hodný *et al.*, 1998; Ricquier & Bouillaud, 2000; Pecqueur *et al.*, 2001; Pedraza *et al.*, 2001; Krauss *et al.*, 2002; Horvath *et al.*, 2003; Rousset *et al.*, 2003). Conversely, UCP2 protein is only found in mouse and rat spleen, lung, stomach, kidney, thymus, WAT, pancreatic islets, macrophages and thymocytes (Ricquier & Bouillaud, 2000; Echtay and Brand, 2001; Pecqueur *et al.*, 2001; Zhang *et al.*, 2001; Krauss *et al.*, 2002; Medvedev *et al.*, 2002).

Several different physiological states have been shown to increase UCP2 mRNA levels in rodents. These include cold exposure (Boss *et al.*, 1997b), 48 hours starvation (Boss *et al.*, 1997b) and leptin administration (Zhou *et al.*, 1997). Lipopolysaccharide (LPS) and starvation has been shown to increase UCP 2 protein expression in lung and stomach (Pecqueur *et al.*, 2001).

1.5.2 Uncoupling Protein 3

While searching for UCP1 homologues in skeletal muscle a third UCP was discovered. Uncoupling Protein 3 (UCP3), a mitochondrial inner membrane protein, was molecularly cloned initially by Boss *et al.* (1997) and shortly thereafter by Vidal-Puig *et al.* (1997) and Gong *et al.* (1997). Their studies indicated that, unlike UCP1 and UCP2, UCP3 exists as two isoforms in humans, a long form ($UCP3_L$) and a short form ($UCP3_S$). The long form consists of 312 amino acid residues, while the short form consists of 275. Like other mitochondrial carriers, UCP3 exists with six transmembrane domains (Boss *et al.*, 1997). $UCP3_S$ lacks the sixth potential trans-membrane region and putative nucleotide binding site implicated in control of coupling efficiency of UCP1. Therefore $UCP3_S$ exerts its biological function without control by purine nucleotides.

Human UCP3 (hUCP3) has a 71 % identical amino acid sequence homology to hUCP2, and 57 % identical sequence homology to hUCP1 (Vidal-Puig *et al.*, 1997) but is much less homologous to other members of the mitochondrial carrier super-family *e.g.* oxoglutarate carrier (~32 % identical) and phosphate carrier (~25 % identical). Based on this high sequence homology with UCP1, it would seem likely that UCP3 uncouples mitochondrial respiration also. Indeed, UCP3 like UCP1 was shown to decrease mitochondrial membrane potential when expressed in yeast and C_2C_{12} myocytes (Gong *et al.*, 1997; Boss *et al*, 1998a ; Zhang *et al.*, 1999). Therefore, it was suggested that UCP3 had some ability to uncouple mitochondria. However, Bienengraeber *et al.* (1998) observed that UCP3 lacked one of the histidine residues vital for proton transport in UCP1 (assuming the 'flip flop' theory presented by Klingenberg is correct). Two possibilities presented themselves, either UCP3 does not transport protons or the mechanism of proton transport differs from that used by UCP1.

UCP3 mRNA is expressed in skeletal muscle of humans (Vidal-Puig *et al.*, 1997). Rodents express UCP3 in skeletal muscle, BAT, spleen and thymus (Gong *et al.*, 1997; Carroll and Porter, 2004). UCP3 mRNA is most abundantly expressed in BAT, and to a lower extent in *tensor fascia latae* (fast- twitch; glycolytic), *tibialis anterior* (fast-twitch; oxidative/glycolytic), *gastrocnemius* (mixed) and less in *soleus* (slow-twitch; oxidative) of rodents, suggesting that UCP3 is expressed more in glycolytic than in oxidative skeletal muscles (Boss *et al.*, 1997a; Vidal-Puig *et al.*, 1997; Cadenas *et al.*, 1999; Giacobino, 1999; Pedraza *et al.*, 2001). UCP 3 protein has been detected in mouse and rat skeletal muscle (Ježek *et al.*, 1999; Gong *et al.*, 2000; Li *et al.*, 2000; Zhou *et al.*, 2000; Vidal-Puig *et al.*, 2000; Cadenas *et al.*, 2002; Harper *et al.*, 2002; Cunningham *et al.*, 2003; Hesselink *et al.*, 2003), BAT mitochondria (Ježek *et al.*, 1999; Gong *et al.*, 2000; Li *et al.*, 2000; Harper *et al.*, 2002; Cunningham *et al.*, 2003) and rat spleen and thymus mitochondria (Carroll and Porter, 2004). The expression of UCP3 in two such thermogenic tissues as skeletal muscle and BAT, and its relative lack of expression in other tissues such as heart (Boss *et al.*, 1997), are consistent with a possible role for UCP3 as a mediator of adaptive thermogenesis. However, it must be pointed out that despite speculation, the biological function of UCP3 is not known.

UCP3 expression is regulated by known stimuli such as thyroid hormone, β_3-adrenergic agonists, starvation, leptin administration and exercise. Thyroid hormone (T3) stimulates increased UCP3 mRNA expression in rat skeletal muscle (Lanni *et al.*, 2003; Schrauwen and Hesselink, 2003; Queiroz *et al.*, 2004; Silvestri *et al.*, 2005). In addition, UCP3 protein expression is increased in skeletal muscle from hyperthyroid rats compared to euthyroid controls (Cunningham *et al.*, 2003). Hypothyroidism in rat skeletal muscle decreased UCP3 mRNA expression. β-adrenergic stimulation of adipose cells causes lipolysis and thermogenesis (Gong *et al.*, 1997). This is mediated largely by β_3-adrenergic receptors (Collins *et al.*, 1994). The selective β_3-adrenergic agonist CL214613 was shown to increase rat UCP3 mRNA levels in white adipose tissue (WAT) but not in BAT (Gong *et al.*, 1997). In addition, β-adrenergic stimulation of L6 myotubes (skeletal muscle cell line) with adrenaline was shown to increase UCP3 mRNA levels transiently (Nagase *et al.*, 2001). Starvation has been shown to increase UCP3 protein expression levels in mouse and rat skeletal muscle mitochondria (Boss *et al.*, 1998a; Cadenas *et al.*, 1999; Sivitz *et al.*, 1999; Moreno *et al.*, 2003). In addition, starvation was shown to increase UCP3 protein expression in thymus and spleen (lymphocyte) mitochondria (Carroll and Porter, 2004). Elevation of free fatty acids by lipid infusion, proposed as a starvation imitating condition, also increases UCP3 gene expression in vivo (Weigle *et al.*, 1998) and in vitro (Hwang and Lane, 1999) in C_2C_{12} cells. High-fat diets increased UCP3 protein expression by approximately 40 %, compared to low fat diets in skeletal muscle mitochondria (Hesselink *et al.*, 2003). Refeeding on a high fat diet resulted in a 2-fold increase in UCP3 protein expression (Crescenzo *et al.*, 2003). Leptin administration increases UCP3 mRNA in skeletal muscle and BAT of genetically obese (ob/ob) mice (lack functional leptin) (Gong *et al.*, 1997). Previous studies have indicated that acute exercise induces large increases in UCP3 in skeletal muscle (Tsuboyama *et al.*, 1998; Zhou *et al.*, 2000; Pilegaard *et al.*, 2000; Schrauwen *et al.*, 2002), whereas endurance training results in marked decreases in skeletal muscle UCP3 (Boss *et al.*, 1998b; Schrauwen *et al.*, 1999 & 2002; Fernström *et al.*, 2003). These divergent changes in UCP3 expression occur at both protein and mRNA levels. Studies on the effect of cold exposure, which increases UCP1 in BAT, had no effect on UCP3 mRNA expression in skeletal muscle in rats (Larkin *et al.*, 1997). However, cold exposure did result in an increase in UCP3 protein expression in rat skeletal muscle (Simonyan *et al.*, 2001; Cunningham *et al.*, 2003). UCP3 deficient mice were shown to have a reduced thermogenic response to the drug MDMA (3,4-

methylenedioxymethamphetamine; ecstasy) and were therefore protected against the dangerously toxic effect of this drug (Mills *et al.*, 2003).

1.5.3 Uncoupling protein 4

More recently, a fourth UCP (UCP4) has been identified (Mao *et al.*, 1999). UCP4 is a 36 kDa protein of 323 amino acids. UCP4 is 29 %, 33 % and 34 % homologous to UCP1, UCP2 and UCP3 respectively. UCP4 transcripts are exclusively expressed in both fetal and adult brain tissues.

1.5.4 Uncoupling protein 5

A fifth novel brain mitochondrial carrier protein exhibiting mitochondrial uncoupling activity was cloned when expressed in yeast (Sanchis *et al.*, 1998). UCP5 is also termed brain-specific mitochondrial carrier protein or BMCP-1. UCP5 mRNA expression is widespread in the brain, with some expression in testis, heart, kidney, and uterus (Yu *et al.*, 2000). UCP5 isoforms have been discovered; a short form ($UCP5_S$), a short form with insert ($UCP5_{SI}$), and a long form ($UCP5_L$).

1.5.5 Plant Uncoupling Proteins

Other members of the uncoupling protein family have been found in plants including *Solanum tuberosum* uncoupling protein (StUCP) in potatoes (Laloi *et al.*, 1997). Vercesi *et al.* (1995) discovered a plant uncoupling protein (PUMP) in potato tubers. cDNAs of a UCP homologue present in *Arabidopsis thaliana* were also cloned and referred to as AtUCP or AtPUMP (Maia *et al.*, 1998). Costa *et al.* (1999) identified PUMP in tomatoes. Interestingly, using antibodies against plant UCP, Jarmuszkiewicz *et al.* (1999) detected a mitochondrial uncoupling protein in the non-photosynthetic soil amoeboid protozoan *Acanthamoeba catellanii.* Similarly, Jarmuszkiewicz *et al.* (2000) identified an uncoupling protein in mitochondria from *Candida parapsilosis* (CpUCP), a non-fermentative parasitic yeast. Recently, a new protein named avUCP, which shares a 70 % amino acid identity with both UCP2 and UCP3, was identified in chicken skeletal muscle (Raimbult *et al.*, 2001).

Despite the existence of several UCP homologues, the study presented here only sought to investigate the expression and physiological function of UCP1 and UCP3.

1.6 Metabolic Adaptation to Training

Both physical and biochemical adaptations occur as a result of performing repeated bouts of exercise over several weeks or months (Maughan *et al.*, 1997). Endurance exercise in particular induces adaptations that significantly improve functional capacities related to oxygen delivery, uptake and use. These adaptations are summarised in table 1.2. The adaptations most relevant to the outcome of this study include, an increase in the size and number of mitochondria (Holloszy and Coyle, 1984; Murakami *et al.*, 1994) and an increase in the capacity of the mitochondrion to generate ATP by oxidative phosphorylation (Maughan *et al.*, 1997).

1.6.1 Muscle Mitochondrial Density

An important metabolic adaptation to endurance training is an increase in mitochondrial density (Schrauwen *et al.*, 1999). Mitochondrial density in skeletal muscle increases after endurance training in rats (Murakami *et al.*, 1994; Gollnick and King, 1969). Using electron microscopic studies increases in both the size and number of mitochondria have been observed (Gollnick and King, 1969). Detailed studies of the enzymatic adaptations of the different skeletal muscle fibre types in rodents have provided some insights regarding the plasticity of mitochondrial composition (Holloszy and Coyle, 1984). In the rat, the levels of the majority of the mitochondrial enzymes are twice as high in the fast twitch red fibres as in the slow twitch red fibres, and 4-8 times as high in the fast twitch red fibres as in the fast twitch white fibres (Holloszy and Coyle, 1984). As UCP3 is found in the MIM a correction factor for changes in mitochondrial density is required as it is important to establish whether UCP3 expression is dependent or independent of mitochondrial abundance.

Citrate synthase is a key enzyme in the mitochondrial tricarboxylic acid cycle and its activity is routinely used as a marker for mitochondria (Murakami *et al.*, 1994). Treadmill run training (12 weeks) has been shown to increase citrate synthase enzyme activities in rat soleus by 47 % (Murakami *et al.*, 1994). Increases in citrate synthase activity have also been observed in *tibialis anterior* (39 %) and *plantaris* (31 %) muscles after 4 weeks of treadmill running (Boss *et al.*, 1998b). This suggests that increases in mitochondrial enzyme activities are due to an increase in mitochondrial enzyme proteins.

Skeletal Muscle Adaptations to Endurance Training
Selective hypertrophy of Type 1 fibres.
Increased number of blood capillaries per muscle fibre.
Increased myoglobin content.
Increased capacity of mitochondria to generate ATP by oxidative phosphorylation.
Increased size and number of mitochondria.
Increased capacity to oxidise lipid and carbohydrate.
Increased reliance on lipids as fuel.
Higher glycogen and triglyceride content.
Increased endurance capacity.

Table 1.2 Summary of the adaptations of skeletal muscle to endurance training

[1.7] UCPs and reactive oxygen species

Transfer of electrons to oxygen in electron transport by cytochrome oxidase occurs one electron at a time. However, upstream of Complex IV in Complex III and Complex I electron transfer is rarely 100% complete, generating incompletely reduced oxygen species. These oxygen species include superoxide, hydrogen peroxide (H_2O_2) and the hydroxyl radical. In addition some enzymes, such as monoamine oxidase and amino acid oxidase, generate H_2O_2 directly. Superoxide, H_2O_2, and hydroxyl radical are more reactive than oxygen, so they are referred to collectively as reactive oxygen species (ROS). Large-scale production of ROS has the potential to inflict considerable damage on the tissues in which they are produced.

Excluding phagocytosis, the majority of ROS are generated by the mitochondrial electron transport chain (Boss *et al.*, 2000). Using isolated mitochondria it has been shown that production of ROS is greatly increased at times when the proton electrochemical gradient is high. Such conditions occur during state 4 respiration in isolated mitochondria when ADP is unavailable. Addition of ADP, which causes proton transport via ATP synthase and consequently decreases electrochemical gradient, or an uncoupling agent, which directly decreases the electrochemical gradient, strongly suppresses superoxide anion formation (Skulachev, 1998). It has been suggested that under conditions which induce increased ROS production, such as cold exposure (Kaushik and Kaur, 2003; Venditti *et al.*,

2004) and endurance exercise (Du *et al.*, 1998; Bejma and Ji, 1999), UCP2 and UCP3 may function as 'mild' uncouplers of oxidative phosphorylation in order to relieve oxidative stress (Skulachev, 1996). To date, there is a limited amount of evidence exists supporting the possibility that UCP2 and UCP3 function to limit ROS production via 'mild' uncoupling. Firstly, UCP3 protein expression has been shown to increase following 8-weeks cold exposure (Cunningham *et al.*, 2003). Secondly, it has previously been shown that the absence of UCP3 led to an increase in ROS production, thereby, implying a role for UCP3 in preventing the formation of ROS in skeletal muscle (Vidal-Puig *et al.*, 2000). Thirdly, superoxide generated using xanthine and xanthine oxidase has been shown to increase proton transport through UCP1, UCP2 and UCP3 in a reaction that is inhibited by nucleotides including GDP (Echtay *et al.*, 2002b). Fourthly, Nègre-Salvayre *et al.* (1997) showed that membrane potential and hydrogen peroxide (H_2O_2) production were increased in mitochondrial fractions isolated from UCP2 containing tissues (BAT, thymus and spleen) when pre-incubated in GDP leading the authors to suggest that their results may indicate that UCP2 acts as a regulator of H_2O_2 production in mitochondria. Finally, it has been shown that the GDP sensitive proton conductance catalysed by UCPs increases on exposure to superoxide (Echtay *et al.*, 2002), or to lipid peroxidation breakdown products such as 4-hydroxy-2-*trans*-nonenal (HNE) (Echtay *et al.*, 2003). These findings support the hypothesis that UCPs may function to limit ROS production.

[1.8] Effects of fatty acids and purine nucleotides on UCP function

BAT UCP1 uncoupling of oxidative phosphorylation is inhibited by purine nucleotides and activated by nanomolar amounts of free fatty acids and by long chain fatty-acyl CoA esters in isolated mitochondria (Nicholls & Rial, 1974). We have recently established that UCP1 transcript and protein is present in thymus mitochondria isolated from room temperature rats (Carroll *et al.*, 2005). We have been able to show that a proportion of the state 4 oxygen consumption by thymus mitochondria isolated from rats housed at room temperature is GDP sensitive and fatty acid activatable in a manner similar to BAT mitochondria (Carroll *et al.*, 2005). Medium to long chain fatty acids induce the uncoupling activity of UCP1 in BAT mitochondria (Klingenberg & Huang, 1999). Fatty acids such as palmitic, oleic and linoleic fatty acids are good activators of UCP1 induced proton transport (Klingenberg & Echtay, 2001). Although the inhibition by nucleotides is well established, the mechanism by which fatty acids activate UCP1 remains controversial

(See Sections 1.4.2 A&B). Experimentally, the fact that uncoupling of UCP1 can be activated by fatty acids and inhibited by purine nucleotides allows a distinction to be made between the UCP1 proton conductance pathway and other pathways of mitochondrial proton conductance. This purine nucleotide inhibition and fatty acid activation of UCP1 activity in BAT mitochondria has become an interesting model for the study of UCP2 and UCP3.

To investigate whether fatty acids activate the function of UCP2 and UCP3, in a similar manner to UCP1, it is necessary to assume that UCP2 and UCP3 are natural uncouplers. There are several lines of evidence to support the hypothesis that UCP2 and UCP3 are natural uncouplers. As stated earlier, UCP2 and UCP3 are 59 % and 57 % homologous to UCP1 respectively and 71 % identical to each other (Lowell, 1999). UCP2 and UCP3 are much less homologous to other members of the mitochondrial carrier super-family (Lowell, 1999). Based upon the high homology of UCP2 and UCP3 with UCP1, compared to its lower homology with other members of the mitochondrial carrier family, it is predicted that UCP2 and UCP3 share biochemical functions with UCP1, including uncoupling activity. The UCP3 gene is found adjacent to that for UCP2 on chromosome 7 in mice and on chromosome 11 in humans (Boss *et al.*, 1997; Fleury *et al.*, 1997; Vidal-Puig *et al.*, 1997). These chromosomes have been linked to hyperinsulinemia and obesity, and it is hypothesized that UCP2 and UCP3 are the peripheral target for energy dissipation in the regulation of body weight (Boss *et al.*, 1997; Fleury *et al.*, 1997; Vidal-Puig *et al.*, 1997). Most of the evidence to date that shows UCP2 and UCP3 are uncoupling proteins came from studies using heterologous yeast expression systems, UCPs reconstituted into proteliposomes, transgenic overexpression systems and gene knock-out studies.

[1.8.1] Heterologous yeast expression systems

Heterologous yeast and mammalian cell expression systems have been used most often in the direct study of the UCP1 homologues. Expression of UCP2 and UCP3 in *Saccharomyces cerevisiae* appears to confirm their uncoupling activities: membrane potential is lowered and state 4 oxygen consumption rates are increased (Echtay *et al.*, 1999; Giacobino, 1999; Hagen *et al.*, 1999; Hinz *et al.*, 1999a & 1999b; Jabůrek *et al.*, 1999). Measurements of mitochondrial State 4 respiration, *i.e.* respiration in the absence of ADP, which is primarily due to proton leak, shows a 50 % increase in mitochondria from

yeast expressing UCP2, compared with that of the control (Fleury *et al.*, 1997). Similarly, UCP3 has been shown to increase whole yeast basal oxygen consumption (Hinz *et al.*, 1999a; Zhang *et al.*, 1999). The increase in whole yeast basal oxygen consumption with UCP3 was even greater than that observed for UCP1 (Zhang *et al.*, 1999). In isolated mitochondria, however, the increase in State 4 respiration with UCP3 (35 %) was small compared to the increase with UCP1 (100 %). However, the increase in state 4 respiration of yeast mitochondria expressing UCP2 and UCP3 was insensitive to 1 mM purine nucleoside di- and tri-phosphates (Hagen *et al.*, 1999; Rial *et al.*, 1999; Zhang *et al.*, 1999; Hagen and Lowell, 2000). These observations suggest that UCP2 and UCP3 exist in a deranged confirmation and do not obtain native function in yeast expression systems (Hinz *et al.*, 1999a; Heidkaemper *et al.*, 2000; Klingenberg & Echtay, 2001; Harper *et al.*, 2002). Other principal concerns with over-expressing a heterologous protein in yeast have been noted in the literature (Stuart *et al.*, 2001). Firstly, the fact that in many of the studies, the heterologous expression of UCP3 in yeast results in a decrease in the fully uncoupled respiration rate attained by FCCP (artificial uncoupler). Rial *et al.* (1999), has previously shown that retinoic acid increases proton transport in yeast mitochondria expressing UCP2. Interestingly, Couplan *et al.* (2002), has shown a lack of sensitivity of UCP2 to retinoic acid, a fatty acid known to activate UCP1, in isolated spleen mitochondria. Additionally, Hagen and Lowell (2000), showed, using heterologous expression systems, that UCP1 was strongly activated by free fatty acids whereas no stimulatory effect on $UCP3_L$ was observed.

[1.8.2] UCPs reconstituted in liposomes

An alternative approach taken to study function and regulation of UCP2 and UCP3 has been to reconstitute these proteins into liposomes after expression in *Escherichia coli* (Jabůrek *et al.*, 1999; Echtay *et al.*, 1999, 2000 & 2001; Jabůrek and Garlid, 2003). It was shown that liposomes, like UCP1, UCP2 and UCP3, catalyze electrophoretic H^+ flux, which requires the presence of free fatty acids. Jabůrek *et al.* (1999), reconstituted the transport activity of human UCP2 and UCP3 purified from recombinant bacteria into liposomes and observed that the two proteins catalysed an electrophoretic flux of protons, similar to UCP1. Jabůrek *et al.* (1999) also reported that fatty acids were obligatory for the proton transport activity of UCP2 and UCP3, again similar to UCP1. These findings led the authors to conclude that UCP2 and UCP3 are true uncoupling proteins. Echtay *et al.* (1999)

also reported the reconstitution of the chloride transport activity of UCP3 and observed an inhibition by purine nucleotides, as with UCP1. More recently, Echtay *et al.* (2000 & 2001) have shown that coenzyme Q (CoQ) is an obligatory cofactor for H^+ transport by *Escherichia coli* expressed UCP1, 2 and 3. On the contrary, Jabůrek and Garlid (2003) have demonstrated that CoQ is not a pre-requisite for uncoupling function in expressed reconstituted UCP1, 2 and 3 (Jabůrek and Garlid, 2003).

[1.8.3] Transgenic over-expression and gene knockout studies

Transgenic mice over-expressing uncoupling proteins and uncoupling protein knock-out (KO) models have been produced as a direct approach to investigate the physiological function of UCPs. Matthias *et al.* (1999) and Monemdjou *et al.* (1999) studied the bioenergetics of BAT mitochondria from UCP1 ablated mice. Interestingly, they found that UCP2 mRNA levels are increased up to 14-fold in the BAT of these mice. BAT mitochondria isolated from UCP1 ablated mice are innately energized as shown by a high membrane potential and a low respiration rate. The UCP1 ablated mice are highly cold intolerant, and this suggests that the heat production lost by UCP1 ablation is not compensated for by other UCPs. Or to put it another way, neither UCP2 nor UCP3 have replaced the proton conductance or thermogenic capacity lost by UCP1-ablation in these mice (Matthias *et al.*, 1999; Nedergaard *et al.*, 2001a & 2001b).

Transgenic mice that over-express human UCP3 in skeletal muscle (UCP3tg mice) have been produced by Clapham *et al.* (2000). Total UCP3 mRNA expression was increased 66-fold in skeletal muscle with little or no expression in other tissues. Despite an increase in food intake, UCP3tg mice weighed less than controls. Skeletal muscle mitochondria isolated from transgenic mice that over-express human UCP3 displayed a 2-3-fold increase in proton conductance, compared to control mice (Cadenas *et al.*, 2000). These results are all consistent with a role of UCP3 in energy expenditure.

More compelling evidence suggesting that UCP3 is an uncoupling protein came from two studies using UCP3 KO mice. Gong *et al.*, (2000), showed that UCP3 KO are not obese and have a phenotype similar to control mice. Therefore, the lack of UCP3 is not associated with obesity. Gong *et al.* (2000) also showed that the proton leak is reduced in skeletal muscle mitochondria isolated from UCP3 KO mice, thus suggesting that UCP3

accounts for some of the proton leak in skeletal muscle. Similar results were found by Vidal-Puig *et al.* (2000), who showed that skeletal muscle mitochondria isolated from UCP3 KO mice are more coupled, as measured by a respiratory control ratio. These results suggest that the mere presence of UCP3 leads to uncoupling activity. Both Gong *et al.* (2000) and Vidal-Puig *et al.* (2000) showed that mitochondria lacking UCP3 showed an increased production of reactive oxygen species (ROS) as determined by measurement of superoxide and aconitase activity. It has previously been shown that mitochondrial membrane potential regulates the generation of ROS (Papa *et al.*, 1997). Thus, a partial uncoupling and its associated decrease in membrane potential could lead to a decreased superoxide production. These results support a role for UCP3 in preventing excessive oxidative damage in skeletal muscle.

Additionally, it has been shown that UCP2 acts as an uncoupling protein in macrophages and pancreatic β-cells, thereby postulating a role for UCP2 as an uncoupler *in vivo* (Couplan *et al.*, 2002). It has been shown that UCP2 is expressed in pancreatic β-cells (Shimabukuro *et al.*, 1997; Zhou *et al.*, 1997; Chan *et al.*, 1999), raising the possibility that UCP2 might influence insulin secretion by regulating the amount of ATP derived from metabolised glucose (Boss *et al.*, 1998c). In support of this view, it was observed that adenovirally mediated expression of UCP2 in pancreatic islets markedly reduced insulin secretion in response to glucose by isolated islets (Chan *et al.*, 1999). Krauss *et al.*, (2002), showed that proton leak activity was lower in thymocytes from UCP2-deficient mice compared to wild-type and that fatty acid analogues (*i.e.* retinoic acid) activated the proton leak in thymocytes isolated from wild-type mice. UCP2 knock-out mice display greater macrophage phagocytic activity and subsequent free radical production (Bai *et al.*, 2005). In addition, this group have recently shown that persistent NF-kappa B activation in UCP2 knock-out mice leads to increased nitric oxide and inflammatory cytokine production suggesting that mitochondrially derived ROS from UCP2 knock-out mice constituitively activates NF-kappa B, resulting in a 'primed' state which both potentiates and amplifies the inflammatory response upon subsequent stimulation.

While data from genetically manipulated systems support an uncoupling function for the UCP1 homologues, experiments on animal models that have been physiologically perturbed do not.

[1.8.4] Evidence against UCP2 and UCP3 being uncoupling proteins arising from physiologically perturbed natural models

Cadenas *et al.* (1999) have shown a 2-fold increase in UCP3 protein expression levels in skeletal muscle mitochondria upon starvation. Despite this increase, the mitochondrial proton conductance in skeletal muscle mitochondria remains unchanged (Cadenas *et al.*, 1999). Similarly, in mice, starvation induced a 3.5-fold increase in soleus UCP3 mRNA expression but it did not increase soleus muscle heat production *in vivo* (Boss *et al.*, 1998a). Cresenzo *et al.* (2003), have shown that re-feeding on a high-fat diet, which exacerbates the suppression of thermogenesis, resulted in a 2-fold elevation in UCP3 protein but no change in state 4 or state 3 respiration. Taken together, these results show an increase in UCP3 mRNA and protein expression but show no change in proton conductance, thereby implying that UCP3 is not an uncoupling protein. Similarly, Jekabsons *et al.* (1999) showed that despite altered UCP2 and UCP3 mRNA expression, non-phosphorylating respiration of skeletal muscle mitochondria is unchanged. Again, these results cast doubts on the involvement of UCP2 and UCP3 in physiological uncoupling.

[1.8.5] Evidence against UCP2 and UCP3 being uncoupling proteins arising from site-directed mutagenesis studies

Site-directed mutagenesis studies have provided evidence disputing the ability of UCP2 and UCP3 to uncouple. In association with the proton buffering model, Bienengraeber *et al.* (1998), has shown that mutation of two histidine residues in UCP1 cause loss of proton transport. The authors' interpretation of this result is that His^{145} and His^{147} comprise part of the proton-conductance pathway in UCP1. As UCP2 contains neither histidine, these authors conclude that UCP2 does not conduct protons. Additionally, as UCP3 contains only one histidine, these authors imply that UCP3 conducts protons only weakly. This may imply a reason why UCP2 and UCP3 cannot conduct protons *in vitro*. Additionally, these two histidine residues were predicted to be located in the second matrix loop of UCP1. Interestingly, a study using chimeric proteins by Hagen & Lowell, (2000), has shown that activation of UCP1 by free fatty acids is mediated by the second repeated domain, since substitution of the second repeat of UCP1 by the equivalent repeat of UCP3 abolishes fatty-acid activation. In contrast, replacing the second repeat domain of UCP3 by the corresponding repeated domain of UCP1 results in fatty acid activation similar to wild-

type UCP1. Taken together, these results indicate that UCP1 and UCP3 are regulated differently and furthermore indicate that sequence difference between UCP1 and UCP3 may result in the lack of fatty acid activation observed in skeletal muscle mitochondria known to contain UCP3. Correspondingly, Nedergaard *et al.* (2001b) identified two very specific sequences, 144SHLHGIKP and the C-terminal sequence RQTVDC(A/T)T conserved solely to UCP1 and not to UCP2 and UCP3. These authors further show that the sequence 144SHLHGIKP, which is probably located on the matrix side of the membrane includes the two histidine residues (His^{145} and His^{147}) previously found to be necessary for UCP1 proton transport but which are not conserved fully in UCP2 and UCP3 (Bienengraeber *et al.*, 1998). Nedergaard *et al.* (2001b), also postulates that these two sequences may therefore be essential for the unique thermogenic function of UCP1 and thus the absence of these sequences in UCP2 and UCP3 may therefore imply a lack of thermogenic function in UCP2 and UCP3.

[1.9] Purine nucleotide binding to UCPs

The binding site for the purine nucleotides was discovered using photo-affinity labelling of BAT mitochondrial membranes with radioactive 8-azido-ATP (Heaton *et al.*, 1978). Nucleotides bind only from the cytosolic side of UCP1 to a high affinity binding site which is independent of the ADP/ATP carrier (Heaton *et al.*, 1978). UCP1 accepts with strong preference the purine ribose di- and tri-nucleotides: GDP, GTP, ATP and ADP, whereas the monophosphates GMP and AMP are poor ligands (Klingenberg, 1988). UCP1 only accepts the free forms of nucleotides, not the Mg^{2+} complexes (Klingenberg, 1988; Huang & Klingenberg, 1995a). UCP1 is predicted to behave as a dimer in the mitochondrial inner membrane (Klingenberg, 1984). Furthermore, it has been shown that only one nucleotide binds per UCP1 dimer (Klingenberg & Huang, 1999). Due to the presence of UCP1, functioning BAT mitochondria are able to adapt to their thermogenic capacity in response to both environmental temperature and dietary signals (Peachey *et al.*, 1988). Rafeal and Heldt, (1976), found that purine nucleotide binding capacity varied with the thermogenic capacity of BAT. Radiolabeled and fluorescent-labelled purine nucleotide binding assays are the most sensitive and specific methods for determining the presence of UCP1 (Milner *et al.*, 1988). The specific binding of radiolabelled GDP has been used extensively as an indication of the thermogenic capacity of BAT (Sundin & Cannon; 1980;

Nedergaard & Cannon, 1985; Sundin *et al.*, 1987). One of the most remarkable features of nucleotide binding to UCP1 is its strong pH dependence (Klingenberg & Huang, 1999). The affinity for purine and pyrimidine nucleotides decreases upon increasing pH, notably above 7.2 (Klingenberg & Huang, 1999). The kinetics of nucleotide binding to UCP1 from BAT mitochondria, previously determined by Huang *et al.* (1998), shows fast and slow phases of binding to UCP1.

It has been observed in some laboratories that the binding capacity of UCP1 varied with short-term changes of temperature (Nedergaard & Cannon, 1985; Trayhurn *et al.*, 1987). On the transfer of rats from 27°C to 4°C for only 20 minutes, GDP binding increased 1.3-fold (Swick & Swick, 1986). Reversibly, on short-term warm adaptation, the binding was masked. Since no *de novo* synthesis occurs in this short time, the results suggested an "unmasking" of binding sites (Swick & Swick, 1986; Klingenberg & Echtay, 2001). The masking phenomenon relates primarily to changes in the number of nucleotide-binding sites after the animal undergoes acute temperature changes *i.e.* before protein synthesis takes place (Desautels *et al.*, 1978; Nedergaard & Cannon, 1985; Gribskov *et al.*, 1986; Peachey *et al.*, 1988; Huang & Klingenberg, 1995). It is known that the UCP1 purine nucleotide binding site in BAT mitochondria isolated from rats or hamsters kept at room temperature or warm acclimated is occupied by endogenous ATP and is therefore masked (Klingenberg & Huang, 1999). A mechanism for masking/unmasking phenomenon incorporating the ATP hypothesis is illustrated in Figure 1.7 (adapted from Klingenberg & Huang, 1999). It is thought that at thermoneutrality (28°C), BAT mitochondria are largely coupled since UCP1 activity is chiefly inhibited by endogenous ATP. The basal free fatty acid concentrations are low. A low basal thermogenic activity is maintained by the small number of free UCP1 molecules. When animals are acutely cold adapted (4°C) or noradrenaline stimulated, fatty acids are released which increase proton transport activity through UCP1 and deplete endogenous ATP by fatty acid activation, where ATP is converted to AMP. This acute drop in endogenous ATP concentration results in dissociation of prebound ATP from UCP1, yielding more free UCP1 molecules and thereby unmasking. The high fatty acid and low ATP concentrations allow a high thermogenic activity (Huang & Klingenberg, 1995). In isolated mitochondria, UCP1 could be completely unmasked by treatment with Dowex at a high pH (Huang & Klingenberg, 1995). Dowex (21K) is an anion exchanger that removes endogenous residual bound

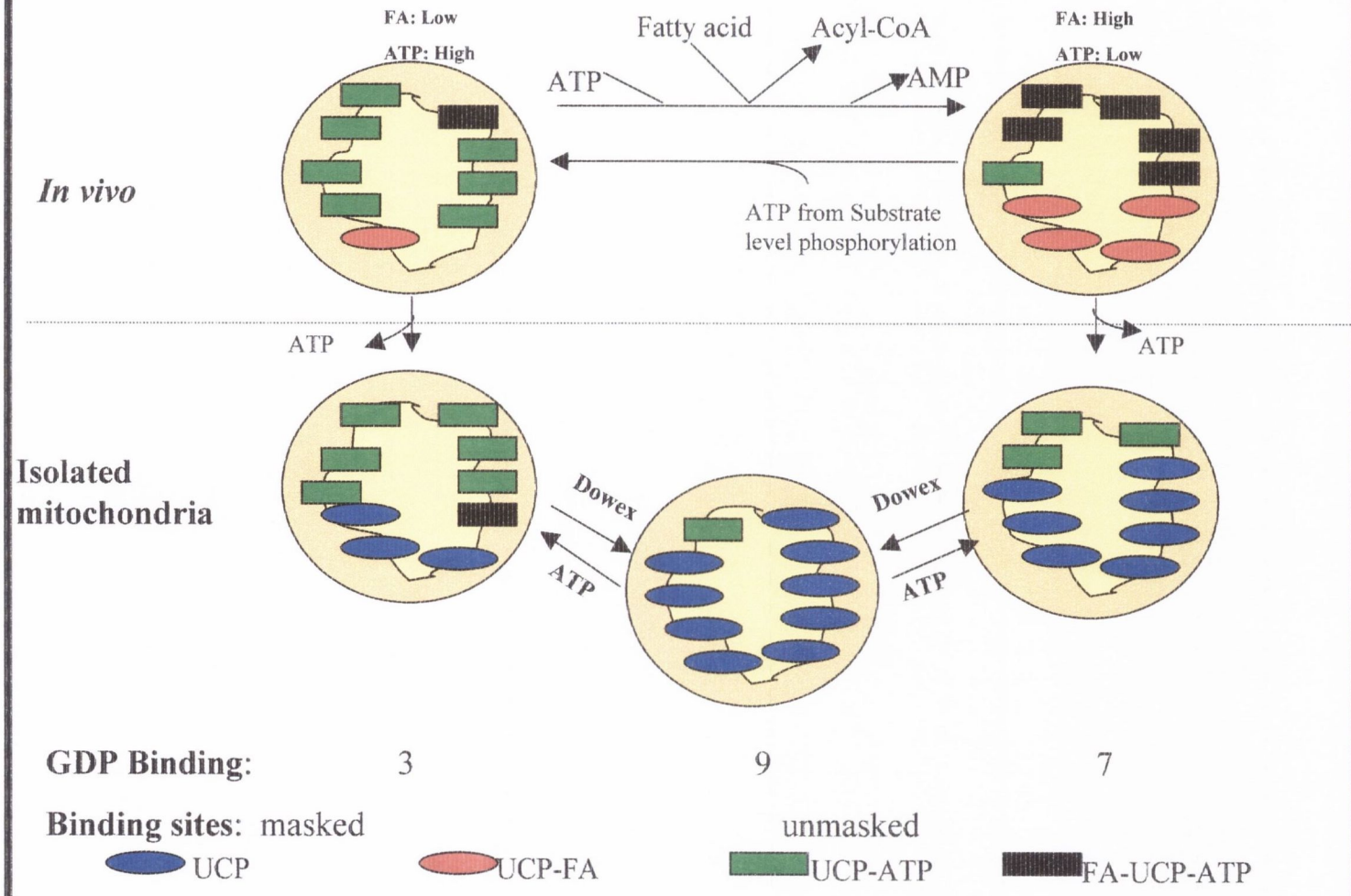


Figure 1.7: Proposed mechanism for the masking/unmasking phenomenon

(as adapted from Klingenberg & Huang, 1999)

nucleotides from isolated mitochondria. [^{3}H] GDP binding studies revealed that thymus mitochondria UCP1 bind GDP with K_D and B_{MAX} binding parameters that are in close accordance with those obtained for BAT mitochondria (Carroll *et al.*, 2005).

Based on the relatively high sequence homology of UCP2 and UCP3 to UCP1, these new UCP homologues were predicted to bind GDP. Some of the amino acids known to be involved in purine nucleotide binding in UCP1 have been identified from chemical modification and site-directed mutagenesis studies (Klaus *et al.*, 1991; Klingenberg & Huang, 1999). The amino acids reported to be involved in purine nucleotide binding in studies on mouse UCP1 are 75-80 % conserved in UCP2 and the long form of UCP3 (UCP 3_L) (Klaus *et al.*, 1991; Klingenberg & Huang, 1999). Chemical modification studies have shown the adjacent sequence **EGPAAFFKG** to be involved in purine nucleotide binding in mouse UCP1 (Klaus *et al.*, 1991). Similar contiguous sequences of **EGPRAFYKG** and **EGPTAFYKG** occur at equivalent positions in UCP2 and UCP3 respectively. In addition, site-directed mutagenesis studies on **Arg 83, Arg 182, Arg 276** (helix 6) of mouse UCP1, have shown them to be essential for purine nucleotide binding (Modriansky *et al.*, 1997; Klingenberg & Huang, 1999; Porter, 2001). Equivalent arginines exist in equivalent positions in UCP2 and the long form of $UCP3_L$. A comparison of rat UCP1 with mouse UCP1 reveals that the consensus sequence **(EGPAAFFKG)** and equivalent arginines **(Arg 84, Arg 183, Arg 277)** are present in rat UCP1. The consensus sequence and equivalently positioned arginines are present in rat UCP2 and rat UCP3 (Figure 1.8). Therefore, there is certainly circumstantial evidence from primary sequence studies that UCP2 and UCP3 can bind purine nucleotides.

Other evidence showing that UCP2 and UCP3 can bind purine nucleotides have come from heterologous yeast and *E. coli* expression systems. Zackova *et al.* (2003) has shown that *E. coli* or yeast expressing UCP2 and UCP3 exhibit high affinity [^{3}H] GTP binding, similar to UCP1. Jekabsons *et al.* (2002) has also shown that recombinant human UCP2, ectopically expressed and solubilised in bacterial inclusion bodies bind purine and pyrimidine nucleoside triphosphates with low micromolar affinity, thus providing more evidence that UCP2 and UCP3 may bind purine nucleotides. However, data showing purine nucleotide binding to isolated mitochondria containing UCP2 and UCP3 has been severely lacking.



Figure 1.8: C-terminal amino acid sequence of rat uncoupling proteins 1, 2 and 3.

The diagram shows the consensus sequence **EGPAAFFKG** in UCP 1 and its equivalent **EGPRAFYKG** in UCP 2 and **EGPTAFYKG** in UCP 3. Also shown are **Arg 277** of rat UCP 1, equivalently positioned **Arg 279** of rat UCP 2 and **Arg 278** of rat UCP 3. Both the contiguous sequence of EGPAAFFKG and the Arg 276 have been implicated in purine nucleotide binding.

1.10 Aims of the Study

As there are very few publications regarding UCP3 protein expression which has also been corrected for mitochondrial density variations in isolated muscle groups following acute and endurance exercise we sought to investigate:

- The effects of acute and endurance exercise on UCP3/unit mass of mitochondria protein expression in *gastrocnemius*, *plantaris*, *soleus* and *extensor digitorum longus* homogenates.

As members of our research team have recently discovered the occurrence of UCP1 in thymus mitochondria, we sought to investigate:

- The effect of cold acclimation on UCP1 protein expression in rat thymus mitochondria.
- In addition, we investigated the effect of cold acclimation on GDP suppressible and fatty acid activatable respiration rates in rat thymus mitochondria.
- Finally, we investigate the effect of cold acclimation on GDP binding parameters in rat thymus mitochondria

As there is a paucity of information in the literature regarding protein expression and functional data of the UCP homologues (UCP2 and UCP3) in natural systems, we also sought to investigate:

- Whether UCP2 and UCP3 are uncoupling proteins in isolated mitochondria and if their uncoupling activity is activated by fatty acids and inhibited by purine nucleotides.
- Whether UCP2 and UCP3 can bind purine nucleotides in isolated mitochondria in a manner similar to UCP1.

Chapter 2

Materials and Methods

Materials and Methods

[2.1] Materials

All chemicals used were obtained from Sigma, BDH or Merck unless otherwise stated (see below). Full source names and addresses are given in Appendix I.

Material	Source
BSA (de-fatted)	Sigma
Commercial peptide antibodies	Calbiochem
Coomassie Blue R	Sigma
Dowex	Fluka
ECL detection reagent	Amersham International
Ecoscint™	National Diagnostics
Folins Ciocalteau's phenol reagent	Merck
[^{3}H] GDP	Amersham International
GDP	Sigma
Liquid nitrogen	Cryoservices
Marvel	Commercially available
Nagarse	Sigma
Palmitate	Sigma
Peptide generated antibodies	Eurogentec
Protein A	Sigma
Protein markers	New England Biolabs
Protogel	National Diagnostics
PVDF	Millipore
Scion Imaging Software	Scion
[^{14}C] Sucrose	Amersham International
Whatman glass fibre filter paper (GF/C)	Whatman
X-OMAT™ LS Film	Kodak

[2.2] Ethics Approval

All animals used in this study were cared for in accordance with the guidelines set out by the Department of Health and Children based on the Cruelty to Animals Act, 1876

and the European Community Directive, 86/609/EC. All animals were obtained from purpose-bred stocks within the bioresources unit (BRU), Trinity College Dublin, Ireland.

[2.3] Animal Treatments

[2.3.1] Acute Exercise

Twenty-seven male CD1 mice (30.5±0.6 g; 8-weeks) were used in this study. Animals were randomly assigned to either a control group (n=9) or a training group to be killed 3 hours after their final training session (n=9) or a second training group to be killed 22 hours after their final training session (n=9). Animals were housed singly under controlled environmental conditions (25±1°C); 12 hour light/dark cycle). Food and water were available *ad libitum* to all animals.

[2.3.2] Endurance Training

Thirteen male CD1 mice (11±1 g; 3 weeks) were used in this study. Animals were randomly assigned to either a control group (n=8) or a training group (n=5), and housed singly under controlled environmental conditions (25±1°C; 12 hour light/dark cycle). Food and water were available *ad libitum* to all animals.

[2.3.3] Temperature Acclimation

Sixty female Wistar rats (124.7±2.5 g) were used in this study. Animals were randomly assigned to either a control group (n=30) or to a cold acclimated group (n=30). Cold-acclimated rats were housed in pairs and held in a temperature-controlled room set at 4±2°C for 5 weeks. Control rats were housed in groups of 6 at 25°C for 5 weeks. All animals were allowed free access to laboratory chow and water. A normal 12 hour light/dark cycle was adhered to. All rats were killed by cervical dislocation.

[2.3.4] Wild Type (WT) and UCP1 Knock-Out (KO) Mice

Six wild type and six knock-out C57BL/6J mice were used in this study. Animals were housed in groups of 6 in a specific pathogen free (SPF) environment at 25±1°C. All animals were allowed free access to food and water and a 12 hour light/dark cycle was in place. All mice were killed by CO_2 asphyxiation.

[2.3.5] Non Specific Pathogen Free Mice

Twelve male CD1 mice (7-8 weeks) were used in this study. Animals were housed in groups of 6 under environmentally controlled conditions (12 hour light/dark cycle; 25±1°C). Mice were housed in a holding facility where they were subject to normally occurring infections and thus were immunologically challenged. All mice were killed by CO_2 asphyxiation.

[2.4] Training Protocols

Animals assigned to the training groups were given 1 week acclimatisation to the swimming water (10 min/day) before either the endurance or acute training program began.

[2.4.1] Endurance Swimming Training

Animals swam for up to 2hr/day, 5days/week for 17 weeks at the same time daily (9 am-11 am). From week 7, when animals were able to maintain a prolonged, endurance type swimming time each session, intensity was increased by introducing weighted swimming (up to 3 % body mass) with fishing weights taped to the tail base of the animals. Animal body mass was measured daily for the first 4 weeks. In the following 13 weeks body mass was measured once per week. Swimming took place in a glass-swimming tank (28 cm deep x 35 cm high x 28 cm wide) filled with tap water maintained at 35±1°C (Nakao *et al.*, 2000). Water temperature was controlled every 10 minutes by the addition of warm water as required. Animals were thoroughly dried under two heating lamps after each training period before being returned to their cages. All animals were killed by CO_2 asphyxiation 22 hours after their final training session and the hind limb muscles were dissected out (see section 2.6).

[2.4.2] Acute Swimming Training

Animals swam for up to 2hr/day, 5days/week for 2 weeks at the same time daily (9am-11am). Swimming took place in a glass-swimming tank (28 cm deep x 35 cm high x 28 cm wide) filled with tap water maintained at 35±1°C (Nakao *et al.*, 2000). Water temperature was controlled every 10 minutes by the addition of warm water as required. Animals were thoroughly dried under two heating lamps after each training period before being returned to their cages. Animals, including sedentary group, were killed 3 or 22 hours

after their final training session by CO_2 asphyxiation and the hind limb muscles were dissected out (see section 2.6).

[2.5] Whole Body Oxygen Consumption

Closed circuit indirect calorimetry (Houlden, 1988) was used to record whole body oxygen consumption rates of both the trained and control groups at 0, 6 and 16 weeks into the endurance swimming training program. The system consisted of 7 chambers, six of which were used for oxygen consumption measurement while the seventh chamber was used as a reference chamber indicating, via changes in pressure, leaks in the system. All chambers were submersed in a heated water bath maintained to 20°C throughout the 3-hour measurement period. All animals were given 3 days of acclimation (2 hours/day) to the chambers before the day of the experiment. On day 4, the measurement day, animals were weighed, and then placed individually in the chambers. The lid was securely closed to prevent water getting into the chamber and the system was started. Carbon dioxide (CO_2) produced by the animals in each chamber was absorbed by soda lime in a basket hanging from the lid of the chamber. Oxygen replaced the CO_2 absorbed during each 3.5 minute cycle of the system. Values from the last hour only were taken to be typical resting measurements of oxygen consumption. Experimental procedures took place at the same time (10 am-1 pm) on each experimental day to limit the effect of circadian rhythm on the metabolic rate. At the end of the 3-hour session the oxygen consumption of each animal was calculated.

[2.6] Skeletal Muscle Dissection

The hind limb muscles *gastrocnemius*, *plantaris*, *soleus* and *extensor digitorum longus* (*EDL*), and were dissected out individually intact and all connective tissue was removed. The muscles were then placed in ice-cold muscle isolation medium consisting (in mM); sucrose 100, EDTA 9, EGTA 1, trizma-base 100, KCl 46, pH 7.5 for storage prior to homogenate preparation.

[2.7] Preparation of Skeletal Muscle Homogenates

Individual muscles were finely chopped on a pre-cooled glass tile, and then frozen in approximately 10 ml of liquid nitrogen in a porcelain mortar. A porcelain pestle was used to grind the frozen muscle to a fine powder. Once ground, individual muscles were re-

suspended in ice-cold muscle isolation medium, 500 µl for both *EDL* and *soleus*, 1 ml for both *gastrocnemius* and *plantaris*. Re-suspended samples were stored in 100 µl aliquots at –20°C until analysis.

[2.8] Mitochondrial Isolations

[2.8.1] Isolation of Brown Adipose Tissue Mitochondria (BAT)

BAT mitochondria were prepared by the method of Scarpace *et al.* (1991). BAT was removed from the interscapular region of the rat between the head and the shoulder blades. BAT was weighed and washed several times in STE buffer (250 mM Sucrose, 1 mM EGTA 5 mM Trizma-base, pH 7.4). Mean ± S.E.M. values for BAT tissue mass (10 rats) were 2.6 ± 0.3 g and 2.2 ± 0.1 g for room temperature and cold acclimated rats respectively. BAT was then placed into a pre-weighed 50 ml beaker containing 30 ml of ice-cold (0-4°C) STE buffer. BAT was chopped carefully in a beaker and poured into a Potter homogeniser tube to a final volume of about 20 ml. The tissue was then homogenised by hand with four passes using a pestle of 0.26 inch (loose) clearance, followed by homogenisation by hand with 6 passes using a pestle of 0.12 inch (tight) clearance. The homogenate was then filtered through four layers of muslin and the filtrate was centrifuged at 8,600 x *g* for 10 minutes at 4°C. The supernatant was discarded and the sides of the centrifuge tube were wiped with tissue to remove any fat deposits. The pellet was re-suspended using a cold finger (a loose-fitting test-tube filled with ice) in approximately 20 ml STE buffer, and centrifuged at 750 x *g* for 10 minutes at 4°C. The pellet was discarded and the supernatant was centrifuged at 8,600 x *g* for 10 minutes at 4°C. The pellet was re-suspended in STE buffer with the addition of 2 % (w/v) de-fatted BSA using a cold-finger and centrifuged at 8,600 x *g* for 10 minutes at 4°C. The pellet was then re-suspended in STE buffer and centrifuged as above. The resulting mitochondrial pellet was re-suspended gently and thoroughly using a cold finger with 0.05 ml of STE buffer per gram of original tissue and used within 6-8 hours of isolation. Mitochondrial protein determination gave significantly different (**$p \leq 0.01$) mitochondrial protein yields of 5.8 ± 1.1 mg/ml and 14.8 ± 1.0 mg/ml for room temperature and cold rats respectively.

[2.8.2] Isolation of Skeletal Muscle Mitochondria

Skeletal muscle mitochondria were isolated from rat hind leg muscle essentially by the method of Bhattacharya *et al.* (1991). 20-30 grams of rat hindquarter muscle (all leg and a small amount of back muscle) was removed and placed into a pre-weighed beaker containing 75 ml of ice-cold (0-4°C) isolation medium (100 mM Sucrose, 9 mM EDTA, 100 mM Trizma-base, 46 mM KCl, pH 7.4). Skeletal muscle was weighed and washed thoroughly in ice-cold medium. Muscle was finely chopped on a pre-cooled glass tile with a razor blade, then added to 200 ml of isolation medium containing 0.5 % (w/v) BSA and 0.02 % (w/v) nagarse (protease) and incubated on ice with stirring for 5 minutes. The tissue was further disrupted using a Waring commercial blender at half max speed for 15 seconds. The homogenate was then centrifuged at 1,500 x *g* for 3 minutes at 4°C. The layer of BSA on top of the supernatant was removed using a spatula and the supernatant was centrifuged at 12,000 x *g* for 10 minutes at 4°C. The pellet was then re-suspended in approximately 25 mls of ice-cold isolation medium containing 2 % (w/v) de-fatted BSA and centrifuged at 12,000 x *g* for 10 minutes at 4°C. The mitochondrial pellet was re-suspended in ice-cold isolation medium and centrifuged as above. The final mitochondrial pellet was re-suspended in ice-cold isolation medium to the desired concentration and stored on ice. Skeletal muscle mitochondria were used within 6-8 hours of isolation.

[2.8.3] Isolation of Liver and Spleen Mitochondria

Mitochondria were prepared by the method of Chappell and Hansford, (1972). Briefly, tissues were removed, trimmed of connective tissue and fat and placed into a pre-weighed beaker containing 50 ml of ice-cold (0-4°C) STE buffer (250 mM Sucrose, 5 mM Trizma-base, 2 mM EGTA, pH 7.4). Tissues were weighed, chopped finely using a scissors and washed several times with ice-cold STE buffer. The tissues were poured into a Potter homogeniser tube to a final volume of approximately 40 ml. The tissues were then homogenised by hand with four passes using a pestle of 0.26 inch (loose) clearance followed by homogenisation by hand with six passes using a pestle of 0.12 inch (tight) clearance. The homogenates were centrifuged at 800 x *g* for 3 minutes at 4°C, pelleting blood and debris. The pellets were discarded and the supernatants were centrifuged at 12,000 x *g* for 10 minutes at 4°C yielding a mitochondrial pellet. The supernatants were discarded and the pellets were re-suspended in approximately 25 ml of ice-cold STE buffer and re-centrifuged at 12,000 x *g* for 10 minutes at 4°C. The resulting pellets containing the

mitochondrial fraction were re-suspended in STE buffer to the desired concentration and used within 6-8 hours of isolation.

[2.8.4] Isolation of Kidney Mitochondria

Rat kidney mitochondria were isolated by the method by Chappell and Hansford (1972). Briefly, kidneys were rapidly dissected out and placed in ice-cold (0-4°C) isolation medium (250 mM sucrose, 5 mM Trizma-base, 1 mM EGTA, pH 7.4). Kidneys were weighed, chopped finely using a scissors and washed several times with ice-cold STE buffer. Tissue was poured into a Potter homogeniser tube to a final volume of approximately 40 ml. The tissues were then homogenised by hand with 10 passes using a pestle of 0.26 inch (loose) clearance. The homogenate was centrifuged at 1,050 x *g* for 3 minutes at 4°C. The ensuing supernatant was stored on ice while the pellets were further homogenised in isolation medium with 5 passes using a pestle of 0.12 inch (tight) clearance. The resulting homogenate was centrifuged at 1,050 x *g* for 3 minutes at 4°C. The supernatants from both centrifugation steps were pooled and centrifuged at 15,000 x *g* for 5 minutes at 4°C. The pellets were re-suspended in approximately 20 ml isolation medium and centrifuged at 15,000 x *g* for 5 minutes at 4°C. The resulting pellet containing the mitochondrial fraction was re-suspended in STE buffer to the desired concentration and used within 6-8 hours of isolation.

[2.8.5] Isolation of Thymus Mitochondria

Thymus mitochondria were prepared by the method of Chappell and Hansford, (1972). The thymus was removed from the abdominal cavity, trimmed of connective tissue and fat and placed into a beaker containing ice-cold (0-4°C) STE buffer (250 mM Sucrose, 5 mM Trizma-base, 2 mM EGTA, pH 7.4). Any BAT present in the vicinity of the thymus was clearly visible and distinguishable from the thymus and was removed prior to the thymus being weighed. Mean ± S.E.M. values for thymus tissue mass (10 rats) were 1.4 ±0.2 g and 1.3 ±0.1 g for room temperature and cold acclimated rats respectively. The thymus was chopped finely using a scissors and washed several times using ice-cold STE buffer. The tissue was poured into a Potter homogeniser tube to a final volume of approximately 40 mls. The tissue was then homogenised by hand with four passes using a pestle of 0.26 inch (loose) clearance followed by homogenisation by hand with six passes

using a pestle of 0.12 inch (tight) clearance. The homogenate was centrifuged at 800 x *g* for 3 minutes at 4°C. The pellet was discarded and the supernatant was centrifuged at 12,000 x *g* for 10 minutes at 4°C yielding a mitochondrial pellet. The supernatant was discarded and the pellet was re-suspended in STE buffer and re-centrifuged at 12,000 x *g* for 10 minutes at 4°C. The pellet was re-suspended in buffer and centrifuged as above. The resulting pellet containing the mitochondrial fraction was re-suspended in STE buffer to the desired concentration and used within 6-8 hours of isolation. Mitochondrial protein determination gave mitochondrial protein yields of 7.6 ± 1.0 mg/ml and 5.8 ± 0.4 mg/ml for room temperature and cold rats respectively.

[2.9] Mitochondrial protein determination using the Markwell Assay

Quantification of protein concentrations in tissue samples was carried out using the commonly employed Markwell assay (Markwell *et al.*, 1978). Standards, ranging in protein content from 0 µg/ml to 50 µg/ml were prepared in triplicate from a stock solution of 1 mg/ml bovine serum albumin (BSA). All re-suspended samples were assayed at two different dilutions. Standards and samples were mixed with 1.5 ml of Markwell C (a 1 in 100 (v/v) dilution of Markwell B (4 % (w/v) copper sulfate) with Markwell A (2 % (w/v) sodium carbonate, 0.4 % (w/v) sodium hydroxide, 0.16 % (w/v) sodium potassium tartrate, 1 % (w/v) SDS). Solutions were vortexed and allowed to stand at room temperature for 15 mins. A 1:1 (v/v) dilution of Folins Ciocalteu's reagent and distilled water was prepared and 150 µl was added to all preparations, which were then vortexed and incubated at room temperature for 45 mins. Standard and sample solutions (200 µl) were pipetted into a standard 96-well plate, placed in a microplate reader/spectrophotometer (Molecular Devices, U.S.A) and absorbance was measured at a wavelength of 650 nm. The concentration of protein in tissue samples was determined from the standard curve obtained.

[2.10] Citrate Synthase Assay

Citrate synthase activity was used as a standard marker of mitochondrial content (Murakami *et al.*, 1994). Briefly, an acrylic cuvette containing 2.8 ml of tris-sucrose (0.1 M trizma base, 0.15 M sucrose, pH 8.1) was placed in a spectrophotometer (Unicam 8625) and the absorbance reading at 412nm was then adjusted to zero. A sample containing 4 µg

of muscle homogenate, as determined by the Markwell protein assay, was added to the cuvette along with 50 µl of a 4 mg/ml 5,5-dithio-bis-nitrobenzoic acid (DTNB) solution and 50 µl acetyl coenzyme A (2 mM). The contents of the cuvette were stirred with a plastic paddle and the chart recorder was started. At this stage the reaction was allowed to proceed for 4 minutes in order to determine the blank rate of the reaction which was subtracted from the actual reaction rate. The assay was started by the addition of 75 µl oxaloacetate (60 mM) and the reaction was allowed to proceed for a further 4 minutes. The assay was completed in triplicate for each sample.

[2.11] Sodium Dodecyl Sulfate Polyacrylamide Gel Electrophoresis (SDS-PAGE)

[2.11.1] Preparation of Samples for Gel Electrophoresis

Protein content of all samples were previously determined (Markwell *et al.*, 1978). Samples were then added to sample buffer consisting of 3.8 ml distilled water, 1 ml tris buffer (1 M; pH 6.8), 0.8 ml glycerol, 1.6 ml 10 % SDS, 0.4 ml bromophenol blue 1 % (w/v). Before use 5 % β-mercaptoethanol was added to the sample buffer. Samples were vortexed briefly then boiled for 5 minutes at 100°C. Positive and negative controls were used on each of the gels. These were prepared by the addition of sample buffer (1:4) and boiling at 100°C for 5 minutes. According to the manufacturer's instructions, pre-stained molecular weight markers were boiled for 3 minutes at 100°C.

[2.11.2] Gel Electrophoresis

Polyacrylamide gels (12 % resolving gel; 5 % stacking gel: Appendix II) were cast between 2 glass plates and fixed to the Miniprotean 3 electrophoresis apparatus (Bio-Rad®, U.K). Running buffer (0.12 M trizma base, 0.96 M glycine, 17.3 mM SDS, pH 8.3) was added to the central reservoir. Samples, molecular weight markers and positive/negative controls were loaded into the wells and run at 200V for 45 minutes at room temperature (Laemmli, 1970). Gels were removed from apparatus and prepared as described in section 2.12 for Western immunoblotting.

[2.12] Western Immunoblotting

One sheet of Polyvinylidene Diflouride (PVDF) membrane (Immobilon-P^{SQ}; Millipore) per gel was pre-soaked in methanol for 30 seconds and then in distilled water for

1 minute. Gels, filter paper and PVDF were soaked in transfer buffer (25 mM trizma base, 192 mM glycine, 10 % (v/v) methanol) for 15-minutes. A layered sandwich was then prepared in which the gel slab was placed on top of 4 sheets of filter paper at the cathode. PVDF was then placed on top of the gel followed by 4 additional sheets of filter paper at the anode. Air bubbles were removed from the sandwich and the cassettes were closed and placed into the transfer cell (Bio-Rad®, U.K.). The transfer cell was then placed into a tank with transfer buffer and an ice block. The lid was secured to the tank and the transfer was carried out for 1-hour at 100 V at room temperature.

Blocking of the membrane was performed by incubating the blot in PWB (PBS containing 0.1 % (w/v) Tween 20) containing 5 % (w/v) Marvel milk powder at room temperature for 1 hour or overnight at 4°C. Blots were then incubated in primary antibody (in PBS-Tween (PBS-T) containing 5 % (w/v) marvel milk powder; see Appendix III) overnight at 4°C or at room temperature for 1-hour containing a 1:1000 dilution of an affinity purified anti-UCP3 peptide antibody, a 1:1000 dilution of a commercial anti-UCP1 peptide antibody (Calbiochem) and a 1:1000 dilution of an antibody to the β-subunit of the F_1-ATP synthase ($F_1\beta$). Following this primary antibody incubation, the blots were washed 3 X 10 minutes in PBS-T. The blots were then incubated with a horseradish peroxidase (HRP) conjugated goat anti-rabbit secondary antibody (1:10000 dilution) in PBS-T containing 5 % Marvel milk powder for 1 hour at room temperature. Following this, blots were further washed for 3 X 10 minutes in PBS-T. Blots were developed using an enhanced chemiluminescence (ECL) detection system (Amersham-Pharmacia) for detecting horseradish peroxidase labelled antibody, by means of the HRP catalysed oxidation of luminol under alkaline conditions and the results were visualised by exposure to Kodak X-Omat LS film.

[2.13] Coomassie Blue R staining of SDS-PAGE gels

Following SDS-PAGE, the laemmli gels were stained using Coomassie blue R according to the method of Laemmli (1970) to ensure all the protein was transferred to the membranes successfully. Laemmli gels were stained using 0.5 % (w/v) Coomassie blue R in 50 % methanol (v/v), 10 % (v/v) acetic acid for 30 minutes on a shaking platform. The Coomassie blue R stain was then discarded and the gels were destained on a shaking platform for 30 minutes using 50 % (v/v) methanol and 10 % (v/v) acetic acid.

[2.14] Densitometry

Following western blot analysis, the relative abundance of UCP1 and UCP3 was determined using densitometry. The band intensities of the exposed film were analysed using Scion Imaging software.

[2.15] Antibodies

Peptide synthesis, conjugation of peptides to BSA and injection of rabbits was undertaken by Eurogentec. Polyclonal antibodies in the resulting rabbit anti-sera were affinity purified on a protein A column. The UCP3 peptide, based on rat sequence to which polyclonal antibodies were raised was as follows:

141....TGGERKYRGTMDAYRC....156

Commercial anti-UCP1 (145aa-159aa) peptide antibody was obtained from Calbiochem. The antibody to the β-subunit of the F_1-ATP synthase was raised to that of *Neurospora crassa* and was a gift from Dr. Matt Harmey, Department of Botany, University College Dublin, Ireland.

[2.16] Affinity purification of the polyclonal antibodies using Protein A-sepharose

The protein A-sepharose column was prepared by swelling 0.5 g of protein A-sepharose in 10 ml of 0.1 M Tris-HCl, pH 8.0 overnight at 4°C. Protein A-sepharose (0.5 g) swells to a bed volume of 2 ml. The column was set by pouring protein A-sepharose into a 10 ml syringe barrel previously plugged with glass wool. The column was allowed to flow by gravity to pack the column bed. The packed affinity resin was then equilibrated with 10 column volumes of 0.1 M Tris-HCl, pH 8.0. In the meantime, the pH of the antibody serum was adjusted to pH 8.0 by adding $1/10^{th}$ the volume of 1 M Tris-HCl, pH 8.0 (*e.g.* 0.05 ml of 0.1 M Tris-HCl, pH 8.0 was added to 0.5 ml of serum sample). The serum sample was then gently applied to the column, ensuring at all times not to disturb the bed surface. The column was then washed with 10 column volumes of 0.1 M Tris-HCl, pH 8.0. The column was further washed with 10 column volumes of 0.01 M Tris-HCl, pH 8.0. The bound immunoglobulin was eluted with 4 column volumes of 0.1 M glycine, pH 3.0. Before beginning elution, eppendorf tubes were set up to collect the entire elution volume as 0.5

ml fractions. Prior to collection of elute, 0.05 ml of neutralization buffer (1 M Tris-HCl, pH 8.0) was added to each tube. Following this, the elution buffer (0.1 M glycine, pH 3.0) was gently added to the top of the resin. 0.5 ml fractions were collected until the elution buffer had just entered the column bed. The immunoglobulin fractions were then quantified spectrophotometrically at 280nm using the formula: 1 OD (optical density) = 0.8 mg/ml. The immunoglobulin fraction consisting of the greatest protein concentration was aliquoted and stored at –20°C prior to western blot analysis. Once the sample had been eluted from the column, the affinity matrix was washed with 2 column volumes of 0.1 M glycine, pH 3.0. This was followed by re-equilibration of the column with at least 10 column volumes of 0.1 M Tris-HCl, pH 8.0. These latter steps were performed to ensure the successful regeneration of the column for future use.

[2.17] Dowex treatment of isolated mitochondria

Endogenous residual bound nucleotides were removed from isolated mitochondria using an anion exchanger (Dowex 21K) according to the procedure described by Huang and Klingenberg (1995). Isolated mitochondria at a concentration of 2 mg/ml in buffer containing 250 mM sucrose, 20 mM Hepes, 1 mM EDTA (pH 8.0), were shaken with Dowex (120 mg/mg protein) at room temperature for 1-hour.

[2.18] GDP binding assay

Measurement of binding of [^{3}H]GDP was performed using a modification of the procedure described by Scarpace *et al.*, 1991 using glass fibre filters that had been soaked in a ligand binding assay buffer (100 mM sucrose, 1.2 mM K-EDTA, 12.2 mM choline chloride, 40 mM TES, pH 7.1). Mitochondria (50 μg) were incubated with various concentrations (0.1 μM-6.0 μM) of [^{3}H] GDP (10.8 & 11.5 Ci/mmol) in ligand binding assay buffer with the addition of 0.1 mg/ml fatty acid free BSA, 2 μM rotenone and 30 μM atractyloside in a total volume 0.25 ml at 37°C. [^{14}C] sucrose (250 μCi/ml) was included in the incubations to calculate the volume of medium trapped on the filter. Non-specific binding was determined in the presence of 1.5 mM unlabelled ligand (GDP). All mitochondrial samples were incubated in triplicate for 15 minutes at 37°C. The incubation mixtures were diluted with 3 ml of ligand binding assay buffer (left at room temperature) and filtered immediately through Whatman glass filter fibres (GF/B, 2.5 cm) that had been

soaked in assay buffer. The filters were then washed with a further 2 x 3 ml of ligand binding assay buffer. The total time taken for filtration and washing was less than 10 seconds. Filters were allowed to dry at room temperature before being placed in scintillation vials. Ecoscint™ scintillation fluid (10 ml) was then carefully added to the dried filters for fluid scintillation counting. Filters in scintillation fluid were vortexed vigorously and left at room temperature overnight to ensure thorough dissolution of the filters. Samples were then counted as described in section [2.19].

[2.19] Liquid scintillation counting

The [^{3}H] isotope and [^{14}C] isotope were measured using a Packard Tricarb 2100 scintillation spectrophotometer. The cocktail used was the commercially available scintillant, ecoscint™, for aqueous samples. The average counting efficiency for [^{3}H] counting using this instrument was calculated to be 45 % and for [^{14}C] sucrose was calculated to be 96 % based on a quench correction curve relating counting efficiency to the spectral index of the external standard.

[2.20] Analysis of saturable binding data

Binding values were obtained as disintegrations per minute (dpm) and converted to pmoles of bound radioligand per milligram of mitochondrial protein using 100 % counting efficiency and specific radioactivity values. The mean values and the standard error of the mean values (S.E.M) were calculated for total and non-specific binding using triplicate samples and the following formula was employed to obtain standard error of the mean values for specific binding values:

$$S.E.M = \sqrt{(E_1)^2 + (E_2)^2}$$

were E_1 = S.E.M for total binding and E_2 = S.E.M for non specific binding. Specific binding was calculated from the difference between total and non-specific binding. The Michaelis dissociation constant (K_D) and the maximal binding capacity (B_{MAX}) were obtained by fitting mean values for specific binding sites on the y-axis and free radioligand concentrations on the x-axis using the computer program Sigma plot (version 5). This program estimates K_D and B_{MAX} parameters after the data are fitted directly to an equation

relating the concentration of the radioligand-receptor complex (bound) and the free radioligand concentration (free ligand):

$$[\text{bound}] = B_{MAX} * [\text{free ligand}]/(\text{free ligand} + K_D)$$

which describes a rectangular hyperbola (and is mathematically equivalent to the Michaelis-Menton equation of enzyme kinetics). The data was fitted by non-weighted, non-linear least squares regression. The data points are represented by a line of best fit.

[2.21] Measurement of oxygen consumption rates in mitochondria isolated from BAT, thymus, liver, kidney, muscle and spleen

Dioxygen uptake (probe for electron flow) by suspensions of isolated mitochondria can be studied using an oxygen electrode. The electrode (Clarke type) consists essentially of a silver/silver chloride reference half-cell, joined to a platinum/O_2 cathode by a saturated KCl bridge. The electrode compartment is isolated from the reaction chamber (in which the mitochondria and their substrates or inhibitors interact) by a thin Teflon membrane. The membrane is permeable to dioxygen and allows this gas to reach the cathode, where it is electrolytically reduced. The reduction allows a current to flow and this is converted to a potential and recorded on a chart recorder. The trace is thus a measure of the dioxygen content of the reaction mixture and both the extent and rate of dioxygen uptake by mitochondria may be measured. The mitochondrial suspension in the reaction chamber was stirred using a magnetic stirrer and thermostatically maintained at 37°C.

[2.22] Fatty acid activation assay

The sensitivity of respiration by non-phosphorylating mitochondria to fatty acids and purine nucleotides was evaluated using the procedure described by González-Barroso *et al.* (1998). Mitochondria (1 mg/ml) were incubated at 37°C in medium containing 120 mM KCl, 5 mM Hepes, 1 mM EGTA (pH 7.4), 16 μM fatty acid free BSA, 5 μM rotenone and 1 μg/ml oligomycin, 5 μM atractyloside. Non-phosphorylating (state 4) oxygen consumption rates were measured as the steady-state rate achieved on addition of 7.5 mM succinate (succinate-KOH, pH 7.4). The sensitivity of this state 4 oxygen consumption rate to GDP (1 mM) was then determined. The sensitivity of the resulting oxygen consumption

rate to palmitate (64 μM) (~40 nM free) was also determined. Finally, the mitochondrial uncoupler 2,4-dinitrophenol (DNP) (30 nM) was added to the chamber to determine the maximum oxygen consumption rate attainable due to uncoupling. The Clarke oxygen electrode was calibrated according to the procedure of Reynafarje *et al.* (1985) assuming 406 nmoles O dissolved in 1 ml of incubation medium held at 37°C.

[2.23] Statistical analysis

All results are expressed as mean ± SEM unless otherwise indicated. Mean values were compared using an unpaired Student's t-test or an ANOVA test. Unless otherwise stated a p value of ≤ 0.05 was taken to indicate significance.

Chapter 3

The effects of acute and endurance exercise on UCP3 protein expression in mouse *gastrocnemius*, *plantaris*, *soleus* and *EDL* muscles

[3.1] Introduction

The relatively recent discovery of UCP3, a UCP isoform whose expression is particularly high in skeletal muscles of rodents and humans, has renewed interest in the study of human energy metabolism (Boss *et al.*, 1997; Vidal Puig *et al.*, 1997; Gong *et al.*, 1997). The almost exclusive expression of UCP3 in skeletal muscle is of great interest as skeletal muscle is an important site of regulated thermogenesis and energy homeostasis in mammals. Therefore, the hypothesis that UCP3 may play a role in controlling thermogenesis and energy expenditure in skeletal muscle is attractive, due to its 57 % sequence homology to UCP1 (Vidal-Puig *et al.*, 1997) and thus, its possible functional equivalence. In fact, UCP3 exhibits properties consistent with an uncoupling function when transfected in C_2C_{12} myocytes (Boss *et al.*, 1998a) and yeast (Gong *et al.*, 1997; Zhang *et al.*, 1999).

UCP3 does not seem to be involved in cold adaptation since acclimation of rats to cold conditions results in a 50 % decrease in skeletal muscle UCP3 expression (Lin *et al.*, 1998; Boss *et al.*, 1998a). Conversely, acute exercise (Tsuboyama *et al.*, 1998; Cortright *et al.*, 1999) and fasting (Gong *et al.*, 1997), situations where one might expect that tight metabolic coupling would be advantageous, result in an increase in UCP3 mRNA expression, which is apparently indicative of an increase in protein and suggests that short term regulation of energy expenditure is not the primary function of this protein. One observation, made by previous investigators regarding the regulation of UCP3 expression by fasting and acute exercise, is that these states result in increases in circulating free fatty acids. Hence, the up-regulation of UCP3 mRNA in skeletal muscle during food deprivation corresponds to increases in serum free fatty acids under such starving conditions (Gong *et al.*, 1997; Millet *et al.*, 1997; Boss *et al.*, 1998a). Elevation of free fatty acids by lipid infusion, proposed as a starvation imitating condition, also increases UCP3 gene expression in vivo (Weigle *et al.*, 1998) and in vitro (Hwang and Lane, 1999) in C_2C_{12} cells. In addition, an acute bout of exercise elevates blood free fatty acid levels and also causes an increase in UCP3 gene expression (Cortright *et al.*, 1999). Taken together these data suggest that UCP3 in skeletal muscle may function primarily as an acute regulator of lipid metabolism and not as a regulator of thermogenesis or short- term energy expenditure.

However, to date the major physiological role(s) and regulation of skeletal muscle UCP3 remain contentious.

The factors that regulate UCP3 gene expression or clearly define its metabolic role are poorly understood. However, UCP3 genes are evidently responsive to the metabolic state of the organism. Due to its possible role in energy metabolism, a number of investigators have studied the adaptive response of UCP3 in skeletal muscle to exercise. Muscle activity by exercise is a well-established model used to profoundly alter the metabolic state of skeletal muscle. For example, protracted physical activity results in elevated metabolic capacity which manifests as an availability of free fatty acids for oxidation (Molé *et al.*, 1971). Many studies have explored the effects of exercise, both acute and endurance, on UCP3 mRNA expression (Tsuboyama *et al.*, 1998; Cortright *et al.*, 1999). However, few studies have established the effect of exercise on UCP3 protein expression. Of the few who have looked at the effect of exercise on skeletal muscle at a protein level, many have failed to correct their results for a number of important metabolic adaptations to training, namely an increase in mitchondrial number and size (Holloszy and Coyle, 1984; Murakami *et al.*, 1994). Since UCPs are mitochondrial proteins, a similar expression of, for example, UCP mRNA in trained and untrained subjects suggests that the expression of UCPs per mitochondrion is decreased in trained subjects. Since it has been previously shown that mRNAs for mitochondrial enzymes involved in energy metabolism are increased in direct proportion to the increase in mitochondrial density in response to training (Puntschart *et al.*, 1995), we have used citrate synthase activity as an indicator of mitochondrial density in both the acute and endurance studies. In addition, we have used $F_1\beta$ expression as a second marker of variations in mitochondrial density in the acute study.

While the detection of UCP3 transcript is useful in ascertaining the role of UCP3, transcript does not necessarily represent the expression of the functional entity, the UCP3 protein. With this in mind we designed a UCP3 peptide antibody, generated by Eurogentec, against which an antibody was raised in rabbit. This antibody has been shown to be sensitive and discriminatory for UCP3 over UCP1, UCP2 and other mitochondrial transporters (Cunningham *et al.*, 2003). Members of our research team have also shown that this UCP3 antibody detects mouse, rat and human forms of UCP3 expressed in *E. coli*,

yeast expression systems, COS cells and in isolated mitochondria (Cunningham *et al.*, 2003).

Previous studies have indicated that acute exercise induces large increases in UCP3 in skeletal muscle, whereas endurance training results in marked decreases in skeletal muscle UCP3 at both mRNA and protein levels. To quantify this, Tsuboyama *et al.* (1998) reported a seven-fold increase in UCP3 mRNA in skeletal muscle of mice 3-hours after a single bout of treadmill running and a sixteen-fold increase in UCP3 mRNA 3-hours after exercise in mice that had been trained for 3-weeks by swimming. In both of these studies the UCP3 mRNA levels returned to sedentary levels in animals killed 22- hours after their last exercise bout. Similarly, Zhou *et al.* (2000) reported an approximate seven-fold increase in UCP3 mRNA in rat skeletal muscle (no specific muscle type) immediately after a 200-minute bout of swimming. A similar response was seen after a bout of treadmill running. Zhou *et al.* (2000) also reported a 3.5-fold increase in UCP3 protein levels in rat skeletal muscle (no specific type) immediately after 100-minutes of running. Pilegaard *et al.* (2000), showed a 2.5-fold increase in UCP3 mRNA four hours after a 4-hour bout of cycling in *vastus lateralis* muscle of human subjects. Schrauwen *et al.* (2002) reported a two-fold increase in *vastus lateralis* UCP3 mRNA expression 4-hours after exercise in men who performed cycle exercise for 2-hours in a fasted state. To summarise, several studies have shown an increase in UCP3 mRNA levels in indiscriminate skeletal muscle as a result of acute exercise (Tsuboyama *et al.*, 1998; Zhou *et al.*, 2000; Pilegaard *et al.*, 2000; Schrauwen *et al.*, 2002).

In contrast to the acute exercise studies discussed above, Boss *et al.* (1998b) reported that an 8-week long program of treadmill running resulted in 76 % and 59 % reductions in UCP3 mRNA in rat *tibialis anterior* and *soleus* muscles respectively. Similarly, Schrauwen *et al.* (1999) reported that endurance trained men had significantly reduced UCP3 mRNA levels in *quadriceps* muscles when compared with untrained men. In addition, Fernström *et al.* (2003) reported a 54 % decrease in UCP3 protein expression in human skeletal muscle (no specific muscle type) following 6-weeks cycling. Conversely, Cortright *et al.* (1999) saw no change in UCP3 mRNA expression in rat skeletal muscle following a 9-week wheel running program.

It has been deduced from rodent studies that the extent and direction in which physical training effects UCP3 mRNA expression is muscle-fibre type specific. Boss *et al.* (1998b) reported a graded scale of UCP3 mRNA expression according to fibre proportions in the different muscles such that fast glycolytic fibres expressed more UCP3 mRNA than slow twitch fibres in rats that had been subjected to treadmill running for 8 weeks. A second study showed an abundant UCP3 protein signal in fibres classed type 2 and only moderate protein expression in type 1 fibres taken from healthy male volunteers (Hesselink *et al.*, 2001). Subclassification of these type 2 fibres revealed UCP3 protein expression to be more abundant in type 2b (fast glycolytic) fibres (Hesselink *et al.*, 2001). In the present study we investigate the effect of exercise on a range of mouse muscle fibre types.

To explore the role of UCP3 in rodent energy metabolism further, we sought to examine for the first time the levels of UCP3 protein expression, per unit mass of mitochondria (citrate synthase activity), in *gastrocnemius*, *plantaris*, *soleus* and *extensor digitorum longus* (*EDL*) homogenates isolated from control, acutely exercised and endurance trained mice. The fibre composition of the four muscle types being used in this study are shown in Table 3.1.

	Type I	Type IIA	Type IIB
	% Slow Oxidative Fibres	% Fast Glycolytic Fibres	% Fast Oxidative/Glycolytic Fibres
Soleus	90	-	10
EDL	5	95	-
Plantaris	-	66.6	33.3
Gastrocnemius	33.3	33.3	33.3

Table 3.1 Muscle fibre composition. Adapted from Boss *et al.* (1998b) and Giacobino. (2001).

[3.2] Results

[3.2.1] Acute Swimming

Male mice were either kept sedentary (control) or exercised by means of swimming for 2 weeks and then sacrificed either 3 hours or 22 hours after their final exercise session. Body mass was measured daily in each of the three cohorts over the 2 week period. UCP3 protein levels in *gastrocnemius*, *plantaris*, *soleus* and *EDL* muscle homogenates from exercised and sedentary animals were measured using a Western blotting technique. Finally, citrate synthase activity and $F_1\beta$ expression were determined as indirect measurements of variation of mitochondrial density.

Figure 3.2.1 illustrates the effect of sedentary conditions and exercised conditions on body mass over a 2 week period. As expected, 2 weeks swimming did not produce significant differences in the body mass between the sedentary and exercised animals (sacrificed either 3 or 22 hours after exercise). Data is expressed as mean ± S.E.M. of 6 independent observations for each of the three animal groups. Statistical differences were assessed using an unpaired Student's t-test.

Figure 3.2.2 reveals that the swimming training protocol used in this study had no effect on citrate synthase activity, an index of mitochondrial abundance, when compared with sedentary animals in any of the four muscle types tested. As expected, high levels of citrate synthase activity were found in the predominantly oxidative muscles. Data is expressed as mean ± S.E.M. of at least 3 independent experiments, each experiment performed in triplicate, for sedentary and trained mice. Statistical analysis was performed using an unpaired Student's t-test.

Figure 3.2.3 illustrates $F_1\beta$ expression in each of the four muscle types as determined by densitometry. There were no significant differences in $F_1\beta$ expression due to acute exercise in either the animals killed 3 or 22 hours post exercise. As expected, the highest levels of $F_1\beta$ expression were found in the highly oxidative *soleus* muscle homogenate. Data is expressed as mean ± S.E.M of 6 independent observations for each of the three groups.

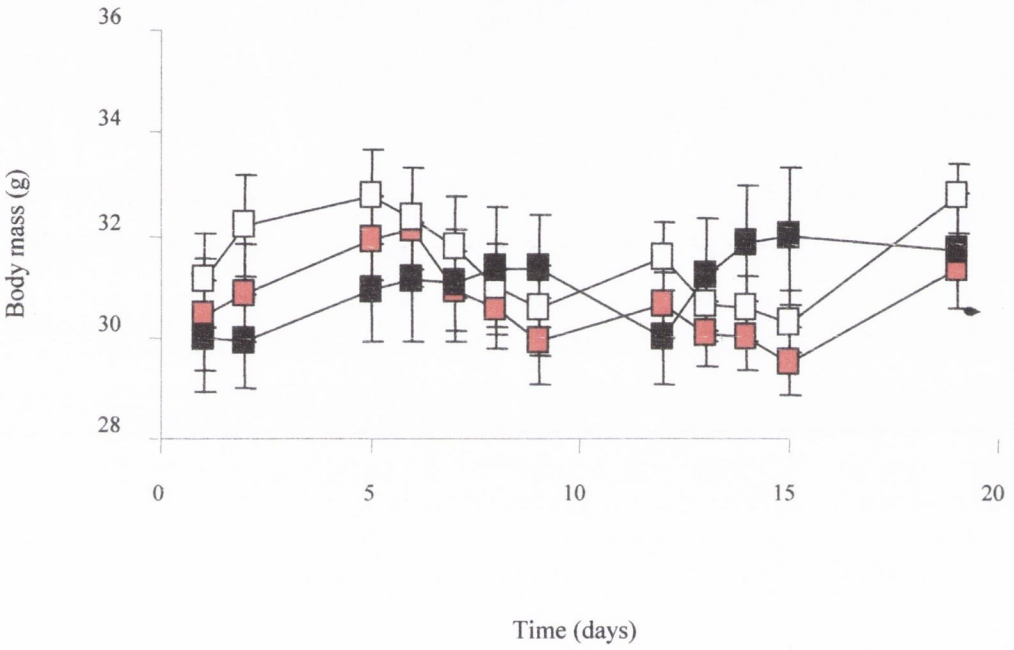


Figure 3.2.1: Effect of acute exercise on body mass.

Exercised animals were subjected to 2 hours swimming, 5 days per week for 2 weeks. Sedentary animals (■) performed no training. Trained animals were divided into 2 groups, which determined how long after the final exercise bout animals would be killed, either 3 hours (■) or 22 hours (□). Animals were weighed daily prior to their swimming session for the duration of the study. Data is expressed as mean ± S.E.M. of 6 independent observations for each cohort.

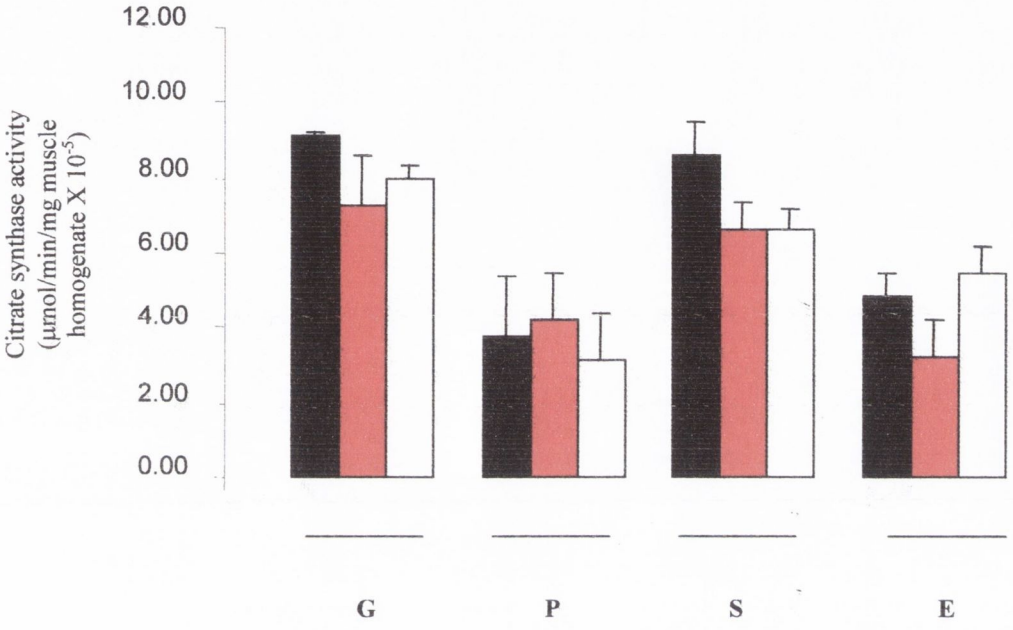


Figure 3.2.2: Citrate synthase activity in *gastrocnemius*, *plantaris*, *soleus* and *EDL* muscle homogenates

Mice were either kept sedentary (■) or exercised by swimming for 2 weeks. Three hours (■) or twenty-two hours (□) after the final exercise bout *gastrocnemius* (G), *plantaris* (P), *soleus* (S) and *EDL* (E) muscles were excised and homogenates were prepared as described in section 2.7. Citrate synthase activity in each of the four muscle types was determined as described in section 2.10. Data is expressed as mean ± S.E.M. of at least 3 experiments each experiment performed in triplicate.

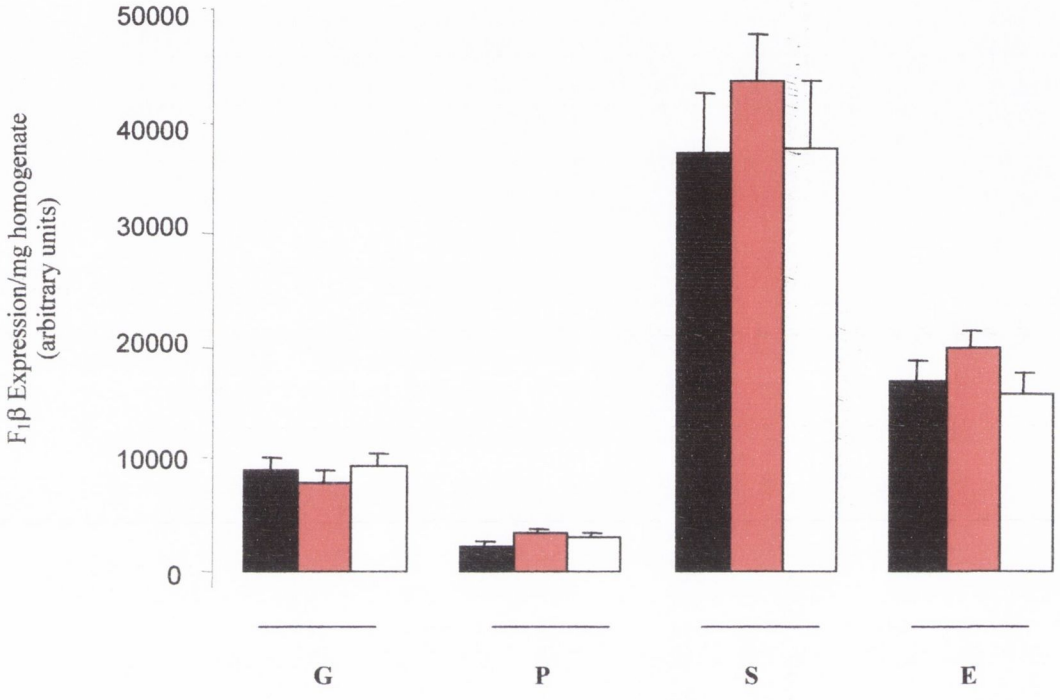


Figure 3.2.3: $F_1\beta$ expression in *gastrocnemius*, *plantaris*, *soleus* and *EDL* muscle homogenates

Mice were either kept sedentary (■) or exercised by swimming for 2 weeks. Three hours (■) or twenty-two hours (□) after the final exercise bout *gastrocnemius* (G), *plantaris* (P), *soleus* (S) and *EDL* (E) muscles were excised and homogenates were prepared as described in section 2.7. All homogenates were subjected to SDS-PAGE and Western blotted using an antibody to the $F_1\beta$ subunit of ATP synthase as described in sections 2.11 & 2.12. Data is expressed as mean ± S.E.M. of 6 mice.

Figure 3.2.4 **(A)** is an immunoblot illustrating, for the first time in the case of the homogenates, our affinity purified anti-UCP3 antibody detecting UCP3 protein in yeast over-expressing UCP3, in control *gastrocnemius* homogenates and in *gastrocnemius* homogenates excised from animals killed 3 and 22 hours post exercise. As expected, no UCP3 protein band was detected in the mouse liver mitochondria. The bar chart **(B)** indicates absolute UCP3 protein expression (*i.e.* UCP3 protein expression values that have not been corrected for potential changes in mitochondrial density due to exercise) per milligram (mg) of *gastrocnemius* homogenate as determined by densitometry. Evidently, the 2 week swimming regime resulted in a significant (* p=0.0304; n=5-6) increase in absolute UCP3 protein expression in the *gastrocnemius* muscle homogenate isolated from mice killed 3 hours post exercise when compared to control animals. However, this increase is transient with absolute UCP3 protein levels decreasing significantly (*p=0.0167; n=6) to pre-exercise levels in animals killed 22 hours post exercise. The bar chart **(C)** shows UCP3 protein expression levels per unit mass of mitochondria in *gastrocnemius* homogenates taken from the control and acutely exercised mice. The UCP3/unit mass of mitochondria protein expression data mirror the data for absolute UCP3 protein expression since the significant increase (*p=0.0186; n=5-6) in UCP3/unit mass of mitochondria protein expression in the animals killed 3 hours post-exercise is followed again by the significant decrease (*p=0.0447; n=5) in UCP3/unit mass of mitochondria protein in the mice killed 22 hours post exercise. All results are expressed as mean ± S.E.M. Data were analysed statistically using an unpaired Student's t-test.

Our anti UCP3 peptide antibody detected UCP3 in yeast over-expressing UCP3 and in *plantaris* muscle homogenates isolated from sedentary and exercised mice as shown in figure 3.2.5 **(A)**. The bar chart **(B)** shows absolute UCP3 protein expression in *plantaris* muscle homogenates isolated from control and exercised animals as determined by densitometry. There was a significant (* p=0.0166; n=3-4) increase in absolute UCP3 protein expression in *plantaris* muscle homogenates isolated from the mice killed 3 hours post exercise when compared with control mice. This increase was maintained in the *plantaris* homogenates isolated from the mice killed 22 hours post exercise (*p=0.0308; n=3-4). The bar chart **(C)** shows the expression of UCP3/unit mass of mitochondria in *plantaris* muscle homogenates excised from control and acutely exercised mice. No significant changes in UCP3/unit mass of mitochondria protein expression were observed

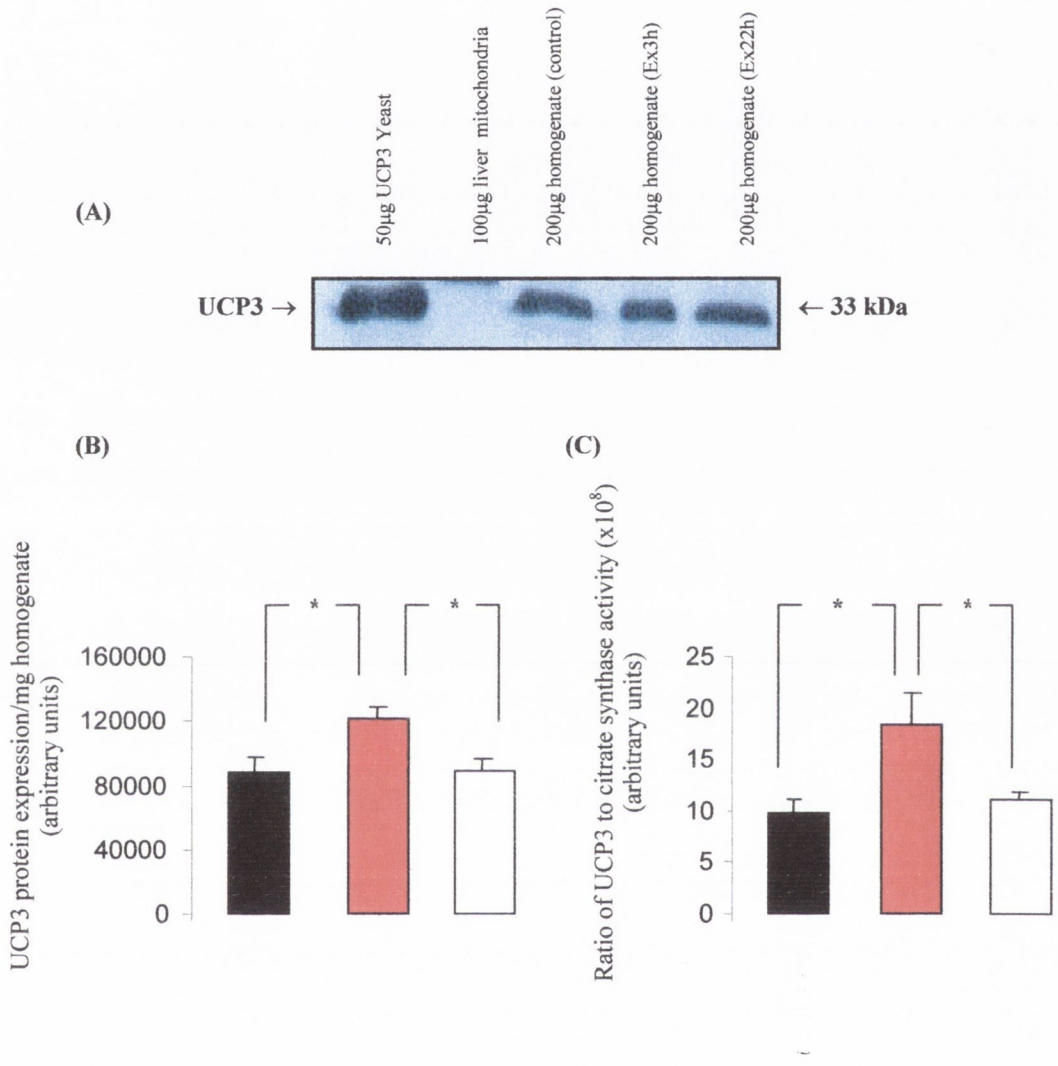


Figure 3.2.4: Effect of acute swimming on expression of UCP3 protein in *gastrocnemius* homogenate.

Mice were either kept sedentary (■) or exercised by swimming for 2 weeks. Three hours (■) or twenty-two hours (□) after the final exercise bout animals were killed and *gastrocnemius* muscle was excised. Homogenates were prepared as described in section 2.7. An immunoblot illustrating in (A) UCP3 protein expression is shown. The bar chart (B) illustrates UCP3 protein expression per mg of *gastrocnemius* homogenate. The bar chart (C) shows UCP3 protein expression relative to citrate synthase activity in *gastrocnemius* homogenate. Data is expressed as mean ± S.E.M. of 5 - 6 mice. Statistical differences are given as $^{*}p \leq 0.05$ as determined by unpaired student t test.

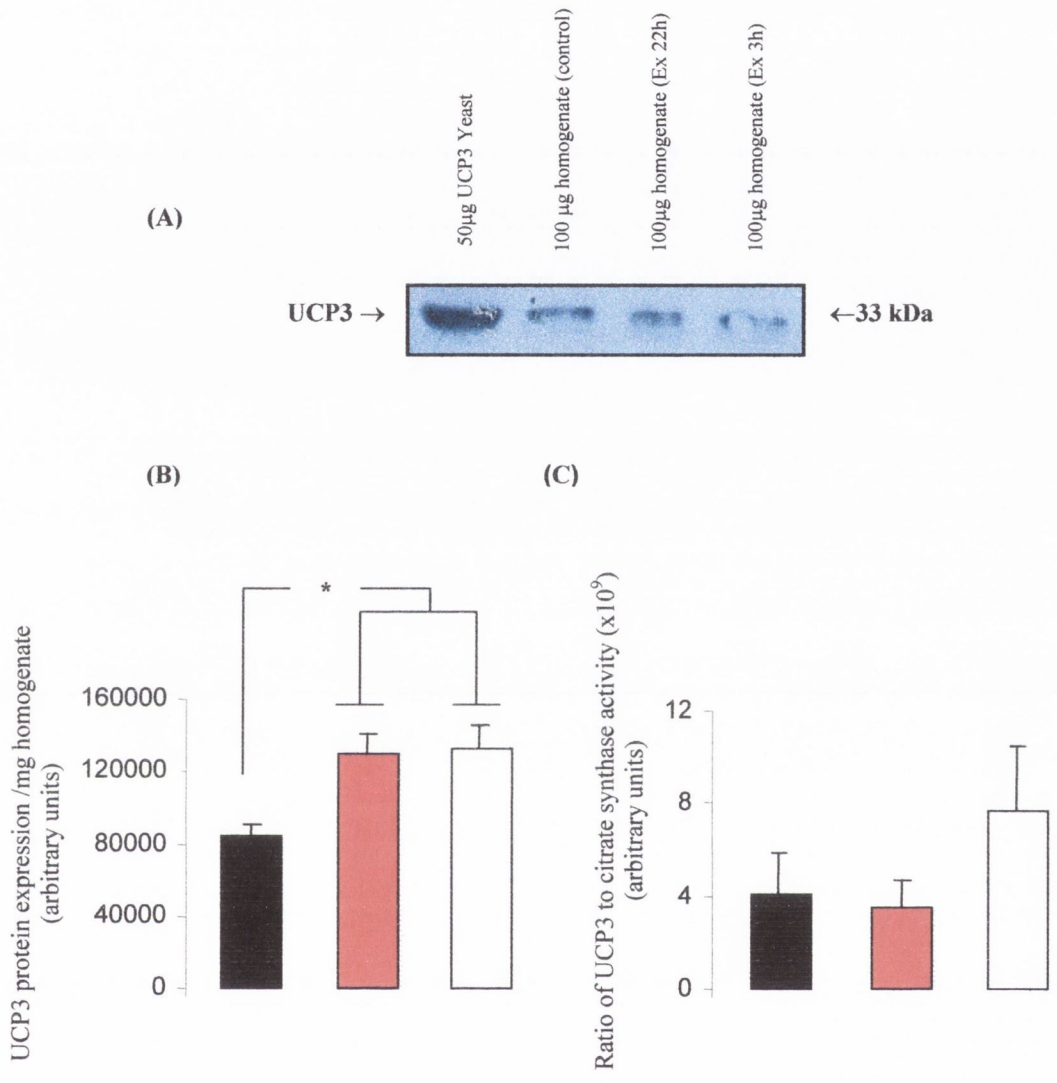


Figure 3.2.5: Effect of acute swimming on expression of UCP3 protein in *plantaris* homogenate.

Mice were either kept sedentary (■) or exercised by swimming for 2 weeks. Three hours (■) or twenty-two hours (□) after the final exercise bout mice were killed and *plantaris* muscle was excised. Homogenates were prepared as described in section 2.7. An immunoblot illustrating in (A) UCP3 protein expression is shown. The bar chart (B) illustrates UCP3 protein expression per mg of *plantaris* homogenate. The bar chart (C) shows UCP3 protein expression relative to citrate synthase activity in *plantaris* homogenate. Data is expressed as mean ± S.E.M. of 3 - 4 mice. Statistical differences are given as $^*p \leq 0.05$ as determined by unpaired student t test.

in any of the groups tested. All data is expressed as mean ± S.E.M. and assessed using unpaired Student's t-tests.

Figure 3.2.6 shows that the acute swimming regime resulted in no significant changes in either absolute UCP3 protein expression or UCP3/unit mass of mitochondria protein expression in the predominantly slow-twitch, oxidative *soleus* muscle homogenates. Figure 3.2.6 **(A)** is an immunoblot depicting UCP3 protein expression in yeast over-expressing UCP3, in control *soleus* homogenate and in *soleus* homogenates prepared from acutely exercised mice killed 3 and 22 hours after their final swimming session. The bar chart **(B)** shows absolute UCP3 protein expression in *soleus* homogenates isolated from each of the three groups as determined by densitometry. The bar chart **(C)** illustrates the expression of UCP3/unit mass of mitochondria in *soleus* muscle homogenates isolated from each of the three groups. Results are expressed as mean ± S.E.M. of 4-5 mice.

Figure 3.2.7 reveals that the 2 week exercise regime had no effect on absolute or UCP3/unit mass of mitochondria protein expression in fast-twitch, glycolytic *EDL* muscle homogenates prepared from control and exercised mice. In figure 3.2.7 **(A)** the anti-UCP3 antibody is shown to detect UCP3 protein in *EDL* muscles from each of the three groups and in yeast over-expressing UCP3. As expected, UCP3 was not detected in liver homogenate. The bar chart **(B)** illustrates absolute UCP3 protein expression, as determined by densitometry, in *EDL* muscle homogenates isolated from control and exercised groups. Figure 3.2.7 **(C)** shows the expression of UCP3/unit mass of mitochondria in soleus homogenates isolated from the three groups. Data is expressed as mean ± S.E.M. of 3-4 mice.

[3.2.2] Endurance Swimming

In the case of the endurance swimming training, mice swam for up to 2hr/day, 5day/week for 17 weeks at the same time daily. From week 7, when animals were able to maintain a prolonged, endurance type swimming time each session, intensity was increased by introducing weighted swimming (up to 3 % body mass) with fishing weights taped to the tail base of the animals. Animal body mass was measured daily for the first 4 weeks. In the following 13 weeks body mass was measured once per week**.** Resting, whole body

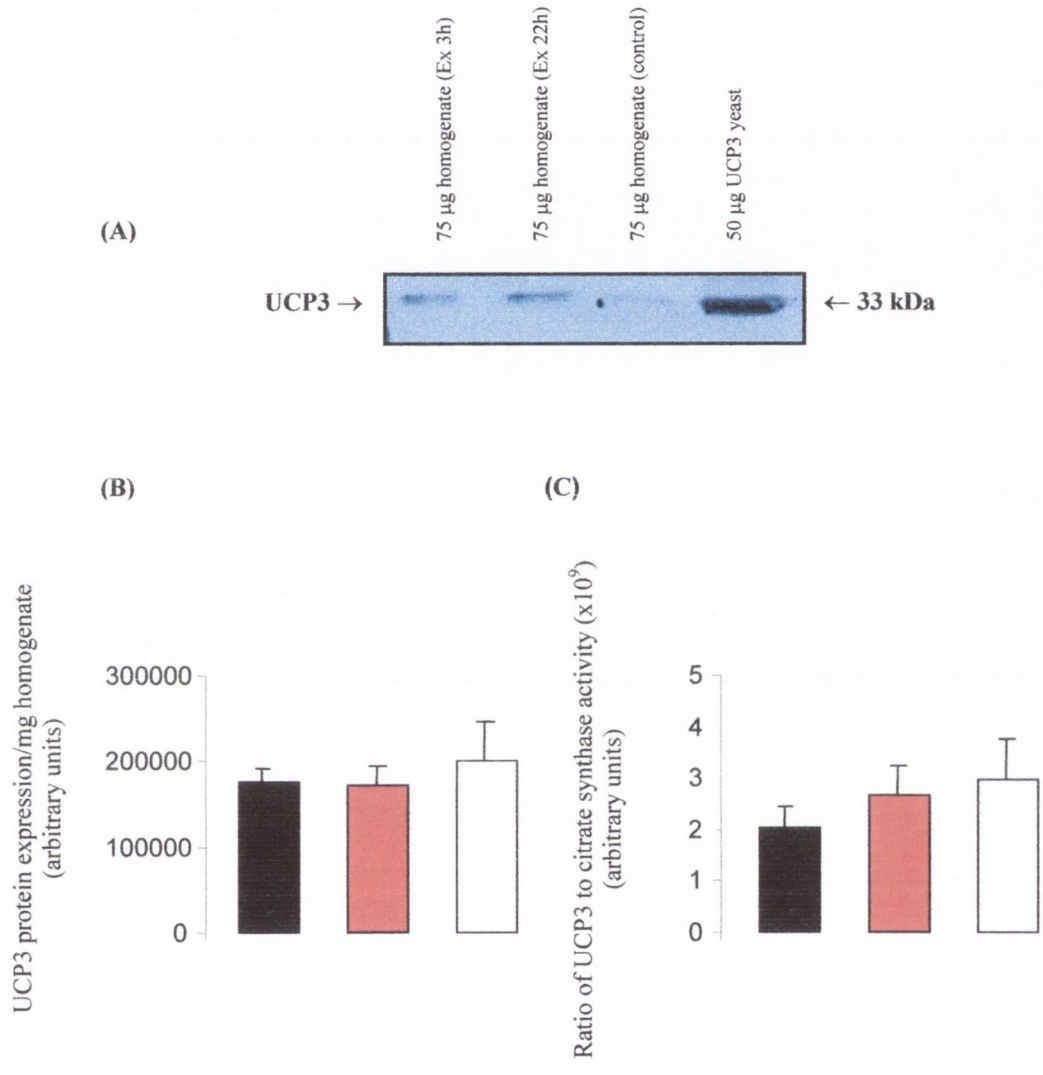


Figure 3.2.6: Effect of acute swimming on expression of UCP3 protein in *soleus* homogenate.

Mice were either kept sedentary (■) or exercised by swimming for 2 weeks. Three hours (■) or twenty-two hours (□) after the final exercise bout animals were sacrificed and *soleus* muscle was excised. Homogenates were prepared as described in section 2.7. An immunoblot illustrating in (A) UCP3 protein expression is shown. The bar chart (B) illustrates UCP3 expression per mg of *soleus* homogenate. The bar chart (C) shows the relative expression of UCP3 protein to citrate synthase activity in *soleus* homogenate. Data is expressed as mean ± S.E.M. of 4 – 5 mice.

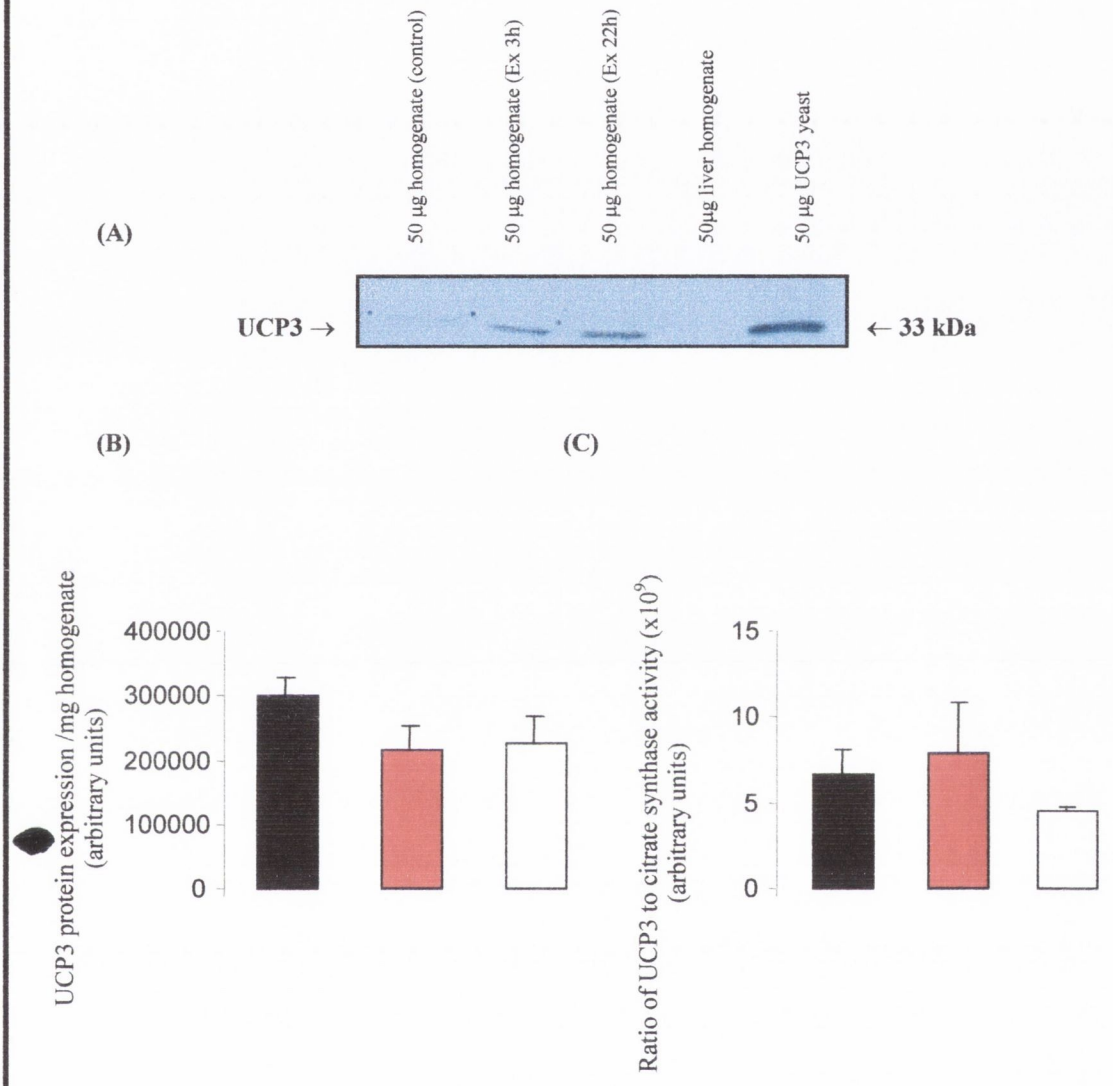


Figure 3.2.7: Effect of acute swimming on expression of UCP3 protein in *EDL* homogenate.

Mice were either kept sedentary (■) or exercised by swimming for 2 weeks. Three hours (■) or twenty-two hours (□) after the final exercise session mice were killed and *EDL* muscle was excised. Homogenates were prepared as described in section 2.7. An immunoblot illustrating in (A) UCP3 protein expression is shown. The bar chart (B) illustrates UCP3 protein expression per mg of *EDL* homogenate. The bar chart (C) shows the relative expression of UCP3 protein to citrate synthase activity in *EDL* homogenates. Data is expressed as mean ± S.E.M. of 3 – 4 mice.

oxygen consumption rates were determined pre-exercise and at 6 and 16 weeks into the training regime. At the end of the training regime mice were killed by CO_2 asphyxiation and *gastrocnemius*, *plantaris*, *soleus* and *EDL* muscles were removed. Muscle homogenates were prepared and UCP3 protein levels from control and exercised animals were measured using a Western blotting technique. Finally, citrate synthase activity was determined.

As expected following 17 weeks of endurance swimming training, the body mass of the trained animals was significantly lower ($*p \leq 0.05$) than that of the sedentary control group as determined by unpaired Student's t-test. Figure 3.2.8 illustrates that this difference in body mass between the groups occurred from week 12 through to the end of the study. Results are presented as mean ± S.E.M. of 8 and 5 independent observations for sedentary and trained animals respectively.

Whole body resting oxygen consumption rates were calculated using a closed circuit indirect calorimetry system as described in section 2.5. Figure 3.2.9 shows that there was a significant ($***p \leq 0.001$) reduction in resting oxygen consumption at 6 and 16 weeks into the training program in both the trained and sedentary groups when compared with the pre-exercise training values as determined by two-way ANOVA. Whole body resting oxygen consumption was not different in trained mice when compared with sedentary mice at any of the time points measured (pre-exercise, 6 and 16 weeks). Results are expressed as mean ± S.E.M. of 5 mice.

Figure 3.2.10 illustrates citrate synthase activity rates in each of the four muscle types in control and endurance trained mice. There was a significant ($*p \leq 0.05$) increase in citrate synthase activity in the trained *plantaris* homogenate when compared with the control homogenate as determined by unpaired Student's t-test. Citrate synthase activity rates did not change significantly in any of the other three muscle types examined. However, there was a trend towards an increase in activity with training. Data is expressed as mean ± S.E.M. of 6 – 7 mice.

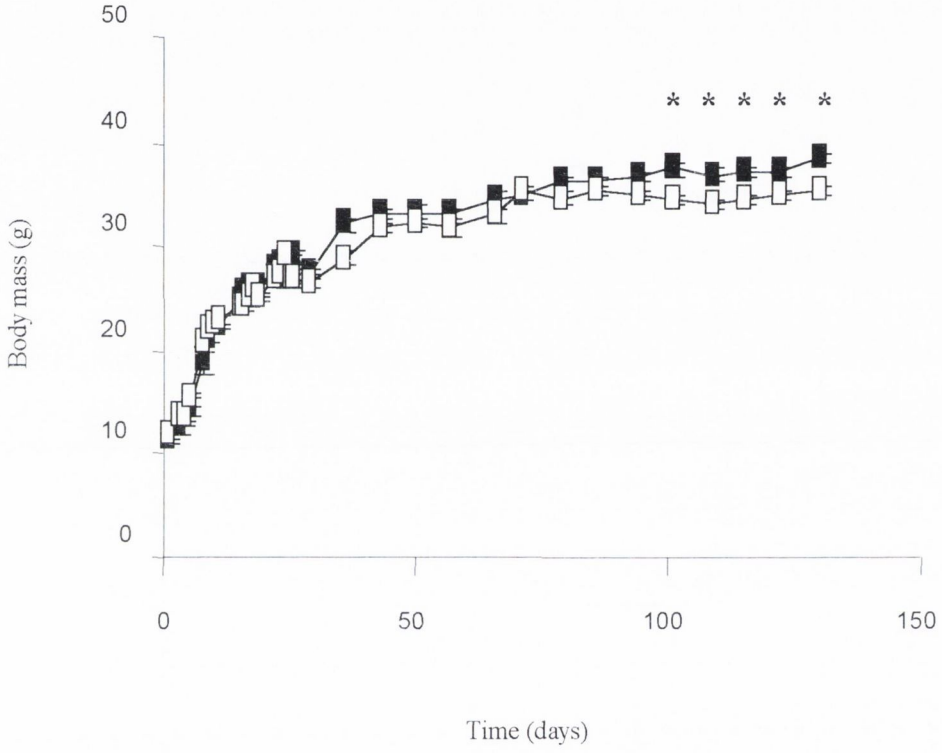


Figure 3.2.8: Effect of endurance training on body mass

Trained animals (□) were subjected to 2 hours swimming, 5 days per week for 17 weeks. Sedentary animals (■) performed no training. Animals were weighed daily prior to their swimming session for the first 4 weeks. In the following 13 weeks body mass was measured once per week. Results are presented as mean ± S.E.M. of 8 and 5 independent observations for sedentary and trained animals respectively. Statistical differences as given as *$p \leq 0.05$ as determined by an unpaired student t test

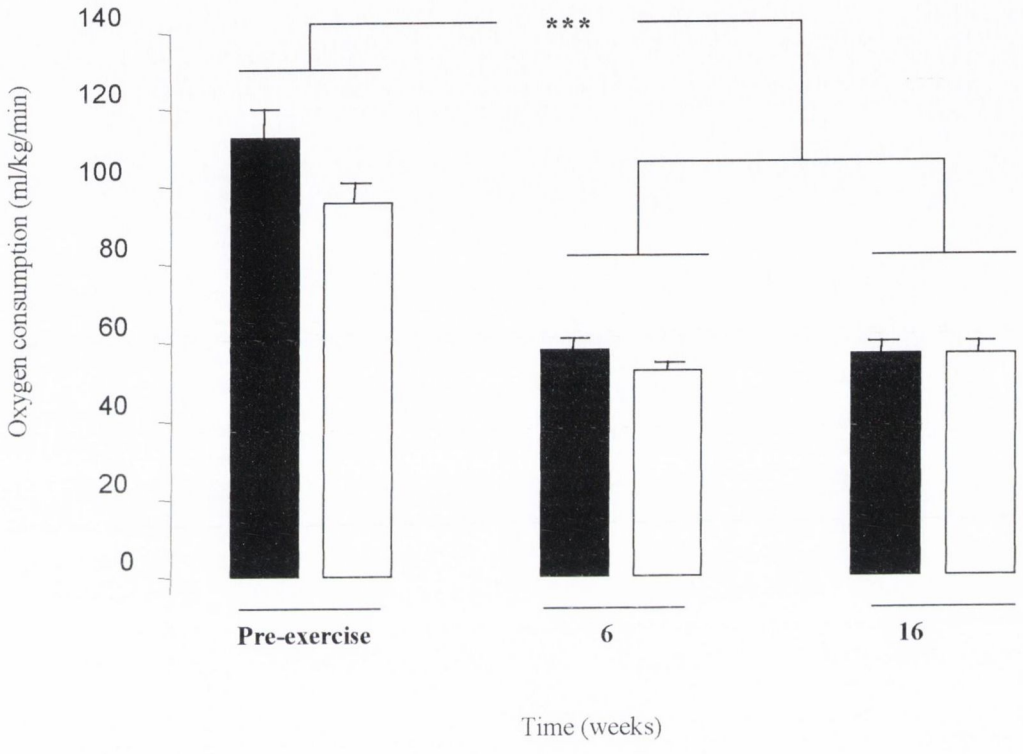


Figure 3.2.9: Whole body resting oxygen consumption pre, mid and post training.

Whole body resting oxygen consumption rates were calculated in sedentary (■) and trained (□) animals using a closed circuit indirect calorimetry system as described in section 2.5. Results are expressed as mean ± S.E.M. of at least 5 animals. Statistical differences are given as ***$p \leq 0.001$ as determined using a two-way ANOVA test.

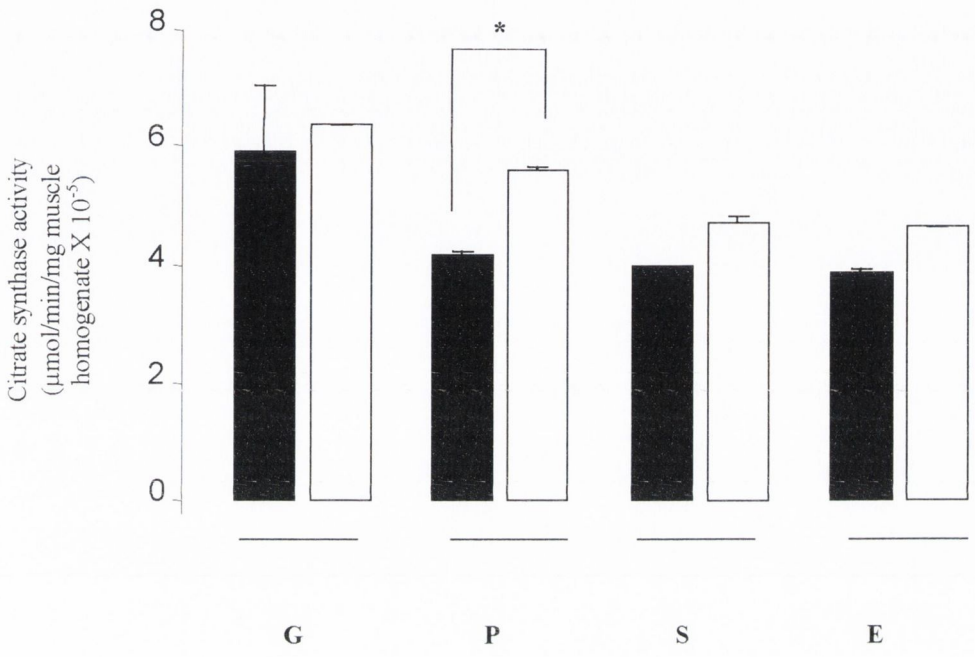


Figure 3.2.10: Citrate synthase activity in *gastrocnemius*, *plantaris*, *soleus* and *EDL* muscle homogenates of endurance trained mice.

Mice were either kept sedentary (■) or exercised (□) by swimming for 17 weeks. Twenty-two hours after the final exercise bout *gastrocnemius*, *plantaris*, *soleus* and *EDL* muscles were excised and homogenates were prepared as described in section 2.7. Citrate synthase activity in each of the four muscle types was determined as described in section 2.10. Data is expressed as mean ± S.E.M. of at least 3 experiments each experiment performed in triplicate. Statistical analysis (student t test) showed a significant (*$p \leq 0.05$) increase in citrate synthase activity in trained *plantaris* muscle homogenate when compared with sedentary control *plantaris* muscle homogenate.

Figure 3.2.11 **(A)** is an immunoblot showing our affinity purified anti-UCP3 antibody detecting UCP3 protein in Cos cells over-expressing UCP3, in skeletal muscle mitochondria isolated from rats, in control gastrocnemius homogenates and in *gastrocnemius* homogenates taken from endurance trained mice. Figure 3.2.11 **(B)** shows absolute UCP3 protein expression in *gastrocnemius* muscle homogenates isolated from control and endurance trained mice as determined by densitometry. The bar chart **(C)** shows UCP3/unit mass of mitochondria protein expression in *gastrocnemius* homogenates. Data is expressed as mean ± S.E.M of 4 and 6 independent observations for control and trained animals respectively. Clearly, endurance training resulted in no change in UCP3 protein expression in gastrocnemius muscle homogenates.

Figure 3.2.12 **(A)** is an immunoblot depicting the expression of UCP3 protein in *plantaris* homogenates prepared from control and trained mice. It also shows our anti-UCP3 antibody detecting UCP3 protein in *EDL* homogenates from fed and 24 hour fasted mice. The bar chart **(B)** shows absolute UCP3 protein expression in *plantaris* muscle homogenate isolated from control and trained mice. The bar chart **(C)** illustrates UCP3/unit mass of mitochondria protein expression in *plantaris* muscle homogenate isolated from control and trained animals. Results are expressed as mean ± S.E.M. of 4 independent observations for each group. Evidently, endurance training resulted in no significant differences in UCP3 protein expression in plantaris muscle homogenates.

Endurance training resulted in no significant differences in UCP3 protein expression in *soleus* muscle homogenates. Figure 3.2.13 **(A)** shows our anti-UCP3 peptide antibody detecting UCP3 protein in *soleus* homogenates isolated from control and trained mice, in normal rat muscle mitochondria and in yeast over-expressing UCP3. The bar chart **(B)** shows absolute UCP3 protein expression, as determined by densitometry, in *soleus* muscle homogenate isolated from control and trained mice. The bar chart **(C)** illustrates UCP3/unit mass of mitochondria protein expression in control and trained animals. Data is expressed as mean ± S.E.M. of 4 independent observations for each group.

Figure 3.2.14 **(A)** shows our affinity purified anti-UCP3 antibody detecting UCP3 protein in yeast over-expressing UCP3 and in control and endurance trained *EDL* muscle

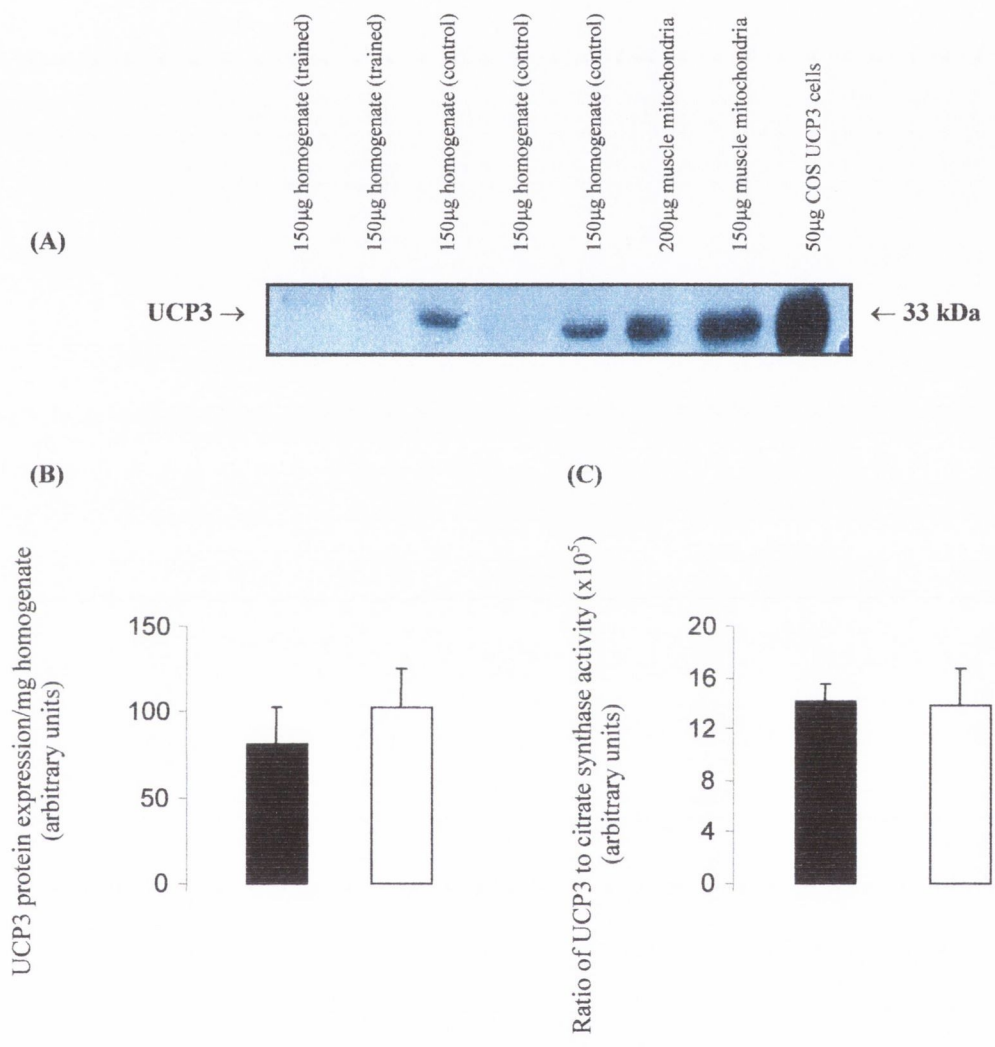


Figure 3.2.11: Effect of 17-weeks endurance swimming training on expression of UCP3 protein in *gastrocnemius* homogenate.

Mice were either kept sedentary (■) or exercised (□) by swimming for 17 weeks. Twenty-two hours after the final exercise bout *gastrocnemius* muscle was excised and homogenates were prepared as described in section 2.7. An immunoblot **(A)** illustrating UCP3 protein expression in *gastrocnemius* homogenate is shown. The bar chart **(B)** illustrates UCP3 protein expression per mg of *gastrocnemius* homogenate. The bar chart **(C)** shows the relative expression of UCP3 protein to citrate synthase activity in *gastrocnemius* homogenates. Data is expressed as mean ± S.E.M. of 4 – 6 mice.

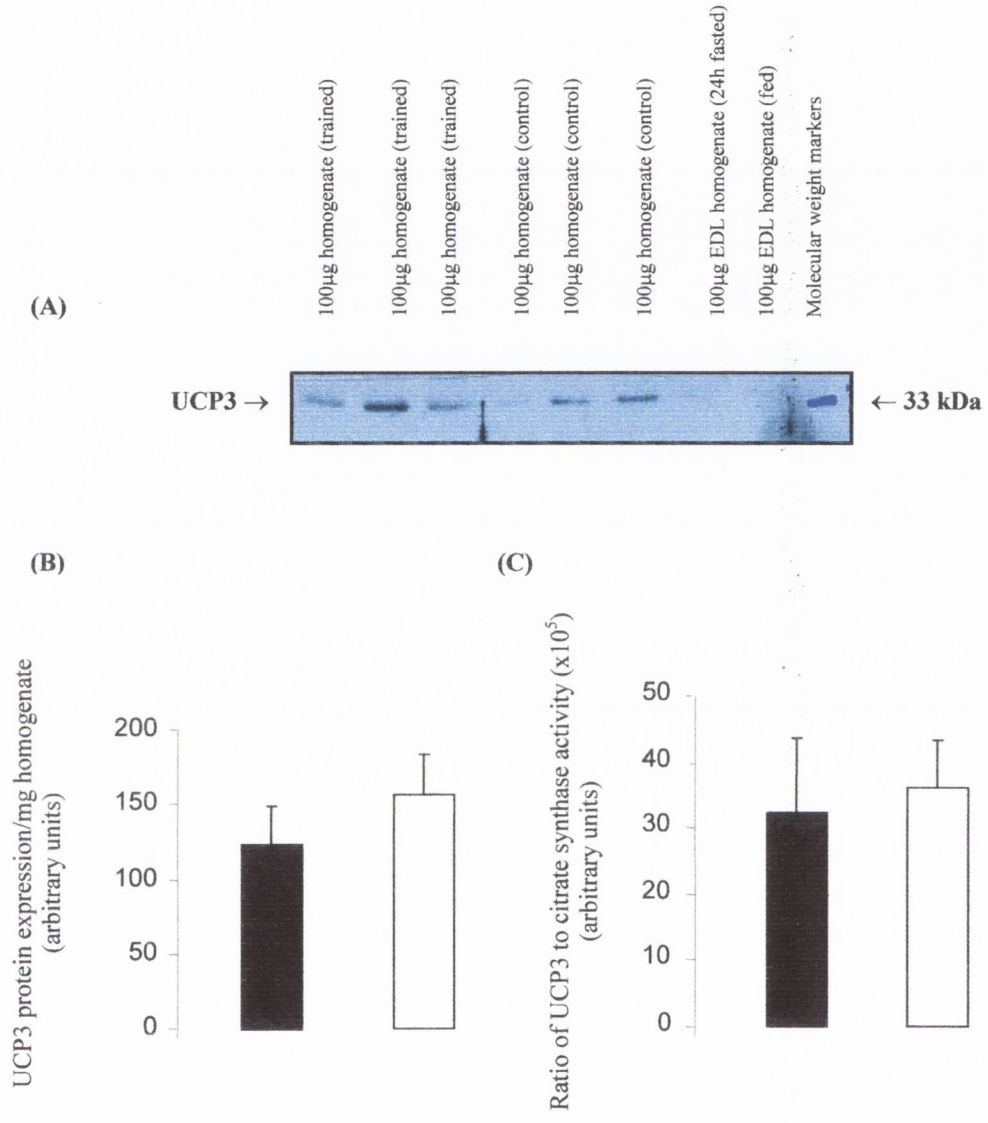


Figure 3.2.12: Effect of 17-weeks endurance swimming training on expression of UCP3 protein in *plantaris* homogenate.

Mice were either kept sedentary (■) or exercised (□) by swimming for 17 weeks. Twenty-two hours after the final exercise bout *plantaris* muscle was excised and homogenates were prepared as described in section 2.7. Figure 3.2.12 **(A)** is an immunoblot illustrating UCP3 protein expression in *plantaris* homogenate. The bar chart **(B)** illustrates UCP3 protein expression per mg of *plantaris* muscle homogenate. The bar chart **(C)** shows the relative expression of UCP3 protein to citrate synthase activity in *plantaris* homogenates. Data is expressed as mean ± S.E.M. of 4 mice.

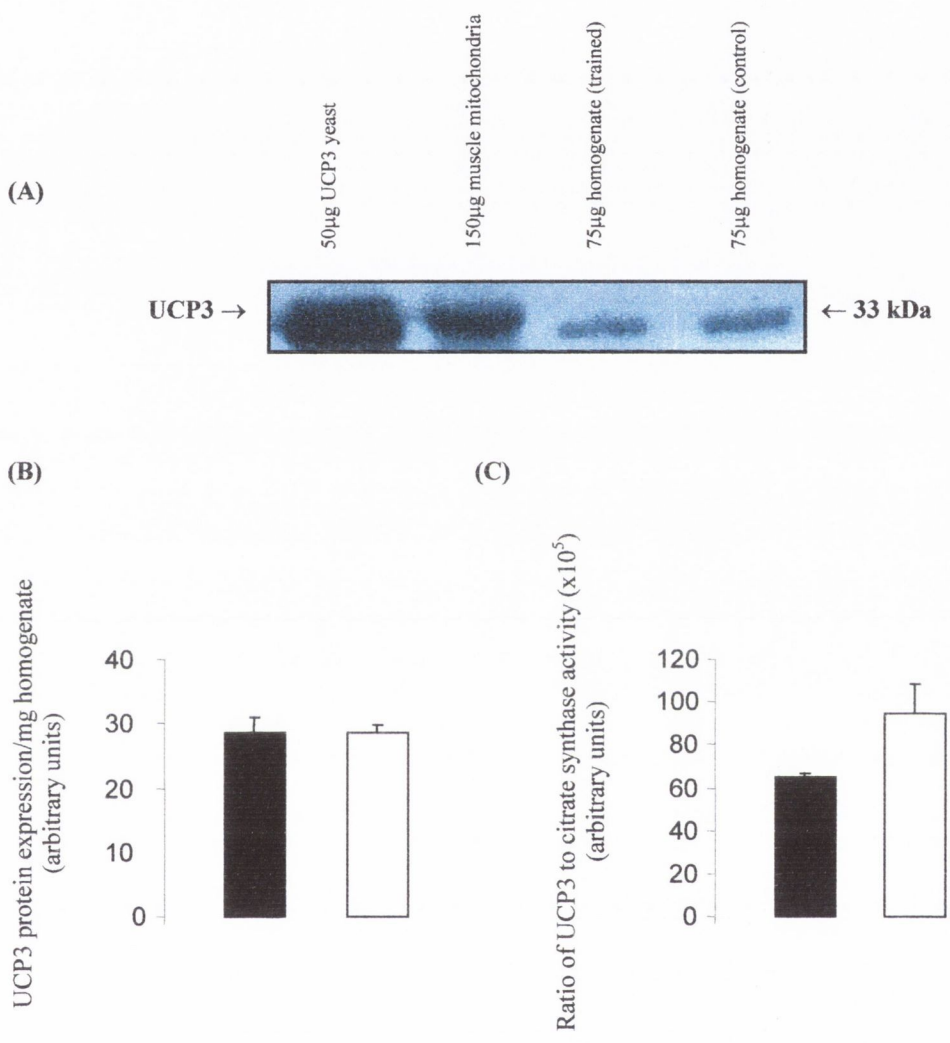


Figure 3.2.13: Effect of 17-weeks endurance swimming training on expression of UCP3 protein in *soleus* homogenate.

Mice were either kept sedentary (■) or exercised (□) by swimming for 17 weeks. Twenty-two hours after the final exercise bout *soleus* muscle was excised and homogenates were prepared as described in section 2.7. An immunoblot illustrating UCP3 protein expression in *soleus* homogenate is shown 3.2.13 **(A)**. The bar chart **(B)** illustrates UCP3 protein expression per mg *soleus* muscle homogenate. The bar chart **(C)** shows the relative expression of UCP3 protein to citrate synthase activity in *soleus* homogenates. Data is expressed as mean ± S.E.M. of 3 mice.

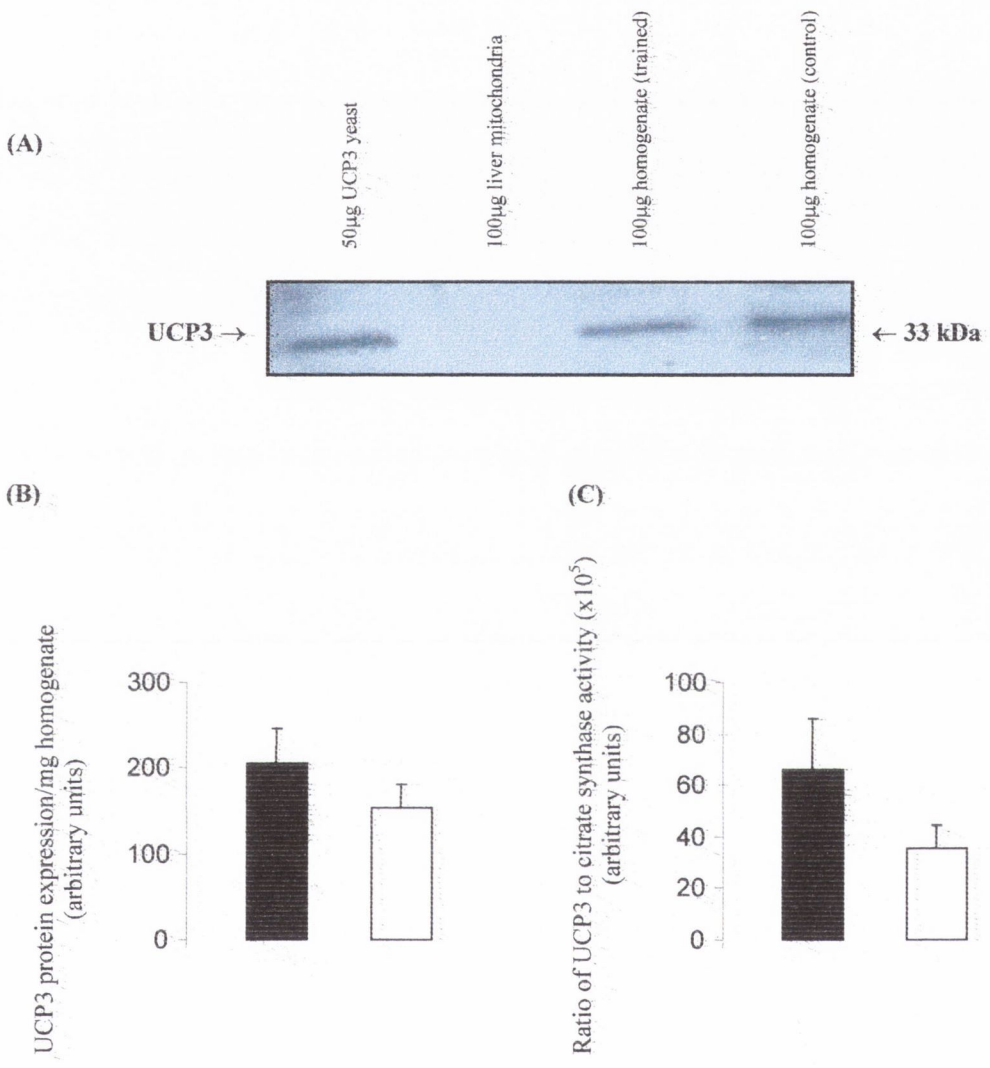


Figure 3.2.14: Effect of 17-weeks endurance swimming training on expression of UCP3 protein in *EDL* homogenate.

Mice were either kept sedentary (■) or exercised (□) by swimming for 17 weeks. Twenty-two hours after the final exercise bout *EDL* muscle was excised and homogenates were prepared as described in section 2.7. An immunoblot illustrating UCP3 protein expression in *EDL* homogenate is shown 3.2.14 **(A)**. The bar chart **(B)** illustrates UCP3 protein expression per mg *EDL* muscle homogenate. The bar chart **(C)** shows the relative expression of UCP3 protein to citrate synthase activity in *EDL* homogenates. Data are expressed as mean ± S.E.M. of 3 - 4 mice.

homogenates. UCP3 protein was not detected in mouse liver mitochondria. Figure 3.2.14 **(B)** shows absolute UCP3 protein expression in *EDL* muscle homogenates isolated from control and trained animals. Figure 3.2.14 **(C)** illustrates the expression of UCP3/unit mass of mitochondria in *EDL* muscle homogenates excised from control and trained animals. Data is expressed as mean ± S.E.M. of 4 and 3 independent observations for control and trained animals respectively.

[3.3] Discussion

The primary physiological role of UCP3 is unclear, as is the mechanism by which its expression is rapidly and substantially increased in fuel-depleted states due to, among other factors, exercise. Previously published studies indicate that UCP3 mRNA and protein expression are increased by acute exercise (Tsuboyama *et al.*, 1998; Cortright *et al.*, 1999; Zhou *et al.*, 2000; Jones *et al.*, 2003;) and are decreased by endurance training (Boss *et al.*, 1998b; Schrauwen *et al.*, 1999) in both rat and mouse skeletal muscle. In the present study, we therefore sought to better understand the effect of exercise on UCP3 protein expression in a number of mouse skeletal muscle types using two models of exercise, acute and endurance.

Many studies have been performed on the metabolic regulation of BAT and skeletal muscle UCP3 mRNA expression, both in humans and rodents. For example, starvation, exercise, leptin and thyroid status have all been investigated as possible regulators of UCP3 in BAT and skeletal muscle (Boss *et al.*, 1998c; Muzzin *et al.*, 1999; Boss *et al.*, 2000). Very few studies, however, have focussed on the regulation of UCP3 expression at the protein level. One of the main reasons for this void is the lack of antibodies specific for UCP3. In this study we use a peptide antibody, designed by members of our laboratory, specific for UCP3 over UCP1 and UCP2 and other mitochondrial transporters (Cunningham *et al.*, 2003). The peptide was synthesised, coupled to adjunct and antibodies were raised to it by Eurogentec. This study examined UCP3 protein expression in a number of skeletal muscle homogenates. The antibody used was sensitive enough to pick up a UCP3 protein signal even in crude homogenates which obviated the need to sacrifice large numbers of animals in order to isolate mitochondria from each of the muscle types.

Neither citrate synthase activity (Figure 3.2.2) nor $F_1\beta$ expression (Figure 3.2.3), both of which act as markers of mitochondrial density, was significantly altered by the acute swimming program in any of the four muscle types tested. Previously, mild exercise, such as that used in this study, was found to have no effect on the levels of respiratory enzymes, such as succinate dehydrogenase, in rat *gastrocnemius* muscle (Holloszy, 1967). These results concur with our data and suggest that the failure of our study to show increases in respiratory enzyme activity following acute exercise resulted from the use of

an insufficient exercise stimulus. In contrast, an important metabolic adaptation following endurance training is the concomitant increase in mitochondrial density and respiratory enzyme activity in skeletal muscle (Holloszy, 1967; Holloszy and Coyle, 1984; Murakami *et al.*, 1994). In particular, citrate synthase activity has been used as a reliable and stable measure of mitochondrial variation upon physical training (Murakami *et al.*, 1994; Boss *et al.*, 1998b). Previously, citrate synthase activity was shown to increase by 39 % and 31 % in rat *tibialis anterior* and rat *plantaris* respectively in response to 8 weeks treadmill running (Boss *et al.*, 1998b). Similar running training in rats (3, 6, 12 weeks) has resulted in significant increases (13 %, 28 %, 47 %) in citrate synthase activity in *soleus* muscle (Murakami *et al.*, 1994). Our results show a significant 26 % increase in citrate synthase activity in *plantaris* muscle homogenate after the 17 week training protocol verifying the results of Boss *et al.* (1998b) (Figure 3.2.10). It has been suggested that *plantaris* muscle is the major load bearing muscle in rodents during swimming which may explain why we see significant increases in citrate synthase activity in this muscle type only. There is also a trend towards greater citrate synthase activity in the other 3 muscle types after the training regime although the increases are not significant. Taken together with the body mass data (Figure 3.2.8), which shows a significantly lower body mass in the trained mice compared with the sedentary mice, our results confirm that the training program used here was effective since citrate synthase activity is also routinely used as a marker of training effectiveness (Boss *et al.*, 1998b). Mitochondria from muscles of trained animals have been shown to exhibit high levels of respiratory control and tightly coupled oxidative phosphorylation (Holloszy and Coyle, 1984). This has provided evidence that the increase in electron transport capacity is associated with concomitant rises in the capacity to generate ATP via oxidative phosphorylation *i.e.* increasing citrate synthase levels are consistent with this. This adaptation may partially account for the increase in aerobic work capacity that occurs with regularly performed, prolonged exercise.

We compared the whole body, resting oxygen consumption rates of trained and untrained mice at different stages during the 17 week endurance-training program. No significant differences in resting oxygen consumption were observed when control mice were compared to trained mice at 0, 6 or 16 weeks (Figure 3.2.9). However, there was a significant reduction in resting oxygen consumption at 6 and 16 weeks into the training program, in both the trained and control groups when compared with the pre-exercise

training values. This time dependent decrease in oxygen consumption is consistent with previous studies (Houlden, 1988).

Tsuboyama *et al.* (1998) reported an 18-fold increase in UCP3 mRNA in *gastrocnemius* muscle isolated from acutely exercised mice killed 3 hours post exercise. The increase in UCP3 mRNA was short-lived, falling to sedentary levels in a subset of exercised animals killed 22 hours post exercise. The data presented in this study suggest that both absolute UCP3 protein expression and UCP3/unit mass of mitochondria protein expression are up-regulated in *gastrocnemius* muscle homogenates in response to acute exercise (Figure 3.2.4). However, the increase in UCP3 protein observed is transitory and disappears within 22 hours. Our study has provided novel results, using a UCP3 specific antibody, showing that the transient effects of acute exercise on UCP3 mRNA in *gastrocnemius* muscle observed by Tsuboyama *et al.* (1998) are also evident at a protein level. In addition, we can confidently dispel concerns that the shifts in UCP3 protein expression observed are in fact due to increasing levels of mitochondria alone. Zhou *et al.* (2000) described increases in UCP3 mRNA and protein expression in rat hind-limb muscle following short term swimming and treadmill running protocols. However, unlike in our study, Zhou *et al.* (2000) do not correct their data for variations in mitochondrial density due to exercise. Furthermore, our study investigated the effects of acute exercise in a number of muscle types of differing muscle fibre composition rather than examining hind-limb muscle as a whole. Cortright *et al.* (1999) presented results that revealed increases of 252 % and 63 % in rat UCP3 mRNA in white and red *gastrocnemius* respectively after an acute bout of treadmill running. UCP3 mRNA was also elevated in mouse *gastrocnemius* following acute exercise but to a lesser extent (Cortright *et al.*, 1999).

In contrast to our *gastrocnemius* data, Jones *et al.* (2003) and Schrauwen *et al.* (1999), who both looked at UCP3 mRNA and protein expression relative to mitochondrial density, reported no significant affect of acute exercise on skeletal muscle UCP3. Jones *et al.* (2003) reported an immediate increase in UCP3 protein expression in rat *triceps* muscles after a 2 x 3-hour bout of swimming exercise. However, this increase in UCP3 was paralleled by a concomitant increase in mitochondrial marker enzyme (COX subunit 1 and cytochrome c). These results led the authors to conclude that the apparent increase in UCP3 in response to acute exercise may in fact reflect an overall increase in mitochondrial

biogenesis. Schrauwen *et al.* (1999) examined the effects of an acute cycling test on UCP3 mRNA in *vastus lateralis* muscles of healthy male volunteers. This group corrected their data for exercise induced changes in mitochondrial density using cytochrome-b and consequently saw no change in UCP3 mRNA expression with acute exercise. In both studies it would appear that UCP3, a mitochondrial component, increased as a component of the exercise induced increase in muscle mitochondria. Our *gastrocnemius* data disputes their findings suggesting that the increases in UCP3 protein that we observed were independent of increases in mitochondrial density post exercise in this muscle type. However, the *plantaris* data collated during the course of this study substantiates their theory that the increases in UCP3 protein observed are in fact due to increased mitochondrial density. Absolute UCP3 protein expression is elevated in *plantaris* muscle of mice killed 3-hours post exercise and this increase is sustained 22-hours after final exercise bout. This increase in *plantaris* muscle is not evident once changes in mitochondrial density have been taken into account. Short-term acute exercise resulted in no significant changes in UCP3 protein expression in *soleus* or EDL muscles either before or after exercise induced changes in mitochondrial density were taken into account.

Our finding that UCP3 protein is elevated in *gastrocnemius* muscle homogenates after 2-weeks swimming is inconsistent with a thermoregulatory role for skeletal muscle UCP3 during or after acute exercise. Clearly, increasing the levels of UCP3 protein at a time when metabolic heat should be dissipated rather than generated is unwise. However, these data do support an association between changes in energy substrate levels (*i.e.* fatty acids) and UCP3 expression. Previously, Weigle *et al.* (1998) reported that elevation of free fatty acids by intralipid infusion resulted in up-regulation of UCP3 mRNA in skeletal muscle. In an attempt to resolve the paradoxical situation where starvation and acute exercise up-regulate UCP3 protein expression Weigle *et al.* (1998) suggested that UCP3 up-regulation may be linked to use of free fatty acids as a fuel rather than to the increased need of the organism to dissipate energy. The up-regulation of UCP3 protein in *gastrocnemius* muscle by acute exercise seen in this study is in agreement with their free fatty acid hypothesis since increased use of lipids and carbohydrates during and after exercise is well known (Brooks and Mercier, 1994). It is possible that increased lipid oxidation rather than glucose oxidation becomes the major stimulus for acute exercise

induced UCP3 up-regulation. Thus the function of skeletal muscle UCP3 may be to act as an acute regulator of lipid metabolism.

A study by Boss *et al.* (1998b) reported that chronic, endurance exercise actually down-regulated UCP3 mRNA expression in *tibialis anterior* and *soleus* muscles of rats. These results were mirrored in studies on human muscle mRNA by Schrauwen *et al.* (1999). When expressed relative to cytochrome-b, *vastus lateralis* UCP3 mRNA expression decreased in trained compared with untrained subjects (Schrauwen *et al.*, 1999). This potentially means, if UCP3 is a functional uncoupler, that there is less uncoupling between ATP synthesis and oxygen consumption in the trained subjects, allowing for higher energy efficiency. A negative correlation, independent of cytochrome-b expression, was also observed between maximal performance and $UCP3_L$ expression (Schrauwen *et al.*, 1999). The hypothesis here is that the decreased UCP3 mRNA per mitochondria in trained subjects and the inverse relationship of $UCP3_L$ and mechanical efficiency that endurance exercise training produces might bring about adaptive physiological responses in skeletal muscles improving energy efficiency. In contrast, Cortright *et al.* (1999) reported no change in UCP3 mRNA expression following a 9-week wheel running program. The present study reports no significant changes in UCP3 protein expression in any of the muscle types tested after the endurance training protocol, supporting the findings of Cortright *et al.* (1999). Given that food consumption post exercise was not monitored in this study, the possibility of differences in feeding behaviour accounting for the disparity in the findings between the studies cannot be excluded. To illustrate, male rats rebound from forced running, given sufficient rest period, by increasing their food intake (Cortright *et al.*, 1999). The potential for the effects of refeeding, which has been shown to decrease UCP3 mRNA in muscle after only 24-hours (Gong *et al.*, 1997), may in part explain the differences in UCP3 mRNA expression observed by different groups.

Another hypothesis regarding the biological role of UCP3 in skeletal muscle is that it has no significant uncoupling function under physiological conditions but serves to transport superoxide anions as a component of the defence mechanism against reactive oxygen species (ROS) (Boss *et al.*, 2000; Echtay *et al.*, 2002). Increasing levels of ROS production are seen during endurance training (Du *et al.*, 1998; Bejma and Ji, 1999). ROS are elevated during exercise as a result of increases in substrate oxidation (Kowaltowski

and Vercesi, 1999). ROS production can lead to the irreversible damage of mitochondrial DNA, membrane lipids and proteins leading to mitochondrial dysfunction and cell death (Skulachev, 1996; Chakraborti *et al.*, 1999; Kowaltowski and Vercesi, 1999). If the concept of UCP3 as a component in the defence mechanism against ROS production is to be believed, one would expect our results to indicate that endurance exercise training results in an increase in skeletal muscle mitochondria that have normal capacity to protect against ROS production by the up-regulation of UCP3 and the consequential UCP3 mediated transport of superoxide anions. We have shown that UCP3 protein expression is unaffected by endurance training (Figures 3.2.11 – 3.2.14) after differences in mitochondrial density have been accounted for suggesting a different role for UCP3.

To date, evidence that UCP3 is a physiological regulator of thermogenesis remains weak. In fact, it would seem that experimental support for this function is stronger in UCP2, a UCP1 homologue (Nègre-Salvayre *et al.*, 1997; Cortez-Pinto *et al.*, 1999; Arsenijevic *et al.*, 2000). Our data would be more consistent with a role for UCP3 in the short-term regulation of fatty acid metabolism, a role which becomes obsolete in more long-term endurance type exercise.

[3.4] Conclusions

This study has shown the novel findings that UCP3 protein expression per unit mass of mitochondria is up-regulated by acute exercise in *gastrocnemius* muscle of mice. It also shows that this increase is transient with levels returning to pre-exercise levels 22-hours after the final exercise bout.

The study confirms the previously published findings that endurance exercise results in no significant changes in skeletal muscle UCP3 protein expression.

The study also confirms the presence of UCP3 protein in skeletal muscle mitochondria and verifies that liver homogenates contain no UCP3.

Our findings are consistent with a role for UCP3 in lipid utilisation rather than thermogenesis.

Chapter 4
Detection of UCP 1 protein expression using Western Blot analysis

[4.1] Introduction

Adaptation of rodents to cold environments involves a physiological process called non- shivering thermogenesis. Brown adipose tissue (BAT) plays the principal role in this response through its capacity to produce heat by uncoupling oxidative phosphorylation from ATP synthesis (Heaton *et al.*, 1978). BAT non-shivering thermogenesis is activated in response to cold exposure or chronic over-eating and depends largely on the activity of UCP1. Consequently, UCP1 is strongly induced by cold exposure. The thermoregulatory role of UCP1 has been emphasized in UCP1 deficient mice, whose resistance to cold is impaired (Enerback *et al.*, 1997; Matthias *et al.*, 1999; Nedergaard *et al.*, 2001b).

The development of high thermogenic capacity in BAT mitochondria isolated from cold-acclimated rats, mice and guinea pigs is characterized by a marked increase in the expression of UCP 1 protein (Ricquier and Kader, 1976; Desautels *et al.*, 1978; Heaton *et al.*, 1978; Swick & Swick, 1986; Sundin *et al.*, 1987; Klaus *et al*, 1991; Nicholls & Rial, 1999; Nedergaard *et al.*, 2001a & 2001b). The fully cold acclimated state is achieved after approximately 3-weeks in the rat (Desautels *et al.*, 1978) and is characterised by a 6–8 fold increase in total cellular mitochondrial mass of BAT (Himms-Hagen, 1986). The concentration of UCP1 is at a minimum at thermoneutrality (27 – 29°C in the laboratory rat) and increases more or less linearly with decreasing temperature (Himms-Hagen, 1986). It is estimated that UCP1 represents 12–15 % of the inner membrane protein of mitochondria from cold acclimated hamsters and rats when measured by immunoassay (Lin and Klingenberg, 1980; Ricquier *et al.*, 1982).

Initial studies of the bioenergetic properties of mitochondria gave rise to the hypothesis that uncoupling protein is brown fat specific (Nicholls and Locke, 1984). This was purportedly confirmed when no significant quantities of UCP1 transcript or protein were detected in immunological studies of liver, heart, epididymal or parametrial white fat, thymus or skeletal muscle (Cannon *et al.*, 1982; Ricquier *et al.*, 1983; Nègre-Salvayre *et al.*, 1997). However, recently studies have appeared in the literature claiming to show UCP1 transcript and protein expression in tissues other than BAT. UCP1 mRNA was detected in the liver of newborn and adult rats after cold exposure (Shinohara *et al.*, 1991). A second study suggests that the β_3-adrenergic agonist, CL316243, induces a functionally

active uncoupling protein in white fat and slow twitch muscle fibres (Yoshida *et al.* 1998). Nibbelink *et al.* (2001) reported that UCP 1 protein was expressed in uterine longitudinal smooth muscle cells. However, the results of Nibbelink *et al.* (2001) were convincingly discredited by Rousset *et al.* (2003). Our laboratory has yielded novel, well-substantiated results illustrating the presence of UCP1 mRNA and protein in thymus mitochondria and UCP1 protein in thymus cell (thymocyte) mitochondria (Carroll *et al.*, 2005). UCP1 expression was established using a commercially available (Calbiochem), polyclonal anti-UCP1 antibody. Specificity of the UCP1 antibody, over UCP2 and UCP3, was established (Carroll *et al.*, 2005). Starvation, a physiological condition which has previously been shown to decrease UCP1 protein expression in BAT mitochondria (Rothwell *et al.*, 1984; Trayhurn and Jennings, 1988; Boss *et al.*, 1998a; Nedergaard *et al.*, 2001a), had no effect on UCP1 expression in thymocyte or thymus mitochondria isolated from fasted rats, compared to fed controls (Carroll *et al.*, 2005). This novel finding of UCP1 expression in rat thymus has been supported by (1) functional studies (2) GDP binding studies, both of which I discuss further in forthcoming chapters (see Chapters 5 & 6), and (3) purification studies (Carroll *et al.*, 2005).

This study seeks to discover whether (a) there is UCP1 expression in mice, (b) whether there is a differential UCP1 expression in mice from the specific pathogen free (SPF) animal facility when compared to the non-SPF mice and (c) whether UCP1 expression in rat thymus is increased after cold acclimation (as has been observed for UCP1 in BAT). Liver mitochondria and BAT mitochondria isolated from UCP1 KO mice are used as negative controls for UCP 1 protein expression. Mitochondria isolated from tissues that constitutively express UCP2 (kidney & spleen) and UCP3 (spleen and skeletal muscle) were also used as controls in this study.

[4.2] Results

Figure 4.2.1 **(A)** shows the anti-UCP1 antibody (Calbiochem) detecting UCP1 protein in BAT and thymus mitochondria isolated from C57BL/6J wild type (WT) mice. UCP1 protein was not detected in BAT or thymus mitochondria isolated from C57BL/6J UCP1 knockout (KO) mice. UCP1 was not detected in liver or kidney mitochondria isolated from WT or from KO mice. $F_1\beta$ expression is shown in Figure 4.2.2 **(B)**.

Figure 4.2.2 **(A)** shows the anti-UCP1 peptide antibody (Calbiochem) detecting UCP1 protein expression in thymus mitochondria isolated from non-specific pathogen free (non-SPF), CD1 mice at varying concentrations (20,40,60,80μg). UCP1 expression was also detected, but to a lesser degree, in thymus mitochondria isolated from specific pathogen free (SPF), C57BL/6J mice at varying concentrations (20 & 40 μg). BAT mitochondria isolated from non-SPF, CD1 mice were also shown to express UCP1. Figure 4.2.1 **(B)** shows that any changes in UCP1 expression in thymus mitochondria due to immunological condition are independent of inaccurate lane loading as indicated by $F_1\beta$ antibody.

Figure 4.2.3 **(A)** shows an anti-UCP1 antibody (Calbiochem) detecting UCP1 protein in BAT mitochondria isolated from both room temperature and cold acclimated rats. UCP1 protein was not detected in rat liver mitochondria isolated from either group. Figure 4.2.3 **(B)** shows $F_1\beta$ expression in rat liver mitochondria and rat BAT mitochondria isolated from animals housed at room temperature and at 4^0C for 5 weeks. Figure 4.2.3 **(C)** shows the relative abundance of UCP1 protein expression as a ratio to $F_1\beta$, as determined by densitometry. Cold acclimation induced a significant ($p \leq 0.05$; $n=3$) 1.7 fold increase in UCP1 protein expression in BAT mitochondria as shown in Figure 4.2.3 **(C)**. Statistical difference was determined using an unpaired Student's t-test. The statistically significant increases observed in UCP1 protein expression levels in BAT mitochondria following cold acclimated cannot be accounted for by differences in lane loading, as indicated by an antibody to the β-subunit of the F_1-ATP synthase.

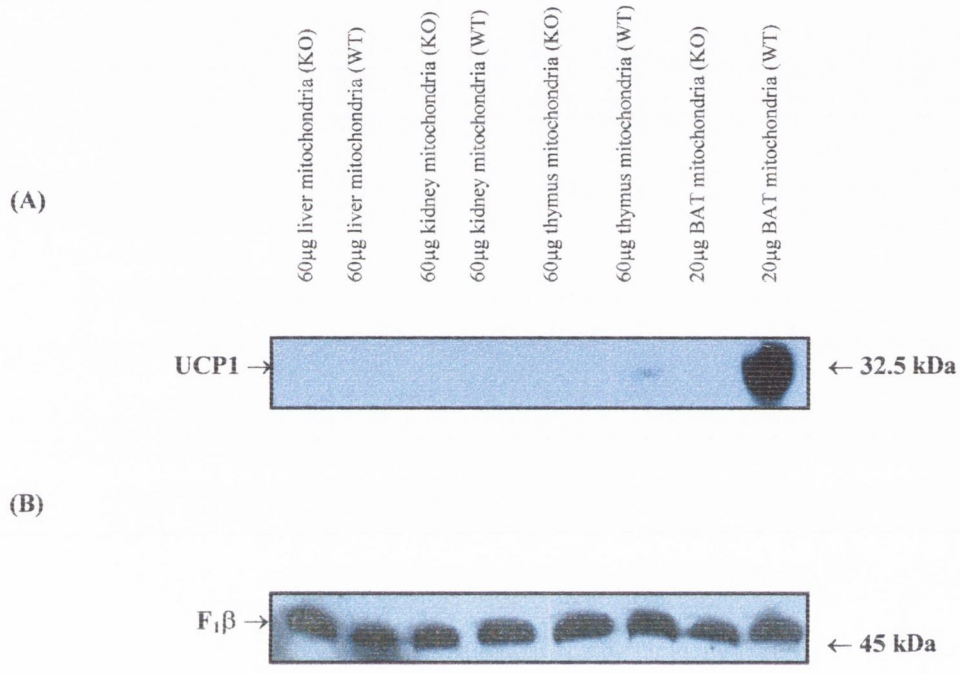


Figure 4.2.1: UCP1 is expressed in thymus mitochondria isolated from WT C57BL/6J mice but is not detected in thymus mitochondria from UCP1 KO C57BL/6J mice.

BAT, thymus, kidney and liver mitochondria were isolated from wild type (WT) and UCP1 knock-out (KO) C57BL/6J mice as described in section 2.8. Mitochondria were subjected to SDS-PAGE and Western blotted using in **(A)** an anti-UCP1 peptide antibody (Calbiochem) and in **(B)** an antibody to the β-subunit of the F_1-ATP synthase. A representative immunoblot depicting detection of UCP1 in WT BAT and WT thymus mitochondria is shown. UCP1 was not detected in KO BAT or KO thymus mitochondria. No UCP1 was detected in liver and kidney mitochondria isolated from WT or KO mice.

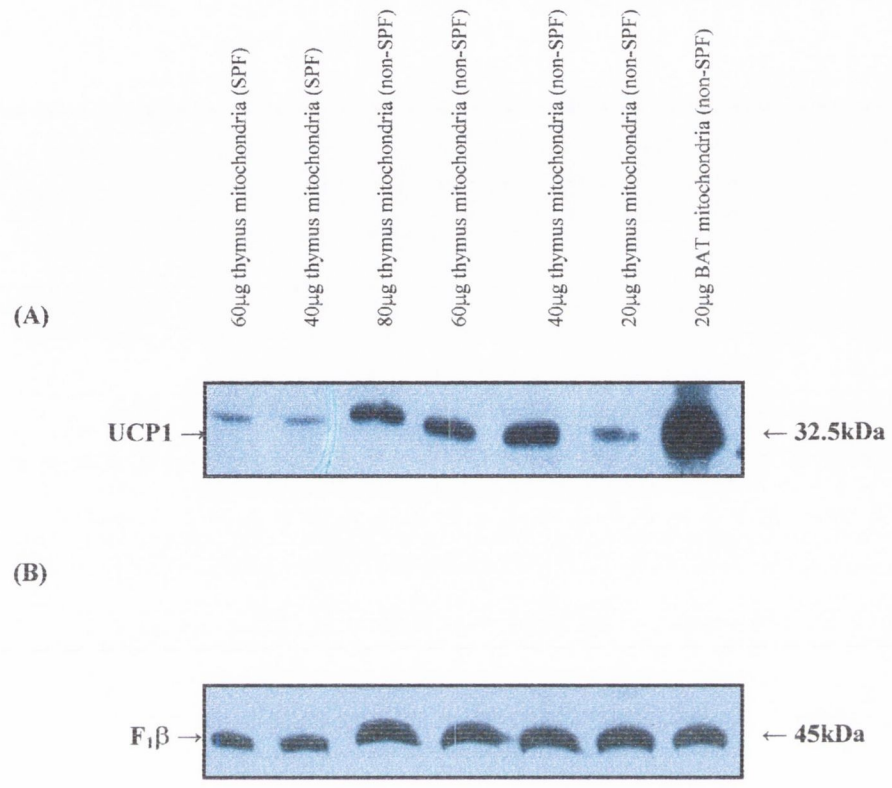


Figure 4.2.2: UCP1 is expressed in thymus mitochondria isolated from specific pathogen free (SPF) and non-SPF mice.

BAT and thymus mitochondria were isolated either from specific pathogen free, CD1 mice or non-specific free C57BL/6J mice as described in sections 2.8.1 & 2.8.5. Mitochondria were subjected to SDS-PAGE and Western blotted using in **(A)** an anti-UCP1 peptide antibody (Calbiochem) or in **(B)** an antibody to the $F_1\beta$ subunit of the ATP synthase.

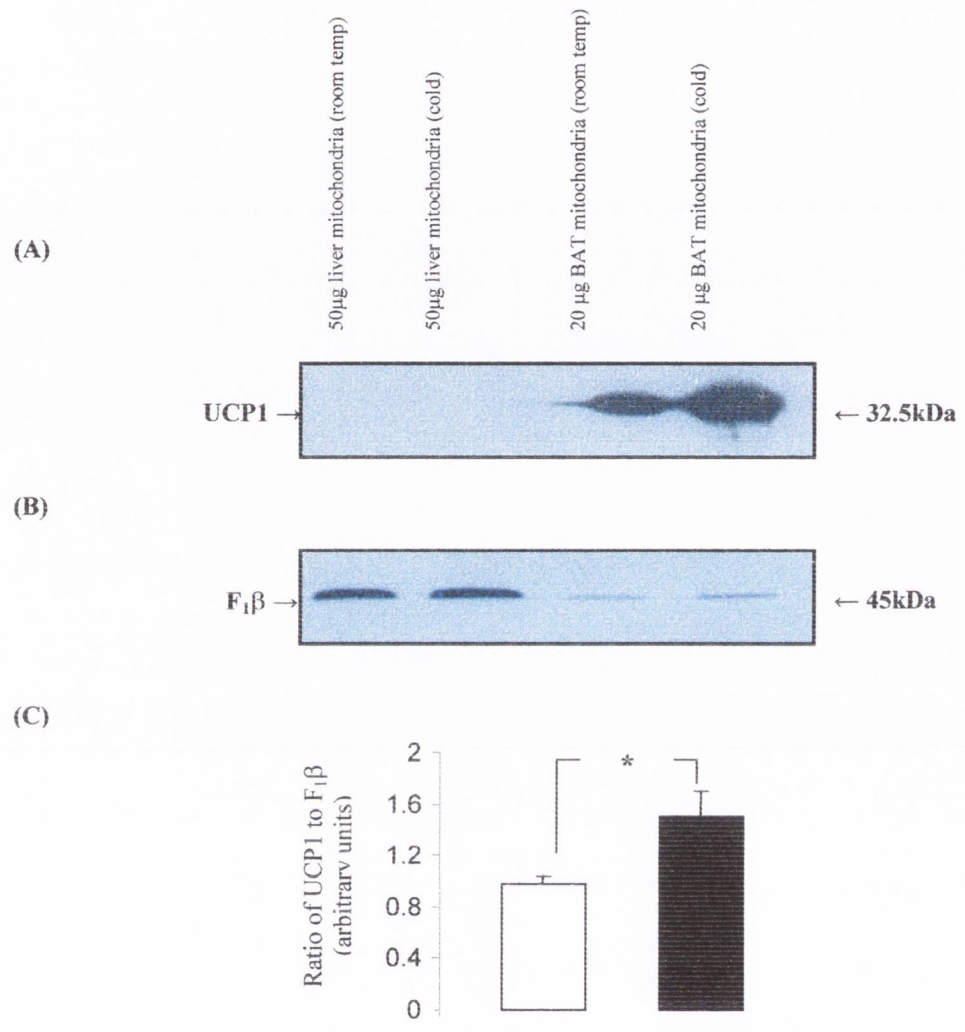


Figure 4.2.3: UCP1 is expressed in BAT mitochondria isolated from room temperature and cold acclimated rats but is not detected in liver mitochondria isolated from these groups.

Mitochondria were isolated either from rats housed at room temperature (□) or at 4°C (■) for 5 weeks. Mitochondria were then subjected to SDS-PAGE and Western blotted using a commercially available anti-UCP1 peptide antibody (Calbiochem) or an antibody to the $F_1\beta$ subunit of the ATP synthase. Figure 4.2.3 **(A)** is a representative immunoblot showing detection of UCP1 in BAT mitochondria isolated from the room temperature and cold acclimated rats. UCP1 was not detected in liver mitochondria from either group. Figure 4.2.3 **(B)** is a typical immunoblot illustrating expression of $F_1\beta$ in liver and BAT mitochondria isolated from room temperature and cold acclimated rats. Figure 4.2.3 **(C)** illustrates the relative expression of UCP1 protein to $F_1\beta$ in room temperature and cold acclimated BAT mitochondria as determined by densitometry. Data are expressed as a mean ± S.E.M. (n=3). Statistical differences are given as $*p \leq 0.05$ as determined by unpaired Student's t-test.

Figure 4.2.4 shows the Calbiochem anti-UCP1 antibody detecting UCP1 in BAT mitochondria isolated from rats housed at room temperature. UCP1 protein was not detected in spleen (UCP2 & 3), kidney (UCP2) or skeletal muscle (UCP3) mitochondria isolated from the room temperature or the cold acclimated rats.

Figure 4.2.5 **(A)** shows the Calbiochem anti-UCP1 antibody detecting UCP1 protein in thymus mitochondria isolated from rats housed at room temperature and in rats housed at 4°C for 5 weeks. UCP1 was also detected in BAT mitochondria isolated from cold acclimated rats. UCP1 protein was not detected in liver mitochondria isolated from cold acclimated rats. Figure 4.2.5 **(B)** shows $F_1\beta$ expression in liver, BAT and thymus mitochondria isolated from cold acclimated rats and in thymus mitochondria isolated from rats housed at room temperature. Figure 4.2.5 **(C)** illustrates the relative abundance of UCP1 protein expression as a ratio of $F_1\beta$, as determined by densitometry. Data is expressed as mean ± S.E.M. Cold exposure for 5 weeks induced a significant ($p=0.0205^*$; $n=3$) 1.7 fold increase in UCP1 protein expression in thymus mitochondria when compared to thymus mitochondria isolated from room temperature rats. Statistical analysis was determined using an unpaired Student's t-test. Changes in UCP1 expression due to cold acclimation in thymus mitochondria cannot be accounted for by differences in lane loading, as indicated by an antibody to the β-subunit of the F_1-ATP synthase.

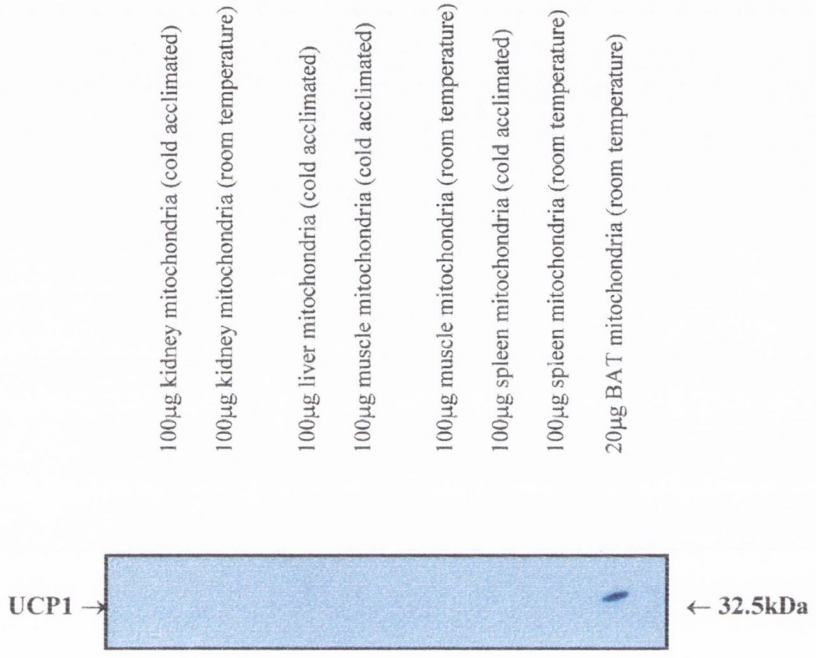


Figure 4.2.4: UCP1 is not detected in spleen, muscle or kidney mitochondria isolated from room temperature and cold acclimated rats.

Mitochondria were isolated from room temperature and cold acclimated rats as described in section 2.8. Mitochondria were then subjected to SDS-PAGE and Western blotted using an anti-UCP1 peptide antibody (Calbiochem). UCP1 protein was detected in room temperature BAT mitochondria but was not detected in spleen, kidney or muscle mitochondria isolated from either the room temperature or the cold acclimated rats.

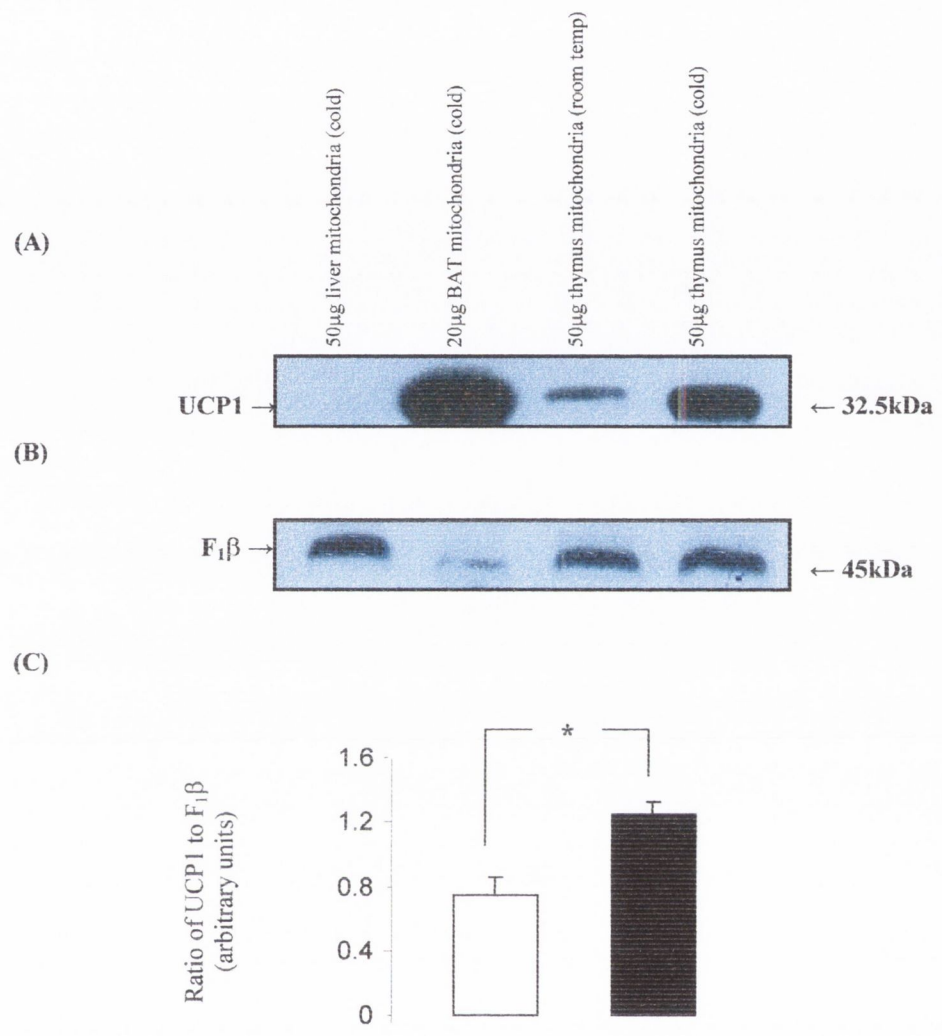


Figure 4.2.5: UCP1 protein expression is increased in thymus mitochondria isolated from rats acclimated to the cold for 5 weeks.

Thymus mitochondria were isolated either from rats housed at room temperature (□) or at 4°C (■) for 5 weeks as described in section 2.8.5. Mitochondria were subjected to SDS-PAGE and Western blotted using in **(A)** an anti-UCP1 (Calbiochem) peptide antibody or in **(B)** an antibody to $F_1\beta$. The bar chart **(C)** illustrates the relative expression of UCP1 protein to $F_1\beta$ in thymus mitochondria isolated from room temperature and cold acclimated rats. A significant 1.7-fold increase in UCP1 protein expression was observed in thymus mitochondria isolated from cold acclimated rats when compared to the room temperature animals. Data is expressed as mean ± S.E.M of 3 rats. Statistical differences are given as $^*p \leq 0.05$ as determined by unpaired Student's t-test.

[4.3] Discussion

In mammalian BAT, non-shivering thermogenesis is explained by uncoupling mitochondrial ATP synthesis from respiration. This phenomenon in the intact animal is fully dependent on the presence of UCP1 as UCP1 allows proton re-entry into the matrix, and thus dissipates the mitochondrial proton electrochemical gradient generated by the electron transport chain, the net result being the production of heat (Rial *et al.*, 1999).

In the present study, we have examined BAT, thymus, liver and kidney mitochondria isolated from C57BL/6J mice in which the UCP1 gene has been genetically knocked out. The Calbiochem UCP1 antibody used previously by Carroll *et al.* (2005) to successfully detect UCP1 in thymus and thymus cell (thymocyte) mitochondria was used in this study also. UCP1 protein was detected in BAT mitochondria isolated from C57BL/6J WT mice (Figure 4.2.1). Using the same amount of protein, no UCP1 signal was obtained in BAT mitochondria isolated from UCP1 KO mice, undoubtedly indicating that the signal detected in the WT mice using the Calbiochem antibody is indeed UCP1. UCP1 protein was not detected in liver or kidney mitochondria isolated from either the WT or UCP1 KO mice. The lack of UCP1 detection in liver and kidney mitochondria from the WT mice is to be expected since liver and kidney mitochondria do not constitutively express UCP1 (Ricquier and Bouillaud, 1986 & 2000; Peachey *et al.*, 1988; Matthias *et al.*, 1999; Nedergaard *et al.*, 2001a) although kidney does constitutively express UCP2 while liver doesn't express any UCPs.

Previously, members of our laboratory have shown that UCP1 mRNA and protein are present in rat thymus and rat thymocyte mitochondria (Carroll *et al.*, 2005). Using the KO and WT mice I have been able to show for the first time that UCP1 protein is detected in thymus mitochondria isolated from the WT but not the UCP1 KO mice (Figure 4.2.1). While UCP1 has been exclusively associated with brown adipose tissue (Nicholls and Locke, 1984; Nicholls, 2001), atypical expression of UCP1 mRNA and protein has also been described in liver (Shinohara *et al.*, 1991) and skeletal muscle (Yoshida *et al.*, 1998). These observations have since been attributed to cross detection between the different UCPs (Rousset *et al.*, 2003). However, in the present study this is unlikely since the UCP1 signals were firstly, not detected in any other UCP containing tissues other than thymus and

BAT and secondly, were not detected in thymus or BAT mitochondria isolated from UCP1 KO mice. This observation challenges the prevailing view that UCP1 expression is exclusive to BAT.

The thymus plays an important role in innate immunity, in determining self-antigens from non-self antigens and is the site of T-lymphocyte maturation and differentiation. We predicted that there would be greater expression of UCP1 in the thymus of mice in the non-SPF unit compared with those held in the SPF unit, if UCP1 has a role in thymus immune function. While every effort is made to keep the non-SPF unit infection free, inevitably, some infections do exist. We found that UCP1 protein expression was higher in the non-SPF mice when compared to the SPF mice (Figure 4.2.2). We suggest that UCP1 is up-regulated in thymus mitochondria in response to non-specific infection.

Using the specific Calbiochem UCP1 antibody, we were able to observe the expected increase in UCP1 protein in BAT mitochondria upon cold acclimation (Figure 4.2.3). Our results show a significant ($p \leq 0.05$) increase (1.7 fold) in UCP1 protein expression in BAT mitochondria isolated from cold acclimated rats when compared to BAT mitochondria isolated from room temperature rats. Our finding correlates well with results obtained by other authors in the literature (Desautels *et al.*, 1978; Heaton *et al.*, 1978; Swick & Swick, 1986; Sundin *et al.*, 1987; Klaus *et al*, 1991; Nicholls & Rial, 1999; Nedergaard *et al.*, 2001a). Despite the fact that Shinohara *et al.* (1991) reported the discovery of UCP1 mRNA in adult rat liver post 1-week cold exposure (4°C), our study reports that UCP1 protein was not detected in adult liver isolated from either room temperature housed or cold exposed rats. In addition, the present study reports that no UCP1 protein was detected in spleen, kidney or skeletal muscle mitochondria isolated from rats housed at either room temperature or 4°C (Figure 4.2.4).

Our results confirm the discovery by Carroll *et al.* (2005) that UCP1 protein is constitutively expressed in thymus mitochondria isolated from rats housed at room temperature. More remarkably however, we show for the first time that UCP1 is present in mouse thymus mitochondria and is significantly ($p \leq 0.05$) up-regulated (1.7 fold) following 5 weeks cold exposure in rats (Figure 4.2.5). A major feature of BAT UCP1 expression is its induction by low temperatures (Ricquier and Kader, 1976; Desautels *et al.*, 1978;

Heaton *et al.*, 1978; Swick & Swick, 1986; Sundin *et al.*, 1987; Klaus *et al*, 1991; Nicholls & Rial, 1999; Nedergaard *et al.*, 2001a & 2001b). Cold exposure has now been shown to strongly induce UCP1 protein in thymus mitochondria as well.

[4.4] Conclusion

In conclusion, our study has shown the novel finding that UCP1 protein is expressed in thymus mitochondria isolated from WT but not UCP1 KO mice. In addition, we provide some preliminary evidence suggesting that the immunological condition of the animal may have some bearing on the role of UCP1 in thymus mitochondria. Furthermore, we show for the first time that cold exposure (5 weeks) up-regulates the expression of UCP1 protein in thymus mitochondria. We also confirm the up-regulation of UCP1 protein in BAT mitochondria post cold exposure and the lack of expression of UCP1 protein in liver, spleen, kidney and skeletal muscle.

We propose that UCP1 expression can no longer be considered as being restricted to BAT and that it is in fact expressed in thymus mitochondria also. The exact role of UCP1 in thymus mitochondria has yet to be revealed. However, the occurrence of UCP1 protein in thymus mitochondria has uncovered an innovative route into the bioenergetics and metabolic function of these immunologically important cells.

Chapter 5

The effect of fatty acids and purine nucleotides on UCP function in cold acclimated rats

[5.1] Introduction

The mitochondria of brown adipose tissue (BAT) are equipped with a high oxidative capacity and are innately uncoupled due to the presence of UCP1. Isolated mitochondrial studies have revealed that BAT UCP1 uncoupling activity can be inhibited by diverse purine di- and triphosphate nucleotides (Rial *et al.*, 1983) and can be activated by medium to long chain fatty acids (Klingenberg and Huang, 1999). While the mechanism by which nucleotides inhibit UCP1 is understood, the method by which fatty acids activate UCP1 remains a matter of debate with two different research groups proposing two models of action; the fatty acid protonophore model (Garlid *et al.*, 1996) and the fatty acid buffering model (Winkler and Klingenberg, 1994). Both of these models are discussed in detail in Chapter 1 (see section 1.4.2). Physiologically, the fact that UCP1 activity can be inhibited and activated by purine nucleotides (GDP in the present study) and fatty acids (palmitate in this study) respectively may be important in allowing BAT to respond to acute changes in the animals need to produce heat in response to changes in environmental temperature.

UCP1 has been exclusively assigned to BAT mitochondria since its discovery in the late 1970s (Heaton *et al.*, 1978). Subsequent studies revealed that UCP1 protein expression in BAT mitochondria is increased upon cold exposure (Ricquier and Kadar, 1976) resulting in the non-shivering thermogenesis phenomenon associated with cold acclimated animals (Ricquier and Bouillaud, 1986). BAT mitochondria isolated from cold acclimated rats exhibit an increased capacity for fatty acid stimulated respiration (Nedergaard and Cannon, 1985) when compared to room temperature controls and show evidence of larger GDP suppressible respiration rates when succinate is used as the principal substrate (Desautels and Himms-Hagen, 1981). The increase in capacity of BAT mitochondria for uncoupled respiration is due to increased UCP1 expression in this tissue after cold exposure. Indeed, we have shown a 1.7-fold increase in expression of UCP1 protein in BAT mitochondria isolated from rats following our 5-week cold exposure study (see Chapter 4). Intriguingly, in our laboratory we have recently discovered UCP1 in thymus mitochondria isolated from room temperature rats (Carroll *et al.*, 2005). We established that a proportion of the state 4 oxygen consumption by thymus mitochondria isolated from rats housed at room temperature is GDP sensitive and fatty acid activatable in a manner similar to BAT

mitochondria (Carroll *et al.*, 2005). Since the present study has determined that the expression of thymus mitochondrial UCP1 protein is significantly increased (1.7-fold) in rats acclimatised to the cold for 5-weeks (see chapter 4), we sought to investigate whether thymus mitochondria, isolated from cold acclimated rats, are more sensitive to GDP-suppressible and palmitate-stimulated oxygen consumption than their room temperature counterparts, as is the case for BAT mitochondria.

Based upon the high sequence homology of UCP2 (59 %) and UCP3 (56 %) with UCP1, it is predicted that UCP1, 2 and 3 share a similar uncoupling function (Lowell, 1999). However, while the uncoupling capabilities of UCP1 are widely accepted, only circumstantial evidence exists purporting a role for UCP2 and UCP3 as uncouplers. Krauss *et al.*, (2002) has shown that endogenously expressed levels of UCP2 appear to mediate proton leak in intact thymocytes. Skeletal muscle mitochondria isolated from transgenic mice over-expressing UCP3 show a 2-3-fold increase in proton conductance compared to control mice (Cadenas *et al.*, 2000). Gong *et al.* (2000) and Vidal-Puig (2000) have both shown that skeletal muscle mitochondria, isolated from UCP3 knockout mice, are more coupled (*i.e.* show reduced proton leak). Furthermore, ecstasy induces a UCP3 dependent thermogenicity in mouse skeletal muscle (Mills *et al.*, 2003) and 4-hydroxy-2-*trans*-nonenal (HNE), a by-product of lipid peroxidation, induces GDP sensitive uncoupling in mitochondria isolated from tissues containing UCP1 (BAT), UCP2 (BAT and kidney) and UCP3 (BAT and skeletal muscle) (Echtay *et al.*, 2003). In addition, superoxide generated using xanthine and xanthine oxidase has been shown to increase proton transport through UCP1, UCP2 and UCP3 in a reaction that is inhibited by nucleotides including GDP (Echtay *et al.*, 2002&2002b). Nègre-Salvayre *et al.* (1997) showed that membrane potential and hydrogen peroxide (H_2O_2) production were increased in mitochondrial fractions isolated from UCP2 containing tissues (BAT, thymus and spleen) when pre-incubated in GDP. The uncoupling agent carbonyl cyanide m-chlorophenylhydrazone (CCCP) reversed the GDP effect leading the authors to suggest that their results may indicate that UCP2 acts as a regulator of H_2O_2 production in mitochondria. In contrast to the aforementioned evidence that UCP2 and UCP3 are functioning uncouplers, several reports have failed to show any uncoupling activity in mitochondria constitutively expressing UCP2 or UCP3 (Porter *et al.*, 1999; Cadenas *et al.*, 1999; Jekabsons *et al.*, 1999; Matthias *et al.*, 1999; Cadenas *et al.*, 2000; Cresenzo *et al.*, 2003). Our assay allows us to re-examine whether

there is a GDP sensitive and fatty acid activatable oxygen consumption in mitochondria from room temperature and cold acclimated rat tissues that contain (a) no UCPs (liver), (b) UCP1 (BAT) (c) UCP2 (BAT, kidney and spleen) and (c) UCP3 (BAT and spleen).

The assay used in this study is based on the method of Gonzalez-Barroso *et al.* (1998) and is ideal for investigating free fatty acid dependent UCP catalysed proton leak. In the assay, proton leak is measured indirectly using oxygen consumption rates (state 4) in the presence of Complex II substrate (succinate), an inhibitor of Complex I electron transport (rotenone), an inhibitor of ATP synthase activity (oligomycin) and an inhibitor of the adenine nucleotide carrier transport function (atractyloside). The assay medium also contains defatted bovine serum albumin which acts as a buffer for fatty acids resulting in concentrations of free fatty acids in the nanomolar range. Previously, similar oxygen consumption experiments have been successfully used to measure UCP1 catalysed uncoupling in cells and isolated mitochondria (Nicholls & Locke, 1984; Matthias *et al.*, 1999; Nedergaard *et al.*, 2001; Carroll *et al.*, 2005). Since this study sought to determine whether fatty acids have a stimulatory effect on oxygen consumption rates resulting from proton leak through UCPs, it was necessary to take precautions to minimise the presence of endogenous free fatty acids associated with the isolation of BAT mitochondria. Firstly, a 2 % de-fatted BSA wash was incorporated into the mitochondrial preparations. The de-fatted BSA was used to 'mop up' any free fatty acids released during the homogenisation stages of the mitochondrial preparations. Incorporation of de-fatted BSA in the isolation medium has been shown to be efficient in minimising the non-UCP dependent uncoupling effects of free fatty acids (Cadenas *et al.*, 1999; Lanni *et al.*, 1999; Matthias *et al.*, 1999). Secondly, fatty acid concentrations were buffered using a 1: 4 de-fatted BSA: fatty acid molar ratio. Gonzalez *et al.* (1998), have demonstrated that a 1: 4 de-fatted BSA: palmitate molar ratio results in a 40 nM concentration of free palmitate. Palmitate at this concentration (40 nM free) causes maximal stimulation of UCP1 uncoupling activity.

[5.2] Results

Figure 5.2.1 shows the effect of purine nucleotides and fatty acids on BAT mitochondria isolated from rats housed at room temperature. In the presence of adenine nucleotide carrier and ATP synthase inhibitors, the state 4 oxygen consumption rate (167.8 ± 14.2 nmoles O/min/mg protein) was significantly decreased 41 % (p=0.01**; n=3) by the addition of GDP (1 mM) (99.5 ± 7.5 nmoles O/min/mg protein). The addition of 64 μM palmitate (~ 40 nM free) significantly increased by 40 % (p=0.02*; n=3) the GDP sensitive state 4 oxygen consumption rate to 139.4 ± 7.5 nmoles O/min/mg protein. The maximal uncoupled oxygen consumption rate attained by the addition of 30 nM 2, 4-dinitrophenol (DNP) was 182.0 ± 5.7 nmoles O/min/mg protein.

This study also sought to reproduce the known effects of fatty acids and purine nucleotides on oxygen consumption rates in BAT mitochondria isolated from rats acclimated to the cold for 5-weeks. Figure 5.2.2 shows that the state 4 oxygen consumption rate (384.2 ± 8.8 nmoles O/min/mg protein) was significantly decreased 56 % (p=0.0012***; n=3) by the addition of 1 mM GDP (169.4 ± 18.2 nmoles O/min/mg protein) in the presence of inhibitors of the ATP synthase and adenine nucleotide carrier. The GDP sensitive state 4 rate was significantly increased 95 % (p=0.0016**; n=3) by the addition of 64 μM palmitate to 330.0 ± 4.0 nmoles O/min/mg protein, close to the maximal uncoupled rate achieved by addition of 30 nM DNP (406.3 ± 3.4 nmoles O/min/mg protein).

Figure 5.2.3 illustrates that state 4 oxygen consumption rates in thymus mitochondria isolated from rats kept at room temperature are sensitive to purine nucleotides and fatty acids. The steady-state oxygen consumption rate (28.0 ± 2.8 nmoles O/min/mg protein; n=3) obtained for thymus mitochondria was significantly decreased 66 % (p=0.0071**; n=3) by the addition of 1 mM GDP (9.6 ± 2.3 nmoles O/min/mg protein). The GDP sensitive state 4 rate was significantly increased by 250 % (p=0.0529*; n=3) upon addition of 64 μM palmitate (33.6 ± 4.3 nmoles O/min/mg protein) to a rate close to the maximal uncoupled rate obtained by the addition of 30 nM DNP (36.4 ± 5.6 nmoles O/min/mg protein).

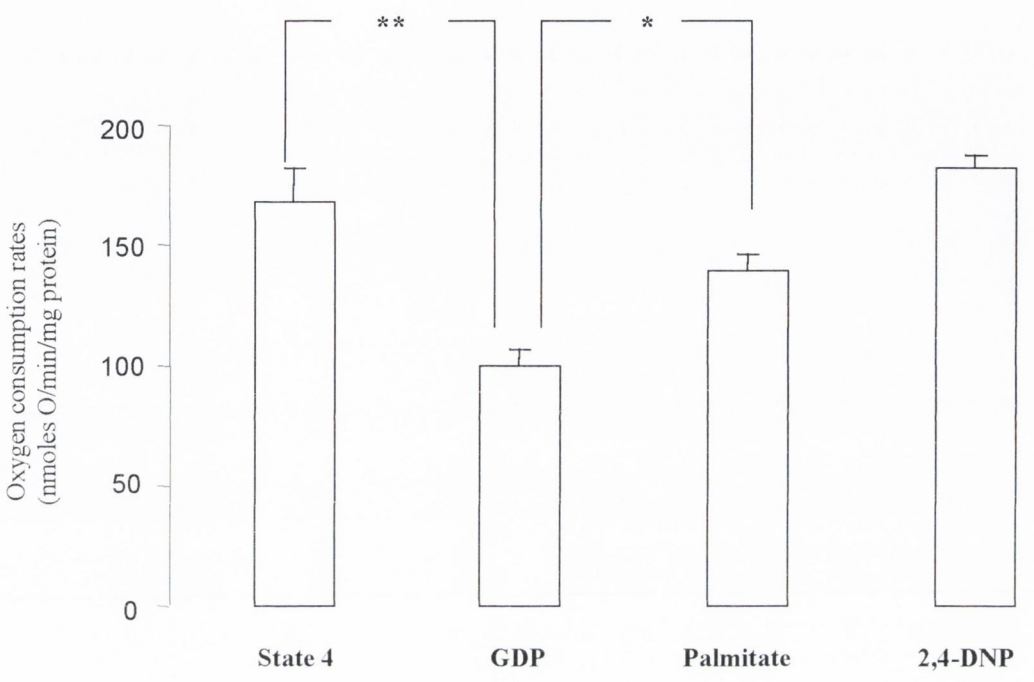


Figure 5.2.1: State 4 oxygen consumption rates in BAT mitochondria, isolated from rats kept at room temperature, are sensitive to purine nucleotides and fatty acids.

BAT mitochondria were isolated from rats housed at room temperature as described in section 2.8.1. BAT mitochondria (1 mg/ml) were incubated at 37°C in the presence of 120 mM KCl, 5 mM Hepes-KOH (pH 7.4), 1 mM EGTA, 16 μM de-fatted BSA, 5 μM rotenone, 1 μg/ml oligomycin, 5 μM atractyloside, and 7.5 mM succinate (K^+-salt) in a pre-calibrated Clarke-type oxygen electrode. Steady-state oxygen consumption rates (state 4) were then measured. 1 mM GDP was added to the chamber followed by the addition of 64 μM palmitate (~40 nM free). Finally 30 nM 2,4-DNP was added. The addition of GDP significantly decreased (P=0.01**; n=3) the state 4 oxygen consumption rate. The addition of 64 μM palmitate increased the oxygen consumption rates significantly (P=0.02*; n=3). Data is expressed as mean ± S.E.M. of at least 3 experiments, each experiment performed in triplicate.

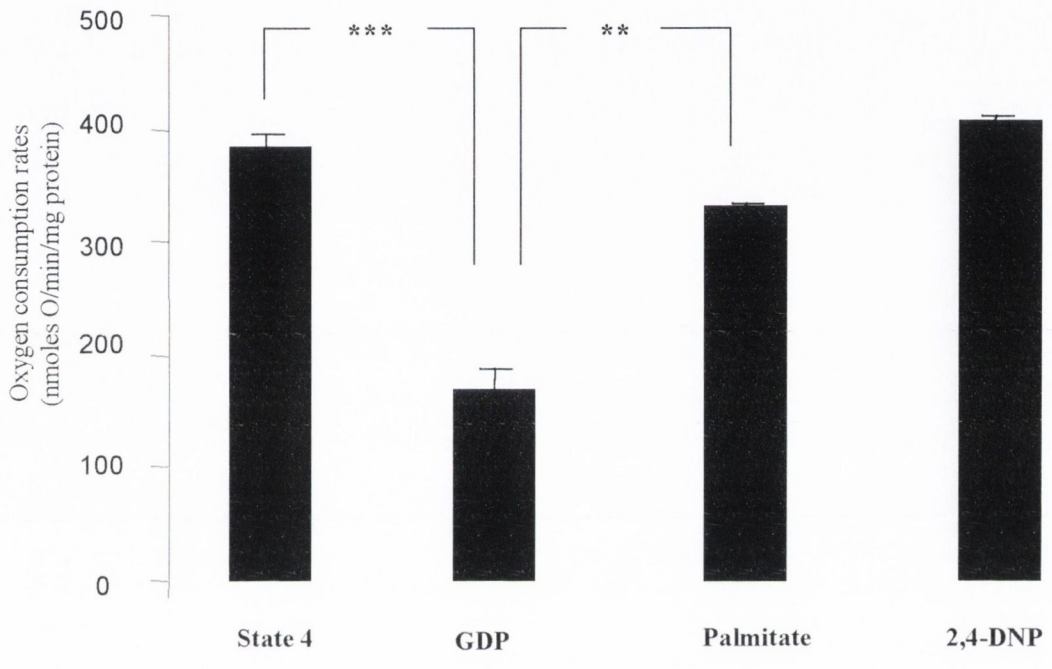


Figure 5.2.2: State 4 oxygen consumption rates in BAT mitochondria, isolated from rats kept at 4°C for 5 weeks, are sensitive to purine nucleotides and fatty acids.

BAT mitochondria were isolated from rats kept at 4°C for 5 weeks as described in section 2.8.1. BAT mitochondria (1 mg/ml) were incubated at 37°C in the presence of 120 mM KCl, 5 mM Hepes-KOH (pH 7.4), 1 mM EGTA, 16 μM de-fatted BSA, 5 μM rotenone, 1 μg/ml oligomycin, 5 μM atractyloside, and 7.5 mM succinate (K^+-salt) in a pre-calibrated Clarke-type oxygen electrode. Steady-state oxygen consumption rates (state 4) were then measured. 1 mM GDP was then added to the chamber followed by the addition of 64 μM palmitate (~40 nM free). Finally 30 nM 2,4-DNP was added. The addition of GDP significantly decreased (P=0.0012***; n=3) the state 4 oxygen consumption rate. The addition of 64 μM palmitate increased the oxygen consumption rates significantly (P=0.0016**; n=3). Data is expressed as mean ± S.E.M. of at least 3 experiments, each experiment performed in triplicate.

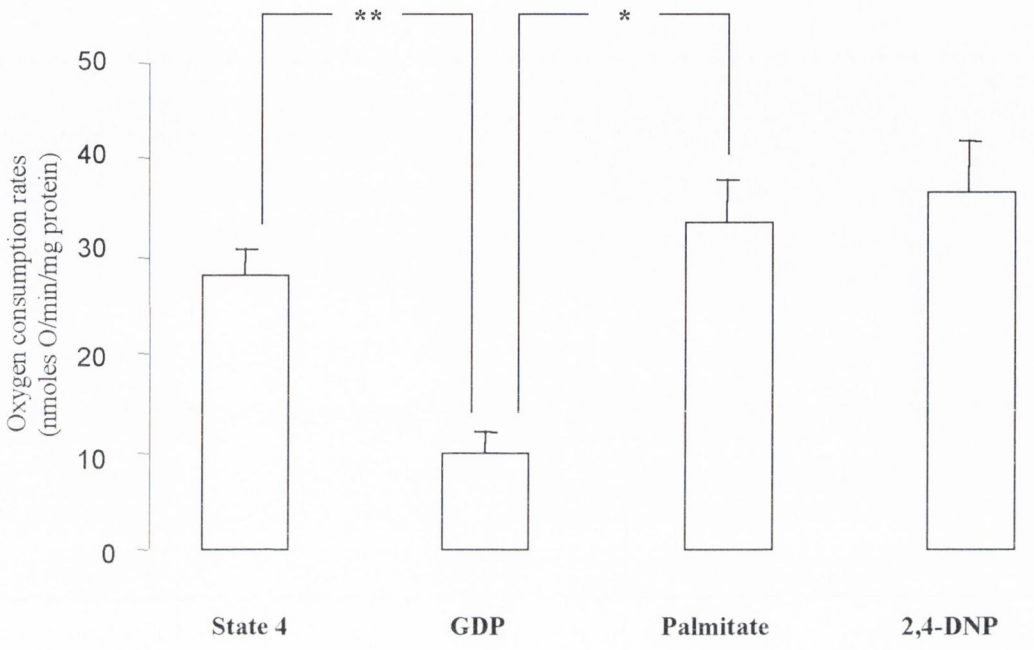


Figure 5.2.3: State 4 oxygen consumption rates in thymus mitochondria, isolated from rats kept at room temperature, are sensitive to purine nucleotides and fatty acids.

Thymus mitochondria were isolated from rats housed at room temperature as described in section 2.8.5. Thymus mitochondria (1 mg/ml) were incubated at 37°C in the presence of 120 mM KCl, 5 mM Hepes-KOH (pH 7.4), 1 mM EGTA, 16 μM de-fatted BSA, 5 μM rotenone, 1 μg/ml oligomycin, 5 μM atractyloside, and 7.5 mM succinate (K^+-salt) in a pre-calibrated Clarke-type oxygen electrode. Steady-state oxygen consumption rates (state 4) were then measured. The effects of the addition of 1 mM GDP followed by the addition of 64 μM palmitate (~40 nM free) on the rates were then measured. Finally, 30 nM 2,4-DNP was added. The addition of GDP significantly decreased (P=0.0071**; n=3) the state 4 oxygen consumption rate. The addition of 64 μM palmitate increased the oxygen consumption rates significantly (P=0.0529*; n=3). Data is expressed as mean ± S.E.M. of at least 3 experiments, each experiment performed in triplicate.

Figure 5.2.4 shows the effects of GDP and palmitate on state 4 oxygen consumption rates in thymus mitochondria isolated from rats housed at 4^0C for 5-weeks. The addition of 1 mM GDP to the electrode chamber significantly decreased by 69 % (p=0.0121**; n=3) the steady state oxygen consumption rate from 41.1 ± 6.2 nmoles O/min/mg protein to 12.6 ± 1.4 nmoles O/min/mg protein. Addition of palmitate (~ 40 nM final free concentration) significantly increased by 339 % (p=0.0121**; n=3) the GDP sensitive state 4 rate to 55.3 ± 7.3 nmoles O/min/mg protein. Finally, the addition of 30 nM DNP stimulated maximal oxygen consumption rates in cold thymus mitochondria (56.2 nmoles O/min/mg protein).

Figure 5.2.5 illustrates the differences between steady state oxygen consumption rates, GDP sensitive rates and palmitate sensitive rates in thymus mitochondria isolated from room temperature and cold rats. State 4 rates were significantly greater (p=0.0220*; n=3) in thymus mitochondria isolated from cold acclimated rats when compared to state 4 rates from thymus mitochondria from room temperature animals. Again, thymus mitochondria from cold acclimated animals displayed significantly greater (p=0.0121**; n=3) GDP sensitive rates than thymus mitochondria isolated from the room temperature cohort. While the trend was towards a faster palmitate rate in cold acclimated thymus mitochondria, this increase was not significantly greater (p=0.0591; n=3) than the palmitate rate observed in the room temperature animals.

Liver mitochondria do not constitutively express uncoupling proteins and were therefore chosen as a negative control in this study. Figures 5.2.6 and 5.2.7 show the effects of GDP (1 mM) and palmitate (~ 40 nM final free concentration) on liver mitochondria isolated from room temperature and cold acclimated rats respectively. It is clear that in the presence of inhibitors of the ATP synthase and the adenine nucleotide carrier, liver mitochondria are insensitive to both GDP and palmitate. The lack of inhibition and activation by GDP and palmitate was not due to poor quality mitochondria as maximal oxygen consumption rates were obtained using 30 nM DNP.

Figures 5.2.8 and 5.2.9 show the effects of GDP and palmitate on state 4 oxygen consumption rates in UCP2 containing kidney mitochondria isolated from room temperature and cold acclimated rats respectively. Steady state oxygen consumption rates,

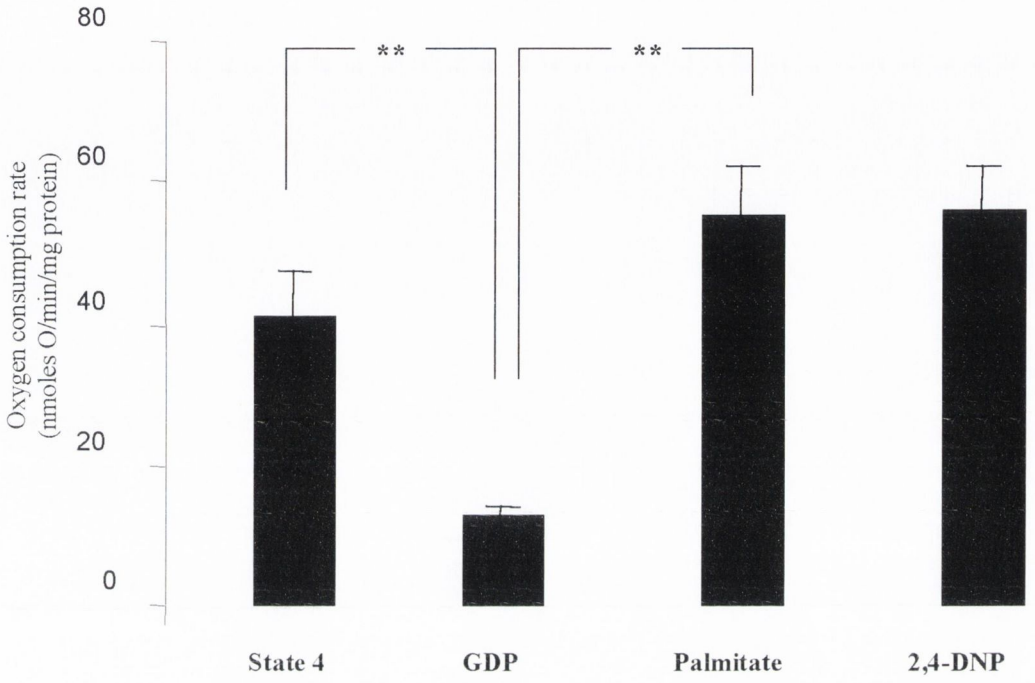


Figure 5.2.4: State 4 oxygen consumption rates in thymus mitochondria, isolated from rats kept at 4°C for 5 weeks, are sensitive to purine nucleotides and fatty acids.

Thymus mitochondria were isolated from rats kept at 4°C for 5 weeks as described in section 2.8.5. Thymus mitochondria (1 mg/ml) were incubated at 37°C in the presence of 120 mM KCl, 5 mM Hepes-KOH (pH 7.4), 1 mM EGTA, 16 μM de-fatted BSA, 5 μM rotenone, 1 μg/ml oligomycin, 5 μM atractyloside, and 7.5 mM succinate (K^+-salt) in a pre-calibrated Clarke-type oxygen electrode. Steady-state oxygen consumption rates (state 4) were then measured. Once a steady-state was achieved 1 mM GDP followed by 64 μM palmitate (~40 nM free) was added. Finally 30 nM 2,4-DNP was added. The addition of GDP significantly decreased (P=0.0121**; n=3) the state 4 oxygen consumption rate. The addition of 64 μM palmitate increased the oxygen consumption rates significantly (P=0.0121**; n=3). Data is expressed as mean ± S.E.M. of at least 3 experiments, each experiment performed in triplicate.

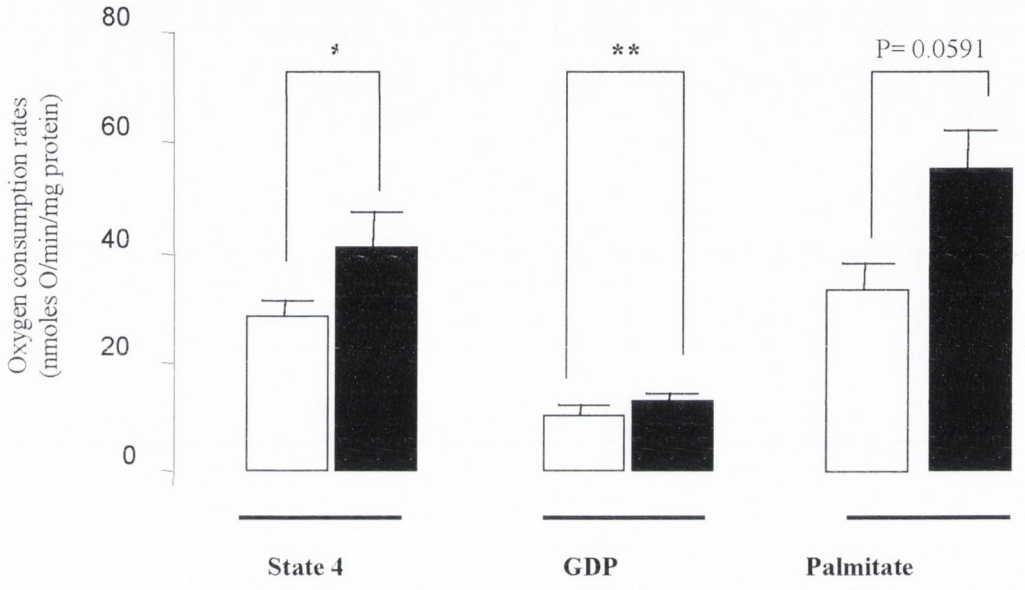


Figure 5.2.5: Comparison of state 4, GDP and palmitate rates in thymus mitochondria isolated from rats housed at room temperature and 4°C.

Mitochondria were isolated from rats housed at room temperature (□) and 4°C (■) as described in section 2.8.5. Steady-state oxygen consumption rates were significantly higher (p= 0.0220*; n=3) in cold acclimated rats than in room temperature rats. GDP sensitive rates were significantly higher (p=0.0121**; n = 3) in cold acclimated rats. Palmitate rates were not quite significantly higher in cold acclimated animals with a p value of 0.0591. Data is expressed as mean ± S.E.M. of 3 independent experiments, each experiment performed in triplicate.

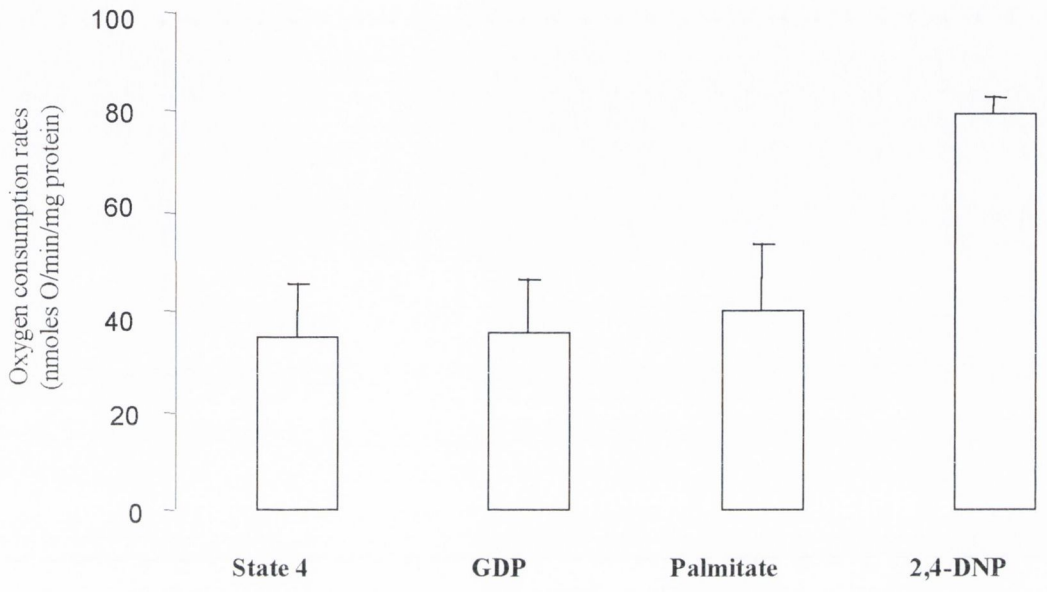


Figure 5.2.6: State 4 oxygen consumption rates in liver mitochondria, isolated from rats kept at room temperature, are insensitive to purine nucleotides and fatty acids.

Liver mitochondria were isolated from rats housed at room temperature as described in section 2.8.3. Liver mitochondria (1 mg/ml) were incubated at 37°C in the presence of 120 mM KCl, 5 mM Hepes-KOH (pH 7.4), 1 mM EGTA, 16 μM de-fatted BSA, 5 μM rotenone, 1 μg/ml oligomycin, 5 μM atractyloside, and 7.5 mM succinate (K^+-salt) in a pre-calibrated Clarke-type oxygen electrode. Steady-state oxygen consumption rates were then measured (State 4). 1 mM GDP was added to the chamber followed by the addition of 64 μM palmitate (~40 nM free). Finally 30 nM 2,4-DNP was added. No significant change in the oxygen consumption rate was observed upon addition of GDP or palmitate. Data is expressed as mean ± S.E.M. of at least 3 independent experiments, each experiment performed in triplicate.

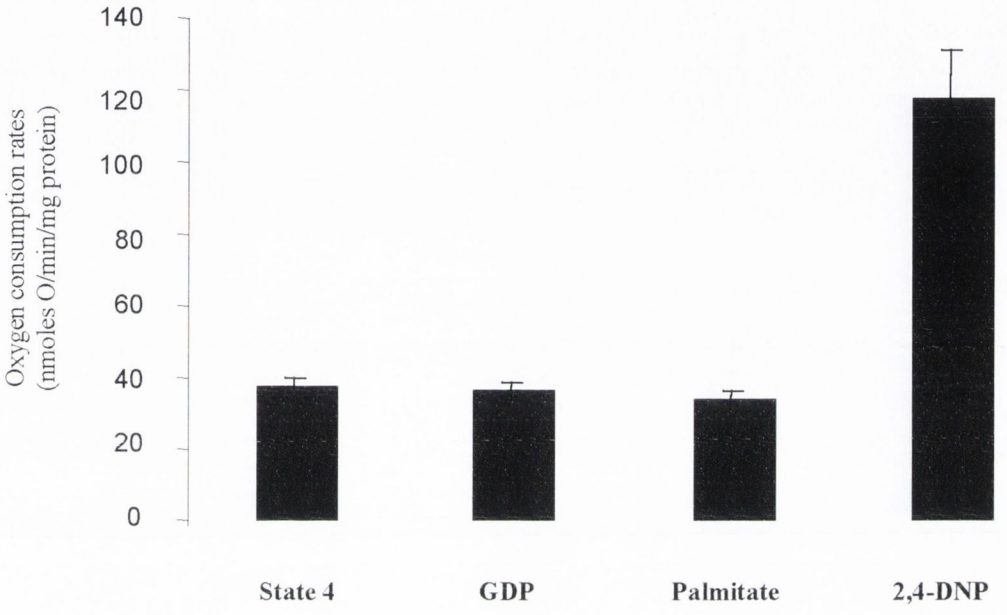


Figure 5.2.7: State 4 oxygen consumption rates in liver mitochondria, isolated from rats kept at 4°C for 5 weeks, are insensitive to purine nucleotides and fatty acids

Liver mitochondria were isolated from rats kept at 4°C for 5 weeks as described in section 2.8.3. Liver mitochondria (1 mg/ml) were incubated at 37°C in the presence of 120 mM KCl, 5 mM Hepes-KOH (pH 7.4), 1 mM EGTA, 16 μM de-fatted BSA, 5 μM rotenone, 1 μg/ml oligomycin, 5 μM atractyloside, and 7.5 mM succinate (K^+-salt) in a pre-calibrated Clarke-type oxygen electrode. Steady-state oxygen consumption rates were then measured (State 4). 1 mM GDP was then added to the chamber followed by the addition of 64 μM palmitate (~40 nM free). Finally 30 nM 2,4-DNP was added. No significant change in the oxygen consumption rate was observed upon addition of GDP or palmitate. Data is expressed as mean ± S.E.M. of at least 3 independent experiments, each experiment performed in triplicate.

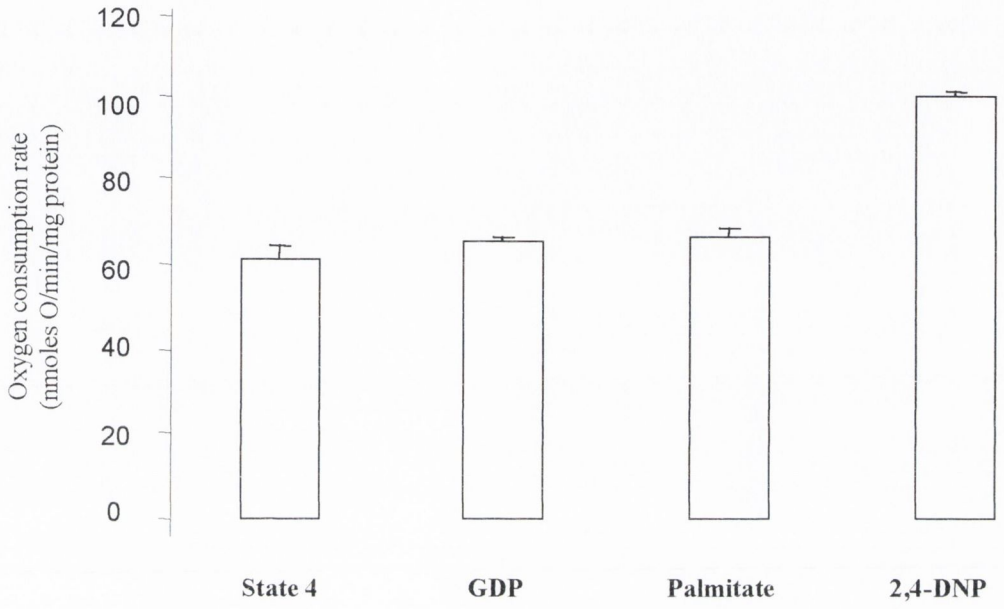


Figure 5.2.8: State 4 oxygen consumption rates in kidney mitochondria, isolated from rats kept at room temperature, are insensitive to purine nucleotides and fatty acids.

Kidney mitochondria were isolated from rats housed at room temperature as described in section 2.8.4. Kidney mitochondria (1 mg/ml) were incubated at 37°C in the presence of 120 mM KCl, 5 mM Hepes-KOH (pH 7.4), 1 mM EGTA, 16 μM de-fatted BSA, 5 μM rotenone, 1 μg/ml oligomycin, 5 μM atractyloside, and 7.5 mM succinate (K^+-salt) in a pre-calibrated Clarke-type oxygen electrode. Steady-state oxygen consumption rates (State 4) were then measured. 1mM of GDP was added to the chamber followed by the addition of 64 μM palmitate (~40 nM free). Finally 30 nM 2,4-DNP was added. No significant change in the oxygen consumption rate was observed upon addition of GDP or palmitate. Data is expressed as mean ± S.E.M. of at least 2 independent experiments, each experiment performed in triplicate.

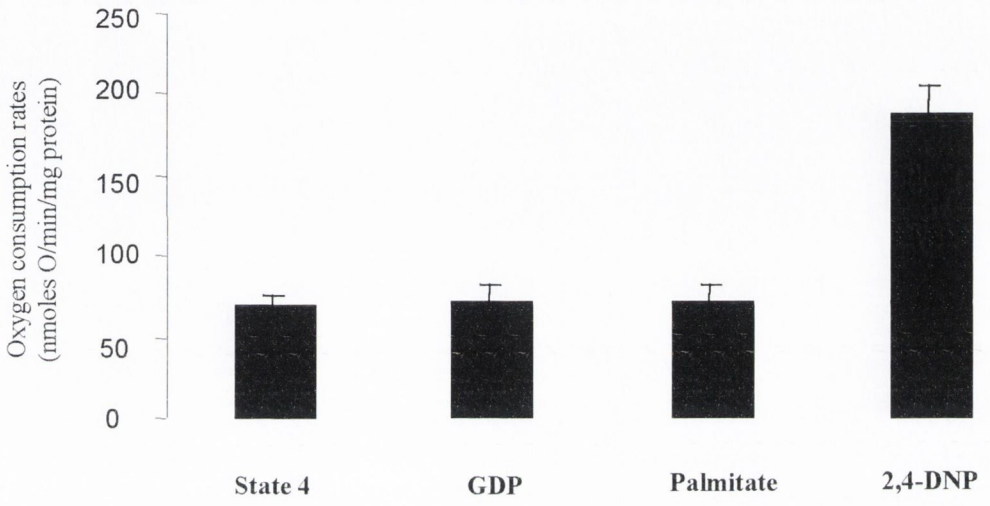


Figure 5.2.9: State 4 oxygen consumption rates in kidney mitochondria, isolated from rats kept at 4°C for 5 weeks, are insensitive to purine nucleotides and fatty acids

Kidney mitochondria were isolated from rats kept at 4°C for 5 weeks as described in section 2.8.4. Kidney mitochondria (1 mg/ml) were incubated at 37°C in the presence of 120 mM KCl, 5 mM Hepes-KOH (pH 7.4), 1 mM EGTA, 16 μM de-fatted BSA, 5 μM rotenone, 1 μg/ml oligomycin, 5 μM atractyloside, and 7.5 mM succinate (K^+-salt) in a pre-calibrated Clarke-type oxygen electrode. Steady-state oxygen consumption rates (state 4) were then measured. 1 mM GDP was added to the chamber. This was followed by the addition of 64 μM palmitate (~40 nM free). Finally 30 nM 2,4-DNP was added. No significant change in the oxygen consumption rate was observed upon addition of GDP or palmitate. Data is expressed as mean ± S.E.M. of at least 3 independent experiments, each experiment performed in triplicate.

in the presence of inhibitors to the adenine nucleotide carrier and ATP synthase were insensitive to the additions of GDP (1 mM) and palmitate (~ 40 nM final free concentration) The insensitivity to long chain fatty acids and purine nucleotides was not due to inferior quality mitochondria as maximal oxygen consumption rates were obtainable upon adding 30 nM DNP to both room temperature and cold acclimated mitochondria.

Figures 5.2.10 and 5.2.11 show the effects of adding GDP and palmitate to UCP2 and UCP3 containing spleen mitochondria isolated from room temperature and cold acclimated rats respectively. The steady state oxygen consumption rate was insensitive to GDP (1 mM) and palmitate (~ 40 nM final free concentration) in the presence of adenine nucleotide carrier and ATP synthase inhibitors. The quality of the mitochondria was not compromised as maximal oxygen consumption rates were obtained upon addition of 30 nM DNP.

Respiratory control ratios (RCR) were determined in this study to check the intactness of the mitochondrial preparations. Table 5.2.1 shows the RCR values for all the mitochondria isolated from the rats kept at room temperature and the cold acclimated rats. In this study the RCR is defined as the (state 3) uncoupled rate (due to the addition of excess artificial uncoupler *i.e.* DNP) divided by the steady state (state 4) oxygen consumption rate.

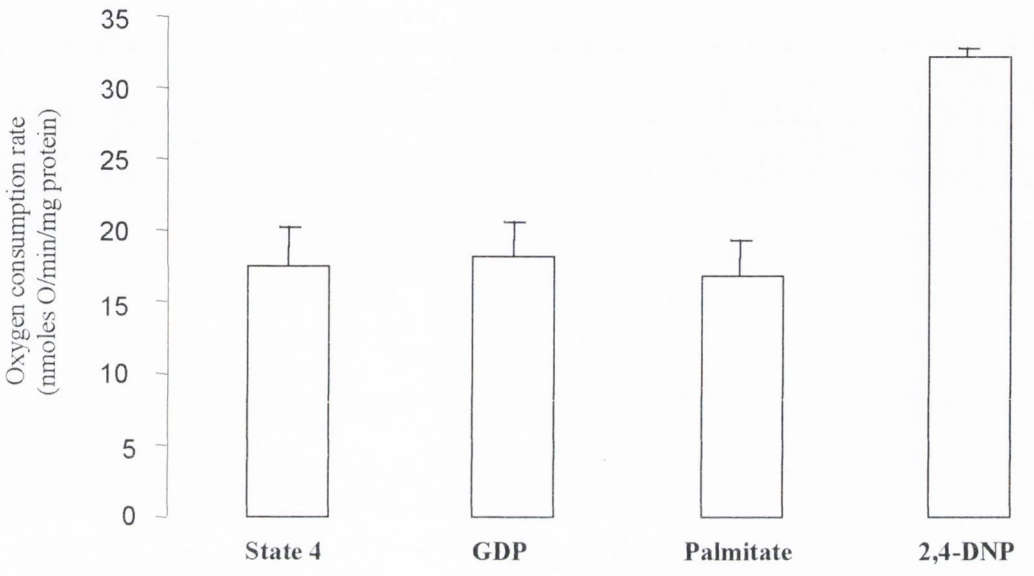


Figure 5.2.10: State 4 oxygen consumption rates in spleen mitochondria, isolated from rats kept at room temperature, are insensitive to purine nucleotides and fatty acids.

Spleen mitochondria were isolated from rats housed at room temperature as described in section 2.8.3. Spleen mitochondria (1 mg/ml) were incubated at 37°C in the presence of 120 mM KCl, 5 mM Hepes-KOH (pH 7.4), 1 mM EGTA, 16 mM de-fatted BSA, 5 mM rotenone, 1 mg/ml oligomycin, 5 mM atractyloside, and 7.5 mM succinate (K^+-salt) in a pre-calibrated Clarke-type oxygen electrode. Steady-state oxygen consumption rates were then measured (State 4). 1 mM GDP was added to the chamber followed by the addition of 64 μM palmitate (~40 nM free). Finally 30 nM 2,4-DNP was added. No significant change in the oxygen consumption rate was observed upon addition of GDP or palmitate. Data is expressed as mean ± S.E.M. of at least 3 independent experiments, each experiment performed in triplicate.

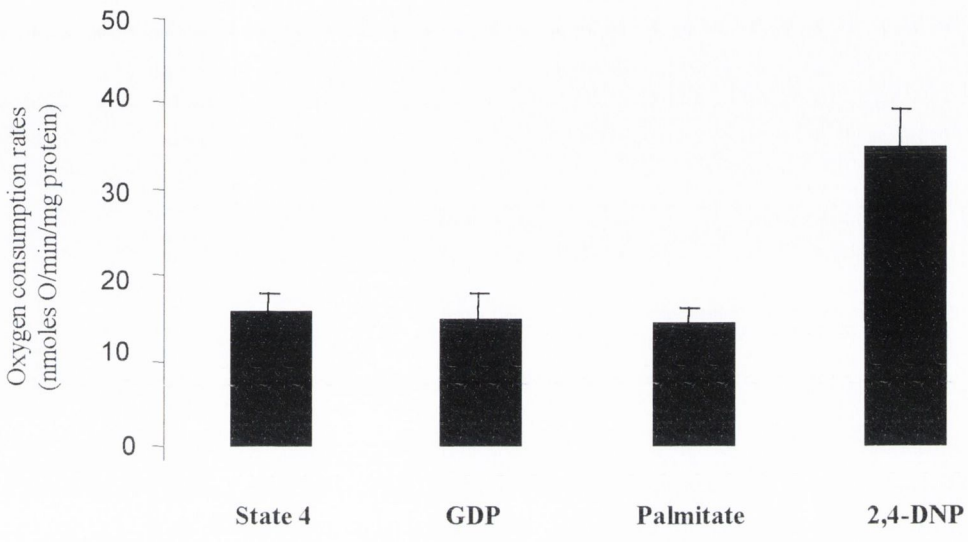


Figure 5.2.11: State 4 oxygen consumption rates in spleen mitochondria, isolated from rats kept at 4°C for 5 weeks, are insensitive to purine nucleotides and fatty acids.

Spleen mitochondria were isolated from rats kept at 4°C for 5 weeks as described in section 2.8.3. Spleen mitochondria (1 mg/ml) were incubated at 37°C in the presence of 120 mM KCl, 5 mM Hepes-KOH (pH 7.4), 1 mM EGTA, 16 μM de-fatted BSA, 5 μM rotenone, 1 μg/ml oligomycin, 5 μM atractyloside, and 7.5 mM succinate (K^+-salt) in a pre-calibrated Clarke-type oxygen electrode. Steady-state oxygen consumption rates (state 4) were then measured. 1 mM GDP was added to the chamber followed by the addition of 64 μM palmitate (~40 nM free). Finally 30 nM 2,4-DNP was added. No significant change in the oxygen consumption rate was observed upon addition of GDP or palmitate. Data is expressed as mean ± S.E.M. of at least 3 independent experiments, each experiment performed in triplicate.

Tissue	RCR (state 3 uncoupled rate/state 4 rate)	RCR (state 3 uncoupled rate/state 4 rate)
	Room temperature	Cold acclimated
BAT	1.0 ± 0.04	1.3 ± 0.1
Thymus	1.3 ± 0.2	1.5 ± 0.2
Skeletal muscle	3.1 ± 0.1	3.0 ± 0.2
Kidney	2.2 ± 0.2	2.5 ± 0.2
Liver	3.2 ± 0.2	3.4 ± 0.3
Spleen	2.2 ± 0.4	2.6 ± 0.2

Table 5.2.1: Respiratory control ratios (RCRs) for mitochondria isolated from rats acclimated to the cold for 5 weeks and from rats kept at room temperature

Mitochondria were isolated from rats as described in section 2.8. Mitochondria (1 mg/ml) were incubated at 37°C in the presence of 120 mM KCl, 5 mM Hepes-KOH, pH 7.4, 1 mM EGTA, 16 μM de-fatted BSA, 5 μM rotenone, 1 μg/ml oligomycin, 5 μM atractyloside, and 7.5 mM succinate (K^+-salt) in a pre-calibrated Clarke-type oxygen electrode. Steady-state oxygen consumption rates were then measured (State 4), followed by the addition of 30 nM 2,4-DNP to stimulate a maximum respiration rate (State 3 uncoupled rate). RCR values were obtained using the formula: State 3 uncoupled/ State 4 respiration rate. Data is expressed as mean ± S.E.M of at least 3 independent experiments, each experiment performed in triplicate.

[5.3] Discussion

BAT mitochondria were used in this study as positive controls to illustrate the well-documented inhibitory effects of GDP and the subsequent stimulatory effects of palmitate on UCP1 uncoupling function. Data presented in this study have confirmed that steady-state (state 4) oxygen consumption rates in BAT mitochondria, isolated from rats housed at room temperature and 4°C (5-weeks), are innately uncoupled *i.e.* show high state 4 oxygen consumption rates in the absence of ATP synthesis. As previously acknowledged, UCP1, present in the inner membrane of BAT mitochondria, is responsible for a significant proportion of this uncoupling. Our results, showing that freshly prepared rat BAT mitochondria are uncoupled, compares well with results obtained by other authors in the literature (Rial *et al.*, 1999; Carroll *et al.*, 2005). The present study also demonstrates that state 4 oxygen consumption rates in BAT mitochondria, isolated from rats kept at room temperature are more coupled when compared to BAT mitochondria isolated from cold acclimated rats. The ability of GDP to inhibit state 4 oxygen consumption rates and nanomolar amounts of palmitate to reactivate the GDP inhibited component of state 4 in BAT mitochondria isolated from room temperature and cold acclimated rats was also confirmed, comparing favourably with previously published work (Desautels and Himms-Hagen, 1981; Nedergaard and Cannon, 1985; Carroll *et al.*, 2005). In addition, our results have confirmed that inhibition of state 4 oxygen consumption rates by GDP and reactivation of GDP inhibited state 4 oxygen consumption rates by palmitate are more pronounced in cold acclimated rats. This result agrees with previously published data (Desautels and Himms-Hagen, 1981; Nedergaard and Cannon, 1985).

Having established that thymus mitochondria isolated from cold acclimated rats exhibit a significant increase in UCP1 protein expression (see Chapter 4; Figure 4.2.5), we sought to determine whether the increase in UCP1 protein per mg of mitochondrial protein would result in increased GDP sensitive and subsequent increased palmitate activation of the GDP sensitive oxygen consumption rate as is the case for cold acclimated BAT mitochondria. In the present study, we confirmed the finding of Carroll *et al.* (2005) that thymus mitochondria isolated from room temperature rats are innately uncoupled (Figure 5.2.3). Furthermore, we were able to verify that thymus mitochondrial oxygen consumption rates are inhibited by GDP. The GDP inhibited component of state 4 oxygen consumption

was reactivated by palmitate. A major finding of the present study is that thymus mitochondria prepared from cold acclimated rats exhibit greater state 4 oxygen consumption rates than mitochondria isolated from thymi of rats housed at room temperature (Figures 5.2.3-5.2.5) as is the case for BAT mitochondria. Moreover, GDP is shown to inhibit the steady state (state 4) oxygen consumption rate of thymus mitochondria isolated from the cold acclimated rats to a greater extent than thymus mitochondria isolated from rats housed at room temperature. We also show that thymus mitochondria, isolated from cold acclimated rats, are more responsive to palmitate activation of the GDP inhibited component of state 4 oxygen consumption, when compared to the room temperature rats. The increased sensitivity of thymus mitochondria to GDP and subsequent increased activation of GDP inhibited oxygen consumption rates by palmitate following cold exposure may be explained in three ways. Firstly, the possibility exists that we may be seeing an increase in natural basal leak *i.e.* leak due to normal, non-UCP related processes. Secondly, the increased sensitivity may be due to an increase in the amount of UCP1 protein present in thymus mitochondria following cold exposure. Thirdly, we may be seeing an increase in the number of 'unmasked' binding sites following cold exposure which results in an increased responsiveness to GDP and hence, increased palmitate activation of GDP inhibited oxygen consumption.

The sequence similarity between UCP1 and two homologues, UCP2 and UCP3, along with evidence from isolated mitochondrial studies, mammalian cell expression systems and heterologous yeast have presented a hypothetical role for UCP2 and UCP3 as uncoupling proteins. The data presented in this study contest this theory. Under our assay conditions, that demonstrate UCP1 uncoupling activity in BAT and thymus mitochondria isolated from both room temperature and cold acclimated rats, we show that mitochondrial state 4 oxygen consumption rates from non-UCP (liver), UCP2 (kidney and spleen) and UCP3 (spleen) containing tissues are unaffected by GDP and palmitate. The insensitivity of non-UCP, UCP2 and UCP3 containing tissues to GDP and nanomolar concentrations of palmitate is not due to poor quality mitochondrial preparations as indicated by the RCR values (Table 5.2.1). However, it is possible that there may be so little UCP2 and UCP3 per mg of mitochondrial protein that our functional assay does not register any changes in oxygen consumption due to GDP or palmitate in these tissues. The lack of mitochondrial uncoupling activity by UCP2 and UCP3 shown in this study corroborates well with other

findings in the literature (Cresenzo *et al.*, 2003; Couplan *et al.*, 2002; Nedergaard *et al.*, 2001; Cadenas *et al.*, 2000; Porter *et al.*, 1999; Matthias *et al.*, 1999; Jekabsons *et al.*, 1999; Cadenas *et al.*, 1999). However, our results contrast with those authors who appear to have shown UCP2 and UCP3 mediated uncoupling. Nègre-Salvayre *et al.* (1997) observed GDP sensitive state 4 oxygen consumption in rat thymus and spleen mitochondria and attributed it to UCP2. Krauss *et al* (2002) observed a decrease in oxygen consumption due to proton leak in thymocytes isolated from UCP2 knock-out mice. Echtay *et al.* (2002 & 2003) and Murphy *et al.* (2003) observed a UCP1, UCP2 and UCP3 dependent leak in BAT, kidney and skeletal muscle triggered by *in vitro* superoxide production and *in vitro* addition of polyunsaturated fatty acid oxidation products (4-hydroxy-2-*trans*-nonenal). Finally, Mills *et al.* (2003) observed a resistance to heat production in skeletal muscle of UCP3 knock-out mice after treatment with ecstasy.

[5.4] Conclusions

In conclusion, we have confirmed that oxygen consumption rates, in BAT mitochondria isolated from both room temperature and cold acclimated rats and in thymus mitochondria isolated from room temperature rats, are inhibited by GDP. Palmitate was then shown to reactivate the GDP inhibited component of state 4 oxygen consumption rates in these tissues.

More remarkably, we have presented novel results illustrating that thymus mitochondrial oxygen consumption rates are more sensitive to (i) GDP inhibition and (ii) palmitate activation of the GDP inhibited component of oxygen consumption following cold acclimation.

In contrast, no GDP inhibition or fatty acid activation of oxygen consumption was detected in UCP2 (spleen, kidney) or UCP3 (spleen) containing mitochondria. Oxygen consumption rates in liver mitochondria, which do not constitutively express any of the UCPs, was unaffected by either GDP or palmitate. Taken together, these results imply that neither UCP2 nor UCP3 are uncouplers in mitochondria or if they do catalyse proton leak, then they are regulated differently to UCP 1.

Chapter 6

Application of a radiolabeled purine nucleotide binding assay to UCP containing mitochondria

[6.1] Introduction

The specific binding of [^{3}H]GDP has been used extensively as a measure of the abundance of UCP1 in BAT. Sympathetic stimulation of BAT, as a result of, for example, cold exposure, increases GDP binding. Chronic cold exposure has been shown to increase the concentration of UCP1 in parallel with the increase in GDP binding (Swick and Swick, 1986; Nicholls and Locke, 1984; Nedergaard and Cannon, 1985; Sundin *et al.*, 1987; Sundin and Cannon, 1980). Having unequivocally established the presence of UCP1 in thymus mitochondria isolated from room temperature rats and the subsequent up-regulation of thymic UCP1 upon cold acclimation (see Chapter 4), this study sought to investigate whether [^{3}H]GDP binding to thymus mitochondria is also elevated following cold exposure. To investigate this we used a radioligand-binding assay specific and sensitive for UCP1 in BAT mitochondria. The [^{3}H]GDP binding assay employed in this study was set up according to the method of Scarpace *et al.* (1991). Similar radioligand-binding assays have been successfully employed to determine saturable binding to UCP1 in BAT mitochondria (Sundin & Cannon, 1980; Nedergaard & Cannon, 1985; Gribskov *et al.*, 1986; Swick & Swick, 1986; Sundin *et al.*, 1987; Milner *et al.*, 1988; Peachey *et al.*, 1988; Scarpace *et al.*, 1991; Huang *et al.*, 1998). BAT mitochondria, isolated from rats acclimated to the cold for 5 weeks, a regime known to increase the thermogenic capacity of UCP1 and thus its GDP binding capabilities, were used as a positive control tissue. Liver mitochondria do not constitutively express UCP1, UCP2 or UCP3, and were used as a negative control tissue for the purpose of this study (Ricquier & Bouillaud, 2000).

This study also sought to investigate whether tissues constitutively expressing UCP2 and UCP3 can bind purine nucleotides in a manner similar to UCP1. The tissues we choose as a source of these mitochondria were spleen which contain UCP2 & UCP3 and kidney which contain UCP2 only. Most of the evidence to date showing that UCP2 and UCP3 can bind purine nucleotides have come from *E. coli* and heterologous yeast expression systems. Jekabsons *et al.* (2002) showed that recombinant human UCP2 ectopically expressed and solublised in bacterial (*E. coli*) inclusion bodies bind purine and pyrimidine nucleoside triphosphates with low micromolar affinity. Zackova *et al.* (2003) also showed that *E. coli* or yeast expressing UCP2 and UCP3 exhibit high affinity [^{3}H]GTP

binding, similar to UCP1. However, data showing purine nucleotide binding to UCP2 and UCP3 containing mitochondria has been somewhat lacking.

Masking has been previously shown to exist in BAT mitochondria containing UCP1 (Huang & Klingenberg, 1995; Gribskov *et al.*, 1986). Masking is the term used to describe the situation when some or all of the nucleotide binding sites for UCPs are already occupied by residual bound purine nucleotides prior to performing the binding assay. The purine nucleotide binding sites in BAT mitochondria has been shown to be masked in rats kept at room temperature but unmasked in BAT mitochondria isolated from cold-acclimated rats. Huang & Klingenberg, (1995) showed that isolated mitochondria could be unmasked by treating the mitochondria with Dowex (a 21K anion exchanger) at pH 8 (see section 2.17; chapter 2). Using Dowex-treated thymus mitochondria isolated from rats kept at room temperature as a control, this study sought to show that non-Dowex treated thymus mitochondria isolated from rats housed at room temperature are masked like non-Dowex treated BAT mitochondria.

[6.2] Results

Figure 6.2.1 shows saturable [^{3}H]GDP binding to Dowex-treated BAT mitochondria isolated from rats housed at room temperature and at 4°C for 5 weeks. The data were fitted to an equation describing a rectangular hyperbola, using non-weighted, non-linear least square regression analysis. The results clearly show saturable binding of [^{3}H]GDP up to 6 μM. The B_{MAX} values obtained were 353 ± 61 (3) and 736 ± 128 (3) pmoles bound/mg of mitochondrial protein for mitochondria isolated from rats housed at room temperature and in the cold respectively. These values were significantly different ($p \leq 0.05$) from one another. The K_D values obtained were 0.5 ± 0.4 μM (3) and 0.8 ± 0.6 μM (3) for room temperature and cold acclimated rats respectively and were not significantly different from one another. Statistical differences were determined using an unpaired Student's t-test. Data are expressed as mean ± S.E.M. of at least 3 experiments each experiment performed in triplicate.

GDP binding was also determined for Dowex-treated liver mitochondria. As liver is known not to express UCPs, it was used as a negative control tissue for the radiolabelled binding assays employed in this study. Figure 6.2.2 shows [^{3}H]GDP binding to liver mitochondria to be non-saturable and thus, prevented the accurate determination of B_{MAX} and K_D values.

Figure 6.2.3 shows saturable binding of [^{3}H]GDP to Dowex-treated thymus mitochondria isolated from room temperature and cold acclimated rats. Saturability was determined using the equation described above. The K_D values determined were 1.4 ± 0.8 μM (3) and 0.9 ± 0.3 μM (3) for mitochondria isolated from rats housed at room temperature and in the cold respectively. B_{MAX} values determined for Dowex-treated thymus mitochondria isolated from room temperature (131 ± 20 pmoles bound/mg protein (3)) and cold acclimated (197 ± 15 pmoles bound/mg protein (3)) were also calculated. No significant difference in K_D values was observed between room temperature and cold acclimated rats. A significant difference ($p \leq 0.05$) was observed in B_{MAX} values when room temperature and cold acclimated rats were compared. Significance was determined using an

unpaired Student's t-test. Results are expressed as mean ± S.E.M. of 3 experiments in triplicate.

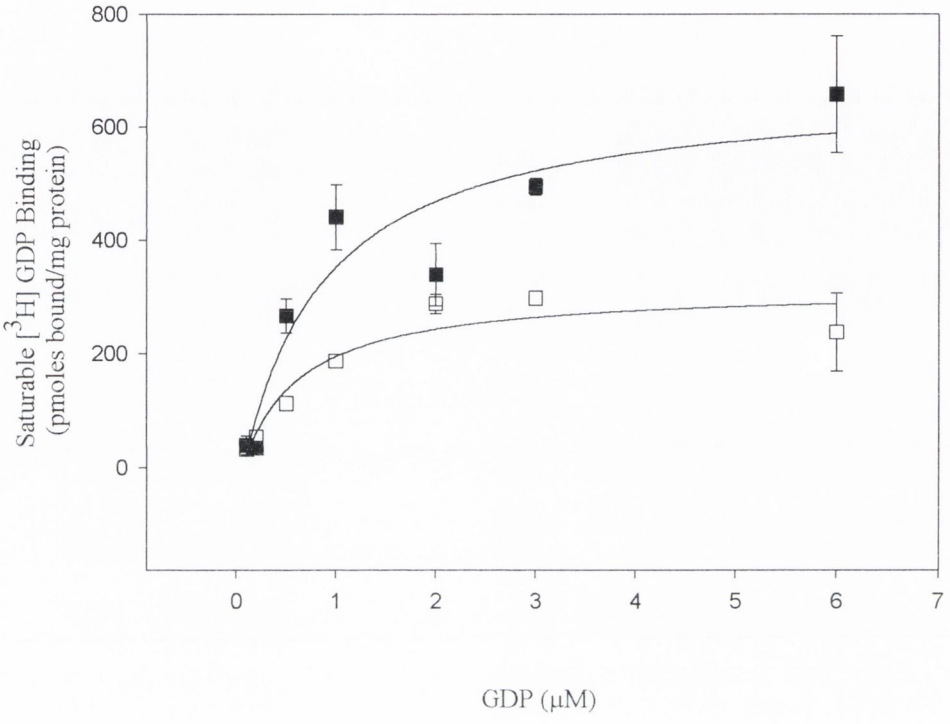


Figure 6.2.1: Comparison of [^{3}H] GDP binding parameters in Dowex-treated BAT mitochondria isolated from room temperature and cold acclimated rats.

BAT mitochondria were isolated from room temperature (□) and cold acclimated (■) rats as described in section 2.8.1. Mitochondria were incubated with [^{3}H] GDP (11.0 Ci/mmol; 0.1 – 6μM) and [^{14}C] sucrose for 15 minutes at 37°C in the absence (total binding) and presence (non-specific binding) of unlabelled GDP (1.5mM) as described in section 2.18. Specific binding was calculated from the difference between total and non-specific binding. Data are expressed as the mean ± S.E.M. of at least 2 experiments, each experiment performed in triplicate. The B_{MAX} values obtained for BAT mitochondria were 352.9 ± 61.1 and 735.6 ± 127.7 for room temperature and cold acclimated rats respectively. The K_D values obtained for BAT mitochondria were 0.5 ± 0.4 and 0.8 ± 0.6 for room temperature and cold acclimated rats respectively. Statistical differences were assessed using an unpaired Student's t-test.

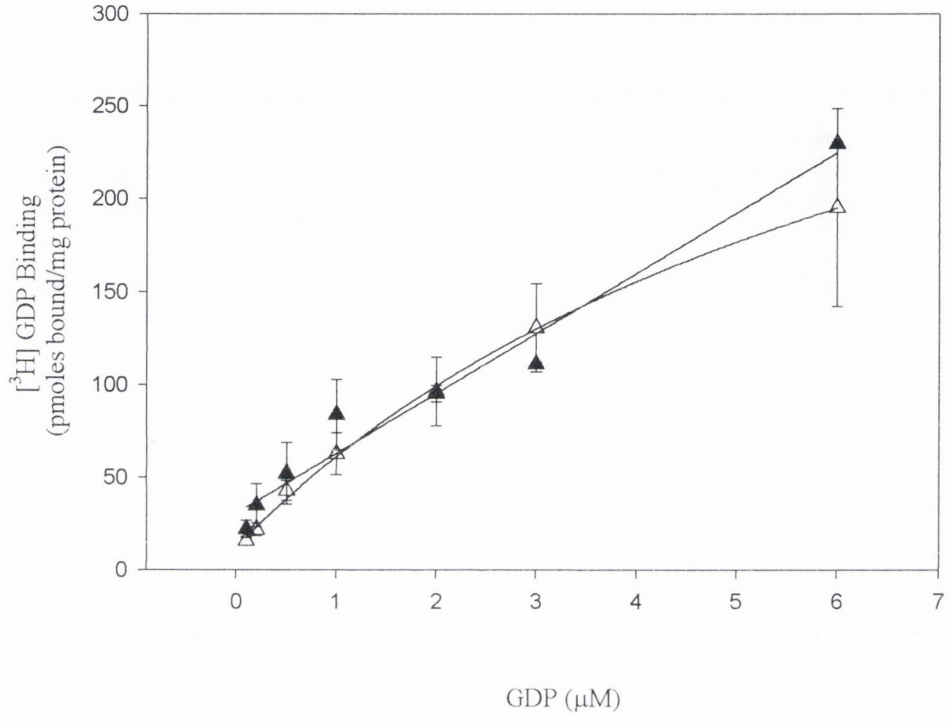


Figure 6.2.2 Comparison of [^{3}H] GDP binding parameters in Dowex-treated liver mitochondria isolated from room temperature and cold acclimated rats.

Liver mitochondria were isolated from room temperature (Δ) and cold acclimated (▲) rats as described in section 2.8.3. Mitochondria were incubated with [^{3}H] GDP (11.0 Ci/mmol; 0.1 – 6μM) and [^{14}C] sucrose for 15 minutes at 37°C in the absence (total binding) and presence (non-specific binding) of unlabelled GDP (1.5mM) as described in section 2.18. Specific binding was calculated from the difference between total and non-specific binding. Data are expressed as the mean ± S.E.M. of at least 3 experiments, each experiment performed in triplicate. Determination of the binding parameters K_D and B_{MAX} for liver mitochondria was unattainable, as the specific binding was not found to be saturable.

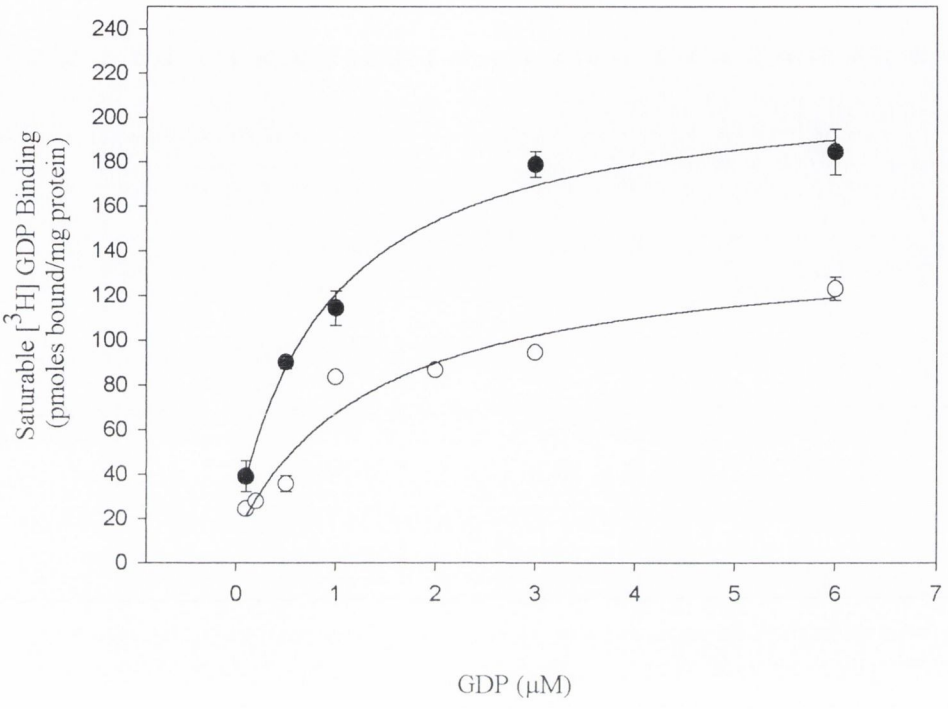


Figure 6.2.3 Comparison of [^{3}H] GDP binding parameters in Dowex-treated thymus mitochondria isolated from room temperature and cold acclimated rats.

Thymus mitochondria were isolated from room temperature (○) and cold acclimated (●) rats as described in section 2.8.5. Mitochondria were incubated with [^{3}H] GDP (11.0 Ci/mmol; 0.1 – 6μM) and [^{14}C] sucrose for 15 minutes at 37°C in the absence (total binding) and presence (non-specific binding) of unlabelled GDP (1.5mM) as described in section 2.18. Specific binding was calculated from the difference between total and non-specific binding. Data are expressed as the mean ± S.E.M. of at least 2 experiments, each experiment performed in triplicate. The B_{MAX} values obtained for thymus mitochondria were 131.4 ± 19.6 and 196.6 ± 14.7 for room temperature and cold acclimated rats respectively. The K_D values obtained for thymus mitochondria were 1.4 ± 0.8 and 0.9 ± 0.3 for room temperature and cold acclimated rats respectively. Statistical differences were assessed using an unpaired Student's t-test.

Figure 6.2.4 shows an overall comparison of the [^{3}H]GDP binding parameters to Dowex-treated BAT and thymus mitochondria isolated from room temperature and cold acclimated rats. The data clearly shows saturable binding of [^{3}H] GDP to thymus and BAT mitochondria up to 6 μM [^{3}H] GDP. Dowex-treated thymus mitochondria bind GDP in a saturable manner with similar binding parameters obtained with Dowex-treated BAT mitochondria. The K_D values determined were 0.5 ± 0.4 μM and 1.4 ± 0.8 μM for Dowex-treated BAT and thymus mitochondria respectively, isolated from room temperature housed rats. The K_D values determined were 0.8 ± 0.6 and 0.9 ± 0.3 for Dowex-treated BAT and thymus mitochondria respectively, isolated from cold acclimated rats. Statistical analysis revealed no significant differences in K_D between BAT and thymus mitochondria isolated from either the room temperature or cold acclimated rats.

Figure 6.2.5 shows [^{3}H]GDP binding to thymus mitochondria isolated from rats housed at room temperature to be non-saturable in the absence of Dowex treatment. Consequently, binding parameters B_{MAX} and K_D were unattainable. In contrast, Dowex-treated thymus mitochondria bind [^{3}H]GDP in a saturable manner up to and including 6 μM GDP.

The kidney has been shown to constitutively express UCP2 protein in its mitochondria. Figure 6.2.6 shows [^{3}H]GDP binding to Dowex-treated kidney mitochondria to be non-saturable. As a result, determination of the binding parameters, B_{MAX} and K_D, was not possible.

The spleen has been shown to constitutively express UCP2 and UCP3 protein in its mitochondria. Figure 6.2.7 shows [^{3}H]GDP binding to Dowex-treated spleen mitochondria to be non-saturable. Therefore, determination of the binding parameters, B_{MAX} and K_D, was not possible.

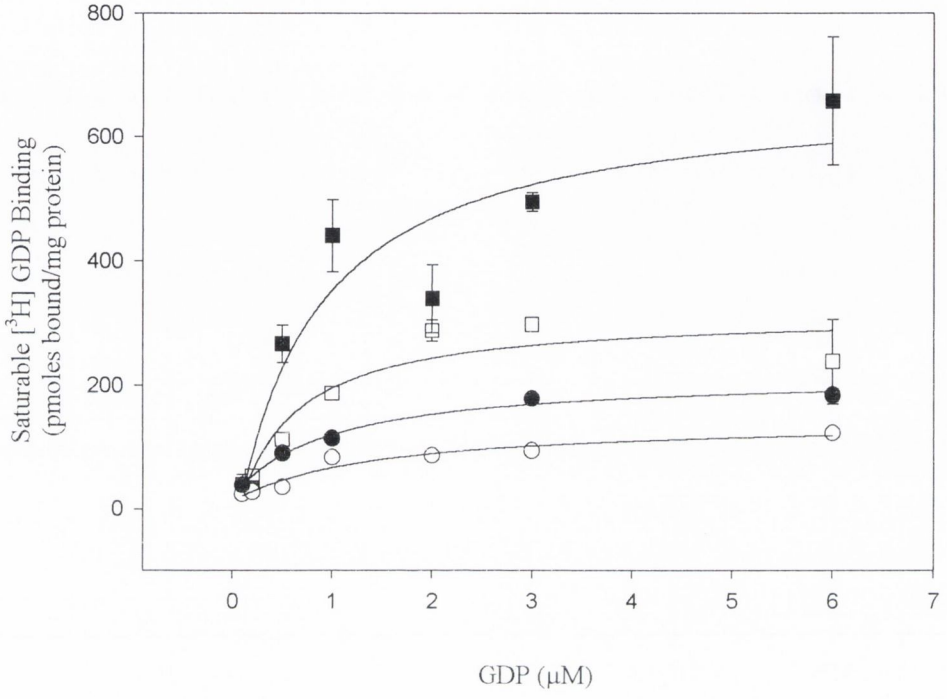


Figure 6.2.4 Comparison of [^{3}H] GDP binding parameters in Dowex-treated BAT and Dowex-treated thymus mitochondria isolated from room temperature and cold acclimated rats.

BAT mitochondria were isolated from room temperature (□) and cold acclimated (■) rats as described in section 2.8.1. Thymus mitochondria were isolated from room temperature (○) and cold acclimated (●) rats as described in section 2.8.5.Mitochondria were incubated with [^{3}H] GDP (11.0 Ci/mmol; 0.1 – 6μM) and [^{14}C] sucrose for 15 minutes at 37°C in the absence (total binding) and presence (non-specific binding) of unlabelled GDP (1.5mM) as described in section 2.18. Specific binding was calculated from the difference between total and non-specific binding. Data are expressed as the mean ± S.E.M. of at least 2 experiments, each experiment performed in triplicate.

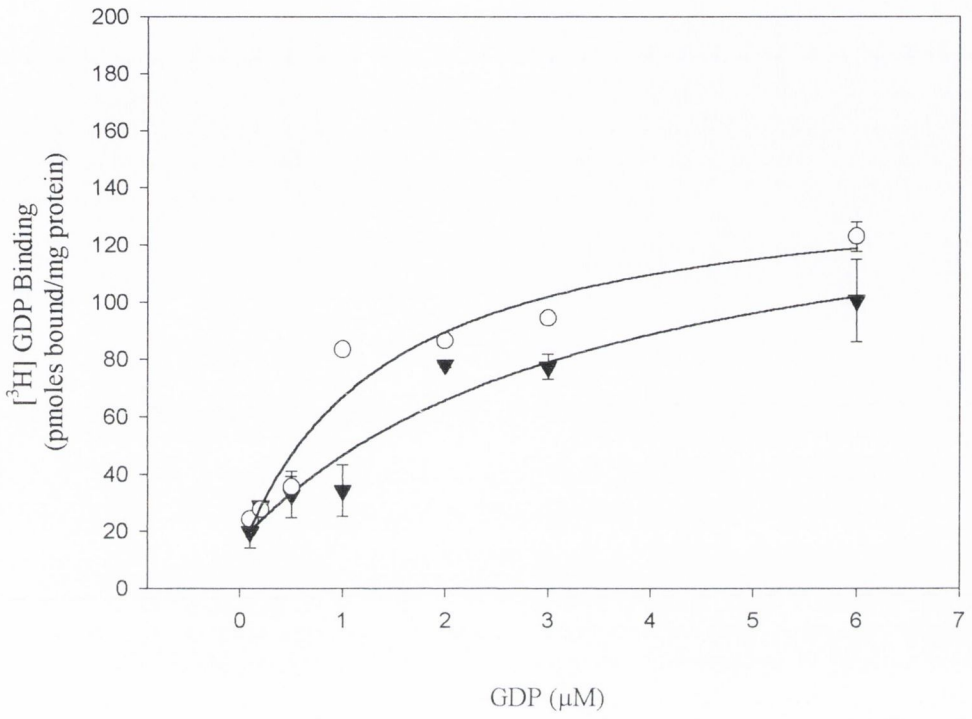


Figure 6.2.5: [^{3}H] GDP binding parameters in Dowex-treated and non-Dowex treated thymus mitochondria isolated from room temperature rats

Dowex treated (○) and non-Dowex treated (▼) thymus mitochondria (50μg) were isolated from rats housed at room temperature as described in section 2.8.4. Mitochondria were incubated with [^{3}H] GDP (11.0Ci/mmol; 0.1 - 6μM) and [^{14}C] sucrose for 15 minutes at 37^{0}C in the absence (total binding) and presence (non specific binding) of unlabelled GDP (1.5mM) as described in section 2.20. Specific binding was calculated from the difference between total and non-specific binding. Data represents the mean ± S.E.M. of at least 3 experiments, each experiment performed in triplicate. Determination of binding parameters K_D and B_{MAX} for room temperature thymus mitochondria were unattainable, as the specific binding was found not to be saturable.

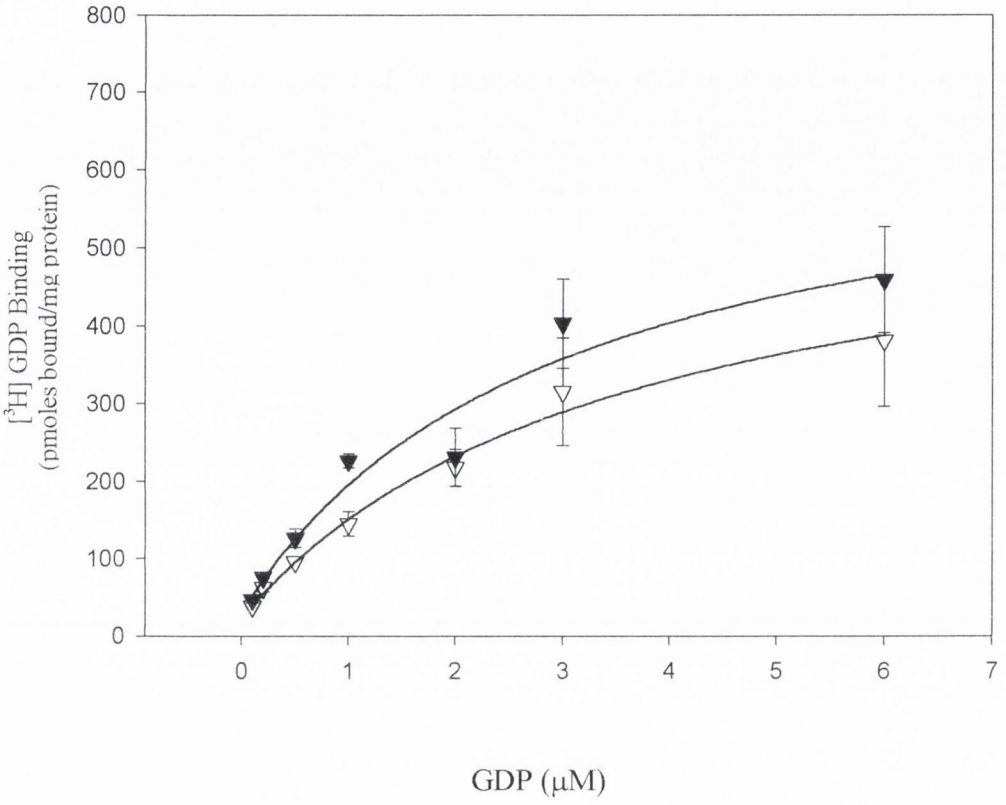


Figure 6.2.6: Comparison of [^{3}H] GDP binding parameters in Dowex treated kidney mitochondria isolated from room temperature and cold acclimated rats.

Kidney mitochondria were isolated from room temperature (▽) and cold acclimated (▼) rats as described in section 2.8.4. Mitochondria were incubated with [^{3}H] GDP (11.0 Ci/mmol; 0.1 – 6μM) and [^{14}C] sucrose for 15 minutes at 37°C in the absence (total binding) and presence (non-specific binding) of unlabelled GDP (1.5mM) as described in section 2.18. Specific binding was calculated from the difference between total and non-specific binding. Data are expressed as the mean ± S.E.M. of at least 3 experiments, each experiment performed in triplicate. Determination of the binding parameters K_D and B_{MAX} for kidney mitochondria was unattainable, as the specific binding was not found to be saturable.

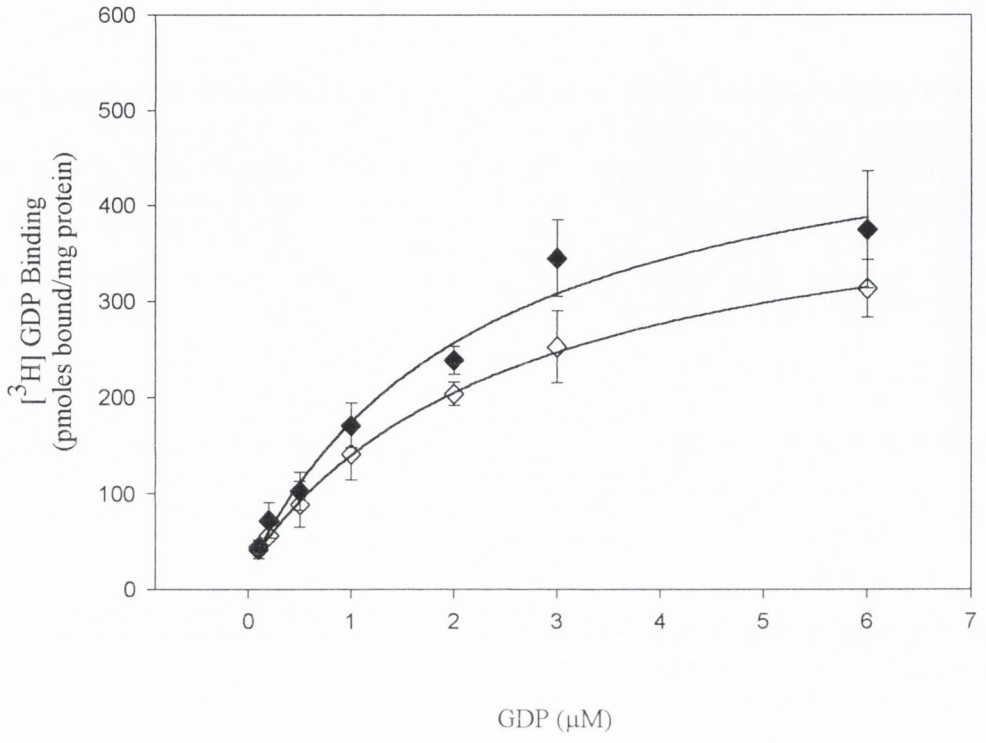


Figure 6.2.7 Comparison of [^{3}H] GDP binding parameters in Dowex-treated spleen mitochondria isolated from room temperature and cold acclimated rats.

Spleen mitochondria were isolated from room temperature (◇) and cold acclimated (◆) rats as described in section 2.8.3. Mitochondria were incubated with [^{3}H] GDP (11.0 Ci/mmol; 0.1 – 6μM) and [^{14}C] sucrose for 15 minutes at 37°C in the absence (total binding) and presence (non-specific binding) of unlabelled GDP (1.5mM) as described in section 2.18. Specific binding was calculated from the difference between total and non-specific binding. Data are expressed as the mean ± S.E.M. of at least 3 experiments, each experiment performed in triplicate. Determination of the binding parameters K_D and B_{MAX} for spleen mitochondria was unattainable, as the specific binding was not found to be saturable.

[6.3] Discussion

Nucleotide binding has been key in identifying and isolating UCP1 from BAT mitochondria (Heaton *et al.*, 1978; Lin & Klingenberg, 1980). UCP1 accepts with strong preference the purine di- and tri-nucleotides: GDP, GTP, ATP and ADP (Klingenberg, 1988). Our study shows BAT mitochondria, isolated from rats housed at room temperature and 4°C for 5 weeks, binding GDP with K_D and B_{MAX} binding parameters that are in close accordance with those obtained by other authors in the literature (Sundin & Cannon, 1980; Nedergaard & Cannon, 1985; Sundin *et al.*, 1987). Furthermore, a significant 2-fold (Figure 6.2.1) increase in GDP binding (B_{MAX}), without a change in K_D, is observed in BAT mitochondria isolated from the cold acclimated rats. The fact that a significant increase in GDP binding to BAT UCP1 upon cold exposure was observed in this study compares favourably with GDP binding studies performed by previous researchers (Swick and Swick, 1986; Nicholls and Locke, 1984; Nedergaard and Cannon, 1985; Sundin *et al.*, 1987; Sundin and Cannon, 1980). Therefore, BAT mitochondria isolated from room temperature and cold acclimated rats act as a positive control tissue for the GDP binding assay employed in this study.

We observed no binding of GDP to Dowex-treated liver mitochondria isolated from rats housed at room temperature or in the cold. We conclude that UCP is not present in liver mitochondria under these conditions. This result is as expected as no UCP protein has been detected in the liver under any physiological condition (Boss *et al.*, 1997; Fluery *et al.*, 1997). Therefore, liver mitochondria act as a negative control tissue for the GDP binding assay used in this study.

One interesting finding of the present study is that thymus mitochondrial UCP1 protein expression is up-regulated upon cold expression in a manner similar to BAT mitochondria (Chapter 4; Figure 4.2.5). As GDP binding to BAT mitochondria UCP1 has been shown to increase in parallel with the increase in UCP1 protein concentration upon cold exposure (Figure 6.2.1), we hypothesized that the observed up-regulation of UCP1 protein in thymus mitochondria upon cold acclimation might also manifest itself as an increase in GDP binding to thymic UCP1. Using Dowex-treated thymus mitochondria isolated from room temperature and cold acclimated rats we were able to show firstly, that

[^{3}H]GDP binding to thymus mitochondrial UCP1 is saturable in both cohorts and secondly, that [^{3}H]GDP binding is indeed significantly ($p=0.05$) increased in the cold acclimated compared to the room temperature animals. The binding curve shown (Figure 6.2.3) demonstrates a 1.5-fold increase in GDP binding in the thymus mitochondria isolated from the cold acclimated rats compared to the room temperature rats and, in both groups, half maximum binding (K_D) is clearly obtained with concentrations of less than 1 μM. It has been shown that the changes in GDP binding observed in BAT mitochondria upon cold exposure reflect changes in the number of binding sites (B_{MAX}), rather than changes in the affinity (K_D) (Peachey *et al.*, 1988; Sundin *et al.*, 1987). The thymus mitochondrial results presented here concur with this finding since we see a significant increase in the B_{MAX} with no apparent difference in K_D values. In addition, the K_D binding parameters obtained for Dowex-treated thymus mitochondria isolated from room temperature and cold acclimated rats are in close accordance with the K_D binding parameters obtained for Dowex-treated BAT mitochondria isolated from the same groups of animals (Figure 6.2.4).

When some or all of the nucleotide binding sites on UCP1 are occupied by residual bound purine nucleotides prior to performing the binding assay, the uncoupling protein is said to be masked. Previously, researchers have shown that UCP1 may exist in BAT mitochondria in either a non-functioning (masked) or functioning form (unmasked) (Huang & Klingenberg, 1995; Gribskov *et al.*, 1986). Huang & Klingenberg, (1995) showed that isolated BAT mitochondria could be unmasked by treatment with Dowex (a 21K anion exchanger) at pH 8 (see section 2.17; chapter 2). The present study sought to determine whether or not UCP1 expressed by thymus mitochondria isolated from room temperature rats displayed a similar masking phenomenon to BAT. To this end we treated some thymus mitochondria with Dowex and left other thymus mitochondria untreated. The results presented suggest that thymus mitochondria are susceptible to masking (Figure 6.2.5). Non-Dowex treated thymus mitochondria exhibited no saturable GDP binding at concentrations up to and including 6 μM GDP while saturable, high affinity binding was observed with the Dowex-treated samples. The unmasking-remasking process in BAT *in vivo* mitochondria appears to be rapid and reversible in response to changes in environmental temperature (Peachey *et al.*, 1988). It has therefore been suggested that masking may represent the acute physiological adaptation of thermogenic activity necessary to maintain body temperature

during the longer period necessary for synthesis and incorporation of new UCP1 into the mitochondria. The apparent occurrence of masking of UCP1 in thymus mitochondria may be consistent with either a thermogenic role for UCP1 or some means by which to control metabolic flux in thymus.

One of the main aims of this chapter was to investigate whether mitochondria containing UCP2 and UCP3 could bind purine nucleotides, in a manner similar to mitochondria containing UCP1. Therefore, we sought to investigate [^{3}H]GDP binding to rat kidney and spleen known to express UCP2 and UCP3 respectively. However, [^{3}H]GDP binding to both kidney and spleen mitochondria was of low-affinity, with no saturable binding up to 6 μM [^{3}H]GDP. To date, no other research group have published data showing [^{3}H]GDP binding to isolated mitochondria containing UCP2 or UCP3. Chemical modification and site-directed mutagenesis studies have shown that the amino acids involved in purine nucleotide binding to UCP1 are conserved in UCP2 and UCP3. Similarly, *E. coli* and heterologous yeast expression systems have shown GDP binding UCP2 and UCP3 (Jekabsons *et al.*, 2002; Zackova *et al.*, 2003). Jekabsons *et al.* (2002) showed that UCP2 expressed in bacterial inclusion bodies and solubilised bind N-methylanthraniloyl-tagged (MANT) purine nucleoside di- and tri-phosphates with low micromolar affinity. Zackova *et al.* (2003) showed that [^{3}H]GTP binding to isolated *E.coli* or yeast-expressing UCP2 or UCP3 exhibit high affinity binding, similar to UCP1. Taken together, circumstantial evidence has thus shown that UCP2 and UCP3 should bind purine nucleotides, akin to UCP1. However, we have shown GDP binding to UCP2 and UCP3 containing mitochondria to be non-saturable. In mitochondria, there may be other proteins regulating the binding capabilities of UCP2 and UCP3 and therefore this may account for the lack of binding observed in our study.

The fact that UCP2 (Nègre-Salvayre *et al.*, 1997; Krauss *et al.*, 2002) and UCP3 (Carroll and Porter, 2004) transcript and protein are expressed in thymus and thymus mitochondria respectively may imply that these UCPs can bind GDP when expressed in thymus mitochondria. Nègre-Salvayre *et al.* (1997) has shown that pre-incubation of thymus mitochondrial fractions with GDP, an inhibitor of UCP1 induced a rise in mitochondrial membrane potential and hydrogen peroxide production (H_2O_2). Up to now, UCP2 has been the only UCP associated with thymus and therefore Nègre-Salvayre *et al.*

(1997) concluded that UCP2 is GDP sensitive and that UCP2 is a regulator of mitochondrial H_2O_2 production. These results obtained by Nègre-Salvayre *et al.* (1997) may imply that UCP2 is associated with the saturable GDP binding observed in thymus mitochondria (Carroll *et al.*, 2005 & Chapter 6). However, although such a role for UCP2 may exist, the conclusion of Nègre-Salvayre *et al.* (1997) remains questionable since GDP binding and inhibition of UCP2 activity by GDP in isolated mitochondria have yet to be adequately demonstrated. Carroll and Porter (2004) have also shown that UCP3 transcript and protein is expressed in human thymus and rat thymus mitochondria. In addition, this group showed that starvation resulted in a 1.5-fold increase in UCP3 protein expression whilst having no effect on UCP1 protein expression in thymus mitochondria. If the GDP binding in thymus mitochondria that Carroll *et al.* observed was associated with UCP3, one might expect to see an increase in [^{3}H]GDP binding in thymus mitochondria isolated from fasted rats. However, it has been shown that [^{3}H]GDP binding to Dowex-treated thymus mitochondria isolated from fasted rats show a slight decrease in the B_{MAX}, whilst having no effect on the K_D (Carroll, unpublished data). This scenario is indicative that GDP binding in thymus mitochondria is not associated with UCP3. Taken together, both the results of Carroll *et al.* (2005) and Nègre-Salvayre *et al.* (1997) strongly imply that the binding parameters obtained for thymus mitochondria are due to the presence of UCP1 and not UCP2 or UCP3.

[6.4] Conclusion

Our results confirm that UCP1 in BAT mitochondria isolated from rats housed at room temperature and acclimated to the cold for 5 weeks bind GDP with binding parameters, K_D and B_{MAX} values very similar to those in the literature.

This study has also substantiated the finding of Carroll *et al.* (2005) that thymus mitochondria have a UCP1 dependent GDP binding site, with binding parameters, K_D and B_{MAX} values, very similar to those obtained for BAT mitochondria. In addition, the present study has provided novel data which show cold exposure significantly increases GDP binding in thymus mitochondria without changing the K_D value in a manner similar to BAT mitochondria. The presence of a functional UCP1 protein in thymus mitochondria has undeniably exposed an innovative route for further research into thymus bioenergetics.

Our findings also confirm that the purine nucleotide binding site in thymus mitochondria isolated from rats housed at room temperature is masked and that Dowex-treating the thymus mitochondria results in the binding site being unmasked.

Taken together, all our binding data shows no saturable GDP binding to mitochondria known to contain UCP2 (kidney) and UCP3 (spleen). The possibility cannot be excluded that a purine nucleotide binding site exists on UCP2 and UCP3 with purine nucleotide selectivity or affinity that is markedly different from that of UCP1. Similarly, UCP2 and UCP3 may only bind purine nucleotides in the presence of activators such as coenzyme Q, superoxide or hydroxynonenals.

Chapter 7
General Discussion

[7.1] UCP3 in skeletal muscle and spleen

We have recently designed a new peptide antibody to UCP3 which is sensitive and discriminatory for UCP3 over UCP2, UCP1 and other mitochondrial carrier transporters (Cunningham *et al.*, 2003). Using the UCP3 peptide antibody, we confirm the presence of UCP3 protein in skeletal muscle mitochondria and lack of expression of UCP3 in liver homogenates (Chapter 3). Moreover, we show the novel result that acute exercise results in a temporary increase in UCP3/mg of mitochondrial protein expression in *gastrocnemius* muscle only which compares favourably to previously published mRNA results for *gastrocnemius* muscle (Tsuboyama *et al.*, 1998). We confirm that endurance exercise results in no significant changes in UCP3/mg of mitochondrial protein expression in *gastrocnemius*, *plantaris*, *soleus* or *EDL* muscle homogenates. Our findings also show that UCP2 (kidney), UCP3 (spleen) and non-UCP (liver) containing mitochondria do not show significant GDP binding (Chapter 6). In addition, we illustrate that purine nucleotides and fatty acids do not inhibit or activate uncoupling in UCP2 (kidney), UCP3 (spleen) or non-UCP (liver) containing mitochondria (Chapter 5).

The physiological functions of UCP2 and UCP3 are as yet unknown. Based on their 59 % (UCP2) and 57 % (UCP3) sequence homology with UCP1, whose physiological function is uncoupling and thermogenesis, UCP2 and UCP3 were attributed with the function of mitochondrial uncoupling through proton leak reactions. Some genetic linkage and association studies as well as UCP mRNA correlation studies are consistent with this view (Harper *et al.*, 2001). Our functional results, from room temperature rats, our consistent with the view that UCP2 and UCP3 are not uncouplers under normal physiological conditions. However, it has been suggested that under conditions which induce increased ROS production, such as cold exposure (Kaushik and Kaur, 2003; Venditti *et al.*, 2004) and endurance exercise (Du *et al.*, 1998; Bejma and Ji, 1999), UCP2 and UCP3 may function as 'mild' uncouplers of oxidative phosphorylation in order to relieve oxidative stress (Skulachev, 1996). Only a limited amount of evidence exists supporting the possibility that UCP2 and UCP3 function to limit ROS production via 'mild' uncoupling. Firstly, UCP3 protein expression has been shown to increase following 8-weeks cold exposure (Cunningham *et al.*, 2003). Secondly, addition of ADP or an uncoupling agent (*e.g.* FCCP or 2,4-DNP) was shown to strongly suppress the formation of

superoxide anions (Skulachev, 1998). Thirdly, it has previously been shown that the absence of UCP3 led to an increase in ROS production, thereby, implying a role for UCP3 in preventing the formation of ROS in skeletal muscle (Vidal-Puig *et al.*, 2000). Finally, 4-hydroxy-2-nonenal (HNE), a by-product of lipid peroxidation, induces GDP sensitive uncoupling in mitochondria isolated from tissues containing UCP1 (BAT), UCP2 (BAT and kidney) and UCP3 (BAT and skeletal muscle) (Echtay *et al.*, 2003).

Our cold and endurance exercise studies present contradictory evidence which suggests that 'mild' uncoupling may not be the function of UCP2 and UCP3 since we see no uncoupling in UCP2 or UCP3 containing mitochondria. We do not see the concomitant increase in state 4 oxygen consumption rates or in inhibition and activation by GDP and palmitate respectively in UCP3 containing mitochondria (spleen) that one would expect if 'mild' uncoupling were the function of UCP3 following cold exposure. In addition, we did not observe any significant increases in UCP3 protein expression following endurance exercise. This is not consistent with a role for UCP3 in the regulation of ROS production. Then again, it is possible that there is so little UCP2 and UCP3 expressed per mg of mitochondrial protein in kidney and spleen respectively that our assay system, which can detect uncoupling in UCP1 containing mitochondria (BAT and thymus), may not be sensitive enough to detect the 'mild' uncoupling function that Skulachev (1996) has proposed for UCP2 and UCP3. Clearly, more experiments are needed to fully evaluate the appealing hypothesis that UCPs functions to reduce ROS production. If UCPs do in fact limit ROS production, then they could play an important role in affecting ageing due to oxidative stress.

The increase in UCP3 protein expression during acute exercise, a time when metabolic heat should be dissipated rather than generated, does not support a primary role for UCP3 in thermoregulation. We believe that our acute exercise UCP3 expression results are more consistent with a role for UCP3 in the regulation of fatty acid oxidation/metabolism than in energy dissipation. Harper *et al.* (2001) and Dulloo *et al.* (2001) have also proposed that the primary role of UCP3 in skeletal muscle is in the regulation of lipids as fuel substrates and/or in controlling the export of fatty acids out of the mitochondria during fatty acid oxidation. In skeletal muscle, physiologic conditions associated with increased levels of circulating free fatty acids, such as cold exposure,

starvation and exercise are correlated with increased UCP3 mRNA and UCP3 protein levels (Boss *et al.*, 1998a; Tsuboyama *et al.*, 1998; Cadenas *et al.*, 1999; Sivitz *et al.*, 1999; Zhou *et al.*, 2000; Pilegaard *et al.*, 2000; Schrauwen *et al.*, 2002; Cunningham *et al.*, 2003; Moreno *et al.*, 2003; Chapter 3). Elevation of free fatty acids by lipid infusion, proposed as a starvation mimicking condition, also increases UCP3 gene expression in vivo (Weigle *et al.*, 1998). Each of these conditions correlates favourably with a role for UCP3 in fatty acid metabolism. However, more investigation is required to ascertain the true physiological function of UCP3.

[7.2] UCP1 in thymus

Using a selective UCP1 peptide antibody, our study has revealed the novel result that UCP1 protein is expressed in thymus mitochondria isolated from wild type mice but is not expressed in thymus mitochondria isolated from UCP1 knock-out mice (Chapter 4). This pattern of expression and non-expression of UCP1 protein in wild type and UCP1 knock-out mice respectively is mirrored in BAT mitochondria. UCP1 is not detected in either UCP2 containing (kidney) or non-UCP containing (liver) mitochondria isolated from wild type or knock-out mice. Our novel finding supports the discovery of UCP1 in thymus and thymocyte mitochondria isolated from rats reported by Carroll *et al.* (2005) and challenges the popularly held belief that UCP1 is solely expressed in BAT mitochondria.

We have also established that rat UCP1 expression is significantly up-regulated following cold acclimation for 5-weeks (Chapter 4). It has previously been shown that UCP1 protein expression in BAT increases upon cold exposure (Ricquier and Kader, 1976; Desautels *et al.*, 1978; Heaton *et al.*, 1978; Swick & Swick, 1986; Sundin *et al.*, 1987; Klaus *et al*, 1991; Nicholls & Rial, 1999; Nedergaard *et al.*, 2001a & 2001b; Chapter 4). The fact that cold exposure increases UCP1 expression in both BAT and thymus mitochondria suggests that UCP1 is regulated in a similar manner in both tissues. However, Carroll *et al.* (2005) reported that acute starvation (48-hours), a condition known to decrease UCP1 expression in BAT (Rothwell *et al.*, 1984; Trayhurn *et al.*, 1988; Boss *et al.*, 1998a; Nedergaard *et al.*, 2001a), resulted in no change in UCP1 expression in thymus or thymocyte mitochondria hinting at a different role for UCP1 in the two tissues. One aspect of future studies will be to investigate UCP1 protein expression in thymus under

varying physiological conditions known to induce changes in UCP1 expression in BAT (*e.g.* thyroid and LPS treatment) and determine whether thymus UCP1 is regulated in the same manner as BAT UCP1.

GDP binding to UCP1 is up-regulated in BAT mitochondria isolated from cold acclimated rats in response to an increase in BAT mitochondrial UCP1 protein expression and an increase in 'unmasked' GDP binding sites (Swick and Swick, 1986; Nicholls and Locke, 1984; Nedergaard and Cannon, 1985; Sundin *et al.*, 1987; Sundin and Cannon, 1980; Chapter 4 & 6). In the present study, the observed up-regulation of UCP1 protein expression in thymus mitochondria in response to cold acclimation (Chapter 4) suggested that we might also expect to see an increase in saturable GDP binding in thymus mitochondria following cold acclimation. Using Dowex-treated thymus mitochondria, to maximize the possibility of detecting GDP binding, from room temperature and cold acclimated rats, we were able to show [^{3}H] GDP binding to be saturable, with K_D values similar to those obtained with BAT mitochondria. In addition, we detected a significant 1.6 fold increase ($p \leq 0.05$) in GDP binding (B_{MAX}) to thymus UCP1 in the cold acclimated group. No significant difference in thymus K_D values were observed between the room temperature and cold acclimated rats. This observation correlates well with our immunoblotting data which shows a 1.7 fold increase in thymus UCP1 protein following 5-weeks cold exposure (Chapter 4). Huang & Klingenberg, (1995) showed that isolated BAT mitochondria from room temperature rats could be unmasked by treatment with Dowex for 1-hour at room temperature. The present study has shown that non-Dowex treated thymus mitochondria exhibited no saturable GDP binding at concentrations up to and including 6 μM GDP while saturable, high affinity binding was observed with the Dowex-treated samples implying that thymus mitochondria are also subject to masking at room temperature.

The present study has also shown that steady state (state 4) oxygen consumption rates are higher in thymus mitochondria isolated from cold acclimated rats (Chapter 5). In addition, our results show that non-phosphorylating oxygen consumption rates in thymus mitochondria, isolated from rats kept at 4°C, are more sensitive to GDP inhibition and are more responsive to reactivation of the GDP inhibited component of state 4 oxygen

consumption by palmitate (Chapter 5). As mentioned in Chapter 5, the increase in state 4 oxygen consumption rates following cold acclimation may be due to one of three events: (i) an increase in basal, non-UCP related, proton leak; (ii) an increase in the number of 'unmasked' GDP binding sites in cold acclimated rats; (iii) an increase in the amount of UCP1 protein expressed in cold acclimated rats. Our results suggest that, as for BAT mitochondria following cold acclimation, the increase in state 4 rates in thymus mitochondria and the increase in responsiveness to GDP and palmitate result from an increase in UCP1 protein expression observed in cold adapted thymus mitochondria (Chapter 4). Although the state 4 oxygen consumption rates for thymus mitochondria, from both room temperature and cold acclimated rats, are noticeably less than those of BAT mitochondria, they are GDP inhibitable and palmitate activatable, which we conclude to be due to the activity of UCP1. Novel inhibitors and activators of the uncoupling activity of UCP1 in rodent thymus mitochondria may be investigated using this sensitive assay system in the future.

	RT BAT	**Cold BAT**	
Tissue Mass (g)	2.6 ± 0.3	2.2 ± 0.1	N.S
mg of mitochondrial protein /g tissue (mg/g)	1.1 ± 0.4	6.9 ± 0.8	**P≤0.01
B_{MAX} (pmoles bound/mg protein)	353 ± 61	736 ± 128	*P≤0.05
UCP1/$F_1\beta$ (arbitrary units)	0.97 ± 0.07	1.5 ± 0.2	*P≤0.05

Table 7.1 Summary of the effects of 5-weeks cold acclimation on tissue mass, mitochondrial protein yield/g tissue, B_{MAX} and UCP1/F1β protein expression in BAT mitochondria. Values are mean ± S.E.M. RT = room temperature; CA= cold acclimated; B_{MAX} = maximal binding capacity.

	RT Thymus	Cold Thymus	
Tissue Mass (g)	1.4 ± 0.2	1.3 ± 0.1	N.S
mg of mitochondrial protein /g tissue (mg/g)	1.7 ± 0.4	1.4 ± 0.1	N.S
B_{MAX} (pmoles bound/mg protein)	131 ± 20	197 ± 15	*p≤0.05
UCP1/$F_1\beta$ (arbitrary units)	0.74 ± 0.12	1.25 ± 0.07	*p≤0.05

Table 7.2 Summary of the effects of 5-weeks cold acclimation on tissue mass, mitochondrial protein yield/g tissue, B_{MAX} and UCP1/F1β protein expression in thymus mitochondria. Values are mean ± S.E.M. RT = room temperature; CA= cold acclimated; B_{MAX} = maximal binding capacity.

Taken together, our expression, binding and functional data illustrate the presence of a functioning UCP1 in rat thymus mitochondria that is significantly increased upon cold acclimation. The next question to be resolved is 'what is the role of UCP1 in thymus'? UCP1 functions in thermoregulation in rodent BAT. However, upon closer inspection, it appears that this may not be the case for UCP1 in rodent thymus (see Table 7.1). Clearly, the expression levels of UCP1/$F_1\beta$, which can be used indirectly to measure the levels of UCP1 per mg of mitochondria, increase in both tissues following cold exposure. In addition, B_{MAX} values increase in both tissues post cold acclimation but greater levels of binding are found in the BAT mitochondria. Finally, and most importantly however, we observed that while the mg of mitochondrial protein per gram of tissue increased significantly in BAT, the mg of mitochondrial protein per gram of tissue stayed the same in the thymus mitochondria which argues against a thermoregulatory role for UCP1 in thymus. Therefore, while thymus UCP1 appears to be temperature sensitive, our results suggest that it is not a general source of heat in the body of these animals.

New perceptions with regard to UCPs, in particular UCP1, are now being revealed with the discovery that UCPs appear to be modulators of mitochondrial ROS production (Nègre-Salvayre *et al.*, 1997; Echtay *et al.*,2002 & 2002b & 2003). Recently, it has been shown that the GDP sensitive proton conductance catalysed by UCPs increases on exposure to superoxide (Echtay *et al.*, 2002), or to lipid peroxidation breakdown products such as 4-hydroxy-2-*trans*-nonenal (HNE) (Echtay *et al.*, 2003). In addition, superoxide generated using xanthine and xanthine oxidase has been shown to increase proton transport through UCP1, UCP2 and UCP3 in a reaction that is inhibited by nucleotides including GDP (Echtay *et al.*, 2002b). Nègre-Salvayre *et al.* (1997) showed that membrane potential and hydrogen peroxide (H_2O_2) production were increased in mitochondrial fractions isolated from UCP2 containing tissues (BAT, thymus and spleen) when pre-incubated in GDP leading the authors to suggest that their results may indicate that UCP2 acts as a regulator of H_2O_2 production in mitochondria. However, Nègre-Salvayre *et al.* (1997) then suggested, that since thymus mitochondria contain no UCP1, but express UCP2 gene, UCP2 must be the regulator of H_2O_2 production. However, our finding that thymus mitochondria do categorically express UCP1 protein puts UCP1 at the forefront as a regulator of H_2O_2 production.

Further evidence, to support the hypothesis that thymus UCP1 functions in the regulation of ROS production, comes in the appearance of reports that chronic cold exposure induces biochemical changes predisposing tissues to oxidative stress. Chronic cold exposure (3-weeks) has previously been shown to detrimentally affect the antioxidant defence system in brain, kidney, liver, heart and small intestine tissues of rats (Kaushik and Kaur, 2003; Venditti *et al.*, 2004). The effects of cold exposure include higher levels of lipid peroxides (LPO) in liver, heart, brain, kidney and intestine, increased xanthine oxidase (XOD) in brain and intestine, and significant diminution of antioxidant enzymes, such as superoxide dismutase (SOD), in liver, kidney, brain, heart and intestine. The fact that we see (i) an increase in UCP1 protein expression in thymus mitochondria, (ii) an increase in [^{3}H] GDP binding to thymus mitochondria and (iii) an increase in GDP inhibition of state 4 oxygen consumption rates and palmitate activatability of GDP inhibited state 4 oxygen consumption rates following cold exposure is consistent with a role for UCP1 in defence against ROS production. One possible aspect of future studies will be to investigate whether a lack of UCP1 in the thymus leads to significant increases in mitochondrial ROS

production under varying physiological conditions conducive to producing oxidative stress (*e.g.* cold exposure).

Evidently, the discovery of UCP1 in rat and mouse thymus mitochondria and its subsequent upregulation in response to cold exposure has revealed a new route for the study of thymus bioenergetics, metabolism, development and function.

References

References

Aquila, H., Link, T.A. and Klingenberg, M. (1985) The uncoupling protein from brown fat mitochondria is related to the mitochondrial ADP/ATP carrier. Analysis of sequence homologies and of folding of the protein in the membrane. *The EMBO J*ournal **4,** 2369 - 2376.

Arsenijevic, D., Onuma, H., Pecqueur, C., Raimbault, S., Manning, B.S., Miroux, B., Couplan, E., Alves-Guerra, M.C., Goubern, M., Surwit, R., Bouillaud, F., Richard, D., Collins, S. and Ricquier, D. (2000) Disruption of the uncoupling protein-2 gene in mice reveals a role in immunity and reactive oxygen species production. *Nature Genetics* **26**, 435 – 439.

Bai, Y., Onuma, H., Bai, X., Medvedev, A., Misukonis, M., Weinberg, J., Cao, W., Robidoux, J., Floering, L., Daniel, K. and Collins, S. (2005) Persistent NF kappa B activation in UCP2 -/- mice leads to enhanced nitric oxide and inflammatory cytokine production. *The Journal of Biological Chemistry* [in press].

Bejma, J. and Ji, L.L. (1999) Aging and acute exercise enhance free radical generation in rat skeletal muscle. *Journal of Applied Physiology* **87,** 465 – 470.

Bhattacharya, S.K., Thakar, J.H., Johnson, P.L. and Shanklin, D.R. (1991) Isolation of skeletal muscle mitochondria from hamsters using ionic medium containing ethylenediaminetetraacetic acid and nagarse. *Analytical Biochemistry* **192**, 344 – 349.

Bienengraber, M., Echtay, K.S. and Klingenberg, M. (1998) H^+ transport by uncoupling protein (UCP-1) is dependent on a histidine pair absent in UCP-2 and UCP-3. *Biochemistry* **37**, 3 -8.

Boss, O., Samec, S., Paoloni-Giacobino, A., Rossier, C., Dulloo, A., Seydoux, J., Muzzin P. and Giacobino, J. (1997a) Uncoupling protein 3: a new member of the mitochondrial carrier family with tissue specific expression. *FEBS Letters* **408**, 39 – 42.

Boss, O., Samec, S., Dulloo, A., Seydoux, J., Muzzin, P. and Giacobino, J.P., (1997b) Tissue dependent regulation of rat UCP2 expression in response to fasting or cold. *FEBS Letters* **412**, 111 - 114.

Boss, O., Samec, S., Kuhne, F., Bijlenga, P., Assimacopoulos-Jeannet, F., Seydoux, J., Giacobino, J. and Muzzin, P. (1998a) Uncoupling protein-3 expression in rodent skeletal muscle is modulated by food intake but not by changes in environmental temperature. *The Journal of Biological Chemistry* **273**, 5 – 8.

Boss, O., Samec, S., Desplanches, D., Mayet, M., Seydoux, J., Muzzin, P. and Giacobino, J. (1998b) Effect of endurance training on mRNA expression of uncoupling proteins 1,2 and 3 in the rat. *FASEB Journal* **12**, 335 – 339.

Boss, O., Muzzin, P. and Giacobino, J.P. (1998c) The uncoupling proteins, a review. *European Journal of Endocrinology* **139**, 1 - 9.

Boss, O., Hagan, T. and Lowell, B.B. (2000) Uncoupling proteins 2 and 3: potential regulators of mitochondrial energy metabolism. *Diabetes* **49**, 143 - 156.

Bouillaud, F., Ricquier, D., Thibault, J. and Weissenbach, J. (1985) Molecular approach to thermogenesis in brown adipose tissue; cDNA cloning of the mitochondrial uncoupling protein. *Proceedings of the National Academy of Science* **82**, 445 - 448.

Brand, M.D. (1977) The stoichiometric relationships between electron transport, proton translocation and adenosine triphosphate synthesis and hydrolysis in mitochondria. *Biochemical Society Trans*actions **5,** 1615 - 1620.

Brand, M.D. (1990) The proton leak across the mitochondrial inner membrane. *Biochimica et Biophysica Acta* **1018**, 128 - 133.

Brand, M.D., Harper, M.E. and Taylor, H.C. (1993) Control of the effective P/O ratio of oxidative phosphorylation in liver mitochondria and hepatocytes. *Biochemical Journal* **291**, 739 - 748.

Brand, M.D., Chein, L-F., Ainscow, E.K., Rolfe, D.F.S. and Porter, R.K. (1994) The causes and functions of mitochondrial proton leak. *Biochimica et Biophysica Acta* **1187**, 132 - 139.

Brand, M.D. (2000) Uncoupling to survive? The role of mitochondrial inefficiency in ageing. *Experimental Gerontology*. **35**, 811 – 820.

Brooks, G.A. and Mercier, J. (1994) Balance of carbohydrate and lipid utilisation during exercise: the 'crossover' concept. *Journal of Applied Physiology* **76**, 2253 – 2261.

Brown, G.C. and Brand, M.D. (1986) Changes in the permeability to protons and other cations at high proton motive force in rat liver mitochondria. *Biochemical Journal* **234**, 75 - 81.

Cadenas, S., Buckingham, J.A., Samec, S., Seydoux, J., Din, N., Dulloo, A.G. and Brand, M.D. (1999) UCP2 and UCP3 rise in starved rat skeletal muscle but mitochondrial conductance remains unchanged. *FEBS Letters* **462**, 257 - 260.

Cadenas, S. Buckingham, J.A., Clapham, J.C. and Brand, M.D. (2000) Human uncoupling protein-3 overexpression increases mitochondrial proton leak. *International Journal of Obesity*. **24**, S187.

Cadenas, S., Echtay, K.S., Harper, J.A., Jekabsons, M.B., Buckingham, J.A., Grau, E., Abiun, A., Chapman, H., Clapham, J.C. and Brand, M.D. (2002) The basal proton conductance of skeletal muscle mitochondria from transgenic mice overexpressing or lacking uncoupling protein 3. *The Journal of Biological Chem*istry **277**, 2773 - 2778.

Cannon, B., Hedin, A. and Nedergaard, J. (1982) Exclusive occurrence of thermogenin antigen in brown adipose tissue. *FEBS Letters* **150**, 129 - 132.

Cannon, B., Jacobsson, A., Rehnmark, S., and Nedergaard, J. (1996). Signal transduction in brown adipose tissue recruitment: noradrenaline and beyond. *International Journal of Obesity* **20**, S36 - S42.

Carroll, A.M., and Porter, R.K. (2004) Starvation sensitive UCP3 expression in rat thymus and spleen. *Biochimica et Biophysica Acta* **1700**, 145 – 150.

Carroll, A.M., Haines, L.R., Pearson, T.W., Fallon, P., Walsh, C., Brennan, C.M., Breen, E.P. and Porter, R.K. (2005) Detection of a functioning UCP1 in thymus. *The Journal of Biological Chemistry* **280**, 15534 – 15543.

Casteilla, L., Klaus, S., Bouillaud, F., Raimbault, S. and Ricquier, D. (1990). The uncoupling protein of brown adipose tissue. Molecular studies. In *Structure, Function and Biogenesis of Energy Transfer Systems*. Edited by Quagliariello *et al.* pp 257-260. Elsevier Science, Amsterdam.

Chakraborti, T., Das, S., Mondal, M., Roychoudhury, S. and Chakraborti, S. (1999) Oxidant, mitochondria and calcium: an overview. *Cell Signal* **11**, 77 – 85.

Chan, C.B., Mac Donald, P.E., Saleh, M.C., Johns, D.C., Marban, E. and Wheeler, M.B. (1999) Over-expression of uncoupling protein-2 inhibits glucose-stimulated insulin secretion from rat islets. *Diabetes*. **48**, 1482 - 1486.

Chappell, J.B. and Hansford, R.G. (1972) In *Subcellular Components: Preparation and Fractionation* (Edited by Birnie, G.D.) pp. 77 – 91. Butterworths, London.

Clapham, J.C., Arch, A.R.S., Chapman, H., Haynes, A., Lister, C., Moore, G.B.T., Piercy, V., Carter, S.A., Lehner, I., Smith, S.A., Beeley, L.J., Godden, R.J., Herrty, N., Skehel, M., Changani, K.K., Hockings, P.D., Reid, D.G., Squires, S.M., Hacher, J., Trail, B., Lactham, J., Rastan, S., Harper, A.J., Cadenas, S., Buckingham, J.A., Brand, M.D. and Abiun, A. (2000) Mice overexpressing human uncoupling protein-3 in skeletal muscle are hyperphagic and lean. *Nature*, **406**, 415 - 418.

Collins, S., Daniel, K., Rolf, E.M., Ramkumar, V., Taylor, I.L. and Gettys, T.W. (1994) Impaired expression and functional activity of the beta3 and beta 1-adrenergic receptors in adipose tissue of congenitally obese (C57BL/6J ob/ob) mice. *Molecular Endocrinology* **8**, 518 - 527.

Cortez-Pinto, H., Lin, H.Z., Yang, S.Q., Da Costa, S.O. and Diehl, A.M. (1999) Lipids upregulate uncoupling protein 2 expression in rat hepatocytes. *Gastroenterology* **116**, 1184 – 1193.

Cortright, R.N., Zheng, D., Jones, J.P., Fluckey, J.D., Dicarlo, S.E., Grujic, D. and Lowell, B.B. (1999) Regulation of skeletal muscle UCP2 and UCP3 gene expression by exercise and denervation. *American Journal of Physiology* **276**, E217 – E221.

Costa, A.D., Nantes, I.L., Jezek, P., Leite, A, Arruda, P. and Vercesi, A.E. (1999) Plant uncoupling mitochondrial protein activity in mitochondria isolated from tomatoes at different stages of ripening. *Journal of Bioenergetics and Biomembr*anes **31**, 527 - 533.

Couplan, E., González-Barroso, M.M., Alves-Guerra, M.C., Ricquier, D., Goubern, M. and Bouillaud, F. (2002) No evidence for a Basal, Retinoic, or Superoxide-induces uncoupling activity of the uncoupling protein 2 present in spleen or lung mitochondria. *The Journal of Biological Chem*istry **277**, 26268 - 26275.

Crescenzo, R., Mainieri, D., Solinas, G., Montani, J.P., Seydoux, J., Liverini, S., Iossa, S. and Dulloo, A.G. (2003) Skeletal muscle mitochondrial oxidative capacity and uncoupling protein 3 are differently influenced by semi-starvation and refeeding. *FEBS Letters* **544**, 138 - 142.

Cunningham, O., McElligott, A.M., Carroll, A.M., Breen, E., Reguenga, C., Oliveira, M.E.M., Azevedo, J.E. and Porter, R.K. (2003) Selective detection of UCP3 expression in skeletal muscle: effect of thyroid status and temperature acclimation. *Biochimica et Biophysica Acta* **1604**, 170 - 179.

Desautels, M., Zaror-Behrens, G. and Himms-Hagen, J. (1978) Increased purine nucleotide binding, altered polypeptide composition and thermogenesis in brown adipose tissue mitochondria of cold-acclimated rats. *Canadian. Journal of Biochem*istry **56**, 378 - 383.

Desautels, M. and Himms-Hagen, J. (1981) Brown adipose tissue mitochondria of cold-acclimated rats: changes in characteristics of purine nucleotide control of the proton electrochemical gradient. *Canadian Journal of Biochemistry* **59**, 619 – 625.

Du, G., Mouithys-Mickalad, A. and Sluse, F.E. (1998) Generation of superoxide anion by mitochondria and impairment of their functions during anoxia and reoxygenation in vitro. *Free Radical Biology and Medicine* **25,** 1066 – 1074.

Echtay, K.S., Liu, Q., Caskey, T., Winkler, E., Frischmuth, K., Bienengräber, M. and Klingenberg, M. (1999) Regulation of UCP3 by nucleotides is different from regulation of UCP1. *FEBS Letters* **450**, 8 - 12.

Echtay, K., Winkler, E. and Klingenberg, M. (2000) Coenzyme Q is an obligatory cofactor for uncoupling protein function. *Nature* **408**, 609 – 613.

Echtay, K.S., Winkler, E., Frischmuth, K. and Klingenberg, M. (2001) Uncoupling protein 2 and 3 are highly active H+ transporters and highly nucleotide sensitive when activated by coenzyme Q (ubiquinone). *Proceedings of the Natural Academy of Sciences* **98**, 1416 – 1421.

Echtay, K.S. and Brand, M.D. (2001) Coenzyme Q induces GDP-sensitive proton conductance in kidney mitochondria. *Biochemical Society Transactions* **29**, 763-768.

Echtay, K.S., Roussel, D., St-Pierre, J., Jekabsons, M.B., Cadenas, S., Stuart, J.A., Harper, J.A., Roebuck, S.J., Morrison, a., Pickering, S., Clapham, J.C. and Brand, M. (2002) Superoxide activates mitochondrial uncoupling proteins. *Nature* **415**, 96 – 99.

Echtay, K.S., Murphy, M.P., Smith, R.A.J., Talbot, D.A. and Brand, M.D. (2002b) Superoxide activates mitochondrial uncoupling protein 2 from the matrix side: Studies using targeted antioxidants. *The Journal of Biological Chemistry* **277**, 47129 - 47135.

Echtay, K.S., Esteves, T.C., Pakay, J.L., Jekabsons, M.B., Lambert, A.J., Portero-Otín, M., Pamplona, R., Vidal-Puig, A.J., Wang, S., Roebuck, S.J. and Brand, M.D. (2003) A signalling role for 4-hydroxy-2-nonenal in regulation of mitochondrial uncoupling. *The EMBO Journal* **22**, 4103 – 4110.

Enerback, S., Jacobsson, A., Simpson, E., Guerra, C., Yamashita, H., Harper, M.E. and Kozak, L.P. (1997) Mice lacking mitochondrial uncoupling protein are cold sensitive but not obese. *Nature* **387**, 90 – 94.

Fernström, M., Tonkonogi, M. and Sahlin, K. (2003) Effects of acute and chronic endurance exercise on mitochondrial uncoupling in human skeletal muscle. *The Journal of Physiology* **554**, 755 – 763.

Fleury, C., Neverova, M., Collins, S., Raimbault, S., Champigigny, O., Levi-Meyruis, C., Seldin, M.F., Surwit, R.S., Riquier, D. and Warden, C.H. (1997) UCP2 a novel gene linked to obesity and hyperinsulinemia. *Nature Genetics* **15**, 269 - 272.

Foster, D.O. and Frydman, M.L. (1979) Tissue distribution of cold-induced thermogenesis in conscious warm- and cold-acclimated rats re-evaluated from changes in tissue blood flow. *Canadian Journal of Physiology and Pharmacology* **57**, 25 - 27.

Foster, D.O. (1986) Quantitative role of brown adipose tissue in thermogenesis. In: *Brown Adipose Tissue* Edited by Trayhurn, P. and Nicholls, D. pp 31 - 52. Arnold, London.

Garlid, K.D., Orosz, D.E., Modriansky, M., Vassanelli, S. and Ježek, P (1996) On the mechanism of fatty acid induced proton transport by mitochondrial uncoupling protein. *The Journal of Biological Chem*istry **271**, 2615 - 2620.

Garlid, K.D., Jabůrek, M. and Ježek, P. (2001) Mechanism of uncoupling protein action. *Biochemical Society Trans*actions **29**, 803 - 806.

Giacobino, J-P. (1999) Effects of dietary deprivation, obesity and exercise on UCP3 mRNA levels. *International Journal of Obesity.* **23**, S60 - S63.

Giacobino, J.P. (2001) Uncoupling protein 3: biological activity. *Biochemical Society Transactions* **29**, 774 – 777.

Gimeno, R., Dembski, M., Weng, X., Deng, N., Shyjan, A., Gimeno, A., Iris, F., Ellis, S.,Woolfe, E. and Tartaglia, L. (1997) Cloning and characterisation of an uncoupling protein homolog. A potential modulator of human thermogenesis. Diabetes **46**, 900 - 906.

Gollnick, P.D. and King, D.W. (1969) Effect of exercise and training on mitochondria of rat skeletal muscle. *American Journal of Physiology* **216**, 1502 – 1509.

Gong, D., He, Y., Karas, M. Karas, M. and Reitman, M. (1997) Uncoupling protein 3 is a mediator of thermogenesis regulated by thyroid hormone, β3 adrenergic agonists and leptin. *The Journal of Biological Chemistry* **272**, 39 – 42.

Gong, D-W., Monemdjou, S., Gavrilova, O., Leon, L.R., Marcus-Samuels, B., Chou, C.J., Everett, C., Kozak, L.P., Li, C., Deng, C., Harper, M-E. and Reitman, M.L. (2000) Lack of obesity and normal response to fasting and thyroid hormone in mice lacking uncoupling protein-3. *The Journal of Biological Chem*istry **275**, 16251 - 16257.

González-Barroso, M., Fleury, C., Bouillaud, F., Nicholls, D.G., and Rial, E. (1998) The uncoupling protein UCP1 does not increase the proton conductance of the inner mitochondrial membrane by functioning as a fatty acid anion transporter. *The Journal of Biological Chemistry* **273**, 15528 – 15532.

Gribskov, C.L., Henningfield, M.F., Swick, A.G. and Swick, R.W. (1986) Evidence for unmasking of rat brown-adipose tissue mitochondrial GDP-binding sites in response to acute cold-exposure. *Biochemical Journal* **233**, 743 – 747.

Hagen, T., Zhang, C-Y., Slieker, L.J., Chung, W.K., Leibel, R.L. and Lowell, B.B. (1999) Assessment of uncoupling activity of the human uncoupling protein 3 short and three mutants of the uncoupling protein gene using a yeast heterologous expression system. *FEBS Letters* **454**, 201 - 206.

Hagen, T. and Lowell, B.B. (2000) Chimeric proteins between UCP1 and UCP 3: the middle third of UCP1 is necessary and sufficient for activation of fatty acids. *Biochemical and Biophysical Research Communications* **276**, 642 - 648.

Hansen, E.S. and Knudsen, J. (1986) Parallel measurements of heat production and thermogenin content in brown fat cells during cold acclimation of rats. *Bioscience Reports* **6**, 31.

Harper, M.E. and Brand, M.D. (1993) The quantitative contributions of mitochondrial proton leak and ATP turnover reactions to the changed respiration rates of hepatocytes from rats of different thyroid status. *The Journal of Biological Chemistry* **268**, 14850 - 14860.

Harper, M-E., Dent, R.M., Bezaire, V., Antoniou, A., Gauthier, A., Monemdjou, S. and Mc Pherson, R. (2001) UCP 3 and its putative function: consistencies and controversies. *Biochemical Society Trans*actions **29**, 768-773.

Harper, J.A., Stuart, J.A., Jekabsons, M.B., Roussel, D., Brindle, K.M., Dickins, K., Jones, R.B. and Brand, M.D. (2002) Artifactual uncoupling by uncoupling protein 3 in yeast mitochondria at the concentrations found in mouse and rat skeletal-muscle mitochondria. *Biochemistry Journal* **361**, 49-56.

Heaton, G.M., Wagenvoord, R.J., Kemp, A. and Nicholls, D.G. (1978) Brown adipose tissue mitochondria: Photoaffinity labelling of the regulatory sites of energy dissipation. *European Journal of Biochemistry* **82**, 515-521.

Heidkaemper, D., Winkler, E., Müller, V., Frischmuth, K., Liu, Q., Caskey, T. and Klingenberg, M. (2000) The bulk of UCP 3 expressed in yeast cells is incompetent for a nucleotide regulated H^+ transport. *FEBS Letters* **480,** 265 - 270.

Hesselink, M.K., Keizer, H.A., Borghouts, L.B., Schaart, G., Kornips, C.F., Slieker, L.J., Sloop, K.W., Saris, W.H. and Schrauwen, P. (2001) Protein expression of UCP3 differs between human type 1, type 2a and type 2b fibres. *FASEB Journal* **15**, 1071 – 1073.

Hesselink, M.K.C., Greenhaff, P.L., Constantin-Toedosiu, D., Hultman, E., Saris, W.H.M., Nieuwlaat, R., Schaart, G., Kornips, E. and Schrauwen, P. (2003) Increased uncoupling protein 3 content does not affect mitochondrial function in human skeletal muscle in vivo. *Journal of Clinical Investigation* **111 (4)**, 479 - 486.

Himms-Hagen, J. (1986) Brown adipose tissue and cold acclimation. In *Brown Adipose Tissue* (Edited by Trayhurn, P. and Nicholls, D.), pp. 214 – 268. Arnold, London.

Himms-Hagen, J. (1990) Brown adipose tissue thermogenesis: Inter-disciplinary studies. *FASEB Journal* **4**, 2890 - 2898.

Hinz, W., Grüninger, S., De Pover, A. and Chiesi, M. (1999a) Properties of the human long and short isoforms of the uncoupling protein-3 expressed in yeast cells. *FEBS Letters* **462**, 411 - 415.

Hinz, W., Faller, B., Grüninger, S., Gazzotti, P. and Chiesi, M. (1999b) Recombinant human uncoupling protein-3 increases thermogenesis in yeast cells. *FEBS Letters* **448**, 57 - 61.

Hodnỳ, Z., Kolřová, P., Rossmeisl, M., Horáková, M., Nibbelink, M., Penicaud, L., Casteilla, L. and Kopeckỳ, J. (1998) High expression of uncoupling protein 2 in foetal liver. *FEBS Letters* **425,** 185 - 190.

Holloszy J.O. (1967) Effects of exercise on mitochondrial oxygen uptake and respiratory enzyme activity in skeletal muscle. *The Journal of Biological Chemistry* **242**, 2278 – 2282.

Holloszy, J.O. and Coyle, E.F. (1984) Adaptations of skeletal muscle to endurance exercise and their metabolic consequences. *Journal of Applied Physiology* **56**, 831 - 838.

Horvath, T.L., Miyamoto, D.S., Barry, S., Gatti, S., Alberati, D., Livaki, A., Lombardi, A., Moreno, M., Goglia, F., Mor, G., Hamilton, J., Kachinskas, D., Horqitz, B. and Warden, C.H. (2003) Uncoupling proteins-2 and 3 influence obesity and inflammation in transgenic mice. *International Journal of Obesity Related Metabolic Disord*ers **27**, 433 - 442.

Houlden, M. (1988) Energy expenditure, thermal performance, and brown fat function of lean and genetically obese (*ob/ob*) mice reared in warm and cold environments. PhD thesis, Department of Physiology, Trinity College, Dublin.

Huang, S. and Klingenberg, M. (1995a) Nature of the masking of nucleotide-binding sites in brown adipose tissue mitochondria. Involvement of endogenous adenosine triphosphate. *European Journal of Biochemistry* **229**, 718 – 725.

Huang, S.G. and Klingenberg, M. (1995b) Fluorescent nucleotide derivatives as specific probes for the uncoupling protein: thermodynamics and kinetics of binding and the control by pH. *Biochemistry*. **34**, 349 – 360.

Huang, S. and Klingenberg, M (1996) Chloride channel properties of the uncoupling protein from brown adipose tissue mitochondria: A patch clamp study. *Biochemistry* **35**, 16806 – 16814.

Huang S.G., Lin, Q.S. and Klingenberg, M. (1998) Slow-phase kinetics of nucleotide binding to the uncoupling protein from brown adipose tissue mitochondria. *The Journal of Biological Chemistry* **273**, 859 – 864.

Hwang, C.S. and Lane, M.D. (1999) Up-regulation of uncoupling protein-3 by fatty acid in C_2C_{12} myotubes. *Biochemical and Biophysical Research Communications* **258**, 464 – 469.

Jabůrek, M., Vařecha, M., Gimeno, R.E., Dembski, M., Ježek, P., Zhang, M., Burn, P., Tartaglia, L.A. and Garlid, K.D. (1999) Transport function and regulation of mitochondrial uncoupling proteins 2 and 3. *The Journal of Biological chemistry* **274**, 26003 - 26007.

Jabůrek, M and Garlid, K.D. (2003) Reconstitution of recombinant uncoupling proteins: UCP 1, -2, -3 have similar affinities for ATP and are unaffected by coenzyme Q_{10}. *The Journal of Biological Chem*istry **278**, 25825 - 25831.

Jarmuszkiewicz, W., Sluse-Goffart, C.M., Hryniewiecka, L. and Sluse, F.E. (1999) Identification and characterization of a protozoan uncoupling protein in *Acanthamoeba castellanii*. *The Journal of Biological Chem*istry **274**, 23198 - 23202.

Jarmuszkiewicz, W., Milani, G., Fortes, F., Schreiber, A.Z., Sluse, F.E. and Vercesi, A.E. (2000) First evidence and characterisation of an uncoupling protein in fungi kingdom: CpUCP of *Candida parapsilosis*. *FEBS Letters* **467**, 145 - 149.

Jekabsons, M.B., Gregoire, F.M., Schonfeld-Warden, N.A., Warden, C.H. and Horwitz, BA. (1999) T_3 stimulates resting metabolism and UCP2 and UCP3 mRNA but not nonphosphorylating mitochondrial respiration in mice. *American Journal of Physiol*ogy **277**, E380 - E389.

Jekabsons, M.B., Echtay, K.S. and Brand, M.D. (2002) Nucleotide binding to human uncoupling protein-2 refolded from bacterial inclusion bodies. *Biochemical Journal* **366**, 565 – 571.

Ježek, P. and Garlid, K.D. (1990) New substrates and competitive inhibitors of the Cl-translocating pathway of the uncoupling protein of brown adipose tissue mitochondria. *Journal of Biological Chem*istry **265**, 19303 - 19311.

Ježek, P., Orosz, D.E., Modriansky, M. and Garlid, K.D. (1994) Transport of anions and protons by the mitochondrial uncoupling protein and its regulation by nucleotides and fatty-acids. A new look at old hypotheses. *Journal of Biological Chemistry* **269**, 26184 - 26190.

Ježek, P., Žáčková, M., Řeháková, Z., Růžička, M., Borecký, J., Škobisová, E., Brucknerová, J., Garlid, K., Gimeno, R.E. and Tartaglia, L.A. (1999) Existence of uncoupling protein-2 antigen in isolated mitochondria from various tissues. *FEBS Letters* **455**, 79 - 82.

Jones, T.E., Baar, K., Ojuka, E., Chen, M. and Holloszy, J. (2003) Exercise induces an increase in muscle UCP3 as a component of the increase in mitochondrial biogenesis. *American Journal of Physiology* **284**, E96 – E101.

Kaushik, S. and Kaur, J. (2003) Chronic cold exposure affects the antioxidant defense system in various rat tissues. *Clin. Chim. Acta.* **333**, 69 – 77.

Klaus, S., Casteilla, L., Bouillaud, F. and Ricquier, D. (1991) The uncoupling protein UCP: A membraneous mitochondrial ion carrier exclusively expressed in brown adipose tissue. *International Journal of Biochemistry* **23**, 791 - 801.

Klingenberg, M. (1984) Characteristics of the uncoupling protein from brown-fat mitochondria. *Biochemical Society Transactions* **12**, 390.

Klingenberg, M. (1988) Nucleotide binding to uncoupling protein. Mechanism of control by protonation. *Biochemistry* **27**, 781 – 791.

Klingenberg, M. (1990) Mechanism and evolution of the uncoupling protein of brown adipose tissue. *Trends in Biochemical Sciences* **15**, 108 – 112.

Klingenberg, M., Echtay, K.S., Biengraeber, M., Winkler, E. and Huang, S.G. (1999). Structure-function relationship in UCP 1. *International Journal of Obesity* **23**, S24 - S29.

Klingenberg, M. and Huang, S.G. (1999) Structure and function of the uncoupling protein from brown adipose tissue. *Biochimica et Biophysica Acta* **1415,** 271 - 296.

Klingenberg, M. and Echtay, K. (2001) Uncoupling Proteins: the issues from a biochemist point of view. *Biochimica et Biophysica Acta* **1504**, 128 – 143.

Kopecky, J., Guerrieri, F., Jezek, P., Drahota, Z. and Houstek, J. (1984) *FEBS Letters* **171**, 186 – 190.

Kowaltowski, A.J. and Vercesi, A.E. (1999) Mitochondrial damage induced by conditions of oxidative stress. *Free Radical Biology and Medicine* **26**, 463 – 471.

Krauss, S., Zhang, C.Y. and Lowell, B.B. (2002) A significant portion of mitochondrial proton leak in intact thymocytes depends on expression of UCP2. *Proceedings of the National Academy of Sciences* **99**, 118 - 122.

Laemmli, U.K. (1970) Cleavage of structural proteins during the assembly of the head of bacteriophage T4. *Nature* **227**, 680 – 685.

Laloi, M., Klein, M., Riesmeier, J.W., Muller-Rober, B., Fleury, F., Bouillaud, F. and Ricquier, D. (1997) A plant cold-induced uncoupling protein. *Nature* **389**, 135 - 136.

Lanni, A., Beneduce, L., Lombardi, A., Moreno, M., Boss, O., Muzzin, P., Giacobino, J.P. and Goglia, F. (1999) Expression of uncoupling protein-3 and mitochondrial activity in the transition from hypothyroid to hyperthyroid state in rat skeletal muscle. *FEBS Letters* **444**, 250 - 254.

Lanni, A., Moreno, M., Lombardi, A. and Goglia, F. (2003) Thyroid hormone and uncoupling proteins. *FEBS Letters* **543**, 5 – 10.

Larkin, S., Mull, E., Miao, W., Pittner, R., Albrandt, K., Moore, C., Young, A., Denaro, M. and Beaumont, K., (1997) Regulation of the third member of the uncoupling protein family, UCP3, by cold and thyroid hormone. *Biochemical and Biophysical Research Communications* **240**, 222 - 227.

Larrouy, D., Laharrague, P., Carrera, G., Viguerie-Bascands, N., Levi-Meyrueis, C., Fleury, C., Pecqueur, C., Nibbelink, M., André, M., Casteilla, L. and Ricquier, D. (1997) Kupffer cells are a dominant site of uncoupling protein 2 expression in rat liver. *Biochemica Biophyica Research Commun*ications **235**, 760 - 764.

Li, B., Nolte, L.A., Ju, J-S., Han, D.H., Coleman, T., Holloszy, J.O. and Semenkovich, C.F. (2000) Skeletal muscle respiratory uncoupling prevents diet-induced obesity and insulin resistance in mice. *Nature Medicine*. **6**, 1115 - 1120.

Lin, C.S. and Klingenberg, M. (1980) Isolation of the uncoupling protein from brown adipose tissue mitochondria. *FEBS Letters* **113**, 299 – 303.

Lin, B., Coughlin, S. and Pilch, P. (1998) Bidirectional regulation of uncoupling protein-3 and GLUT-4 mRNA in skeletal muscle by cold. *American Journal of Physiology* **275**, E386 – E391.

Lowell, B.B. (1999) Uncoupling protein-3 (UCP 3): a mitochondrial carrier in search of a function. *International Journal of Obesity* **23**, S43 - S45.

Maia, I.G., Benedetti, L.E., Leite A., Turcinelli, S.R., Vercesi, A.E. and Arruda, P. (1998) AtUCP: an *Arabidopsis* gene encoding a plant uncoupling protein. *FEBS Letters* **429**, 403 - 406.

Mao, W., Yu, X.X., Zhong, A., Li, W., Brush, J., Sherwood, S.W., Adams, S.H., and Pan, G. (1999) UCP4, a novel brain-specific mitochondrial protein that reduces membrane potential in mammalian cells. *FEBS Letters* **443**, 326 - 330.

Markwell, M.A. and Haas, S.M. (1978) A modification of the Lowry procedure to simplify protein determination in membrane and lipoprotein samples. *Analytical Biochemistry* **87 (1)**, 206 – 210.

Matthias, A. Jacobsson, A., Cannon, B. and Nedergaard, J. (1999) The bioenergetics of brown fat mitochondria from UCP1-ablated mice. UCP1 is not involved in fatty acid-induced de-energisation (uncoupling). *The Journal of Biological Chemistry* **274**, 28150 – 28160.

Maughan, R., Gleeson, M. and Greenhaff, P.L. (1997) In *Biochemistry of Exercise and Training* pages 178-184. Oxford University Press (Oxford, New York and Tokyo).

Medvedev, A., Robidoux, J., Bai, X., Cao, W., Floering, L., Daniel, K., Collins, S. (2002) Regulation of the uncoupling protein-2 gene in INS-1 beta-cells by oleic acid. *The Journal of Biological Chemistry* **277**, 42639 – 42644.

Millet, L., Vidal, H., Andreelli, F., Larrouy, D., Riou, J., Ricquier, D., Laville, M. and Langin, D. (1997) Increased uncoupling protein 2 and 3 mRNA expression during fasting in obese and lean humans. *Journal of Clinical Investigation* **100**, 2665 – 2670.

Mills, E.M., Banks, M.L., Sprague, J.E. and Finkel, T. (2003) Uncoupling the agony from ecstasy. *Nature*. **426**, 403 - 404.

Milner, R.E., Wilson, S., Arch, J.R.S. and Trayhurn, P. (1988) Acute effects of β-adrenoceptor agonist (BRL 26830A) on rat brown-adipose tissue mitochondria. *Biochemical Journal* **249**, 759 - 763.

Mitchell, P. (1961) Coupling of phosphorylation to electron and hydrogen transfer by a chemiosmotic type of mechanism. *Nature*. **191**, 144 - 148.

Modriansky, M., Murdza-Inglis, D.L., Hasmukh, V.P., Freeman, K.B. and Garlid, K.D. (1997) Identification by site-directed mutagenesis of three arginines in uncoupling protein that are essential for nucleotide binding and inhibition. *The Journal of Biological Chemistry* **272**, 24759 - 24762.

Molé, P.A., Oscai, L.B. and Holloszy, J.O. (1971) Increase in levels of palmityl CoA synthesase, carnitine palmityltransferase and palmityl CoA dehydrogenase, and in the capacity to oxidise fatty acids. *Journal of Clinical Investigation* **50**, 2323 – 2330.

Monemdjou, S., Kozak, L. and Harper, M.E. (1999) Mitochondrial proton leak in brown adipose tissue mitochondria of *Ucp*1-deficient mice is GDP insensitive. *American Journal of Physiology* **276**, E1073 – E1082.

Moreno, M., Lombardi, A., Del Lange, P., Silvestri, E., Ragni, M., Lanni, A. and Goglia, F. (2003) Fasting, lipid metabolism, and triiodothyonine in rat gastrocnemius muscle: interrelated roles of uncoupling protein 3, mitochondrial thioesterase and coenzyme Q. *FASEB Journal* **17**, 1112 – 1114.

Murakami, T., Shimamura, Y., Fujitsuka, N., Nakai, N., Sugiyama, S., Ozawa, T., Sokabe, M., Horai, S., Tokuyama, K. and Suzuki, M. (1994) Enzymatic and genetic adaptations of soleus muscle mitochondria to physical training in rats. *American Journal of Physiology* **267**, E388 - E395.

Murphy, M.P., Echtay, K.S., Blaikie, F.H., Asin-Cayuela, J., Cochemé, H.M., Green, K., Buckingham, J., Taylor, E.R., Hurrell, F., Hughes, G., Miwa, S., Cooper, C.E., Svistunenko, D.A., Smith, R.A.J. and Brand, M.D. (2003) Superoxide activates uncoupling proteins by generating carbon-centred radicals and initiating lipid peroxidation: studies using a mitochondria-targeted spin trap derived from α-phenyl-*n*-*tert*-butylnitrone. *The Journal of Biological Chem*istry **278,** 48534 - 48545.

Muzzin, P., Boss. O. and Giacobino, J.P. (1999) Uncoupling protein 3: its possible role and mode of regulation in rodents and humans. *Journal of Bioenergetics and Biomembranes* **31**, 467 - 473.

Nakao, C., Ookawara, T., Kizaki, T., Oh-Ishi, S., Miyazaki, H., Haga, S., Sato, Y. and Ohno, H. (2000) Effects of swimming training on three superoxide dismutase isoenzymes in mouse tissues. *Journal of Applied Physiology* **88**, 649 - 654.

Nagase, I., Yoshida, T. and Saito, M. (2001) Up-regulation of uncoupling proteins by beta-adrenergic stimulation in L6 myotubes. *FEBS Letters* **494**, 175 – 180.

Néchad, M. (1986) Structure and development of brown adipose tissue. In *Brown Adipose Tissue* (Edited by Trayhurn, P. and Nicholls, D.), pp. 1 - 30. Arnold, London.

Nedergaard, J., and Cannon, B. (1985) [^{3}H] GDP binding and thermogenin amount in brown adipose tissue mitochondria from cold-exposed rats. *American Journal of Physiology* **248**, C365 – C371.

Nedergaard, J. and Cannon, B. (1992) The uncoupling protein thermogenin and mitochondrial thermogenesis. In *New Comprehensive Biochemistry, Molecular Mechanisms in Bioenergetics* (edited by Ernster, L.) **Vol. 23** p.p 385 – 420. Elsevier, Amsterdam.

Nedergaard, J., Golozoubova, V., Matthias, A., Asadi, A., Jacobsson, A. and Cannon, B. (2001a) UCP1: the only protein able to mediate adaptive non-shivering thermogenesis and metabolic inefficiency. *Biochimica et Biophysica Acta* **1504**, 82 - 106.

Nedergaard, J., Golozoubova, V., Matthias, A., Shabalina, I., Ohba, K.-i., Ohlson, K., Jacobsson, A. and Cannon, B. (2001b) Life without UCP1: mitochondrial, cellular and organismal characteristics of the UCP1 ablated mice. *Biochemical Society Transactions* **29,** 756 - 762.

Nègre-Salvayre, A., Hirtz, C., Carrera, G., Cazenave, R., Troly, M., Salvayre, R., Pénicaud, L. and Casteilla, L. (1997) A role for uncoupling-protein 2 as a regulator of mitochondrial hydrogen peroxide generation. *FASEB Journal* **11**, 809 - 815.

Nibbelink, M., Moulin, K., Arnaud, E., Duval, C., Penicaud, L. and Casteilla, L. (2001) Brown fat UCP1 is specifically expressed in uterine longitudinal smooth muscle cells. *The Journal of Biological Chemistry* **276**, 47291 – 47295.

Nicholls, D.G. and Rial, E. (1974) Measurement of proton leakage across mitochondrial inner membranes and its relation to protonmotive force. *Methods in Enzymology* **174**, 85 - 94.

Nicholls, D.G. (1974) The influence of respiration and ATP hydrolysis on the proton-electrochemical gradient across the inner membrane of rat liver mitochondria, as determined by ion distribution. *European Journal of Biochemistry* **50**, 305 - 315.

Nicholls, D.G. and Locke, R.M. (1984) Thermogenic mechanism in brown fat. *Physiological Reviews* **64**, 1 – 64.

Nicholls, D.G. and Ferguson, S.J. (1992) In *Bioenergetics 2*. London: Academic Press.

Nicholls, D.G. and Rial, E. (1999) A History of the first Uncoupling Protein, UCP1. *Journal of Bioenergetics and Biomembranes* **31**, 399 - 406.

Nicholls, D.G. (2001) A history of UCP 1. *Biochemical Society Trans*actions **29**, 75 -755.

Nobes, C.D., Brown, G.C., Olive, P.N. and Brand, M.D. (1990) Non-ohmic proton conductance of the mitochondrial inner membrane in hepatocytes. *The Journal of Biological Chemistry* **265**, 12903 - 1290.

Palou, A., Picó, C., Bonet, M.L. and Oliver, P. (1998) The uncoupling protein, thermogenin. *The International Journal of Biochemistry and call Biology* **30**, 7 – 11.

Papa, S. and Skulachev, V.P. (1997) Reactive oxygen species, mitochondria, apoptosis and aging. *Molecular and Cellular Biochemistry* **174**, 305 - 319.

Parascandola, J. (1974) Dinitrophenol and Bioenergetics: A Historical Perspective. *Molecular and Cellular Biochemistry* **5,** 69 - 77.

Peachey, T., French, R. andYork, D. (1988) Regulation of GDP binding and uncoupling-protein concentration in brown adipose tissue mitochondria. The effects of cold acclimation, warm reacclimation and noradrenaline. *Biochemical Journal* **249,** 451 – 457.

Pecqueur, C., Alves-Guerra, M.C., Gelly, C., Levi-Meyrueis, C., Couplan, E., Collins, S., Ricquier, D., Bouillaud, F. and Miroux, B. (2001) Uncoupling protein 2, *in vivo* distribution, induction upon oxidative stress, and evidence for translational regulation. *The Journal of Biological Chemistry* **276**, 8705 - 8712.

Pedraza, N., Solanes, G., Iglesias, R., Vázqeuz, M., Giralt, M. and Villarroya, F. (2001) Differential regulation of expression of genes encoding uncoupling proteins 1 and 3 in brown adipose tissue during lactation in mice. *Biochemical J*ournal **355,** 105 - 111.

Pilegaard, H., Ordway, G.G., Saltin, B. and Neufer, P.D. (2000) Transcriptional regulation of gene expression in human skeletal muscle during recovery from exercise. *American Journal of Physiology* **279**, E806 – E814.

Porter, R.K. and Brand, M.D. (1995) Causes of the differences in respiration rate of hepatocytes from mammals of different body mass. *American Journal of Physiol*ogy **269**, R1213 - R1224.

Porter, R.K. and Andrews, J.F. (1998) Effects of leptin on mitochondrial "proton leak" and uncoupling proteins: implications for mammalian energy metabolism. *Proceedings of the Nutrition Society* **57**, 455 - 460.

Porter, R.K., Joyce, O.J., Farmer, M.K., Heneghan, R., Tipton, K.F., Andrews, J.F., McBennett, S.M., Lund, M.D., Jensen, C.H. and Melia, H. P. (1999) Indirect measurement of mitochondrial proton leak and its applications. *International Journal of Obesity* **23**, S12 – S18.

Porter, R.K. (2001) Mitochondrial proton leak: a role for uncoupling protein 2 and 3. *Biochimica et Biophysica Acta* **1504**, 120 - 127.

Puntschart, A., Claassen, H., Jostarndt, K., Hoppeler, H., Billeter, R. (1995) mRNAs of enzymes involved in energy metabolism and mtDNA are increased in endurance-trained athletes. *American Journal of Physiology* **269**, C619 – C625.

Queiroz, M.S., Shao, Y. and Ismail-Beigi, F. (2004) Effect of thyroid hormone on uncoupling protein 3 mRNA expression in rat heart and skeletal muscle. *Thyroid* **14,** 177 – 185.

Rafael, J., Ludolph, H.J. and Hohorst, H.J. (1969) Mitochondria from brown adipose tissue: uncoupling of oxidative phosphorylation by long chain fatty acids and recoupling by guanosine triphosphate. *Hoppe-Seyler's Z. Physiological Chemistry* **350**, 1121 - 1131.

Rafael, J. and Heldt, H. (1976) Binding of guanine nucleotides to the outer surface of the inner membrane of guinea pig brown fat mitochondria in correlation with the thermogenic activity of the tissue. *FEBS Letters* **63**, 304 – 308.

Raimbult, S., Dridi, S., Denjean, F., Lacheur, J., Couplan, E., Bouillaud, F., Bordas, A., Duchamp, C., Taouis, M. and Ricquier, D. (2001) An uncoupling protein homologue putatively involved in facultative muscle thermogenesis. *Biochemical J*ournal **353**, 441 - 444.

Reynafarje, B., Costa,. L.E. and Lehninger, A.L. (1985) Oxygen solubility in aqueous media determined by a kinetic method. *Analytical Biochemistry* **145**, 406 – 419.

Rial, E., Aguirregoitia, E., Jimenez-Jimenez, J. and Ledesma, A. (2004) Alkylsulfonates activate the uncoupling protein UCP1: implications for the transport mechanism. *Biochimica et Biophysica Acta* **1608**, 122 – 130.

Rial, E., González-Barroso, M.M., Fluery, C., Iturrizaga, S., Sanchis, d., Jiménez-Jiménez, J., Ricquier, D., Goubern, M. and Bouillaud, F. (1999) Retinoids activate proton transport by the uncoupling proteins UCP1 and UCP2. *The EMBO J*ournal **18,** 101 - 108.

Rial, E., Poustie, A. and Nicholls, D. (1983) Brown adipose tissue mitochondria; the regulation of the 32 000 M_r uncoupling protein by fatty acids and purine nucleotides. *European Journal of Biochemistry* **137**, 197 – 203.

Ricquier, D. and Kader, J. (1976) Mitochondrial protein alteration in active brown fat: a sodium dodecyl sulfate polyacrylamide electrophoretic study. *Biochemical and Biophysical Research Communications* **73,** 577 – 583.

Ricquier, D. Lin, C.S. and Klingenberg, M. (1982) Isolation of the GDP binding protein from brown adipose tissue mitochondria of several animals and amino acid composition study in rat. *Biochemical and Biophysical Research Communications* **106**, 582 – 589.

Ricquier, D., Barlet, J., Garel, J., Combes-George, M. and Dubois, M. (1983) An immunological study of the uncoupling protein of brown adipose tissue mitochondria. *Biochemical Journal* **210**, 859 – 866.

Ricquier, D. and Bouillaud, F. (1986) Brown adipose tissue mitochondrial uncoupling protein. In: *Brown Adipose Tissue* (Edited by Trayhurn, P. and Nicholls, D.), pp. 86 - 104, Arnold Publishers, London.

Ricquier, D., Bouillaud, F., Toumelin, P., Mory, G., Bazin, R., Arch, J, Penicaud, L. (1986) Expression of uncoupling protein mRNA in thermogenic or weakly thermogenic brown adipose tissue. Evidence for a rapid beta-adrenoceptor-mediated and transcriptionally regulated step during activation of thermogenesis. *Journal of Biological Chemistry* **261**, 13905 - 13910.

Ricquier, D. and Bouillaud, F. (2000) The uncoupling protein homologues: UCP1, UCP2, UCP 3, StUCP and AtUCP. *Biochemical Journal* **345**, 161 - 179.

Rolfe, D.F.S., Newman, J.M.B., Buckingham, J.A., Clark, M.G. and Brand, M.D. (1999) Contribution of mitochondrial proton leak to respiration rate in working skeletal muscle and liver and to standard metabolic rate. *American Journal of Physiology* **276**, C692 - 699.

Rolfe, D.F.S. and Brand, M.D. (1996) Contribution of mitochondrial proton leak to skeletal muscle respiration and to standard metabolic rate. *American Journal of Physiology* **271**, C1380 - 1389.

Rothwell, N.J. and Stock, M.J. (1979) A role for brown adipose tissue in diet-induced thermogenesis. *Nature*, **281**, 31 - 33.

Rothwell, N.J. and Stock, M.J. (1982) Effect of chronic food restrictions on energy balance, thermogenic capacity and brown adipose tissue activity in the rat. *Bioscience Reports* **2**, 543 – 549.

Rothwell, N.J., Saville, M.E. and Stock, M.J. (1984) Brown fat activity in fasted and refed rats. *Bioscience Reports* **4,** 351 - 357.

Rousset, S., Alves-Guerra, M.C., Ouadghiri-Bencherif, S., Kozak, L.P., Miro, B.,Richard, D., Bouillaud, F., Ricquier, D. and Cassard-Doulcier, A.M. (2003) Uncoupling protein 2, but not uncoupling protein 1, is expressed in the female mouse reproductive tract. *The Journal of Biological Chem*istry **278**, 45843 - 45847.

Runswick, M.J., Powell, J.T., Nyren, P. and Walker, J.E. (1987) Sequence of bovine mitochondrial phosphate carrier: structural relationship to ADP/ATP translocase and the brown fat mitochondrial uncoupling protein. The *EMBO Journal* **6**, 1367 - 1373.

Sanchis, D., Fleury, C., Chomiki, N., Goubern, M., Haung, Q.L., Neverova, M.,Gregoire, F., Easlick, J., Raimbault, S. and Levi-Meyrueis, C. (1998) BMCP1, a novel mitochondrial carrier with high expression in the central nervous system of humans and rodents, and respiration uncoupling activity in recombinant yeast. *The Journal of Biological Chemistry* **273**, 34611 - 34615.

Scarpace, P.J., Bender, B.S. and Borst, S.E. (1991) *Escherichia coli* peritonitis activates thermogenesis in brown adipose tissue: relationship to fever. *Canadian Journal of Physiological Pharmacology* **69**, 761 – 766.

Schrauwen, P. and Hesselink, M. (2003) Uncoupling protein 3 and physical activity: the role of uncoupling protein 3 in energy metabolism revisited. *Proceedings of the Nutrition Society* **62,** 635 – 643.

Schrauwen, P., Hesselink, M., Vaartjes, I., Kornips, E., Saris, W., Giacobino, J. and Russell, A. (2002) Effect of acute exercise on uncoupling protein 3 is a fat metabolism mediated effect. *American Journal of Physiology* **282**, E11 – E17.

Schrauwen, P., Troost, F.J., Xia, J., Ravussin, E. and Saris, W.H.M. (1999) Skeletal muscle UCP2 and UCP3 expression in trained and untrained male subjects. *International Journal of Obesity* **23**, 966 - 972.

Shimabukuro, M., Zhou, Y.T., Lee, Y. and Unger, R.H. (1997) Induction of uncoupling protein-2 mRNA by troglitazone in the pancreatic islets of Zucker diabetic fatty rats. *Biochemical and Biophysical Research Communications* **237**, 359 – 361.

Shinohara, Y., Shima, A., Kamida, M. and Terada, H. (1991) Uncoupling protein is expressed in liver mitochondria of cold-exposed and newborn rats. *FEBS Letters* **293**, 173 – 174.

Silvestri, E., Moreno, M., Lombardi, A., Ragni, M., de Lange, P., Alexson, S., Lanni, A. and Goglia, F. (2005) Thyroid hormone effects on putative biochemical pathways involved in UCP3 activation in rat skeletal muscle mitochondria. *FEBS Letters* **579**, 1639 – 1645.

Simonyan, R.A., Jimenez, M., Ceddia, R.B., Giacobino, J-P., Muzzin, P. and Skulachev, V.P. (2001) Cold-induced changes in the energy coupling and the UCP 3 level in rodent skeletal muscles. *Biochimica et Biophysica Acta* **1505**, 271 – 279.

Sivitz, W.I., Fink, B.D. and Donohue, P.A. (1999) Fasting and leptin modulate adipose and muscle uncoupling protein: divergent effects between messenger ribonucleic acid and protein expression. *Endocrinology*. **140**, 1511-1519.

Skulachev, V.P. (1991) Fatty acid circuit as a physiological mechanism of uncoupling of oxidative phosphorylation. *FEBS Letters* **294,** 158-162.

Skulachev, V.P., (1996) Why are mitochondria involved in apoptosis? Permeability transition pores and apoptosis as selective mechanisms to eliminate superoxide-producing mitochondria and cell. *FEBS Letters* **397,** 7 – 10.

Skulachev, V.P. (1998) Uncoupling: new approaches to an old problem of bioenergetics. *Biochimica et Biophysica Acta* **1363**, 100 – 124.

Stuart, J.A., Cadenas, S., Jekabsons, M.B., Roussel, D. and Brand, M.D. (2001) Mitochondrial proton leak and the uncoupling protein 1 homologues. *Biochemica et Biophysica Acta* **1504**, 144-158.

Stuart, J.A., Brindle, K.M., Harper, J.A. and Brand, M.D. (1999) Mitochondrial proton leak and the uncoupling proteins. *Journal of Bioenergetics and Biomembranes* **31,** 517- 525.

Sundin, U., Moore, G., Nedergaard, J. and Cannon, B. (1987) Thermogenin amount and activity in hamster brown fat mitochondria: effect of cold acclimation. *American Journal of Physiology* **252**, R822-R832.

Sundin, U and Cannon, B. (1980) GDP-binding to the brown fat mitochondria of developing and cold-adapted rats. *Comparative Biochemistry and Physiology (Part B)* **65**, 463 – 471.

Swick, A.G. and Swick, R.W. (1986) Rapid changes in number of GDP binding sites on brown adipose tissue mitochondria. *American Journal of Physiol*ogy **251**, E192-E195.

Trayhurn, P. and Nicholls, D.G. (1986) In *Brown adipose tissue* (Edited by Trayhurn, P. and Nicholls, D.) Arnold, London.

Trayhurn, P., Ashwell, M., Jennings, G., Richard, D. and Stirling, D.M. (1987) Effect of warm or cold exposure on GDP binding and uncoupling protein in rat brown fat. *American Journal of Physiol*ogy **252**, E237 - E243.

Trayhurn, P. and Jennings, G. (1988) Non-shivering thermogenesis and the thermogenic capacity of brown fat in fasted and/or refed mice *American Journal of Physiol*ogy **254,** R11 - R16.

Tsuboyama-Kasaoka, N., Tsunoda, N., Maruyama, K., Takahashi, M., Kim, H., Ikemoto, S. and Ezaki, O. (1998) Up-regulation of uncoupling protein-3 mRNA by exercise training and down-regulation of UCP-3 by denervation in skeletal muscles. *Biochemical and Biophysical Research Communications* **247**, 498 – 503.

Venditti, P., De Rosa, R. and Di Meo, S. (2004) Effect of cold induced hyperthyroidism on H_2O_2 production and susceptibility to stress conditions of rat liver mitochondria. *Free Radical Biology and Medicine*. **36**, 348 – 358.

Vercesi, A.E., Martins, I.S., Silva, M.A.P., Leite, H.M.F., Cuccovia, I.A. and Chaimovich, H. (1995) PUMPing Plants. *Nature* **375,** 24.

Vidal-Puig, A., Grujic, D., Zhang, C-Y., Hagen, T., Boss, O., Ido, Y., Szszepanik, A., Wade, J., Mootha, V., Cortright, R., Muoio, D.M. and Lowell, B.B. (2000) Energy metabolism in uncoupling protein 3 gene knockout mice. *The Journal of Biological Chem*istry **275**, 16258 - 16266.

Vidal-Puig, A., Solanes, G., Grujic, D., Flier, J.S. and Lowell, B.B. (1997) UCP3: An uncoupling protein homologue expressed preferentially and abundantly in skeletal muscle and brown adipose tissue. *Biochemical and Biophysical Research Communications* **235**, 79 – 82.

Weigle, D.S., Selfridge, L.E., Schwartz, M.W., Seeley, R.J., Cummings, D.E., Havel, P.J., Kuijper, J.L. and Baltrandelrio, H. (1998) Elevated free fatty acids induce uncoupling protein 3 expression in muscle: a potential explanation for the effect of fasting. *Diabetes* **47**, 298-302.

Winkler, E. and Klingenberg, M. (1994) Effect of fatty acids on proton transport activity of the reconstituted uncoupling protein. *The Journal of Biological Chemistry* **269,** 2508 -2515.

Yoshida, T., Umekawa, T., Kumamoto, K., Sakane, N., Kogure, A., Kondo, M., Wakabayashi, Y., Kawada, T., Nagase, I. and Saito, M. (1998) β3-adrenergic agonist

induces a functionally active uncoupling protein in fat and slow-twitch muscle fibres. *American Journal of Physiology* **274**, E469 – E475.

Yu, X.X., Mao, W., Zhong, A., Schow, P., Brush, J., Sherwood, S.W., Adams, S.H. and Pan, G. (2000) Characterisation of novel UCP 5/BMCP1 isoforms and differential regulation of UCP4 and UCP5 expression through dietary or temperature manipulation. *FASEB J*ournal **14**, 1611 - 1618.

Žáčková, M., Škibisová, E., Urbanková, E. and Ježek, P. (2003) Activating omega-6 polyunsaturated fatty acids and inhibitory purine nucleotides are high affinity ligands for novel mitochondrial uncoupling proteins UCP2 and UCP3. *The Journal of Biological Chem*istry **278**, 20761 – 20769.

Zhang, C., Baffy, G., Perret, P., Krauss, S., Peroni, O., Grujic, D., Hagen, T., Vidal-Puig, A., Boss, O., Kim, Y., Zheng, X., Wheeler, M., Shulman, G., Chan, C. and Lowell, B. (2001) Uncoupling protein-2 negatively regulates insulin secretion and is a major link between obesity, beta cell dysfunction and type 2 diabetes. *Cell* **105**, 745 – 755.

Zhang, C., Hagen, T., Mootha, V., Lawrence, S. and Lowell, B. (1999) Assessment of uncoupling activity of uncoupling protein 3 using a yeast heterologous expression system. *FEBS Letters* **449**, 129 – 134.

Zhou, T., Shimabukuro, M., Lee, L., Wong, M., Triev, F., Newgard, C.B., Koyama, K. and Unger, R.H. (1997) Induction by leptin of uncoupling protein-2 and enzymes of fatty acid oxidation. *Proceedings of National Academy of Science* (USA) **94**, 6386 - 6390.

Zhou, M., Lin, B., Coughlin, S., Vallega, G. and Pilch, P. (2000) UCP3 expression in skeletal muscle: effects of exercise, hypoxia and AMP-activated protein kinase. *American Journal of Physiology* **279**, E622 – E629.

Appendix

Appendix 1

Suppliers	Address
Amersham International Plc.	Amersham Place, LittleChalfont, BuckinghamshireHP79NA, United Kingdom.
Bachem Ltd.	Hegenheimer, Strasse 59576, Weil am Rhein, Germany.
BioRad Laboratories Inc.	c/o alpha Technologies, Poulreva House, Grove Road, Dublin 6, Ireland.
BioResources Unit	Department of Biochemistry, Trinity College, Dublin 2, Ireland.

Biosciences	3 Charlemont Terrace, Crofton Road, Dunlaoghaire, Co. Dublin, Ireland.
British Drug House (BDH) Chemicals Ltd.	Broom Road, Poole, Dorset BH12 4NN, United Kingdom.
Calbiochem Novabiochem (U.K.) Ltd.	Unit C2A, Boulevard Industrial Park, Beeston, Nottingham NG9 2JR, United Kingdom.
Cryoservices Ltd.	BallymountIndustrial Estate Tallaght, Dublin 24.
Eurogentec	Parc Scientifique du Sart Tilman, 4102 Seraing, Belgium.
Kodak	Eastman Kodak Company, Rochester, New York 14650,

	U.S.A.
Fluka	c/o Sigma-Aldrich Ltd., Dublin, Ireland.
Lennox	JFK Drive, Naas Road, Dublin 12, Ireland.
Merck	Merck KgaA, D-64271 Darmstadt, Germany.
Millipore	The Boulevard, Blackmoor Lane, Watford, Hertfordshire WD1 8YW, United Kingdom.
National Diagnostics	305 Patton Drive, Atlanta, Georgia 30336, U.S.A.
New England Biolabs (U.K. Ltd.)	Knowl Piece, Wilbury Way, Hitchin, Hertfordshire SG4 OTY, United Kingdom.

Sarstedt Ltd.	68 Boston Road, Leicester, Leicestershire LE4 IAW, United Kingdom.
Scion Corporation	Maryland, U.S.A.
SERVA Electrophoresis GmbH	Carl-Benz-Str.7, P.O.B 105260, 69115 Heidelberg, Germany.
Sigma Chemical Company Ltd.	Fancy Road, Poole, Dorset, United Kingdom.
Tocris Cookstown Ltd.	Langford, Bristol B540 SDW, United Kingdom.
Whatman International Ltd.	Whatman House, St Leonard's Road, 20.20 Maidstone, Kent SG1 OLS, United Kingdom.

Appendix II

Acrylamide Gels

Stacking Gel 5% (2 X 1.5mm gels)	
30% (w/v) acrylamide, 0.8% (v/v) Bis-acrylamide (protogel™)	8ml
Distilled H_2O	6.7ml
0.5M Tris-HCl (pH 6.8)	5ml
10% (w/v) SDS	200µl
10% (w/v) Ammonium persulfate	100µl
TEMED	15µl

Resolving Gel 12% (2 X 1.5mm gels)	
Distilled H_2O	12.2ml
1.5M Tris-HCl (pH 8.8)	5ml
30% (w/v) acrylamide, 0.8% (v/v) Bis-acrylamide (protogel™)	2.66ml
10% (w/v) SDS	200µl
10% (w/v) Ammonium Persulfate	100µl
TEMED	20µl

Appendix III

10X PBS Composition

1.4M	NaCl
27mM	KCl
114.5 mM	Na_2HPO_4
17.6mM	KH_2PO_4

To make 1X PBS-T dilute 50ml 10X PBS in 450ml distilled H_2O and add in 500µl tween to give a final concentration of 0.1%PBS-T

Publications

Carroll, A.M., Haines, L.R., Pearson, T.W., Fallon, P. Walsh, C., Brennan, C.M., Breen, E.P. and Porter, R.K. (2005) Detection of a functioning UCP1 in thymus. *J. Biol. Chem.* In print

Carroll, A.M., Haines, L.R., Pearson, T.W., Brennan, C.M., Breen, E.P. and Porter, R.K. (2004) Immunodetection of UCP1 in rat thymus. *Biochem. Soc. Trans.* 32 (6), 1066 – 1067.

Brennan, C.M., McElligott, A.M., Warmington, S.A. and Porter, R.K. (2002) Skeletal muscle UCP3 expression following endurance swimming training in mice. *Proc. J. Physiol.* 543, 119.